



**SAPIENZA**  
UNIVERSITÀ DI ROMA

**S100B and PGE<sub>2</sub>: key enteric glial-derived signalling molecules  
in the gut pathophysiology**

A Dissertation for the Degree of Doctor of Philosophy in Pharmacology and Toxicology

STEFANO GIGLI

Department of Physiology and Pharmacology “Vittorio Erspamer”  
“Sapienza” University of Rome

**Director of PhD Program**

Prof. Maura Palmery

**Thesis Advisor**

Prof. Giuseppe Esposito

# SUMMARY

Chapter 1 .....	5
THE ENTERIC NERVOUS SYSTEM.....	5
1.1. Overview .....	5
1.2. Cellular Organization and Localization .....	7
1.3. The Enteric Glial Cells.....	8
1.3.1. Discovery .....	8
1.3.2 Morphological and Molecular Composition .....	10
1.3.3. Physiological Functions of EGCs.....	13
1.3.3.1. Support for Enteric Neurons .....	14
1.3.3.2. Regulation of Neurotransmission.....	15
1.3.3.3. Interaction with Immune System .....	16
1.3.3.5. Intestinal Motility.....	17
1.3.3.6. Modulation of Intestinal Epithelial Barrier .....	18
1.3.4. Pathological Functions .....	22
1.3.4.1. Morphological and Functional Changes.....	22
1.3.4.2. Interaction with Immune System .....	25
1.3.4.3. The Role of S100B in inflammation and cancer .....	26
1.3.4.3. The Role of PGE <sub>2</sub> in inflammation and leaky gut.....	29
1.4. Aim of the study.....	32
1.5. References .....	34
Chapter 2 .....	53
THE ROLE OF S100B ON HUMAN COLON CANCER.....	53
2.1 Introduction .....	53
2.2 Materials and Methods .....	56
Experimental Design.....	56
Western Blot.....	57
Electrophoretic mobility shift assay (EMSA) .....	58

NO quantification.....	59
Myeloperoxidase assay .....	59
Lipid peroxidation assay .....	60
Enzyme-linked immunosorbent assay.....	60
Statistical analysis .....	60
2.3 Results .....	61
Basal level of S100B and the relative RAGE/NF-κB pathway activation increase with the severity of lesions.....	61
p53 <sup>w<sup>t</sup></sup> protein decreases with the degree of specimens severity .....	63
Oxidative stress S100B-induced extends proportionally with the injury degree .....	64
Exposure to exogenous S100B induces a protein expression profile similar to tumoral specimens.....	65
2.4 Discussion .....	68
2.5 References .....	71
Chapter 3 .....	76
IMPACT OF GLIAL-DERIVED PGE <sub>2</sub> ON INTESTINAL FUNCTIONS..	76
3.1 Introduction .....	76
3.2 Materials and Methods .....	79
Experimental Design .....	79
<i>In vivo</i> Intestinal Permeability Assay .....	80
<i>In vivo</i> Total Transit Time Measurement .....	80
Immunohistochemical Staining.....	80
Statistical analysis .....	81
3.3 Results .....	82
DSS administration induces a marked increase in mPGES1 protein expression in myenteric plexi.....	82
In basal condition, mPGES1 deletion induces an intestinal permeability decrease in female and a transit time increase in male.....	84
mPGES1 deletion did not affect total transit time and permeability increase DSS-induced .....	85
mPGES1 deletion accelerates DSS effects during colitis development	87

3.4 Discussion .....	88
3.5 References .....	91

# Chapter 1

## THE ENTERIC NERVOUS SYSTEM

---

### 1.1. Overview

The Enteric Nervous System (ENS) is a division of the Autonomic Nervous System (ANS) located along the gastrointestinal tract, from the esophagus until the anus, including also pancreas, gallbladder and biliary tree. It integrates the informations about the state of gastroenteric tract in coordination with Central Nervous System (CNS) with which is connected through the afferent and efferent fibers of sympathetic and parasympathetic systems (Furness, 2012) In particular, these fibers compose three different pathways joining the ENS to distinct regions of CNS: the vagal pathway, connecting the esophagus and the stomach directly to the medulla oblongata; the sympathetic pathway, linking mainly the small and large intestine with the thoracolumbar spinal cord; pelvic pathway, joining the rectum and the lumbosacral defecation center (Figure 1.1). Nevertheless, the ENS actively participates in regulating gut motility, fluid exchange with the lumen, local blood flow and host-pathogen defense (Costa et al., 2000).

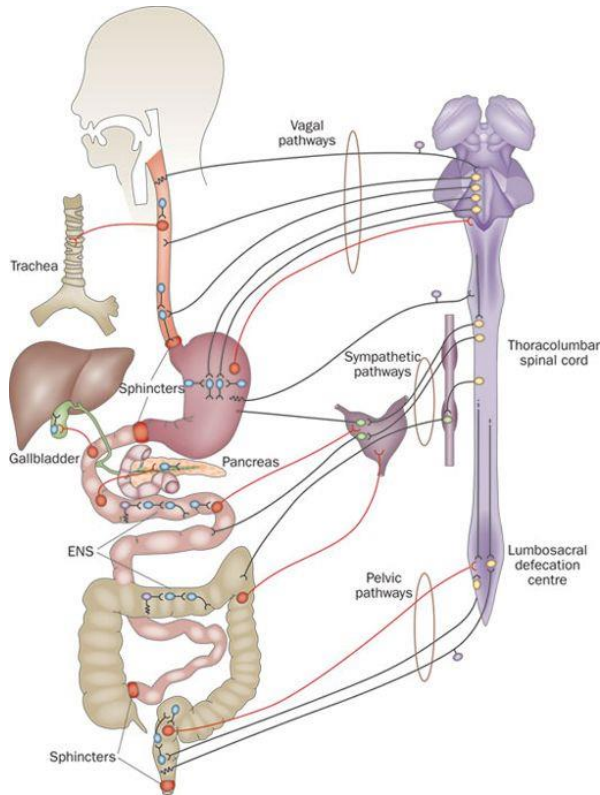


**Figure 1.1.** The innervation of the gastrointestinal tract (from Furness JB 2012).

Despite its extensive connections with CNS, the ENS is also capable of local and autonomous activity without any input from the brain. This surprising feature was observed for the first time in the beginning of XX century by a pioneering study of Bayliss and Starling. They showed that the peristaltic reflexes in dog intestines persisted even after anesthesia or transection of gut extrinsic nerves, advancing the hypothesis of an intrinsic nervous activity and independent integration center (Bayliss and Starling, 1900). A few years later, these findings were confirmed by similar studies (Langley and Magnus, 1905; Trendelenburg, 1917). Currently, it is widely accepted that ENS is able to regulate GI functions in absence of extrinsic neural connections as it includes primary afferent neurons, interneurons and motor neurons necessary for reflex circuitry (Furness et al, 2003). In fact, the ENS is considered as “second brain”

in our body characterized by specific functionality with promising clinical implications (Gershon, 1999).

## 1.2. Cellular Organization and Localization

The ENS is composed of about 100-500 millions of enteric neurons (1 to 5 times more than the spinal cord) and a number up to 10 times more enteric glial cells (EGCs) (Grundy and Schemann, 2007; Furness, 2012). These cellular populations are organized into complexes structures, called ganglia, connected to each other through interganglionic fibres. They are divided mainly in two classes: the submucosal plexus and myenteric plexus, located into strategic regions of gastroenteric tract according to their functions (Figure 1.2).

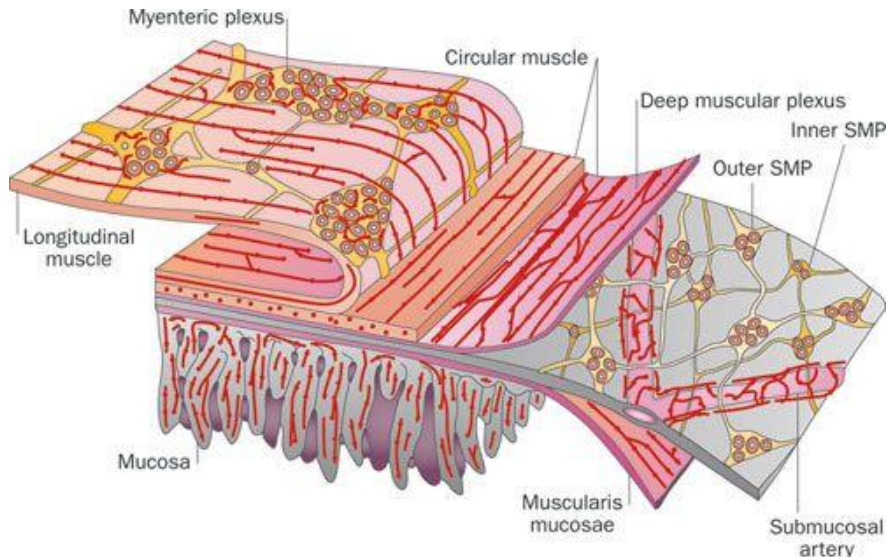


**Figure 1.2.** Anatomy of Enteric Nervous System (adapted from Furness JB, The Enteric Nervous System (Blackwell, Oxford, 2006)).

The submucosal plexus, also called Meissner's plexus, is composed by a gangliated network lying within the submucosal layer, between the circular muscle layer and the mucosa of the small and the large intestines. Then, it is present only from the duodenum to the rectum displaying a prominent role in the modulation of mucosal secretion and fluid exchange with the lumen (Furness, 2012). The submucosal plexus is divided itself in three different portions: the inner one (immediately under the intestinal mucosa), the outer one, or Schabadasch's plexus (crossing the bottom of the circular muscle layer) and the intermediate one (between the previous plexi) (Hoyle and Burnstock, 1989; Timmermans et al., 2001). The myenteric plexus, also called Auerbach's plexus, extends between the longitudinal and the circular muscle layer throughout the gastrointestinal tract, from the esophagus to the anal sphincter. Because of its location, the myenteric plexus is normally involved in the control of peristaltic movements and intestinal motility (Furness, 2012).

### **1.3. The Enteric Glial Cells**

#### **1.3.1. Discovery**

Enteric glia was described for the first time by Dogiel in 1899 (Dogiel, 1899). His work was focused on the characterization of submucosal and myenteric plexi using the blue methylene staining technique, in order to classify enteric neurons and find a correlation between their structural and functional features. But he also reported the presence of nucleated satellite cells surrounding neurons within enteric ganglia. However, over the next fifty years this observation was largely ignored. Using the Bielschowsky silver stain method, in 1952 Stohr studied the structure of ENS classifying enteric glia as Schwann cells, term adapted in "ganglionic Schwann cells" by Cook and



Burnstock (Stohr, 1952; Cook and Burnstock, 1976). The first studies focused specifically on enteric glial cells were conducted by Gabella in the 70's. He recognized the unique nature of enteric glia and refused the previous terminology because of their extensive branched processes surrounded by single basement membrane (Gabella, 1972). His analysis illustrated the characteristic structural features of this cellular population referring to it, for the first time, with the label of “enteric glial cells” (Gabella, 1981).

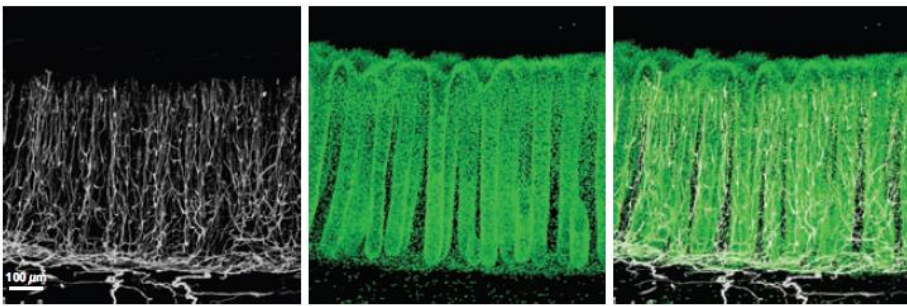


**Figure 1.3.** Gross view of enteric glial cells projections into mucosa. S100B positive cells are stained in white and nuclei are stained in green. Figure adapted from Liu et al, 2013.

Enteric glial cells (EGCs) are located in close proximity to enteric neurons and, within intestinal mucosa, they form a dense network that extend from the lamina propria to the top of colonic crypts and intestinal villi getting in direct contact with enteroendocrine cells, as observed in Figure 1.3 (Liu et al., 2013; Bohorquez et al., 2014). Although enteric glial cells represent the largest cellular population composing the ENS, the ratio between glia and neurons is strongly dependent by species. For instance, it has been estimated that in myenteric plexi this ratio can vary from 1:1 in mice until 7:1 in human (Gabella, 1984; Hoff et al., 2008). Moreover, their dimension can change from myenteric to submucosal plexi. Indeed, myenteric glia is larger than their submucosal counterpart (Hoff et al., 2008). Conversely, any significant difference between age or gender was observed.

### 1.3.2 Morphological and Molecular Composition

Similarly to the astrocytes into the CNS, enteric glial cells are star-shaped cells composed by small cell bodies containing mainly nucleus with small cytoplasmatic portion. The cell body cover about 1/10 of whole glial surface (Hanani and Reichenbach, 1994). The remaining part is accounted by their extensive branched processes tightening around neurons into enteric ganglia, producing an extracellular space of about 10 nm (Cook and Burnstock, 1976). It is relevant to point up that EGCs are also located close the interganglionic fibers as well as epithelial and endothelial cells (Gershon and Rothman, 1991; Boesmans et al., 2015). Because of their high irregular morphology and different localization, in 1994 EGCs have been classified in four different subtypes based on structural similarities with astrocytes (Hanani and Reichenbach, 1994) (Figure 1.4). Type I or “protoplasmic” gliocytes are star-

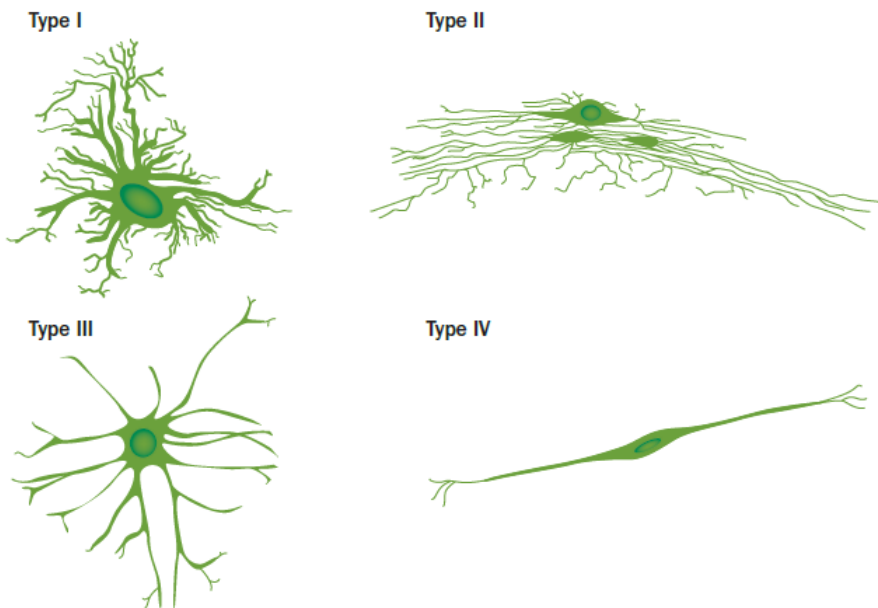


**Figure 1.4.** Schematic illustration of different morphological types of enteric glial cells. Figure adapted from Gulbransen and Sharkey, 2012.

shaped cells characterized by short and irregular projections in a similar way to protoplasmic astrocytes into CNS. Type II or “fibrous” gliocytes are found into interganglionic fibers which explains their elongated and tapered shape. Finally, type III or “mucosal” gliocytes are star-shaped cells with several long processes extending along the intestinal mucosa. Type IV or “intramuscular” gliocytes are elongated glia running the nervous fibers through intestinal muscular layers. However, several evidences highlighted a marked molecular and functional heterogeneity among different glial subpopulations, proposing new essential criteria and parameters for a more complete and exhaustive classification (Nasser et al., 2006; Costagliola et al., 2009).

Several molecular markers are widely used to study the EGCs (Figure 1.5). The branched processes of enteric glia are mainly composed by gliofilaments enriched in vimentin and glial fibrillary acid protein (GFAP) (Jessen and Mirsky, 1980, 1985). Vimentin is predominantly expressed during the development of enteric glia. Conversely, GFAP is a cytoskeleton protein strongly expressed by mature enteric glia as well as astrocytes (Jessen and Mirsky, 1980), in fact it is mostly used to investigate glial morphology. In this regard, preclinc studies demonstrated the higher GFAP expression following pro-inflammatory stimuli, such as lipopolysaccharide (LPS), according to what observed in patients affected by inflammatory bowel diseases (von Boyen et al., 2004; Rosenbaum et al., 2016; da Cunha Franceschi et al., 2017). S100B is a calcium-binding protein present in the cytoplasm where can modulate the calcium homeostasis (Zimmer et al., 1995; Heizmann et al., 2002). It can be also released exerting a neurotrophic action, as largely observed in the CNS (Marshak, 1990; Selinfreund et al., 1991; Heizmann et al., 2002). Although it is expressed also by other cellular populations, including myofibroblasts and oligodendrocytes (Arcuri et al., 2002; Hachem et al., 2005), S100B is considered a specific glial marker for EGCs within intestinal and colonic wall (Rühl, 2005). Sox10 belongs to SRY-related HMG-box family of transcription factor. It is widely expressed by progenitors cells of enteric nervous system in

the neural crest as well as differentiated enteric glia and displays a prominent role in the gliogenesis, especially in the last phase of ENS development (Kelsh, 2006; Bondurand and Sham, 2013). Conversely, differentiated neurons do not express Sox10 protein. Sox10 is mainly used in research application for nuclei staining and relative glial quantification, but it does not provide informations about glial morphology. Although GFAP, S100B and Sox10 represent the most common glial markers, they are not co-expressed in the whole enteric glial population, reminding the morphological heterogeneity already described (Boesmans et al., 2015).

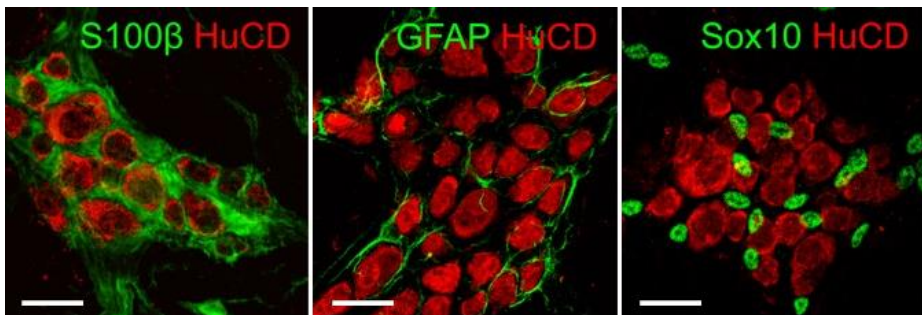


**Figure 1.5.** Interaction between enteric neurons (red) and enteric glial cells identified with different specific markers (green). Scale bar: 25  $\mu$ m. Figure adapted from Boesmans et al, 2013.

### 1.3.3. Physiological Functions of EGCs

At first, EGCs were considered as cells responsible for neuronal mechanical support (as suggested by their name, “glia” from the Greek γλία, “glue”) and trophic functions. In the last decades, an active role displayed by this cellular population in the intestinal homeostasis has been widely accepted, including the interaction with immune system and the modulation of intestinal motility and permeability as briefly described in Figure 1.6.

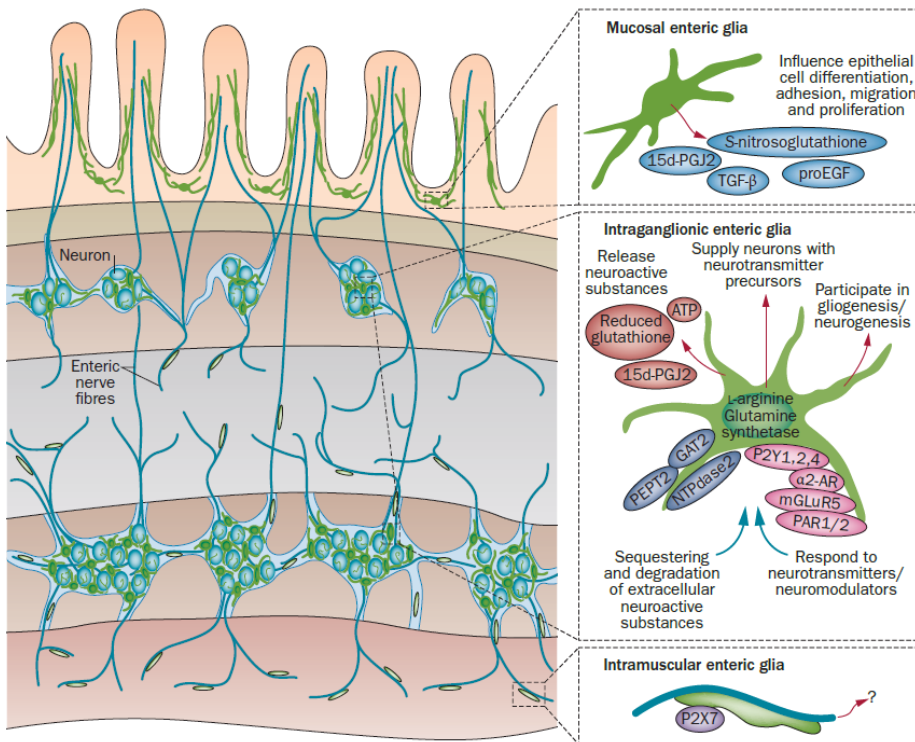


**Figure 1.6.** Schematic representation of the main physiological functions displayed by enteric glial cells. Figure adapted from Gulbransen and Sharkey, 2012.

### **1.3.3.1. Support for Enteric Neurons**

The supporting role in sustaining the integrity and the architecture of enteric nervous system was the first function attributed to EGCs. As observed by Gabella in 1990, EGCs firmly anchor on the surface of nerve fibers and ganglia through their gliofilament, stabilizing the entire structure of ENS (Gabella, 1990). Besides their mechanical support, enteric glia is also involved in homeostatic mechanisms of enteric neurotransmission supplying neurons with precursors necessary for neurotransmitters such as L-arginine and glutamine (via glutamine synthase), responsible for the synthesis of nitric oxide (NO) and  $\gamma$ -amino butyric acid (GABA), respectively (Jessen and Mirsky, 1983; Aoki et al., 1991; Nagahama et al., 2001; Gulbransen and Sharkey, 2012). Moreover, in physiological conditions antioxidants and growth factors are also provided to the enteric neurons (von Boyen and Steinkamp, 2006; Abdo et al., 2010, 2012). Interestingly, EGCs maintain the enteric neurotransmission by regulating the bioavailability of neuroactive compounds in the extracellular milieu through specific surface enzymes and glial channels. For instance, transporters for GABA (GAT-2) and oligopeptides are enzymes located on the glial surface responsible for the removal of neuroactive substances (GABA and vasoactive intestinal peptide VIP, respectively) from extracellular space (Fletcher et al., 2002; Rühl et al., 2005). In addition, EGCs also express ectonucleotidase, nucleoside triphosphate diphosphohydrolase 2 (eNTPDase2) able to degrade of neuroactive compound nearby enteric neurons (Braun et al., 2004; Lavoie et al., 2011). In a different way, glial potassium channels prevent neuronal death caused by excitotoxicity with consequent stabilization of neurotransmission (Hanani et al., 2000; Costagliola et al., 2009), exerting analogous effects of glutamine synthase also expressed by enteric glia because of its ability to recue glutamate levels producing glutamine (Jessen and Mirsky, 1983; Kato et al., 1990). Neuroprotective properties just mentioned are well

elucidated. Indeed, in 1998 Bush et al observed a marked neurodegeneration into myenteric plexi after the specific deletion of GFAP+ cells using a transgenic murine model (Bush et al., 1998). Later, several compounds have been identified as glial mediators of neuroprotection such as 15-deoxy- $\Delta^{12,14}$ -Prostaglandin J<sub>2</sub> (15dPGJ<sub>2</sub>), glial cells-derived neurotrophic factor (GDNF), nerve growth factor (NGF) and neurotrophine 3 (Hoehner et al., 1996; von Boyen and Steinkamp, 2006; Abdo et al., 2012).

### **1.3.3.2. Regulation of Neurotransmission**

Enteric glia takes part actively in the modulation of neurotransmission, beyond their ability to regulate the neurotransmitters bioavailability described above. Indeed, EGCs expressed different receptors able to detect signaling molecules released by enteric neurons triggering a neuron-glia communication, as demonstrated by *in vitro* and *in situ* studies (Kimball and Mulholland, 1996; Gomes et al., 2009; Gulbransen and Sharkey, 2009). Although more investigations are necessary to explain the exact mechanisms on the basis of this crosstalk, a large amount of neuroactive compounds involved have been identified including ATP, norepinephrine (NE), glutamate, thrombin, lipid signaling molecules, serotonin (5-HT), bradykinin, histamine and endothelins (Kimball and Mulholland, 1996; Garrido et al., 2002; Vanderwinden et al., 2003; Segura et al., 2004; Nasser et al., 2006, 2007; Zhang et al., 2010; Boesmans et al., 2013). Interestingly, it has been described that enteric glia respond to acetylcholine (ACh) and 5-HT released from enteric neurons with an increase in intracellular calcium concentration inducing a marked ATP release (Zhang et al., 2003; Boesmans et al., 2013). This process can propagate into neighboring glial cells via Cx43 gap junctions resulting in a modulation of neuronal activity in the ENS (McClain et al., 2014). To confirm that, recent evidences showed that pharmacological inhibition or

deletion of glial Cx43, preventing the diffusion of  $\text{Ca}^{2+}$  response, reduce neuronal activity and affect secretomotor intestinal functions in mice (McClain et al., 2014; Grubisic and Gulbransen, 2017). These evidences strongly suggest that EGCs can release gliotransmitters with which they communicate with enteric neurons, modulating directly the gut functions in a complex and synergic system.

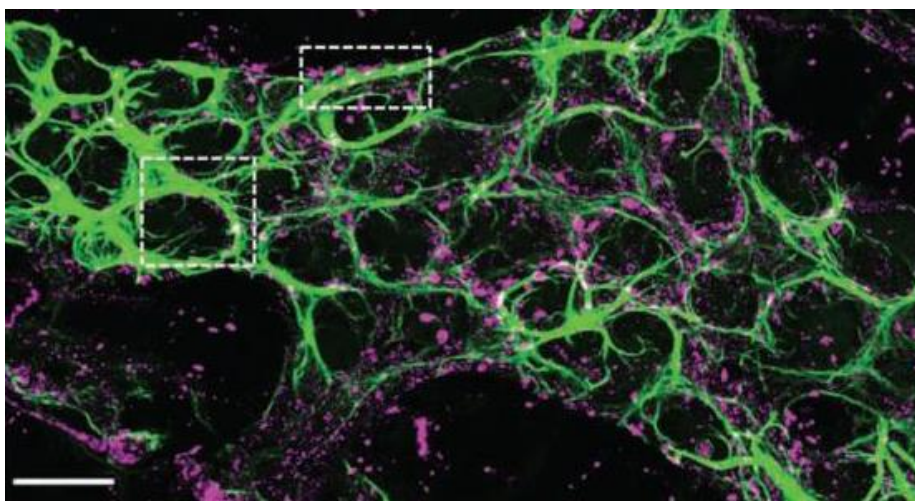


**Figure 1.7.** Localization of Cx43 (magenta) on the enteric glial cells identified with anti-GFAP antibody (green). Scale bar: 20  $\mu\text{m}$ . Figure adapted from McClain et al, 2015.

### 1.3.3.3. Interaction with Immune System

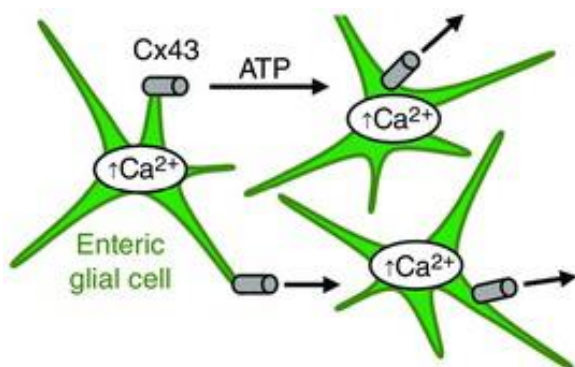
EGCs actively participate in the defense of the intestinal mucosa through a close interaction with immune system. In the last years, it has been well accepted how enteric glia can initiate and sustain inflammatory processes following detrimental noxia. At the beginning of XXI century, *in vitro* studies elucidated the ability of glial cells to produce  $\text{IL-1}\beta$ ,  $\text{TNF}\alpha$  and  $\text{IL-6}$  after



immunological stimulation (Ruhl et al., 2001; Rühl, 2005). The mechanisms on the basis of IL-1 $\beta$  and TNF $\alpha$  release are still unclear, but it has been demonstrated that EGCs express the receptor for IL-1 $\beta$ , responsible for glial-derived IL-6 release that act in a negative feedback way on its own secretion (Ruhl et al., 2001; Rühl, 2005). Moreover, enteric glia expresses the major histocompatibility complex class II (MHC II) in disease states, confirming the critical role displayed by EGCs in intestinal immune responses (Hirata et al., 1986; da Silveira et al., 2011). In addition, toll-like receptors (TLRs) family is expressed by enteric glia, especially TLR4, providing evidences that EGCs recognize invading microbes and, then, trigger the inflammatory process (Barajon et al., 2009; Esposito et al., 2014).

### 1.3.3.5. Intestinal Motility

In the last years, the hypothesis of enteric glia implication in the control of intestinal motility has been investigated through evaluation of gastric emptying and fecal transit in different models of glial ablation (Aubé et al., 2006; Rao et al., 2017). Unlike neurons, enteric glia are not capable to generate action



potentials (Hanani et al., 2000). Their excitability is not mediated by electricity but by calcium fluxes transmitted to nearby EGCs in a

**Figure 1.8.** Schematic representation of Ca<sup>2+</sup> waves propagation between nearby enteric glial cells. Figure adapted from Grubisic and Gulbransen, 2017.

paracrine/autocrine manner releasing ATP and Ca<sup>2+</sup> through the Cx43 gap junction (Zhang et al., 2003; Grubisic and Gulbransen, 2017) (Figure 1.8). Recent studies demonstrated that glial excitability is necessary for intestinal motility. Indeed, the ablation of Cx43 expressed by EGCs reduced the *ex vivo* contraction of smooth muscles and *in vivo* intestinal motility and fecal transit (McClain et al., 2014, 2015). Moreover, the same effect was observed following neuronal activation induced by electric stimulation, suggesting that decreasing in intestinal motility is importantly regulated by enteric glia (McClain et al., 2014, 2015). Anyway, the precise mechanisms on the basis of this modulation are not fully elucidated yet.

### **1.3.3.6. Modulation of Intestinal Epithelial Barrier**

Similarly to astrocytes in the CNS and their ability to modulate brain blood barrier permeability, enteric glia represent one of the most key regulators of intestinal barrier functions. In particular, mucosal enteric gliocytes (type III) are mainly located in the intestinal mucosa (up to 0.5-2 μm from the epithelial cells) where they can modulate permeability, cellular differentiation and proliferation via releasing several factors (Liu et al., 2013; Neunlist et al., 2013) (Figure 1.9).

**Intestinal Permeability.** The first evidence of the direct involvement of EGCs in maintaining of intestinal barrier architecture and, consequently, in the modulation of permeability was reported by Bush in 1998. This pioneering study showed that the total ablation of enteric glia in transgenic mice induced a fulminant jejuno-ileitis with significant loss in mucosal integrity suggesting

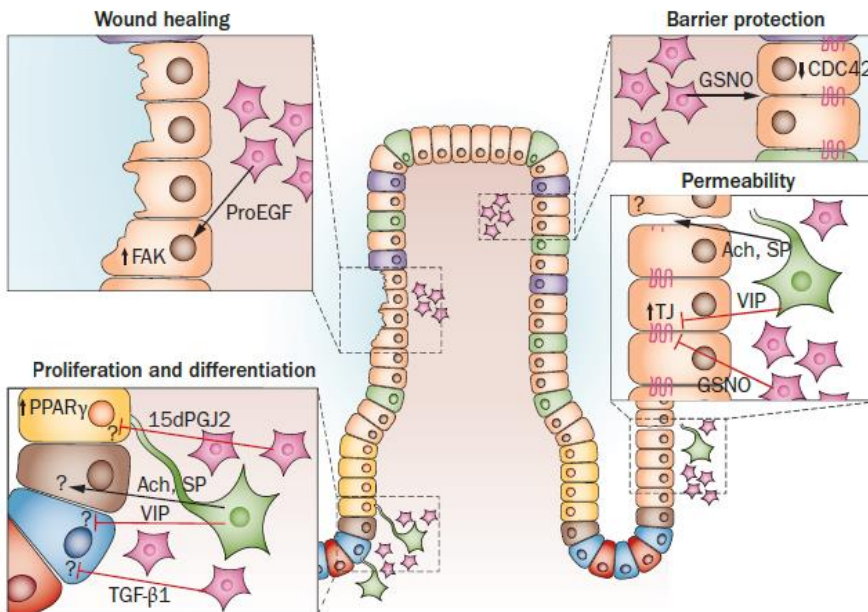


**Figure 1.9.** Schematic representation of the main soluble factors released by enteric glia responsible for the modulation of intestinal epithelial barrier homeostasis. Figure adapted from Neunlist et al, 2012.

an essential role of EGCs in intestinal homeostasis and contribution in mechanisms underlying inflammatory bowel disease (Bush et al., 1998). A significant increase of paracellular permeability in absence or before of inflammatory processes was also observed in models of less severe glial ablation (Aubé et al., 2006; Arrieta et al., 2009). The most important glial mediator of this effect has been identified in the S-nitrosoglutathione (GSNO) (Savidge et al., 2007; Flamant et al., 2011). During inflammatory conditions, the release of this nitric oxide donor by enteric glia is directly associated with a significant reduction in paracellular permeability related to a marked increase in tight junction protein expression, including zonula occludens 1 (ZO-1) and occludin (Savidge et al., 2007; Flamant et al., 2011). Among the proposed mechanism for these effects, it is well established that GSNO

protects intestinal integrity by reducing CDC42 which has a crucial role in cytoskeleton assembly and bacterial invasion (Flamant et al., 2011). Recently, it has been showed that 15-hydroxyeicosatetraenoic acid (15-HETE) contribute in intestinal barrier permeability (Pochard et al., 2016). This metabolite of arachidonic acid is released by enteric glia in pathological conditions, such as Crohn's disease, and exerts protective effects reducing intestinal permeability through AMPK inhibition and ZO-1 expression (Pochard et al., 2016). Interestingly, the same negative modulation glia-mediated in permeability was observed following different pro-inflammatory stimuli, for instance cytokines cocktail (TNF $\alpha$ , IL-1 $\beta$  and IFN $\gamma$ ), lipopolysaccharide (LPS) or nitric oxide exposure (MacEachern et al., 2011; Xiao et al., 2011; Cheadle et al., 2013).

**Cellular Proliferation and Differentiation.** Enteric glia has also a consistent antiproliferative action mainly mediated by releasing transforming growth factor- $\beta$ 1 (TGF- $\beta$ 1) and 15-deoxy- $\Delta$ 12,14-prostaglandin J2 (15dPGJ2) (Neunlist et al., 2007; Bach-Ngohou et al., 2010). The mechanisms on the basis of these factors is different and do not include any apoptotic process. Indeed, TGF- $\beta$ 1 inhibits intestinal epithelial proliferation interfering with the cell cycle. It is well accepted that this factor downregulates G1/S cyclins and cyclin-dependent kinases expression and, conversely, upregulates cyclin-dependent kinases inhibitors, mediating a synergic effect in blockade the cell cycle (Neunlist et al., 2007). In a different way, the lipidic mediator 15dPGJ2 exerts its antiproliferative effect with a peroxisome proliferator-activated receptor (PPAR)- $\gamma$ -dependent mechanism (Bach-Ngohou et al., 2010). It is also interesting to highlight that these effects are associated with a significant promotion of cellular differentiation. Indeed, recent evidences *in vitro* showed that EGCs are able to modulate the expression of genes controlling cell-to cell and cell-to-matrix adhesion toward a general increase in intestinal epithelial cells differentiation (Van Landeghem et al., 2009).

**Mucosal Healing.** The impact of enteric glia on the modulation of intestinal epithelial barrier has been observed in the mucosal repair after different kind of barrier injury. An elegant study in 2011 demonstrated that the conditional ablation of enteric glia in transgenic mice is related to a marked worsening in damage DSS-mediated and delaying of tissue healing from ulcerations induced by diclofenac (Van Landeghem et al., 2011). This statement was confirmed by *in vitro* analysis showing that EGCs increased intestinal epithelial wound healing and spreading. The main responsible for this activity is represented by the soluble factor pro-epidermal growth factor (proEGF) which is released by EGCs and contribute to epithelial restitution in a EGFR-dependent manner (Van Landeghem et al., 2011). Recently, another lipidic mediator secreted by enteric glia has been observed to participate in epithelial repair (Coquenlorge et al., 2016). 11- $\beta$  prostaglandin F<sub>2</sub> (11 $\beta$ PGF<sub>2</sub> $\alpha$ ) is a metabolite of arachidonic acid involved in intestinal epithelial barrier healing and spreading through the activation of PPAR $\gamma$  and DP2 receptors, as observed in isolated EGCs/Caco2 co-culture studies (Coquenlorge et al., 2016).

### 1.3.4. Pathological Functions

A growing concept in gastroenterology is the active role of ENS in the gastrointestinal pathophysiology. In particular, a large amount of evidences demonstrated the direct involvement of enteric glia in the initiation and propagation of intestinal inflammatory processes and related pathologies, such as ulcerative colitis and Chron's disease.

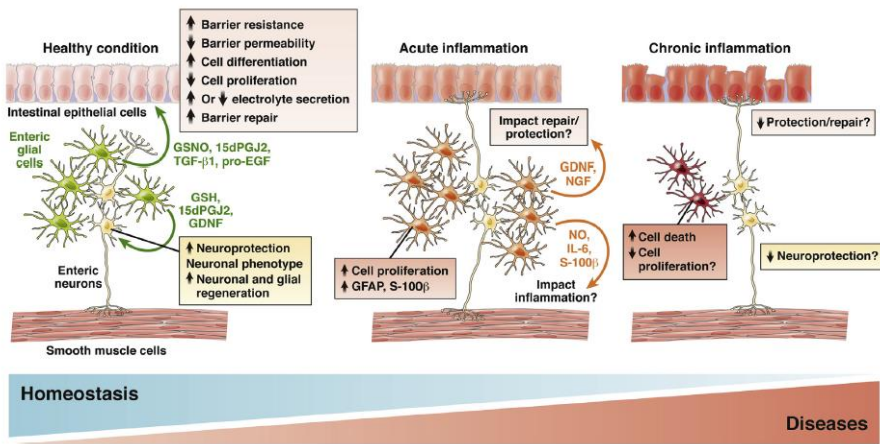


**Figure 1.10.** Schematic representation of enteric glia involvement with related glial mediators in both intestinal healthy and inflammatory conditions. Figure adapted from Neunlist et al, 2014.

#### 1.3.4.1. Morphological and Functional Changes

Changes in the number of EGCs are associated to inflammatory bowel diseases, diverticular disease, Chagas disease and pathology not directly related to gastrointestinal tract, such as type II diabetes or Parkinson's disease (Cornet et al., 2001; Wedel et al., 2010; da Silveira et al., 2011; von Boyen et al., 2011; Devos et al., 2013; Stenkamp-Strahm et al., 2013). The nature of these alteration can vary depending on the single pathology and is usually

studied by GFAP and S100 immunoreactivity. We can assume that, globally, glial density is reduced in the diseases course with due exceptions. For instance, a significant decrease in GFAP protein expression was observed in non-inflamed areas from patients with Crohn's disease, but not in ulcerative colitis (Cornet et al., 2001; von Boyen et al., 2011). Conversely, the inflamed regions of both inflammatory bowel diseases are characterized by high GFAP levels, although less pronounced in Chron's disease (Cornet et al., 2001; von Boyen et al., 2011). Similar results were provided for Chagas disease but with a decreased S100B immunoreactivity (da Silveira et al., 2011). Actually, it is not surprising this difference between the glial markers expression because of their cellular localization, as explained above. Nevertheless, it is clear a greater expression of glial markers in inflamed tissues in comparison with non-inflamed regions. In support of this statement, several evidences showed a marked sensitiveness of EGCs to proinflammatory stimuli (Figure 1.11). The exposure to  $TNF\alpha$  or  $IL-1\beta$ , as well as bacterial lipopolysaccharide (LPS), induce S100B and GFAP protein expression, also in autocrine way by release

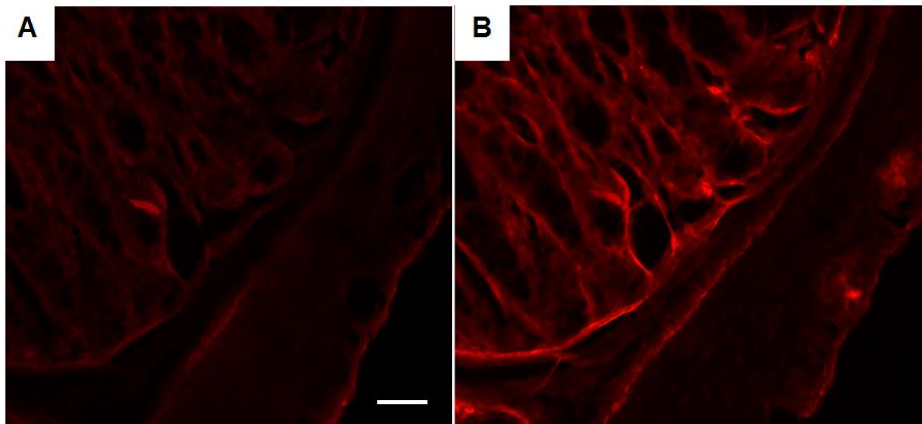


**Figure 1.11.** Difference in S100B immunoreactivity (red) between enteric glia in absence of proinflammatory challenge (A) and activated-EGCs during inflammation (B).

of glial endothelin-1 (von Boyen et al., 2004; Cirillo et al., 2009; von Boyen and Steinkamp, 2010). Interestingly, these morphological alterations in glial phenotype are reflected in functional changes represented by expression of receptors and enzymes and glial proliferation (Nasser et al., 2007; Joseph et al., 2011). Furthermore, *in vivo* and *in vitro* studies showed an increase in glial activity through the upregulation of early gene c-Fos in both submucosal and myenteric plexi and translocation of signal transducer and activator of transcription 5 (STAT-5) in cultured enteric glia following IL-1 $\beta$  and TNF $\alpha$  application, respectively (Tjwa et al., 2003; Rehn et al., 2004). In addition to cytokines, other proinflammatory mediators can modulate glial activity. Thrombin is capable to activate the glial protease-activated receptors (PARs) resulting in a marked Ca<sup>2+</sup> responses and contributing to inflammatory process (Garrido et al., 2002). Moreover, EGCs are very responsive to extracellular purines, released and less hydrolyzed during inflammation (Wynn et al., 2004; Lomax et al., 2005). All these findings support the evidence that enteric glia can detect inflammatory extracellular substances and, in response, promote and participate actively to inflammatory processes. No less importantly, these functional abnormalities also translate in the loss of neuroprotective and physiological actions of enteric glia inducing, among other effects, a significative neuronal death in pathological conditions.

A recent lipidomic study highlighted a marked reduction in different polyunsaturated fatty acids (PUFAs) metabolites produced by enteric glia isolated from Crohn's disease patients in comparison with healthy subjects (Coquenlorge et al., 2016). At the same time, EGCs have lost their ability to modulate tissue healing and intestinal permeability in these patients, suggesting that these metabolites are responsible, at least in part, for glial activity. In particular, the arachidonic acid 11 $\beta$ PGF2 $\alpha$  has been associated with impaired effect of enteric glia in Crohn's disease.



### 1.3.4.2. Interaction with Immune System

Currently, the concept of an important cross-talk between enteric glia and immune system has been hypothesized and largely recorded. One of the most interesting observations describes EGCs as antigen presenting cells (APC) able to evoke immune cells during inflammation. Not for nothing, enteric glia express inducible major histocompatibility complex (MHC) class II receptor on the cellular surface in Crohn's disease and in Chagas disease with the costimulatory proteins CD80 and CD86 (Koretz et al., 1987; da Silveira et al., 2011). In support, *in vitro* evidences also showed an increasing of glial MHC class II peptides and intercellular adhesion molecules 1 (ICAM-1) expression (Hollenbach et al., 2000). Consistently, these data are related to a high lymphocyte density nearby. Moreover, in inflammatory conditions mast cells are recruited by enteric ganglia and degranulated mast cells result often in contact with EGCs and S100 positive nerve fibers (Bassotti et al., 2011).

It is worth noting that enteric glia is able to detect invading bacteria because of the expression of Toll-like receptor 4 (TLR-4). The binding with bacterial LPS activates a signaling cascade inducing downstream the transcription of different genes encoding for proinflammatory cytokines and regulators. An elegant study by Esposito in 2014 demonstrated that glial TLR-4 is overexpressed in human colonic tissues isolated from patients affected by ulcerative colitis as well as in DSS-treated mice. Interestingly, this upregulation is tightly associated with a marked phosphorylation of p38 MAPK, ERK, JNK and NF- $\kappa$ B activation, identifying a possible mechanism on the basis of enteric glia response following detrimental noxia (Esposito et al., 2014).

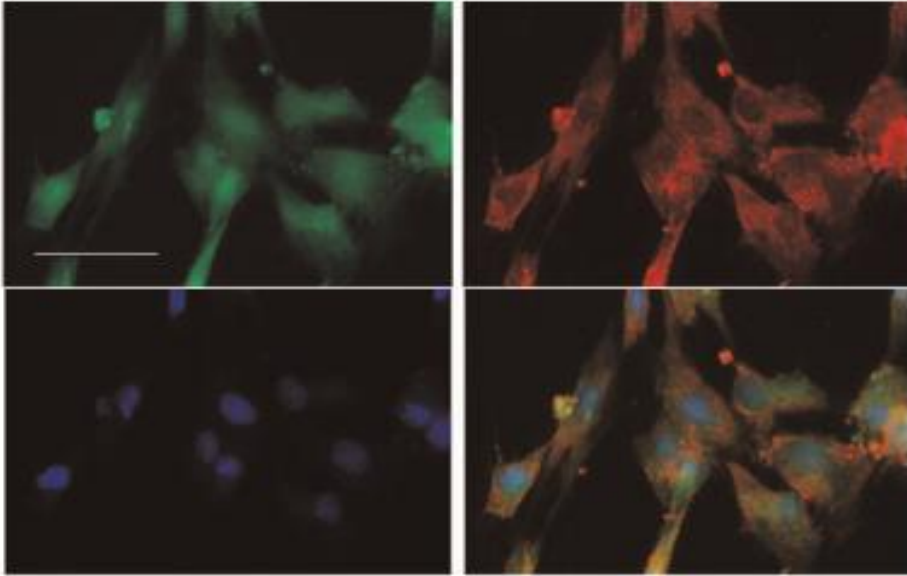


**Figure 1.12.** Co-expression of S100B (red) and TLR-4 (green) on enteric glia. Nuclei were stained with Hoechst (blue). Figure adapted from Turco et al, 2013. Scale Bar: 40  $\mu\text{m}$ .

### **1.3.4.3. The Role of S100B in inflammation and cancer**

S100B belongs to  $\text{Ca}^{2+}/\text{Zn}^{2+}$  binding protein family and represents the main glial mediator involved in inflammatory responses. It is physiologically localized at cytoplasmatic and/or nuclear level in both nervous and non-nervous tissues. In the brain, astrocytes release S100B which can exert opposite effects depending upon its concentrations. At nanomolar concentrations, S100B acts as a neurotrophic factor, promoting neuronal survival and astrocytes proliferation (Zimmer et al., 2005; Bramanti et al., 2010; Chow et al., 2010). Conversely, at micromolar concentrations has toxic effects with important implications in neurodegenerative diseases, including Alzheimer's disease and Down syndrome (Griffin et al., 1989; Van Eldik and Griffin, 1994). In the gut, a tight association between high levels of S100B and

the severity of inflammatory states has been described. Actually, S100B is considered a specific enterogial marker and behaves similarly to what observed in the CNS. More specifically, S100B effects are mediated by activation of membrane receptor for advanced glycation end products (RAGE) through the S100B accumulation on the extracellular portion of the receptor (Schmidt et al., 2001; Adami et al., 2004; Cirillo et al., 2009). The activation of RAGE induces different reactions at the intracellular level: lipids peroxidation and p38 mitogen-activated protein kinase (p38-MAPK) phosphorylation. Lipoperoxidation increases cellular oxidative state with a massive production of reactive oxygen species (ROS) (Esposito et al., 2006; Capoccia et al., 2015a). The phosphorylation of p38-MAPK triggers the nuclear translocation of transcription factor nuclear factor- $\kappa$ B (NF- $\kappa$ B), responsible for the transcriptions of genes encoding for proinflammatory mediators and cytokines, including iNOS and COX-2 (Esposito et al., 2006; Capoccia et al., 2015a). In view of the above, the causality between high levels of S100B and NO release in inflammatory states has been reported in different gut pathologies. Indeed, a significant increase in S100B mRNA and protein expression associated with the extent of iNOS expression has been shown in duodenal mucosa of patients with celiac disease as well as in rectal mucosa of ulcerative colitis patients (Esposito et al., 2007; Cirillo et al., 2009). Moreover, in the same studies the exposure to micromolar concentration of exogenous S100B induced a massive release of NO in healthy tissue (Esposito et al., 2007; Cirillo et al., 2009). Along this line, an elegant *in vitro* study demonstrated that an inflammatory stimulus represented by LPS and IFN $\gamma$ , increase S100B protein expression and release on isolated human EGCs, associated with a significative increment of iNOS expression and nitrite release (Cirillo et al., 2011). To confirm whether S100B is crucial for the inflammatory response, effects on iNOS expression and nitrite production were reduced in presence of RAGE antibody and S100B antibody (Cirillo et al., 2011). More recently, in a model of secretory diarrhea HIV-1 Tat-induced, a marked neuroinflammation

mediated by EGCs was observed. The activation of enteric glia resulted in a significant increase in GFAP, S100B and iNOS expression with a massive release of S100B and nitrite (Esposito et al., 2017). All the effects were abolished inhibiting glial activity with lidocaine administration (Esposito et al., 2017). Taken together, these data highlighted the pivotal role of EGCs in intestinal inflammatory processes whose activity is principally mediated by S100B.

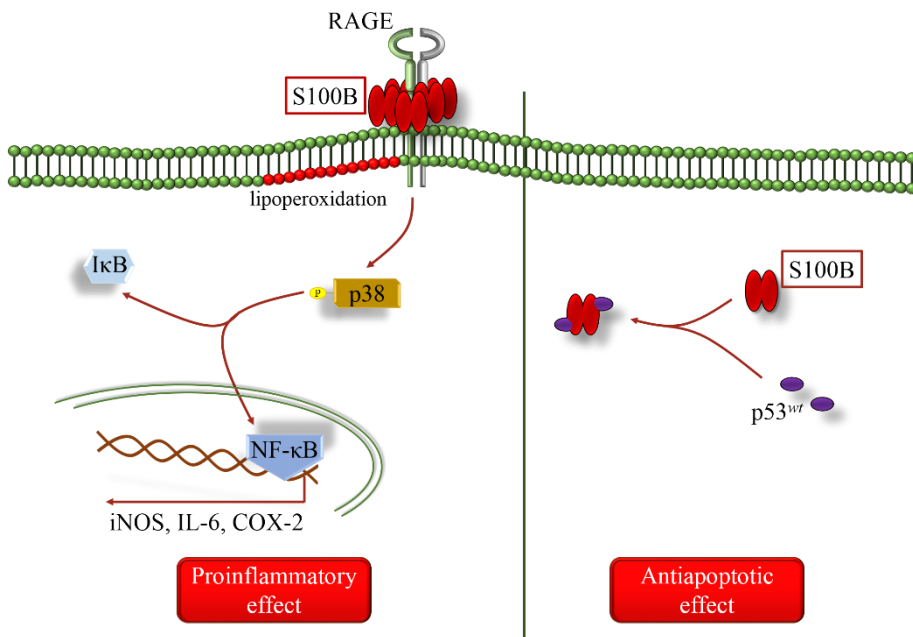


**Figure 1.13.** Schematic representation of mechanisms underlying the proinflammatory and anti-apoptotic effect of S100B protein.

Over the past decades it has been demonstrated a close relationship between chronic inflammatory states and colon cancer (Quante et al., 2013; Garcia et al., 2014). Indeed, intestinal inflammation is considered the earliest step in the adenoma-carcinoma sequence because of its ability to promote a pro-malignant microenvironment (Quante et al., 2013; Garcia et al., 2014). For instance, the production of ROS during inflammatory process induces genetic mutations

exceeding the control of p53 via apoptosis. Under these circumstances, S100B may make a large contribution in cancer promotion associated to chronic inflammation. Actually, S100B generates an overwhelming genomic instability due to ROS production and induces NF- $\kappa$ B activation, that contribute to carcinogenesis acting as protooncogene. Moreover, S100B is able to inhibit p53 protein functions. It interacts with the C-terminus of p53 preventing its tetramerization, phosphorylation protein kinase C-mediated and transcriptional activity (Delphin et al., 1999; Fernandez-Fernandez et al., 2008). Although studies concerning the involvement of S100B in colorectal cancer are still missing, several evidences support this statement for different malignancies, including melanoma and glioma (Lin et al., 2004; Capoccia et al., 2015b). It is currently used as biomarker in the diagnosis and prognosis of melanoma where it results overexpressed (Andres et al., 2004; Weide et al., 2012). Similarly, S100B upregulation was associated with early relapse and liver metastasis after curative resection in patients affected by colorectal cancer (Hwang et al., 2011; Huang et al., 2012). Based on this background, S100B may display an essential role in the promotion of colitis-associated colon cancer and, consequently, may be a possible molecular target of intervention in the prevention of this pathology.

#### **1.3.4.3. The Role of PGE<sub>2</sub> in inflammation and leaky gut**

Prostaglandin E<sub>2</sub> (PGE<sub>2</sub>) is a bioactive lipid produced by enteric glia in pathological condition exerting several biological effects associated with inflammation and cancer. PGE<sub>2</sub> belongs to the prostanoid family and is synthesized by sequential reactions operated by different enzymes. In the first place, free fatty acids, including arachidonic acid, are produced by phospholipases, enzymes responsible for the hydrolysis of membrane

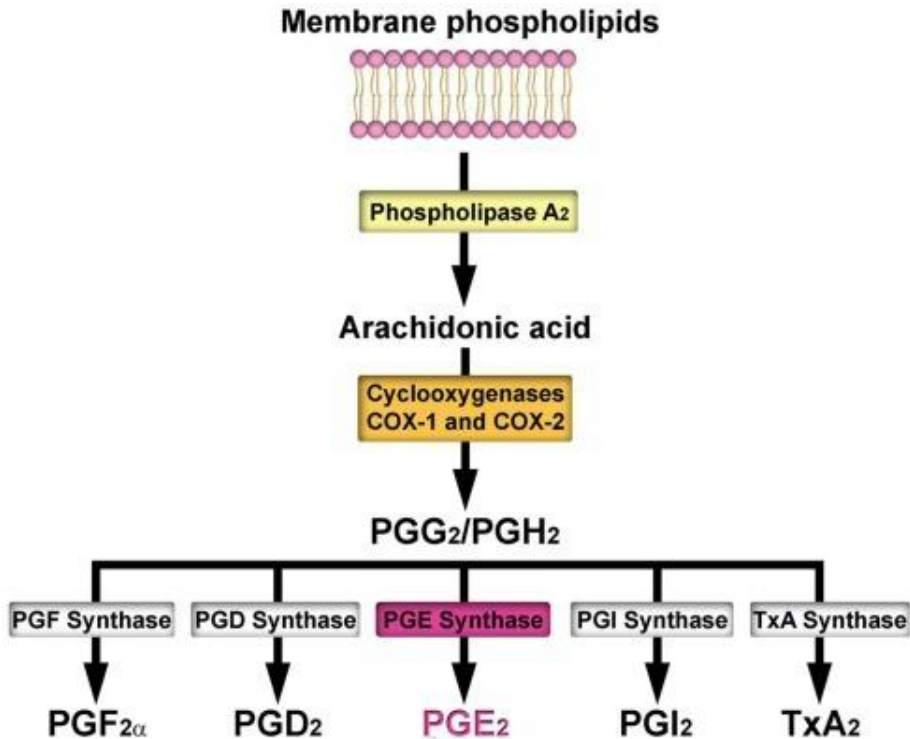


**Figure 1.13.** Schematic representation of PGE<sub>2</sub> synthesis. Figure adapted from Clasadonte et al, 2011.

phospholipids. Then, membrane-released arachidonic acid is oxidized in unstable product, PGG<sub>2</sub> which is reduced in PGH<sub>2</sub> by the same enzyme, called cyclooxygenase (COX). The inducible isoform is COX-2 and is highly expressed by several tissue following proinflammatory and mitogenic stimuli (Wang and Dubois, 2006). Finally, PGH<sub>2</sub> can be converted in different prostaglandin by specific terminal synthases. Specifically, PGE<sub>2</sub> is produced by microsomal PGE synthase-1 (mPGES1), mPGES2 and cytosolic PGE synthase (cPGES) (Jakobsson et al., 1999; Wang et al., 2005b). While mPGES2 and cPGES are constitutively expressed, during inflammation mPGES1 is highly induced in association with COX-2 to generate high

temporary concentrations of PGE<sub>2</sub> (Murakami et al., 2000). Beside to classic inflammatory activity acting as vasodilator and pyrogenic agent, PGE<sub>2</sub> interact with immune system enhancing the resolution of inflammation and tissue repair. For instance, PGE<sub>2</sub> inhibits the synthesis of IL-2 cytokine and the relative receptor expression by T cells counteracting their proliferation and activation (Kalinski, 2012). Similarly, cytotoxic activities of natural killer (NK) and activated T cells are abolished by the prostanoid as well as the production of the chemokine CCL19 responsible for attracting naïve T cells in the site of infection (Martinet et al., 2010; Muthuswamy et al., 2010). In the gut, several evidences *in vivo* demonstrated the protective role of PGE<sub>2</sub> in support of barrier permeability and integrity. Indeed, it has been reported that genetic deletion of mPGES1 in mice induce the presence of spontaneous colonic ulcerations underlying the key role displayed by PGE<sub>2</sub> in mucosal homeostasis and wound repair (Nakanishi et al., 2011). Accordingly, another study showed that the absence of mPGES1 in KO mice resulted in marked severity of ulcerative colitis starting from day 1 of dextran sodium sulfate (DSS) administration, due to a higher sensitiveness to DSS treatment in comparison with wild type mice (Hara et al., 2010). It has been hypothesized that PGE<sub>2</sub> may protect the mucosal integrity by the interaction with EP4 receptor. Indeed, EP4 agonist administration prevent mucosal damage DSS-induced and, along this line, a worsening of intestinal injury and barrier integrity after DSS administration in EP4 deficient mice has been observed (Kabashima et al., 2002). Among the other mechanism proposed, PGE<sub>2</sub> mediates tissue repair and epithelial regeneration through the activation of the PI3K/Akt pathway and the Wnt cascade as well as the transactivation of epidermal growth factor receptor (EGFR) (Buchanan et al., 2003; Castellone et al., 2005). Interestingly, these mechanisms are also responsible for epithelial proliferation and colon cancer promotion suggesting a prominent role of PGE<sub>2</sub> in the colon tumorigenesis. This statement is supported by several researches using different animal models. Direct evidences showed that the administration

of PGE<sub>2</sub> in rats induces cellular proliferation and reduces apoptotic processes resulting in a marked increase in colon cancer incidence and multiplicity (Kawamori et al., 2003; Wang et al., 2005a). Furthermore, less production of PGE<sub>2</sub> due to genetic deletion of mPGES1 in *Apc*-mutant mice is associated with a persistent suppression of tumor growth (-66%) and adenomas formation (-95%) (Nakanishi et al., 2008). Along this line, Nakanishi et al. evaluated the impact of mPGES1 gene deletion in A/J mice which are more sensitive to colon carcinogenesis. mPGES1 KO mice showed a significant decrease in colon cancer multiplicity (-80%) and incidence (-90%) compared to wild type animals (Nakanishi et al., 2011). The data from all these studies converge on the consistent contribution of PGE<sub>2</sub> in inflammation as well as in promoting of pro-malignant microenvironment that leads to tumorigenic drift. Interestingly, COX-2 protein expression and PGE<sub>2</sub> release are markedly induced by S100B after enteric glia activation in pathological condition (Esposito et al., 2007; Cirillo et al., 2009). Hence, it can be assumed that PGE<sub>2</sub> act as glial mediator in modulating mucosal integrity and permeability by mediating a “leaky gut” condition that underlies the majority of gut pathologies, including inflammatory bowel disease and colon cancer. Nevertheless, evidences about the role of specific glial-derived PGE<sub>2</sub> because of the ubiquitous expression of the prostanoid. Although more investigations are necessary, targeting PGE<sub>2</sub> production by controlling mPGES1 or COX-2 expression and/or by modulating enteric glia activity may represent a promising strategy in the management of gut pathologies.

#### **1.4. Aim of the study**

The present research is focused on providing new insights in the pathophysiological functions of enteric glia identifying novel molecular target



for the intervention of gastrointestinal disorders. Specifically, we focused on the role of two different glial mediators: S100B and PGE<sub>2</sub>. S100B is a calcium-binding protein physiologically released by EGCs acting as neurotrophic factor. An aberrant production of S100B represents a key step in several intestinal diseases, including ulcerative colitis, celiac diseases and melanoma. However, evidences about the implication of S100B in colon cancer outcome are still missing. On the other hand, PGE<sub>2</sub> is a bioactive lipid belonging to prostanoid family exhibiting different actions in intestinal inflammation, tissue repair as well as colon cancer. Although the involvement of PGE<sub>2</sub> in the homeostasis and pathological conditions of gastrointestinal tract is well established, any investigations about PGE<sub>2</sub> as glial mediator have been reported yet.

In this scenario, the present study aimed to:

- i) elucidate the role of S100B in *ex vivo* culture of human colorectal cancer;
- ii) evaluate the impact of glial-derived PGE<sub>2</sub> on intestinal functions in both physiological and pathological conditions in mPGES1-S100B-deleted mice.

## 1.5. References

- Abdo H, Derkinderen P, Gomes P, Chevalier J, Aubert P, Masson D, Galmiche J-P, Vanden Berghe P, Neunlist M, Lardeux B. 2010. Enteric glial cells protect neurons from oxidative stress in part via reduced glutathione. *FASEB J* 24:1082–1094.
- Abdo H, Mahe MM, Derkinderen P, Bach-Ngohou K, Neunlist M, Lardeux B. 2012. The omega-6 fatty acid derivative 15-deoxy-Delta(1)(2),(1)(4)-prostaglandin J2 is involved in neuroprotection by enteric glial cells against oxidative stress. *J Physiol* 590:2739–2750.
- Adami C, Bianchi R, Pula G, Donato R. 2004. S100B-stimulated NO production by BV-2 microglia is independent of RAGE transducing activity but dependent on RAGE extracellular domain. *Biochim Biophys Acta* [Internet] 1742:169–77. Available from: <http://www.ncbi.nlm.nih.gov/pubmed/15590067>
- Andres R, Mayordomo JI, Zaballos P, Rodino J, Isla D, Escudero P, Elosegui L, Filipovich E, Saenz A, Polo E, Tres A. 2004. Prognostic value of serum S-100B in malignant melanoma. *Tumori* 90:607–610.
- Aoki E, Semba R, Kashiwamata S. 1991. Evidence for the presence of L-arginine in the glial components of the peripheral nervous system. *Brain Res* 559:159–162.
- Arcuri C, Giambanco I, Bianchi R, Donato R. 2002. Annexin V, annexin VI, S100A1 and S100B in developing and adult avian skeletal muscles. *Neuroscience* 109:371–388.
- Arrieta MC, Madsen K, Doyle J, Meddings J. 2009. Reducing small intestinal permeability attenuates colitis in the IL10 gene-deficient mouse. *Gut* 58:41–48.

- Aubé A, Cabarrocas J, Bauer J, Philippe D, Aubert P, Doulay F, Liblau R, Galmiche JP, Neunlist M. 2006. Changes in enteric neurone phenotype and intestinal functions in a transgenic mouse model of enteric glia disruption. *Gut*:630–638.
- Bach-Ngohou K, Mahe MM, Aubert P, Abdo H, Boni S, Bourreille A, Denis MG, Lardeux B, Neunlist M, Masson D. 2010. Enteric glia modulate epithelial cell proliferation and differentiation through 15-deoxy-12,14-prostaglandin J2. *J Physiol* 588:2533–2544.
- Barajon I, Serrao G, Arnaboldi F, Opizzi E, Ripamonti G, Balsari A, Rumio C. 2009. Toll-like receptors 3, 4, and 7 are expressed in the enteric nervous system and dorsal root ganglia. *J Histochem Cytochem* 57:1013–23.
- Bassotti G, Villanacci V, Nascimbeni R, Cadei M, Manenti S, Sabatino G, Maurer CA, Cathomas G, Salerni B. 2011. Colonic mast cells in controls and slow transit constipation patients. *Aliment Pharmacol Ther* 34:92–99.
- Bayliss WM, Starling EH. 1900. The movements and the innervation of the large intestine. *J Physiol* [Internet] 26:107–118. Available from: <http://www.ncbi.nlm.nih.gov/pmc/articles/PMC1540523/>
- Boesmans W, Lasrado R, Vanden Berghe P, Pachnis V. 2015. Heterogeneity and phenotypic plasticity of glial cells in the mammalian enteric nervous system. *Glia* 63:229–241.
- Boesmans W, Martens MA, Weltens N, Hao MM, Tack J, Cirillo C, Vanden Berghe P. 2013. Imaging neuron-glia interactions in the enteric nervous system. *Front Cell Neurosci* [Internet] 7:183. Available from: <http://www.ncbi.nlm.nih.gov/pmc/articles/PMC3801083/>
- Bohorquez D V, Samsa LA, Roholt A, Medicetty S, Chandra R, Liddle RA.

2014. An enteroendocrine cell-enteric glia connection revealed by 3D electron microscopy. *PloS one* 9:e89881.
- Bondurand N, Sham MH. 2013. The role of SOX10 during enteric nervous system development. *Develop Biol* [Internet] 382:330–343. Available from:  
<http://www.sciencedirect.com/science/article/pii/S0012160613002169>
- von Boyen G, Steinkamp M. 2006. The enteric glia and neurotrophic factors. *Z Gastroenterol* 44:985–990.
- von Boyen G, Steinkamp M. 2010. The role of enteric glia in gut inflammation. *Neuron Glia Biol* 6:231–236.
- von Boyen GBT, Schulte N, Pfluger C, Spaniol U, Hartmann C, Steinkamp M. 2011. Distribution of enteric glia and GDNF during gut inflammation. *BMC Gastroenterol* 11:3.
- von Boyen GBT, Steinkamp M, Reinshagen M, Schafer K-H, Adler G, Kirsch J. 2004. Proinflammatory cytokines increase glial fibrillary acidic protein expression in enteric glia. *Gut* 53:222–228.
- Bramanti V, Tomassoni D, Avitabile M, Amenta F, Avola R. 2010. Biomarkers of glial cell proliferation and differentiation in culture. *Front Biosci (Schol Ed)* 2:558–570.
- Braun N, Sevigny J, Robson SC, Hammer K, Hanani M, Zimmermann H. 2004. Association of the ecto-ATPase NTPDase2 with glial cells of the peripheral nervous system. *Glia* 45:124–132.
- Buchanan FG, Wang D, Bargiacchi F, DuBois RN. 2003. Prostaglandin E2 regulates cell migration via the intracellular activation of the epidermal growth factor receptor. *J Biol Chem* 278:35451–35457.
- Bush TG, Savidge TC, Freeman TC, Cox HJ, Campbell EA, Mucke L,

- Johnson MH, Sofroniew M V. 1998. Fulminant Jejuno-Ileitis following Ablation of Enteric Glia in Adult Transgenic Mice. *Cell* [Internet] 93:189–201. Available from:  
<http://www.sciencedirect.com/science/article/pii/S0092867400815718>
- Capoccia E, Cirillo C, Gigli S, Pesce M, D'Alessandro A, Cuomo R, Sarnelli G, Steardo L, Esposito G. 2015a. Enteric glia: A new player in inflammatory bowel diseases. *Int J Immunopathol Pharmacol* 28:443–51.
- Capoccia E, Cirillo C, Marchetto A, Tiberi S, Sawikr Y, Pesce M, D'Alessandro A, Scuderi C, Sarnelli G, Cuomo R, Steardo L, Esposito G. 2015b. S100B-p53 disengagement by pentamidine promotes apoptosis and inhibits cellular migration via aquaporin-4 and metalloproteinase-2 inhibition in C6 glioma cells. *Oncol Lett* [Internet] 9:2864–2870. Available from:  
<http://www.ncbi.nlm.nih.gov/pmc/articles/PMC4473713/>
- Castellone MD, Teramoto H, Williams BO, Druey KM, Gutkind JS. 2005. Prostaglandin E2 promotes colon cancer cell growth through a Gs-axin-beta-catenin signaling axis. *Science* 310:1504–1510.
- Cheadle GA, Costantini TW, Lopez N, Bansal V, Eliceiri BP, Coimbra R. 2013. Enteric glia cells attenuate cytomix-induced intestinal epithelial barrier breakdown. *PloS one* 8:e69042.
- Chow S-K, Yu D, Macdonald CL, Buibas M, Silva G a. 2010. Amyloid  $\beta$ -peptide directly induces spontaneous calcium transients, delayed intercellular calcium waves and gliosis in rat cortical astrocytes. *ASN neuro* [Internet] 2:e00026. Available from:  
<http://www.pubmedcentral.nih.gov/articlerender.fcgi?artid=2810812&tool=pmcentrez&rendertype=abstract>

- Cirillo C, Sarnelli G, Esposito G, Grosso M, Petruzzelli R, Izzo P, Calì G, D'Armiento FP, Rocco A, Nardone G, Iuvone T, Steardo L, Cuomo R. 2009. Increased mucosal nitric oxide production in ulcerative colitis is mediated in part by the enteroglial-derived S100B protein. *Neurogastroenterol Motil* 21:1209-e112.
- Cirillo C, Sarnelli G, Turco F, Mango A, Grosso M, Aprea G, Masone S, Cuomo R. 2011. Proinflammatory stimuli activates human-derived enteroglial cells and induces autocrine nitric oxide production. *Neurogastroenterol Motil* 23:e372-82.
- Cook RD, Burnstock G. 1976. The ultrastructure of Auerbach's plexus in the guinea-pig. II. Non-neuronal elements. *J Neurocytol* [Internet] 5:195–206. Available from: <https://doi.org/10.1007/BF01181656>
- Coquenlorge S, Van Landeghem L, Jaulin J, Cenac N, Vergnolle N, Duchalais E, Neunlist M, Rolli-Derkinderen M. 2016. The arachidonic acid metabolite 11 $\beta$ -ProstaglandinF2 $\alpha$  controls intestinal epithelial healing: deficiency in patients with Crohn's disease. *Sci Rep* [Internet] 6:25203. Available from: <http://dx.doi.org/10.1038/srep25203>
- Cornet A, Savidge TC, Cabarrocas J, Deng WL, Colombel JF, Lassmann H, Desreumaux P, Liblau RS. 2001. Enterocolitis induced by autoimmune targeting of enteric glial cells: a possible mechanism in Crohn's disease? *Proc Natl Acad Sci USA* [Internet] 98:13306–11. Available from: <http://www.pubmedcentral.nih.gov/articlerender.fcgi?artid=60866&tool=pmcentrez&rendertype=abstract>
- Costa M, Brookes S, Hennig G. 2000. Anatomy and physiology of the enteric nervous system. *Gut* [Internet] 47:iv15-iv19. Available from: <http://www.ncbi.nlm.nih.gov/pmc/articles/PMC1766806/>

- Costagliola A, Van Nassauw L, Snyders D, Adriaensen D, Timmermans J-P. 2009. Voltage-gated delayed rectifier K<sup>v</sup> 1-subunits may serve as distinctive markers for enteroglia cells with different phenotypes in the murine ileum. *Neurosci Lett* 461:80–84.
- da Cunha Franceschi R, Nardin P, Machado CV, Tortorelli LS, Martinez-Pereira MA, Zanotto C, Goncalves C-A, Zancan DM. 2017. Enteric glial reactivity to systemic LPS administration: Changes in GFAP and S100B protein. *Neurosci Res* 119:15–23.
- Delphin C, Ronjat M, Deloulme JC, Garin G, Debussche L, Higashimoto Y, Sakaguchi K, Baudier J. 1999. Calcium-dependent interaction of S100B with the C-terminal domain of the tumor suppressor p53. *J Biol Chem* 274:10539–10544.
- Devos D, Lebouvier T, Lardeux B, Biraud M, Rouaud T, Pouclet H, Coron E, Bruley des Varannes S, Naveilhan P, Nguyen J-M, Neunlist M, Derkinderen P. 2013. Colonic inflammation in Parkinson's disease. *Neurobiol Dis* 50:42–48.
- Dogiel AS. Über den bau der ganglien in den geflechten des darmes und der gallenblase des menschen und der säugetiere . *Arch Anat Physiol (Leipzig) Anat Abt Jg.* 1899:130–158.
- Van Eldik LJ, Griffin WS. 1994. S100 beta expression in Alzheimer's disease: relation to neuropathology in brain regions. *Biochim Biophys Acta* 1223:398–403.
- Esposito G, Capoccia E, Gigli S, Pesce M, Bruzzese E, Alessandro AD, Cirillo C, Cerbo A, Cuomo R, Steardo L, Sarnelli G. 2017. HIV-1 Tat-induced diarrhea evokes an enteric glia-dependent neuroinflammatory response in the central nervous system. *Sci Rep* 7:7735.
- Esposito G, Capoccia E, Turco F, Palumbo I, Lu J, Steardo A, Cuomo R,

- Sarnelli G, Steardo L. 2014. Palmitoylethanolamide improves colon inflammation through an enteric glia/toll like receptor 4-dependent PPAR- $\alpha$  activation. *Gut* 63:1300–12.
- Esposito G, Cirillo C, Sarnelli G, De Filippis D, D'Armiento FP, Rocco A, Nardone G, Petruzzelli R, Grosso M, Izzo P, Iuvone T, Cuomo R. 2007. Enteric glial-derived S100B protein stimulates nitric oxide production in celiac disease. *Gastroenterology* 133:918–25.
- Esposito G, De Filippis D, Cirillo C, Sarnelli G, Cuomo R, Iuvone T. 2006. The astroglial-derived S100beta protein stimulates the expression of nitric oxide synthase in rodent macrophages through p38 MAP kinase activation. *Life Sci* 78:2707–2715.
- Fernandez-Fernandez MR, Rutherford TJ, Fersht AR. 2008. Members of the S100 family bind p53 in two distinct ways. *Protein Sci [Internet]* 17:1663–1670. Available from: <http://www.ncbi.nlm.nih.gov/pmc/articles/PMC2548378/>
- Flamant M, Aubert P, Rolli-Derkinderen M, Bourreille A, Neunlist MR, Mahe MM, Meurette G, Marteyn B, Savidge T, Galmiche JP, Sansonetti PJ, Neunlist M. 2011. Enteric glia protect against *Shigella flexneri* invasion in intestinal epithelial cells: a role for S-nitrosoglutathione. *Gut* 60:473–484.
- Fletcher EL, Clark MJ, Furness JB. 2002. Neuronal and glial localization of GABA transporter immunoreactivity in the myenteric plexus. *Cell Tissue Res* 308:339–346.
- Furness JB, Clerc N, Vogalis F, Stebbing MJ. The enteric nervous system and its extrinsic connections. In: Yamada T, Alpers DH, eds. *Textbook of Gastroenterology*. Philadelphia: Lippincot Williams, 2003: 12–34
- Furness JB. 2012. The enteric nervous system and. *Nat Rev Gastroenterol*



- HepatoJ [Internet] 9:286–294. Available from:  
<http://dx.doi.org/10.1038/nrgastro.2012.32>
- Gabella G. 1972. Fine structure of the myenteric plexus in the guinea-pig ileum. *J Anat* 111:69–97.
- Gabella G. 1981. Ultrastructure of the nerve plexuses of the mammalian intestine: the enteric glial cells. *Neuroscience* 6:425–436.
- Gabella G. 1984. Size of neurons and glial cells in the intramural ganglia of the hypertrophic intestine of the guinea-pig. *J Neurocytol* 13:73–84.
- Gabella G. 1990. On the plasticity of form and structure of enteric ganglia. *J Auton Nerv Syst* 30 Suppl:S59-66.
- Garcia SB, Stopper H, Kannen V. 2014. The contribution of neuronal-glial-endothelial-epithelial interactions to colon carcinogenesis. *Cell Mol Life Sci* 71:3191–3197.
- Garrido R, Segura B, Zhang W, Mulholland M. 2002. Presence of functionally active protease-activated receptors 1 and 2 in myenteric glia. *J Neurochem* [Internet] 83:556–564. Available from:  
<https://doi.org/10.1046/j.1471-4159.2002.01119.x>
- Gershon MD. 1999. The Enteric Nervous System : A Second Brain The Enteric Nervous System : A Second Brain. *Hosp Pract* 34:31–52.
- Gershon MD, Rothman TP. 1991. Enteric glia. *Glia* 4:195–204.
- Gomes P, Chevalier J, Boesmans W, Roosen L, van den Abbeel V, Neunlist M, Tack J, Vanden Berghe P. 2009. ATP-dependent paracrine communication between enteric neurons and glia in a primary cell culture derived from embryonic mice. *Neurogastroenterol Motil* 21:870-e62.

- Griffin WSUET, Stanley LC, Ling C, White L, Macleod V, Perrot LJ, Iii CLW, Araoz C. 1989. Brain interleukin 1 and S-100 immunoreactivity are elevated in Down syndrome and Alzheimer disease. *Proc Natl Acad Sci USA* 86:7611–7615.
- Grubisic V, Gulbransen BD. 2017. Enteric glial activity regulates secretomotor function in the mouse colon but does not acutely affect gut permeability. *J Physiol* 595:3409–3424.
- Grundy D, Schemann M. 2007. Enteric nervous system. *Curr Opin Gastroenterol* 23:121–126.
- Gulbransen BD, Sharkey KA. 2009. Purinergic neuron-to-glia signaling in the enteric nervous system. *Gastroenterology* 136:1349–1358.
- Gulbransen BD, Sharkey KA. 2012. Novel functional roles for enteric glia in the gastrointestinal tract. *Nat Rev Gastroenterol Hepatol* 9:625–632.
- Hachem S, Aguirre A, Vives V, Marks A, Gallo V, Legraverend C. 2005. Spatial and temporal expression of S100B in cells of oligodendrocyte lineage. *Glia* 51:81–97.
- Hanani M, Francke M, Hartig W, Grosche J, Reichenbach A, Pannicke T. 2000. Patch-clamp study of neurons and glial cells in isolated myenteric ganglia. *Am J Physiol Gastrointest Liver Physiol* 278:G644-51.
- Hanani M, Reichenbach A. 1994. Morphology of horseradish peroxidase (HRP)-injected glial cells in the myenteric plexus of the guinea-pig. *Cell Tissue Res* 278:153–160.
- Hara S, Kamei D, Sasaki Y, Tanemoto A, Nakatani Y, Murakami M. 2010. Prostaglandin E synthases: Understanding their pathophysiological roles through mouse genetic models. *Biochimie* 92:651–659.
- Heizmann CW, Fritz G, Schafer BW. 2002. S100 proteins: structure,

functions and pathology. *Front Biosci* 7:d1356-68.

- Hirata I, Austin LL, Blackwell WH, Weber JR, Dobbins WO. 1986. Immunoelectron microscopic localization of HLA-DR antigen in control small intestine and colon and in inflammatory bowel disease. *Dig Dis Sci* [Internet] 31:1317–1330. Available from: <https://doi.org/10.1007/BF01299810>
- Hoehner JC, Wester T, Pahlman S, Olsen L. 1996. Localization of neurotrophins and their high-affinity receptors during human enteric nervous system development. *Gastroenterology* 110:756–767.
- Hoff S, Zeller F, von Weyhern CWH, Wegner M, Schemann M, Michel K, Ruhl A. 2008. Quantitative assessment of glial cells in the human and guinea pig enteric nervous system with an anti-Sox8/9/10 antibody. *J Comp Neurol* 509:356–371.
- Hollenbach E, Ruhl A, Zoller M, Stremmel W. 2000. T cell activation by enteric glia - A novel pathway for the amplification of inflammatory responses in the enteric nervous system (ENS). *Gastroenterology* [Internet] 118:A184–A185. Available from: [https://doi.org/10.1016/S0016-5085\(00\)82813-9](https://doi.org/10.1016/S0016-5085(00)82813-9)
- Hoyle CH, Burnstock G. 1989. Neuronal populations in the submucous plexus of the human colon. *J Anat* [Internet] 166:7–22. Available from: <http://www.ncbi.nlm.nih.gov/pmc/articles/PMC1256735/>
- Huang M-Y, Wang H-M, Chang H-J, Hsiao C-P, Wang J-Y, Lin S-R. 2012. Overexpression of S100B, TM4SF4, and OLFM4 Genes Is Correlated with Liver Metastasis in Taiwanese Colorectal Cancer Patients. *DNA Cell Biol* [Internet] 31:43–49. Available from: <http://www.ncbi.nlm.nih.gov/pmc/articles/PMC3246415/>
- Hwang C-C, Chai H-T, Chen H-W, Tsai H-L, Lu C-Y, Yu F-J, Huang M-Y,

- Wang J-Y. 2011. S100B protein expressions as an independent predictor of early relapse in UICC stages II and III colon cancer patients after curative resection. *Ann Surg Oncol* [Internet] 18:139–145. Available from: <http://europepmc.org/abstract/MED/20628824>
- Jakobsson PJ, Thoren S, Morgenstern R, Samuelsson B. 1999. Identification of human prostaglandin E synthase: a microsomal, glutathione-dependent, inducible enzyme, constituting a potential novel drug target. *Proc Natl Acad Sci USA* 96:7220–7225.
- Jessen KR, Mirsky R. 1980. Glial cells in the enteric nervous system contain glial fibrillary acidic protein. *Nature* [Internet] 286:736. Available from: <http://dx.doi.org/10.1038/286736a0>
- Jessen KR, Mirsky R. 1983. Astrocyte-like glia in the peripheral nervous system: an immunohistochemical study of enteric glia. *J Neurosci* 3:2206–2218.
- Jessen KR, Mirsky R. 1985. Glial fibrillary acidic polypeptides in peripheral glia. *J Neuroimmunol* [Internet] 8:377–393. Available from: [https://doi.org/10.1016/S0165-5728\(85\)80074-6](https://doi.org/10.1016/S0165-5728(85)80074-6)
- Joseph NM, He S, Quintana E, Kim Y-G, Núñez G, Morrison SJ. 2011. Enteric glia are multipotent in culture but primarily form glia in the adult rodent gut. *J Clin Invest* [Internet] 121:3398–3411. Available from: <https://doi.org/10.1172/JCI58186>
- Kabashima K, Saji T, Murata T, Nagamachi M, Matsuoka T, Segi E, Tsuboi K, Sugimoto Y, Kobayashi T, Miyachi Y, Ichikawa A, Narumiya S. 2002. The prostaglandin receptor EP4 suppresses colitis, mucosal damage and CD4 cell activation in the gut. *J Clin Invest* 109:883–893.
- Kalinski P. 2012. Regulation of immune responses by prostaglandin E2. *J Immunol* 188:21–28.

- Kato H, Yamamoto T, Yamamoto H, Ohi R, So N, Iwasaki Y. 1990. Immunocytochemical characterization of supporting cells in the enteric nervous system in Hirschsprung's disease. *J Pediatr Surg* 25:514–519.
- Kawamori T, Uchiya N, Sugimura T, Wakabayashi K. 2003. Enhancement of colon carcinogenesis by prostaglandin E2 administration. *Carcinogenesis* 24:985–990.
- Kelsh RN. 2006. Sorting out Sox10 functions in neural crest development. *BioEssays* 28:788–798.
- Kimball BC, Mulholland MW. 1996. Enteric glia exhibit P2U receptors that increase cytosolic calcium by a phospholipase C-dependent mechanism. *J Neurochem* 66:604–612.
- Koretz K, Momburg F, Otto HF, Möller P. 1987. Sequential induction of MHC antigens on autochthonous cells of ileum affected by Crohn's disease. *Am J Pathol* [Internet] 129:493–502. Available from: <http://www.ncbi.nlm.nih.gov/pmc/articles/PMC1899812/>
- Van Landeghem L, Chevalier J, Mahe MM, Wedel T, Urvil P, Derkinderen P, Savidge T, Neunlist M. 2011. Enteric glia promote intestinal mucosal healing via activation of focal adhesion kinase and release of proEGF. *Am J Physiol Gastrointest Liver Physiol* 300:G976-87.
- Van Landeghem L, Mahé MM, Teusan R, Léger J, Guisle I, Houlgatte R, Neunlist M. 2009. Regulation of intestinal epithelial cells transcriptome by enteric glial cells: impact on intestinal epithelial barrier functions. *BMC Genomics* 10:507.
- Langley JN, Magnus R. 1905. Some observations of the movements of the intestine before and after degenerative section of the mesenteric nerves. *J Physiol* 33:34–51.

- Lavoie EG, Gulbransen BD, Martin-Satue M, Aliagas E, Sharkey KA, Sevigny J. 2011. Ectonucleotidases in the digestive system: focus on NTPDase3 localization. *Am J Physiol Gastrointest Liver Physiol* 300:G608-20.
- Lin J, Yang Q, Yan Z, Markowitz J, Wilder PT, Carrier F, Weber DJ. 2004. Inhibiting S100B restores p53 levels in primary malignant melanoma cancer cells. *J Biol Chem* 279:34071–34077.
- Liu YA, Chung YC, Pan ST, Shen MY, Hou YC, Peng SJ, Pasricha PJ, Tang SC. 2013. 3-D imaging, illustration, and quantitation of enteric glial network in transparent human colon mucosa. *Neurogastroenterol Motil* 25:e324-38.
- Lomax a E, Fernández E, Sharkey K a. 2005. Plasticity of the enteric nervous system during intestinal inflammation. *Neurogastroenterology and motility : the official journal of the European Gastrointestinal Motility Society* [Internet] 17:4–15. Available from: <http://www.ncbi.nlm.nih.gov/pubmed/15670258>
- MacEachern SJ, Patel BA, McKay DM, Sharkey KA. 2011. Nitric oxide regulation of colonic epithelial ion transport: a novel role for enteric glia in the myenteric plexus. *J Physiol* 589:3333–3348.
- Marshak DR. 1990. S100 beta as a neurotrophic factor. *Prog Brain Res* 86:169–181.
- Martinet L, Jean C, Dietrich G, Fournié J-J, Poupot R. 2010. PGE2 inhibits natural killer and  $\gamma\delta$  T cell cytotoxicity triggered by NKR and TCR through a cAMP-mediated PKA type I-dependent signaling. *Biochem Pharmacol* [Internet] 80:838–845. Available from: <http://www.sciencedirect.com/science/article/pii/S0006295210003412>
- McClain J, Grubisic V, Fried D, Gomez-Suarez RA, Leininger GM,

- Sevigny J, Parpura V, Gulbransen BD. 2014. Ca<sup>2+</sup> responses in enteric glia are mediated by connexin-43 hemichannels and modulate colonic transit in mice. *Gastroenterology* 146:497–507.e1.
- McClain JL, Fried DE, Gulbransen BD. 2015. Agonist-Evoked Ca<sup>2+</sup> Signaling in Enteric Glia Drives Neural Programs That Regulate Intestinal Motility in Mice. *Cell Mol Gastroenterol Hepatol* [Internet] 1:631–645. Available from: <http://www.ncbi.nlm.nih.gov/pmc/articles/PMC4673674/>
- Murakami M, Naraba H, Tanioka T, Semmyo N, Nakatani Y, Kojima F, Ikeda T, Fueki M, Ueno A, Oh S, Kudo I. 2000. Regulation of prostaglandin E2 biosynthesis by inducible membrane-associated prostaglandin E2 synthase that acts in concert with cyclooxygenase-2. *J Biol Chem* 275:32783–32792.
- Muthuswamy R, Mueller-Berghaus J, Haberkorn U, Reinhart TA, Schadendorf D, Kalinski P. 2010. PGE(2) transiently enhances DC expression of CCR7 but inhibits the ability of DCs to produce CCL19 and attract naive T cells. *Blood* 116:1454–1459.
- Nagahama M, Semba R, Tsuzuki M, Aoki E. 2001. L-arginine immunoreactive enteric glial cells in the enteric nervous system of rat ileum. *Biol Signals Recept* 10:336–340.
- Nakanishi M, Menoret A, Tanaka T, Miyamoto S, Montrose DC, Vella AT, Rosenberg DW. 2011. Selective PGE(2) suppression inhibits colon carcinogenesis and modifies local mucosal immunity. *Cancer Prev Res (Phila)* 4:1198–1208.
- Nakanishi M, Montrose DC, Clark P, Nambiar PR, Belinsky GS, Claffey KP, Xu D, Rosenberg DW. 2008. Genetic deletion of mPGES1 suppresses intestinal tumorigenesis. *Cancer Res* 68:3251–3259.

- Nasser Y, Ho W, Sharkey KA. 2006. Distribution of adrenergic receptors in the enteric nervous system of the guinea pig, mouse, and rat. *J Comp Neurol* 495:529–553.
- Nasser Y, Keenan CM, Ma AC, McCafferty D-M, Sharkey KA. 2007. Expression of a functional metabotropic glutamate receptor 5 on enteric glia is altered in states of inflammation. *Glia* [Internet] 55:859–872. Available from: <https://doi.org/10.1002/glia.20507>
- Neunlist M, Aubert P, Bonnaud S, Van Landeghem L, Coron E, Wedel T, Naveilhan P, Ruhl A, Lardeux B, Savidge T, Paris F, Galmiche JP. 2007. Enteric glia inhibit intestinal epithelial cell proliferation partly through a TGF-beta1-dependent pathway. *Am J Physiol Gastrointest Liver Physiol* 292:G231-41.
- Neunlist M, Van Landeghem L, Mahe MM, Derkinderen P, des Varannes SB, Rolli-Derkinderen M. 2013. The digestive neuronal-glia-epithelial unit: a new actor in gut health and disease. *Nat Rev Gastroenterol Hepatol* 10:90–100.
- Pochard C, Coquenlorge S, Jaulin J, Cenac N, Vergnolle N, Meurette G, Freyssinet M, Neunlist M, Rolli-Derkinderen M. 2016. Defects in 15-HETE Production and Control of Epithelial Permeability by Human Enteric Glial Cells From Patients With Crohn’s Disease. *Gastroenterology* 150:168–180.
- Quante M, Varga J, Wang TC, Greten FR. 2013. The gastrointestinal tumor microenvironment. *Gastroenterology* 145:63–78.
- Rao M, Rastelli D, Dong L, Chiu S, Setlik W, Gershon MD, Corfas G. 2017. Enteric Glia Regulate Gastrointestinal Motility but Are Not Required for Maintenance of the Epithelium in Mice. *Gastroenterology* [Internet] 153:1068–1081.e7. Available from:



<https://doi.org/10.1053/j.gastro.2017.07.002>

Rehn M, Hubschle T, Diener M. 2004. TNF-alpha hyperpolarizes membrane potential and potentiates the response to nicotinic receptor stimulation in cultured rat myenteric neurones. *Acta Physiol Scand* 181:13–22.

Rosenbaum C, Schick MA, Wollborn J, Heider A, Scholz C-J, Cecil A, Niesler B, Hirrlinger J, Walles H, Metzger M. 2016. Activation of Myenteric Glia during Acute Inflammation In Vitro and In Vivo. *PLoS one* 11:e0151335.

Rühl A. 2005. Glial cells in the gut. *Neurogastroenterol Motil* [Internet] 17:777–790. Available from: <https://doi.org/10.1111/j.1365-2982.2005.00687.x>

Ruhl A, Franzke S, Collins SM, Stremmel W. 2001. Interleukin-6 expression and regulation in rat enteric glial cells. *Am J Physiol Gastrointest Liver Physiol* 280:G1163-71.

Rühl A, Hoppe S, Frey I, Daniel H, Schemann M. 2005. Functional expression of the peptide transporter PEPT2 in the mammalian enteric nervous system. *J Comp Neurol* [Internet] 490:1–11. Available from: <https://doi.org/10.1002/cne.20617>

Savidge TC, Newman P, Pothoulakis C, Ruhl A, Neunlist M, Bourreille A, Hurst R, Sofroniew M V. 2007. Enteric glia regulate intestinal barrier function and inflammation via release of S-nitrosoglutathione. *Gastroenterology* 132:1344–58.

Schmidt AM, Yan S Du, Yan SF, Stern DM. 2001. Multiligand receptors The multiligand receptor RAGE as a progression factor amplifying immune and inflammatory responses. *J Clin Invest* 108:949–955.

Segura BJ, Zhang W, Cowles RA, Xiao L, Lin TR, Logsdon C, Mulholland

- MW. 2004. Lysophosphatidic acid stimulates calcium transients in enteric glia. *Neuroscience* 123:687–693.
- Selinfreund RH, Barger SW, Pledger WJ, Van Eldik LJ. 1991. Neurotrophic protein S100 beta stimulates glial cell proliferation. *Proc Natl Acad Sci USA* [Internet] 88:3554–3558. Available from: <http://www.ncbi.nlm.nih.gov/pmc/articles/PMC51490/>
- da Silveira ABM, de Oliveira EC, Neto SG, Luquetti AO, Fujiwara RT, Oliveira RC, Brehmer A. 2011. Enteroglial cells act as antigen-presenting cells in chagasic megacolon. *Hum Pathol* 42:522–532.
- Stenkamp-Strahm CM, Kappmeyer AJ, Schmalz JT, Gericke M, Balemba O. 2013. High-fat diet ingestion correlates with neuropathy in the duodenum myenteric plexus of obese mice with symptoms of type 2 diabetes. *Cell Tissue Res* 354:381–394.
- Stohr PJ. 1952. Synopsis of research results on the microscopic innervation of the gastrointestinal tract. *Ergeb Anat Entwicklungsgesch* 34:250–401.
- Timmermans J, Hens J, Adriaensen D. 2001. Outer Submucous Plexus : An Intrinsic Nerve Network Involved in Both Secretory and Motility Processes in the Intestine of Large. 78:71–78.
- Tjwa ET, Bradley JM, Keenan CM, Kroese ABA, Sharkey KA. 2003. Interleukin-1beta activates specific populations of enteric neurons and enteric glia in the guinea pig ileum and colon. *Am J Physiol Gastrointest Liver Physiol* 1:1268–1276.
- Trendelenburg P. 1917. Physiologische und pharmakologische Versuche uber die Dunndarmperistaltik", *Arch. Exp. Pathol. Pharmacol.* 81, 55-129, 1917. Naunyn Schmiedebergs *Arch Pharmacol*:55–129.

- Vanderwinden J-M, Timmermans J-P, Schiffmann SN. 2003. Glial cells, but not interstitial cells, express P2X7, an ionotropic purinergic receptor, in rat gastrointestinal musculature. *Cell Tissue Res* [Internet] 312:149–154. Available from: <https://doi.org/10.1007/s00441-003-0716-2>
- Wang D, Buchanan FG, Wang H, Dey SK, DuBois RN. 2005a. Prostaglandin E2 enhances intestinal adenoma growth via activation of the Ras-mitogen-activated protein kinase cascade. *Cancer Res* 65:1822–1829.
- Wang D, Dubois RN. 2006. Prostaglandins and cancer. *Gut* 55:115–122.
- Wang D, Mann JR, DuBois RN. 2005b. The role of prostaglandins and other eicosanoids in the gastrointestinal tract. *Gastroenterology* 128:1445–1461.
- Wedel T, Busing V, Heinrichs G, Nohroudi K, Bruch H-P, Roblick UJ, Bottner M. 2010. Diverticular disease is associated with an enteric neuropathy as revealed by morphometric analysis. *Neurogastroenterol Motil* 22:407–14, e93-4.
- Weide B, Elsässer M, Büttner P, Pflugfelder A, Leiter U, Eigentler TK, Bauer J, Witte M, Meier F, Garbe C. 2012. Serum markers lactate dehydrogenase and S100B predict independently disease outcome in melanoma patients with distant metastasis. *Br J Cancer* [Internet] 107:422. Available from: <http://dx.doi.org/10.1038/bjc.2012.306>
- Wynn G, Ma B, Ruan HZ, Burnstock G. 2004. Purinergic component of mechanosensory transduction is increased in a rat model of colitis. *Am J Physiol Gastrointest Liver Physiol* 287:G647-57.
- Xiao W-D, Chen W, Sun L-H, Wang W-S, Zhou S-W, Yang H. 2011. The protective effect of enteric glial cells on intestinal epithelial barrier function is enhanced by inhibiting inducible nitric oxide synthase activity under lipopolysaccharide stimulation. *Mol Cell Neurosci*

46:527–534.

Zhang DK, He FQ, Li TK, Pang XH, Cui DJ, Xie Q, Huang XL. 2010. Glial-derived neurotrophic factor regulates intestinal epithelial barrier function and inflammation and is therapeutic for murine. *J Pathol*:213–222.

Zhang W, Segura BJ, Lin TR, Hu Y, Mulholland MW. 2003. Intercellular calcium waves in cultured enteric glia from neonatal guinea pig. *Glia* [Internet] 42:252–262. Available from:  
<https://doi.org/10.1002/glia.10215>

Zimmer DB, Chaplin J, Baldwin A, Rast M. 2005. S100-mediated signal transduction in the nervous system and neurological diseases. *Cell Mol Biol*:201–214.

Zimmer DB, Cornwall EH, Landar A, Song W. 1995. The S100 protein family: history, function, and expression. *Brain Res Bull* 37:417–429.

# Chapter 2

## THE ROLE OF S100B ON HUMAN COLON CANCER

---

### 2.1 Introduction

Colorectal cancer (CRC) is the third most common cancer in men and the second in women throughout the world (Ferlay et al., 2015; Aran et al., 2016). Almost 55% of colorectal cancer cases occurred in more developed countries representing one of the leading cause of malignancy worldwide (Marley and Nan, 2016). Elegant reports, over the past decades, have recognized that accumulating genetic mutations in epithelial stem cells are crucial in the multi-step cascade of events leading to colon carcinogenesis (Barker et al., 2009; Zeki et al., 2011). Interestingly, an increased incidence of colon adenocarcinoma has been observed in patients affected by inflammatory bowel diseases, such as ulcerative colitis, suggesting that an intestinal long-standing state of inflammation may be an agent of epithelial cell mutations leading to CRC (Freeman, 2008; Jess et al., 2012). Actually, it has been recognized that the production of reactive oxygen species (ROS) during chronic inflammation is able to induce genetic mutations, that may be repaired by p53-dependent cell cycle checkpoint, preventing the replication of mutated cells. From these perspectives, the overwhelming genomic instability promoted by chronic inflammatory states and able to exceed the control of p53 protein, appears to be the fundamental step in the progression of colonic neoplastic lesions (Schwitalla et al., 2013).

In this composite scenario, among the cellular populations composing the enteric nervous system (ENS), the enteric glial cells (EGCs) has been recently

discovered as a key cellular element in the gut homeostasis maintenance as well as in the triggering and perpetuating of gut inflammation, intestinal barrier permeability and epithelial cells proliferation (Cornet et al., 2001; Aubé et al., 2006; Neunlist et al., 2007; Capoccia et al., 2015). In particular, EGCs react to different external stimuli acting as antigen-presenting cells (APC) and thus releasing specific signaling molecules and cytokines. Among these factors, S100B belongs to a multigene family of diffusible  $\text{Ca}^{+2}/\text{Zn}^{+2}$ -binding proteins and it is physiologically and specifically expressed by EGCs in the gut (Esposito et al., 2007; Cirillo et al., 2009, 2011b). S100B represents an intriguing glial mediator because of its dual activity in mediating inflammation and cellular proliferation. Indeed, at micromolar concentration, S100B accumulates at the level of Receptor for Advanced Glycation End products (RAGE) and activates RAGE/NF- $\kappa$ B pathway that is accompanied by ROS production. Downstream the protooncogene NF- $\kappa$ B can move in the nucleus promoting the transcription of proinflammatory cytokines (including IL-6) and mediators (iNOS and COX-2) which are crucial in the inflammatory response but also in the pathogenesis of colorectal cancer (Heizmann et al., 2002; Romano et al., 2016). Additionally, S100B is able to inhibit the activity of tumor suppressor p53 protein (Lin et al., 2001). In fact, S100B binds p53 through a protein-protein interaction forming a complex that prevents p53 tetramer formation and, consequently, its transcriptional activity aimed at regulating cell cycle (Delphin et al., 1999; Fernandez-Fernandez et al., 2008). The final proliferative effect contributes importantly to carcinogenic process, as already seen in melanoma (Lin et al., 2004, 2010; Yoshimura et al., 2013). Starting from this background, it can be assumed that S100B may be a promising molecular target in the treatment of colorectal cancer. Indeed, it is already used as biomarker in the diagnosis and prognosis of melanoma and its involvement in other malignancies is under study. Nevertheless, evidences about the contribution of S100B in the colon cancer outbreak are still missing.

Therefore, we aimed at investigating the role of entero-glial derived S100B protein in ex vivo culture of human colon cancer providing information about the S100B/p53 interaction as potential therapeutic strategy for the treatment of the pathology.

## **2.2 Materials and Methods**

### **Experimental Design**

Biopsy specimens of peritumoral and tumoral areas from 8 patients diagnosed with colon cancer (5 women; mean age 47 years) has been used for the experiments. None of the patients had familiar history of colon cancer, hence all the cancers were considered as sporadic. Patients were diagnosed with left (3 patients, 1 woman) and sigmoid (5 patients, 4 women) sporadic colon cancer with no evidence of lymph nodes or distant metastasis and/or local invasion at pre-operative staging (T1 or T2, N0, M0). As positive controls, we collected four mucosal biopsies from the recto-sigmoid region of 8 patients with diagnosed UC (5 women; mean age 47 years) undergoing colonoscopy for relapse of rectal bleeding. All patients had proven histological diagnosis of UC with a MAYO 2 score at endoscopy and none of them had dysplastic modifications at routine histopathological examination. Four recto-sigmoid biopsies from 8 otherwise control subjects (2 women; mean age 50 years) undergoing colonoscopy for colon cancer screening, served as controls.

Human colonic specimens were used for the experiments and were divided in the 4 groups, as follows: 1) control group comprising colonic specimens collected from 8 control undergoing colonoscopy for colon cancer screening (2 women; mean age 50 years); 2) peritumoral group comprising surgical specimens of peritumoral areas collected from 8 patients diagnosed with colon cancer (5 women; mean age 47 years); 3) UC group comprising surgical colonic specimens collected from 8 patients diagnosed with ulcerative colitis, (5 women; mean age 47 years); 4) tumoral group comprising surgical specimens of tumoral areas collected from 8 patients diagnosed with colon cancer (5 women; mean age 47 years). All patients received and signed an



informed consent and all procedures were approved by the ethical committee of the University of Naples “Federico II”.

Surgical specimens were cut in thin slices (400  $\mu\text{m}$ ) using a Vibratome VT1200 (Leica Microsystem) to get organotypic culture in according to the procedure described by Vaira et al (Vaira et al., 2010). Specimens were rapidly washed in ice-cold sterile 1X PBS, orientated and immobilized using cyanoacrylate glue. Slicing speed was optimized depending on tissue type and density: 0.03-0.08 mm/s for inflamed tissue and 0.01-0.08 mm/s for normal tissue. Vibration amplitude was set at 2.95-3.00 mm. Then slices were cultured on specific organotypic inserts with FBS-supplemented Dulbecco Modified Eagle’s Medium (DMEM) at 37°C in 5% CO<sub>2</sub>/95% for 24h. In another set of experiments, control group whole-mount specimens were exposed to S100B at increasing concentrations (0.005, 0.05, 0.5 and 5  $\mu\text{M}$ ). At the end of experiments, surnatants were collected and specimens were homogenized to perform biochemical analysis as described below.

## **Western Blot**

Whole-mount specimens were homogenized in ice-cold hypotonic lysis buffer to obtain cytosolic extracts; thus, protein concentration was determined using Bio-Rad protein assay kit (Bio-Rad, Milan, Italy). Equivalent amounts (50  $\mu\text{g}$ ) of each homogenate underwent electrophoresis through a polyacrilamide minigel. Proteins were transferred onto nitrocellulose membrane that were saturated with non-fat dry milk and then incubated with either mouse anti-S100B (Neo-Marker, Milan, Italy), mouse anti-iNOS, rabbit anti-COX2, rabbit anti-RAGE, mouse anti-PCNA, rabbit anti-Bax, rabbit anti-p53<sup>wt</sup> (all Abcam, Cambridge, UK), rabbit anti-total p38 MAPK, rabbit anti-phospho p38 MAPK (all Cell Signaling Technology, Euroclone, Pero, Milan, Italy), mouse anti- $\beta$ -actin (Santa Cruz Biotechnology, Santa Cruz, California,

USA). Membranes were then incubated with the specific secondary antibodies conjugated to horseradish peroxidase (HRP) (Dako, Milan, Italy). Immune complexes were revealed by enhanced chemiluminescence detection reagents (Amersham Biosciences, Milan, Italy). Blots were analyzed by scanning densitometry (GS-700 imaging densitometer; Bio-Rad). Results were expressed as OD (arbitrary units; mm<sup>2</sup>) and normalized on the expression of the housekeeping protein  $\beta$ -actin.

### **Electrophoretic mobility shift assay (EMSA)**

EMSA was performed to detect NF- $\kappa$ B activation in nuclear extracts of whole-mount specimens. Double stranded oligonucleotides containing the NF-kappaB recognition sequence for (5': AGTTGAGGGGACTTTCCCAGCC) were end-labelled with <sup>32</sup>P $\gamma$ -ATP. Nuclear extracts were incubated for 15 min with radiolabeled oligonucleotides (2.5–5.0 x 10<sup>4</sup> cpm) in 20 ml reaction buffer containing 2 mg poly dI-dC, 10 mM Tris-HCl (pH 7.5), 100 mM NaCl, 1 mM EDTA, 1 mM dl-dithiothreitol, 1 mg/ml bovine serum albumin, 10% (v/v) glycerol. Nuclear protein-oligonucleotide complexes were resolved by electrophoresis on a 6% non-denaturing polyacrylamide gel in 1 Tris Borate EDTA buffer at 150 V for 2 hrs at 4°C. The gel was dried and autoradiographed with an intensifying screen at -80°C for 20 hrs. Subsequently, the relative bands were quantified by densitometric scanning with Versadoc (Bio-Rad Laboratories) and a computer software (Quantity One Software, Bio-Rad Laboratories). <sup>32</sup>P $\gamma$ -ATP was from Amersham (Milan, Italy). Poly dI-dC was from Boehringer-Mannheim (Milan, Italy). Oligonucleotide synthesis was performed to our specifications by Tib Molbiol (Boehringer-Mannheim).

## **NO quantification**

NO was measured as nitrite ( $\text{NO}_2^-$ ) accumulation in human biopsies supernatants by a spectrophotometer assay based on the Griess reaction (Di Rosa et al., 1990). Briefly, Griess reagent (1% sulphanilamide, 0.1% naphthylethylenediamine in  $\text{H}_3\text{PO}_4$ ) was added to an equal volume of supernatant and the absorbance was measured at 550 nm. Nitrite concentration (nM) was thus determined using a standard curve of  $\text{NaNO}_2$ .

## **Myeloperoxidase assay**

Myeloperoxidase (MPO), a marker of polymorphonuclear leukocyte accumulation and general inflammation occurring in colonic tissues, was determined as previously described (Cassini-Vieira et al., 2015). After removal, human colonic tissues were rinsed with a cold saline solution, opened and deprived of the mucosa using a glass slide. The resulting layer was then homogenized in a solution containing 0.5% hexadecyltrimethylammonium bromide (Sigma-Aldrich) dissolved in 10 mM potassium phosphate buffer and centrifuged for 30 min at  $20\,000\times g$  at  $37^\circ\text{C}$ . An aliquot of the supernatant was mixed with a solution of tetramethylbenzidine (1.6 mM; Sigma-Aldrich) and 0.1 mM hydrogen peroxide (Sigma-Aldrich). The absorbance was then spectrophotometrically measured at 650 nm. MPO activity was determined as the amount of enzyme degrading 1 mmol/min of peroxide at  $37^\circ\text{C}$  and was expressed in milliunits per 100 mg of wet tissue weight.

## **Lipid peroxidation assay**

Malonyl dialdehyde (MDA) was measured by the thiobarbituric acid colorimetric assay in human biopsies supernatants. Briefly, 1 mL 10% (w/v) trichloroacetic acid was added to 450  $\mu$ l of tissue lysate. After centrifugation, 1.3 mL 0.5% (w/v) thiobarbituric acid was added and the mixture was heated at 80°C for 20 min. After cooling, MDA formation was recorded (absorbance 530 nm and absorbance 550 nm) in a Perkin Elmer (Waltham, Massachusetts, USA) spectrofluorimeter and the results were presented as ng MDA/mL.

## **Enzyme-linked immunosorbent assay**

Enzyme-linked immunosorbent assay (ELISA) for S100B and PGE<sub>2</sub> (Biovendor R&D, Brno, Czech Republic) was carried out on human biopsies supernatants according to the manufacturer's protocol. Absorbance was measured on a microtitre plate reader. S100B levels were determined using standard curves method.

## **Statistical analysis**

Results were expressed as mean  $\pm$  SEM of experiments. Statistical analysis was performed using parametric one-way analysis of variance (ANOVA) and multiple comparisons were performed by Bonferroni's post hoc test. p values <0.05 were considered significant.

## 2.3 Results

### **Basal level of S100B and the relative RAGE/NF- $\kappa$ B pathway activation increase with the severity of lesions**

S100B protein expression and release were significantly higher in colon cancer specimens than control groups (all  $p < 0.001$ ; Figure 2.1 A-C). Comparing all the experimental groups, the increase of S100B production in culture media was proportional to the degree of lesion severity (peritumoral:  $p < 0.01$  and UC:  $p < 0.001$  vs control; Figure 2.1A). Accordingly, an ever greater amount in S100B protein expression has been detected in the UC, peritumoral and tumoral specimens, respectively (peritumoral:  $p < 0.05$  and UC:  $p < 0.001$  vs control; Figure 2.1 B-C). Interestingly, RAGE/NF- $\kappa$ B signaling proteins follow a similar trend to S100B. Therefore, a proportional upregulation in RAGE expression (peritumoral:  $p < 0.01$ , UC:  $p < 0.001$  and tumoral:  $p < 0.001$  vs control; Figure 2.1 B, D), p38 MAPK phosphorylation (UC:  $p < 0.05$  and tumoral:  $p < 0.001$  vs control; Figure 2.1 B, E) and NF- $\kappa$ B activation (UC:  $p < 0.05$  and tumoral:  $p < 0.001$  vs control; Figure 2.1 B, E) was observed.

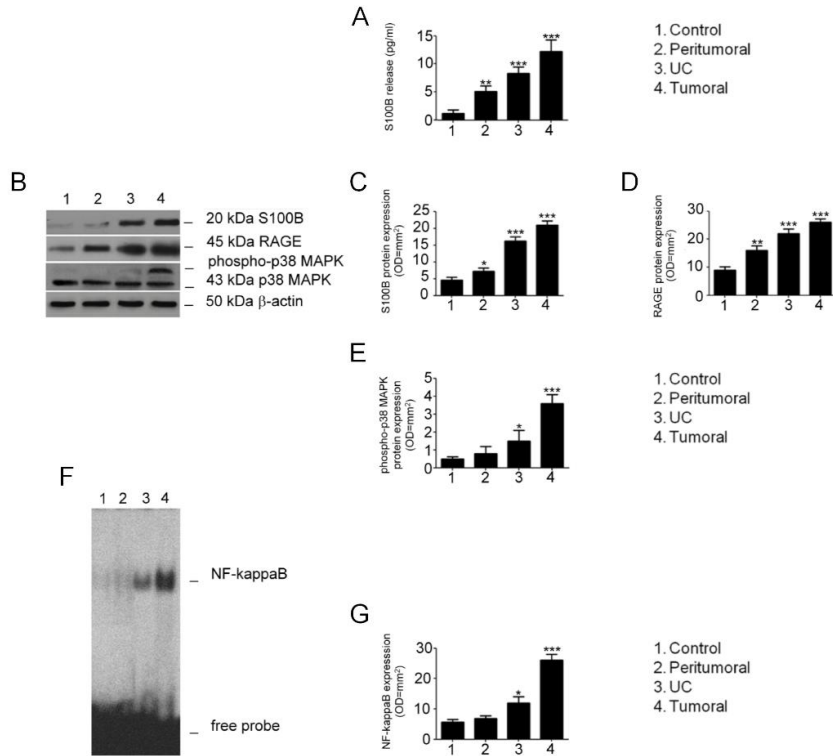


**Figure 2.1.** S100B basal level and RAGE/NF- $\kappa$ B pathway in peritumoral, UC and tumoral specimens. (A) The panel shows S100B basal release in the different tissues. (B-E) Densitometric analysis and relative quantification of the corresponding immunoreactive bands for S100B, RAGE and phospho-p-38 MAPK (arbitrary units normalized on the expression of the housekeeping protein  $\beta$ -actin). (F-G) The panel shows representative NF- $\kappa$ B activation complex bands and their densitometric quantification (OD= optical density in mm<sup>2</sup>). Results are expressed as mean $\pm$ SEM of *n*= 5 experiments performed in triplicate. \* *p*<0.05, \*\* *p*<0.01 and \*\*\* *p*<0.001 versus control.

## p53<sup>wt</sup> protein decreases with the degree of specimens severity

S100B is able to bind tumor suppressor p53 inhibiting its proapoptotic activity. Because of this interaction, the expression of p53<sup>wt</sup> and S100B protein were inversely related, yielding to an ever more significant reduction of p53<sup>wt</sup> protein expression in UC, peritumoral and tumoral groups, respectively (peritumoral:  $p < 0.01$ , UC:  $p < 0.001$  and tumoral:  $p < 0.001$  vs control; Figure 2.2 A-B). Along this line, an ever more decrease in pro-apoptotic Bax protein expression was observed in comparison with control group (peritumoral:  $p < 0.01$ , UC:  $p < 0.001$  and tumoral:  $p < 0.001$ ; Figure 2.2 A, C). Conversely, the proliferative marker PCNA is markedly increased in tumoral tissues when compared to control group ( $p < 0.001$ ; Figure 2.2 A, D). Again, correlating all other experimental groups, PCNA upregulation was proportional to the severity of lesions (UC:  $p < 0.05$  vs control; Figure 2.2 A, D).

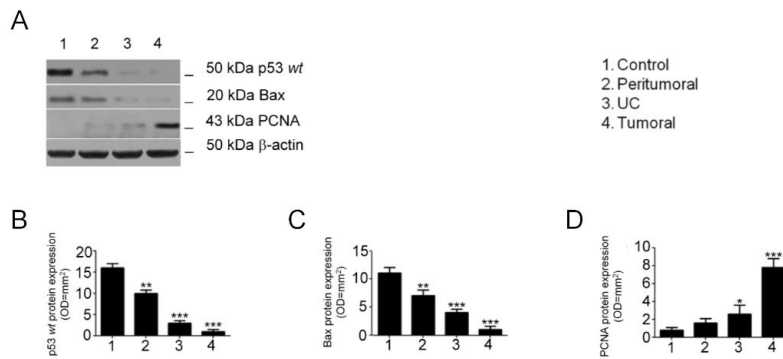
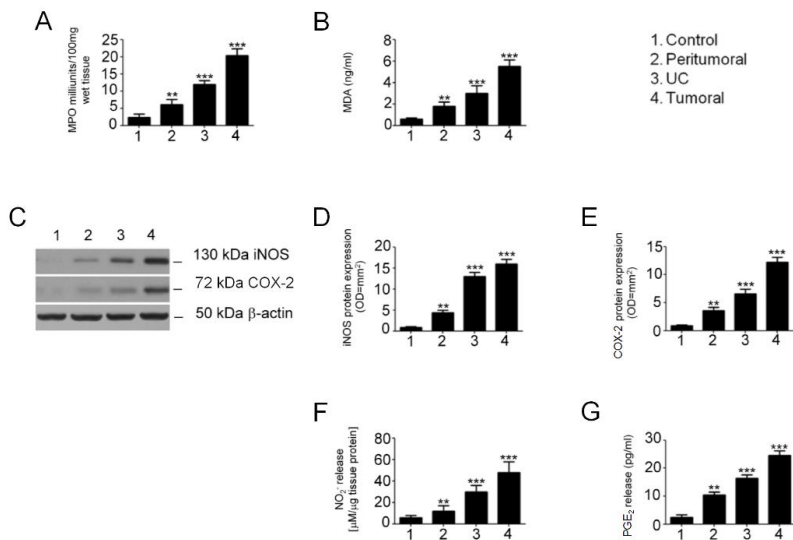


**Figure 2.2.** Pro-apoptotic and proliferative profile of peritumoral, UC and tumoral specimens. (A-D) Densitometric analysis and relative quantification of the corresponding immunoreactive bands for p53<sup>wt</sup>, Bax and PcNA (arbitrary units normalized on the expression of the housekeeping protein  $\beta$ -actin). Results are expressed as mean $\pm$ SEM of  $n= 5$  experiments performed in triplicate. \*  $p < 0.05$ , \*\*  $p < 0.01$  and \*\*\*  $p < 0.001$  versus control.

## Oxidative stress S100B-induced extends proportionally with the injury degree

S100B contributes importantly to cellular oxidative stress promoting lipid peroxidation and iNOS expression through the activation of RAGE/NF- $\kappa$ B pathway. To assess oxidative stress, we evaluated myeloperoxidase (MPO) and malonaldehyde (MDA) concentrations, as well as iNOS expression and mucosal NITRITE production. In colon cancer specimens, a significant raise



in MPO **Figure 2.3**. Oxidative stress in peritumoral, UC and tumoral specimens. The panel shows (A) MPO and (B) MDA production in the different tissues. (C-E) Densitometric analysis and relative quantification of the corresponding immunoreactive bands for iNOS and COX-2 (arbitrary units normalized on the expression of the housekeeping protein  $\beta$ -actin). The panel shows (F) nitrite and (G) PGE<sub>2</sub> release in the culture medium of different specimens. Results are expressed as mean  $\pm$  SEM of  $n=5$  experiments performed in triplicate. \*\*  $p < 0.01$  and \*\*\*  $p < 0.001$  versus control.



and MDA concentrations was observed compared with control groups (all  $p < 0.001$ ; Figure 2.3 A-B) showing a proportional increase when all the experimental groups are compared (all peritumoral:  $p < 0.01$  and UC:  $p < 0.001$  vs control; Figure 2.3 A,B). Similarly, mucosal iNOS protein expression and NITRITE production in the culture medium were ever higher in UC, peritumoral and tumoral groups, respectively (all peritumoral:  $p < 0.01$ , UC:  $p < 0.001$  and tumoral:  $p < 0.001$ ; Figure 2.3 C-D, F). In association with oxidative stress, a significant increase in COX-2 protein expression and PGE<sub>2</sub> release in a proportional manner with the severity of injuries was observed (all peritumoral:  $p < 0.01$ , UC:  $p < 0.001$  and tumoral:  $p < 0.001$ ; Figure 2.3 C, E, G).

### **Exposure to exogenous S100B induces a protein expression profile similar to tumoral specimens**

To address the role of S100B protein upregulation in colon cancer specimens, whole-mount specimens from the control group were exposed to exogenous S100B at increasing concentrations (0.005, 0.05, 0.5 and 5  $\mu\text{M}$ ). After 24h incubation, exogenous S100B induced a significant decrease in p53<sup>wt</sup> protein expression in a dose-dependent fashion (0.005  $\mu\text{M}$ :  $p < 0.05$ , 0.05-5  $\mu\text{M}$ :  $p < 0.001$  vs control; Figure 2.4 A-B). In parallel, both concentration dependent decrease in Bax protein expression (0.005  $\mu\text{M}$ :  $p < 0.05$ , 0.05  $\mu\text{M}$ :  $p < 0.01$ , 0.5-5  $\mu\text{M}$ :  $p < 0.001$  vs control; Figure 2.4 A, C) and increase in PCNA protein expression (0.05  $\mu\text{M}$ :  $p < 0.05$ , 0.5-5  $\mu\text{M}$ :  $p < 0.001$  vs control; Figure 2.4 A, D) were detected, demonstrating a raising proliferative profile after exogenous S100B exposure. This finding was associated with an increasing of oxidative stress state. Indeed, exogenous S100B markedly increased MPO (0.005  $\mu\text{M}$ :  $p < 0.01$ , 0.05-5  $\mu\text{M}$ :  $p < 0.001$  vs control; Figure 2.4 I) and MDA (0.05-5  $\mu\text{M}$ :  $p < 0.001$  vs control; Figure 2.4 J) level in a concentration-dependent fashion,

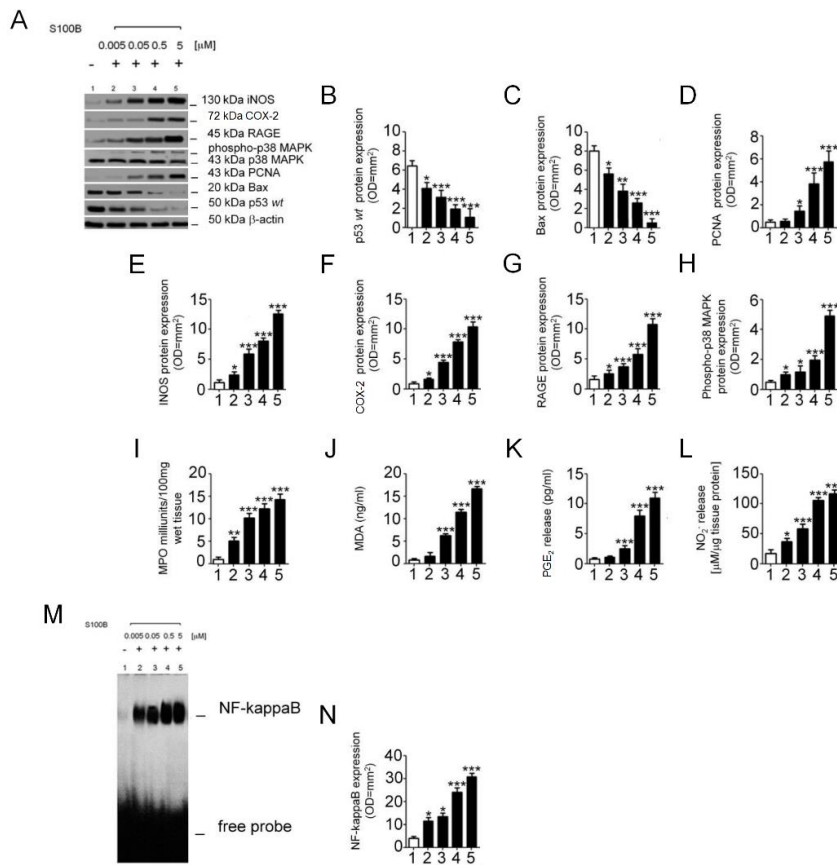


**Figure 2.3.** Exogenous S100B induces a tumor-like profile in a concentration-dependent manner. (A-H) Densitometric analysis and relative quantification of the corresponding immunoreactive bands for p53<sup>wt</sup>, Bax, PCNA, iNOS, COX-2, RAGE and phospho-p38 MAPK (arbitrary units normalized on the expression of the housekeeping protein  $\beta$ -actin). The panel shows (I) MPO, (J) MDA, (K) PGE<sub>2</sub> and (L) nitrite production in the different tissues. Representative NF- $\kappa$ B activation complex bands and their densitometric quantification (OD= optical density in mm<sup>2</sup>). Results are expressed as mean $\pm$ SEM of  $n=5$  experiments performed in triplicate. \*  $p<0.05$ , \*\*  $p<0.01$  and \*\*\*  $p<0.001$  versus control.

as well as iNOS (0.005  $\mu$ M:  $p<0.05$ , 0.05-5  $\mu$ M:  $p<0.001$  vs control; Figure 2.4 A, E) and COX-2 (0.005  $\mu$ M:  $p<0.05$ , 0.05-5  $\mu$ M:  $p<0.001$  vs control;

Figure 2.4 A, F) protein expression with nitrite (0.005  $\mu\text{M}$ :  $p<0.05$ , 0.05-5  $\mu\text{M}$ :  $p<0.001$  vs control; Figure 2.4 K) and  $\text{PGE}_2$  (0.05-5  $\mu\text{M}$ :  $p<0.001$  vs control; Figure 2.4 L) release in the culture media. As expected, increasing doses of S100B induced an ever more expression of RAGE/NF- $\kappa\text{B}$  signaling proteins. In particular RAGE expression (0.005  $\mu\text{M}$ :  $p<0.05$ , 0.05-5  $\mu\text{M}$ :  $p<0.001$  vs control; Figure 2.4 A, G), p38 MAPK phosphorylation (0.005-0.05  $\mu\text{M}$ :  $p<0.05$ , 0.5-5  $\mu\text{M}$ :  $p<0.001$  vs control; Figure 2.4 A, H) and NF- $\kappa\text{B}$  activation (0.005-0.05  $\mu\text{M}$ :  $p<0.05$ , 0.5-5  $\mu\text{M}$ :  $p<0.001$  vs control; Figure 2.4 M-N) have been investigated.

## 2.4 Discussion

In the present study, we showed for the first time that enteroglia-derived S100B protein is involved in the promotion of colon carcinogenesis by sustaining an inflammatory and oxidative microenvironment and by inhibiting p53<sup>wt</sup> function. To test whether S100B may be the main responsible for tumorigenic drift, we also demonstrated that control specimens exposed to exogenous S100B showed a significant decrease in the expression of p53 protein associated to a protein expression profile similar to tumoral tissues.

Even though genetic mutations in epithelial stem cells are considered the mainstay step in colon cancer development, recent data suggest that primary dysfunction in the intestinal microenvironment can be critical for cancer development and progression (Quante et al., 2013; Garcia et al., 2014). This scenario is strongly supported by the perpetuation of chronic inflammation that promote alterations on colonic epithelial cells and eventually evolve into tumorigenic drift (McConnell and Yang, 2009). In fact, inflammatory bowel diseases rank as third highest factor risk to develop colorectal cancer (Kim and Chang, 2014). S100B protein may represent an ideal bridge between chronic inflammation and colon cancer acting as the main promoter of the carcinogenic processes. S100B is a neurotrophin expressed and released by enteric glia displaying a prominent role in the onset and maintaining of neuroinflammatory responses to detrimental noxia (Cirillo et al., 2011a; Capoccia et al., 2015). Interestingly, it is also commonly up-regulated in cancers and is often associated with tumor progression and prognosis (Andres et al., 2004; Hwang et al., 2011; Huang et al., 2012). To test whether S100B is involved in the colon carcinogenesis, we investigated its expression and release in association with related inflammatory and proliferative mediators in human tumoral specimens in comparison with healthy tissues. Our results showed that in colon cancer there is a marked upregulation of S100B directly related to a raise in oxidative

stress and nitric oxide (NO) production through the increased expression of iNOS. In fact, it is well established that ROS are among the initiating factors in colon cancer because of their ability to induce genetic mutations. Interestingly, our data showed also an increase in COX-2 protein expression and consequent PGE<sub>2</sub> release in tumoral specimens, suggesting a possible implication of this bioactive lipid in the cancer outcome when released by enteric glia. Furthermore, tumor suppressor p53<sup>wt</sup> expression is inversely related to S100B due to their protein-protein interaction resulting in a blocking of apoptotic activity of p53<sup>wt</sup>. Accordingly, proapoptotic Bax protein is downregulated but proliferative marker PCNA is overexpressed. Interestingly, we found that S100B-induced pro-apoptotic proteins expression and oxidative mediators profiles closely resemble those observed in UC specimens, even in less quantity and in the absence of dysplastic modification of the epithelium. In line with previously reported data, we observed that p53<sup>wt</sup> function was significantly inhibited in UC specimens, further supporting the evidence that the impairment of p53<sup>wt</sup> is an early modification in chronic inflammatory conditions, as UC. These evidences support that this inflammatory-driven pro-malignant microenvironment may precede cancer development, rather than be its consequence.

There are limited evidences for a role of EGCs and S100B in the pathophysiology of colon cancer. In a previous report, the disruption of EGCs network, ranging from altered EGCs morphology to total loss of S100B immunoreactivity, has been linked to cancer development (Neunlist et al., 2007). The authors concluded that EGCs may exert anti-proliferative effects on epithelial cells, thus protecting against cancer development (Neunlist et al., 2007). In contrast, an *in vivo* study on 357 CRC patients showed that an increased immuno-stained reactivity for S100B protein was a reliable prognostic factor of recurrence after curative resection (Hwang et al., 2011). Even if conflicting, these results possibly depend on the dual activity of enterogial derived factors, particularly S100B (Fano et al., 1995; Van Eldik and

Wainwright, 2003). EGCs may indeed display either pro-proliferative and anti-apoptotic functions or toxic effects depending on the concentration of S100B released in the extracellular milieu. In this perspective, functional alterations in EGCs and consequently in their secreted factors may have opposite roles in cancer, either displaying a tumor suppressor function by increasing immunosurveillance against cancer cells or facilitating tumor progression by promoting cells proliferation and invasion.

Aimed to clarify the involvement of enteric glia and especially of S100B as putative promoter of tumorigenic drift, we investigated the effects of exogenous S100B exposure on control tissues. Intriguingly, our data support the hypothesis that EGCs, fueling intestinal inflammation, can build a pro-malignant microenvironment S100B-mediated that eventually initiates tumor growth. Actually, exposure to exogenous S100B generates a tumor-like protein expression profile. Our results demonstrated that S100B induced a dose-dependent increase of RAGE/NF- $\kappa$ B signaling protein expression resulting in a large expression of iNOS and massive release of nitrite. Likewise, an ever more extent oxidative stress in a concentration-dependent manner was detected. More importantly, S100B reduced dose-dependently proapoptotic Bax and p53<sup>wt</sup> tumor suppressor expression confirming its ability to bind p53<sup>wt</sup> and block its function to regulate cell cycle.

Although further investigations are necessary to better characterize the role of EGCs in the pathophysiology of colon cancer, our study provides relevant evidences about the crucial role of S100B in the onset of colon cancer. Because of its effect on mediating chronic inflammation and oxidative stress in addition to proliferative activity via p53<sup>wt</sup> inhibition, S100B represents a promising molecular target in the colon cancer therapy. More specifically, compound able to inhibit S100B activity and disrupts S100B/p53 interaction may be a new possible therapeutic strategy in the treatment of this pathology.

## 2.5 References

- Andres R, Mayordomo JI, Zaballo P, Rodino J, Isla D, Escudero P, Elosegui L, Filipovich E, Saenz A, Polo E, Tres A. 2004. Prognostic value of serum S-100B in malignant melanoma. *Tumori* 90:607–610.
- Aran V, Victorino AP, Thuler LC, Ferreira CG. 2016. Colorectal Cancer: Epidemiology, Disease Mechanisms and Interventions to Reduce Onset and Mortality. *Clin Colorectal Cancer* 15:195–203.
- Aubé A, Cabarrocas J, Bauer J, Philippe D, Aubert P, Doulay F, Liblau R, Galmiche JP, Neunlist M. 2006. Changes in enteric neurone phenotype and intestinal functions in a transgenic mouse model of enteric glia disruption. *Gut*:630–638.
- Barker N, Ridgway RA, van Es JH, van de Wetering M, Begthel H, van den Born M, Danenberg E, Clarke AR, Sansom OJ, Clevers H. 2009. Crypt stem cells as the cells-of-origin of intestinal cancer. *Nature* 457:608–611.
- Capoccia E, Cirillo C, Gigli S, Pesce M, D'Alessandro A, Cuomo R, Sarnelli G, Steardo L, Esposito G. 2015. Enteric glia: A new player in inflammatory bowel diseases. *Int J Immunopathol Pharmacol* 28:443–451.
- Cassini-Vieira P, Moreira CF, da Silva MF, Barcelos LS. 2015. Estimation of Wound Tissue Neutrophil and Macrophage Accumulation by Measuring Myeloperoxidase (MPO) and N-Acetyl- $\beta$ -D-glucosaminidase (NAG) Activities. *Bio Protoc* 5:e1662.
- Cirillo C, Sarnelli G, Esposito G, Grosso M, Petruzzelli R, Izzo P, Calì G, D'Armiento FP, Rocco A, Nardone G, Iuvone T, Steardo L, Cuomo R. 2009. Increased mucosal nitric oxide production in ulcerative colitis is

- mediated in part by the enteroglia-derived S100B protein. *Neurogastroenterol Motil* 21:1209-e112.
- Cirillo C, Sarnelli G, Esposito G, Turco F, Steardo L, Cuomo R. 2011a. S100B protein in the gut: the evidence for enteroglia-sustained intestinal inflammation. *World J Gastroenterol* 17:1261–1266.
- Cirillo C, Sarnelli G, Turco F, Mango A, Grosso M, Aprea G, Masone S, Cuomo R. 2011b. Proinflammatory stimuli activates human-derived enteroglia cells and induces autocrine nitric oxide production. *Neurogastroenterol Motil* 23:e372-82.
- Cornet A, Savidge TC, Cabarrocas J, Deng WL, Colombel JF, Lassmann H, Desreumaux P, Liblau RS. 2001. Enterocolitis induced by autoimmune targeting of enteric glial cells: a possible mechanism in Crohn's disease? *Proc Natl Acad Sci USA* 98:13306–11.
- Delphin C, Ronjat M, Deloulme JC, Garin G, Debussche L, Higashimoto Y, Sakaguchi K, Baudier J. 1999. Calcium-dependent interaction of S100B with the C-terminal domain of the tumor suppressor p53. *J Biol Chem* 274:10539–10544.
- Van Eldik LJ, Wainwright MS. 2003. The Janus face of glial-derived S100B: beneficial and detrimental functions in the brain. *Restorative neurology and neuroscience* 21:97–108.
- Esposito G, Cirillo C, Sarnelli G, De Filippis D, D'Armiento FP, Rocco A, Nardone G, Petruzzelli R, Grosso M, Izzo P, Iuvone T, Cuomo R. 2007. Enteric glial-derived S100B protein stimulates nitric oxide production in celiac disease. *Gastroenterology* 133:918–25.
- Fano G, Biocca S, Fulle S, Mariggio MA, Belia S, Calissano P. 1995. The S-100: a protein family in search of a function. *Prog Neurobiol* 46:71–82.



- Ferlay J, Soerjomataram I, Dikshit R, Eser S, Mathers C, Rebelo M, Parkin DM, Forman D, Bray F. 2015. Cancer incidence and mortality worldwide: sources, methods and major patterns in GLOBOCAN 2012. *Int J Cancer* 136:E359-86.
- Fernandez-Fernandez MR, Rutherford TJ, Fersht AR. 2008. Members of the S100 family bind p53 in two distinct ways. *Protein Sci* 17:1663–1670.
- Freeman H-J. 2008. Colorectal cancer risk in Crohn's disease. *World J Gastroenterol* 14:1810–1811.
- Garcia SB, Stopper H, Kannen V. 2014. The contribution of neuronal-glia-endothelial-epithelial interactions to colon carcinogenesis. *Cell Mol Life Sci* 71:3191–3197.
- Heizmann CW, Fritz G, Schafer BW. 2002. S100 proteins: structure, functions and pathology. *Front Biosci* 7:d1356-68.
- Huang M-Y, Wang H-M, Chang H-J, Hsiao C-P, Wang J-Y, Lin S-R. 2012. Overexpression of S100B, TM4SF4, and OLFM4 Genes Is Correlated with Liver Metastasis in Taiwanese Colorectal Cancer Patients. *DNA Cell Biol* 31:43–49.
- Hwang C-C, Chai H-T, Chen H-W, Tsai H-L, Lu C-Y, Yu F-J, Huang M-Y, Wang J-Y. 2011. S100B protein expressions as an independent predictor of early relapse in UICC stages II and III colon cancer patients after curative resection. *Ann Surg Oncol* 18:139–145.
- Jess T, Rungoe C, Peyrin-Biroulet L. 2012. Risk of colorectal cancer in patients with ulcerative colitis: a meta-analysis of population-based cohort studies. *Clin Gastroenterol Hepatol* 10:639–645.
- Kim ER, Chang DK. 2014. Colorectal cancer in inflammatory bowel disease: the risk, pathogenesis, prevention and diagnosis. *World J Gastroenterol*

20:9872–9881.

Lin J, Blake M, Tang C, Zimmer D, Rustandi RR, Weber DJ, Carrier F. 2001. Inhibition of p53 transcriptional activity by the S100B calcium-binding protein. *J Biol Chem* 276:35037–35041.

Lin J, Yang Q, Wilder PT, Carrier F, Weber DJ. 2010. The calcium-binding protein S100B down-regulates p53 and apoptosis in malignant melanoma. *J Biol Chem* 285:27487–27498.

Lin J, Yang Q, Yan Z, Markowitz J, Wilder PT, Carrier F, Weber DJ. 2004. Inhibiting S100B restores p53 levels in primary malignant melanoma cancer cells. *J Biol Chem* 279:34071–34077.

Marley AR, Nan H. 2016. Epidemiology of colorectal cancer. *Int J Mol Epidemiol Genet* 7:105–114.

McConnell BB, Yang VW. 2009. The Role of Inflammation in the Pathogenesis of Colorectal Cancer. *Curr Colorectal Cancer Rep* 5:69–74.

Neunlist M, Aubert P, Bonnaud S, Van Landeghem L, Coron E, Wedel T, Naveilhan P, Ruhl A, Lardeux B, Savidge T, Paris F, Galmiche JP. 2007. Enteric glia inhibit intestinal epithelial cell proliferation partly through a TGF-beta1-dependent pathway. *Am J Physiol Gastrointest Liver Physiol* 292:G231-41.

Quante M, Varga J, Wang TC, Greten FR. 2013. The gastrointestinal tumor microenvironment. *Gastroenterology* 145:63–78.

Romano M, DE Francesco F, Zarantonello L, Ruffolo C, Ferraro GA, Zanus G, Giordano A, Bassi N, Cillo U. 2016. From Inflammation to Cancer in Inflammatory Bowel Disease: Molecular Perspectives. *Anticancer Res* 36:1447–1460.

Di Rosa M, Radomski M, Carnuccio R, Moncada S. 1990. Glucocorticoids

inhibit the induction of nitric oxide synthase in macrophages. *Biochem Biophys Res Commun* 172:1246–1252.

Schwitala S, Ziegler PK, Horst D, Becker V, Kerle I, Begus-Nahrman Y, Lechel A, Rudolph KL, Langer R, Slotta-Huspenina J, Bader FG, Prazeres da Costa O, Neurath MF, Meining A, Kirchner T, Greten FR. 2013. Loss of p53 in enterocytes generates an inflammatory microenvironment enabling invasion and lymph node metastasis of carcinogen-induced colorectal tumors. *Cancer Cell* 23:93–106.

Vaira V, Fedele G, Pyne S, Fasoli E, Zadra G, Bailey D, Snyder E, Favarsani A, Coggi G, Flavin R, Bosari S, Loda M. 2010. Preclinical model of organotypic culture for pharmacodynamic profiling of human tumors. *Proc Natl Acad Sci USA* 107:8352–6.

Yoshimura C, Miyafusa T, Tsumoto K. 2013. Identification of small-molecule inhibitors of the human S100B-p53 interaction and evaluation of their activity in human melanoma cells. *Bioorg Med Chem* 21:1109–1115.

Zeki SS, Graham TA, Wright NA. 2011. Stem cells and their implications for colorectal cancer. *Nat Rev Gastroenterol Hepatol* 8:90–100.

# Chapter 3

## IMPACT OF GLIAL-DERIVED PGE<sub>2</sub> ON INTESTINAL FUNCTIONS

---

### 3.1 Introduction

Enteric glial cells are a cellular population composing the enteric nervous system involved in several processes of intestinal homeostasis (Rühl et al., 2004; Neunlist et al., 2014). Although EGCs have been considered for years as passive bystanders of gut pathophysiology, recently a new concept has emerged based on the actively contribution of enteric glia in intestinal physiological and pathological functions (Cabarrocas et al., 2003; Bassotti et al., 2007; Capoccia et al., 2015). In fact, EGCs can modulate cellular epithelial differentiation and proliferation as well as tissue repair and intestinal permeability through the release of specific mediators, including growth factors (such as proEGF and TGF $\beta$ 1) and bioactive lipids (for instance, 11 $\beta$ -PGF2 $\alpha$  and 15dPGJ2) (Savidge et al., 2007; Van Landeghem et al., 2011; Abdo et al., 2012; Coquenlorge et al., 2016). Moreover, several evidences highlighted the prominent role displayed by enteric glia in the initiation and propagation of inflammatory processes following detrimental noxia (Esposito et al., 2007, 2017; Cirillo et al., 2009). In particular, it is well established that the Ca<sup>+2</sup>/Zn<sup>+2</sup>-binding protein S100B is over-released by enteric glia promoting inflammatory states through ROS production and the expression of proinflammatory cytokines and mediators (Esposito et al., 2007; Cirillo et al.,

2011; Capoccia et al., 2015). Among these factors, COX2 enzymes expression is significantly induced and, consequently, a large amount of PGE<sub>2</sub> is release.

PGE<sub>2</sub> is a bioactive eicosanoid produced from arachidonic acid by sequential reactions catalyzed by different enzymes, including the terminal enzyme mPGES1 (Jakobsson et al., 1999; Park et al., 2006). PGE<sub>2</sub> exerts a wide range of effects in the gut pathophysiology, including proinflammatory activity and tissue repair, through the interaction with prostaglandin E2 receptors (EPs) (Dey et al., 2006). Interestingly, PGE<sub>2</sub> displays also an important function in the regulation of intestinal permeability and barrier integrity. In fact, *in vitro* studies reported a marked decrease in transepithelial resistance, tight junctions expression and epithelial barrier integrity in both T84 and Caco2 cells mediated by PGE<sub>2</sub> in an EP4 receptor-dependent manner (Lejeune et al., 2010; Rodriguez-Lagunas et al., 2010). Conversely, a preventive action in mucosal integrity and permeability DSS-induced was observed after administration of EP4 agonist (Kabashima et al., 2002). Along this line, genetic deletion of mPGES1 in mice induced an exacerbation of colitis induced by DSS exposure suggesting the protective role of PGE<sub>2</sub> in maintaining intestinal permeability and barrier integrity (Hara et al., 2010). However, more investigations are necessary to elucidate the clear role of PGE<sub>2</sub> but it appears evident its ability to modulate intestinal permeability and mucosal integrity. More specifically, it is interesting to investigate the contribution of PGE<sub>2</sub> in mediating a condition of leaky gut which underlies several intestinal diseases, including ulcerative colitis and colon cancer. In fact, permeability and intestinal barrier impairment mediated by leaky gut allows the external antigens to come to contact with the organism from the lumen, triggering immune or inflammatory responses. In support of this hypothesis, studies focused on the role of S100B in ulcerative colitis and celiac disease, similarly to previous chapter on colon cancer, reported a marked increase in COX2 protein expression and PGE<sub>2</sub> release (Esposito et al., 2007; Cirillo et al., 2009). Thus, it can be speculated that PGE<sub>2</sub> may act not only as

proinflammatory marker but also as glial mediator contributing to the outbreak of these pathologies through the promotion of a leaky gut condition that usually underlies the majority of gut diseases. Unfortunately, no evidences about the activity of glial-derived PGE<sub>2</sub> on intestinal permeability have been provided yet.

In order to clarify the role of PGE<sub>2</sub> released specifically by enteric glia on intestinal functions, this study aims to elucidate in S100B-mPGES1-deleted mice: i) the impact of PGE<sub>2</sub> glial-derived by deletion of mPGES1 in S100B positive cells on intestinal permeability e permeability; ii) difference in basal and inflammatory conditions; iii) difference between male and female.

## 3.2 Materials and Methods

### Experimental Design

All housing and experimental procedures were carried out in compliance with the local ethical review panel of INSERM U1235 (Nantes, France). Both male and female 8-weeks-old S100B-mPGES1-deleted mice were used for the experiments. S100B-mPGES1-deleted mice were obtained by crossing S100B<sup>CreER</sup> mice and mPGES1<sup>flox/flox</sup> mice. Both male and female animals were randomly divided in the following experimental groups ( $n=8-10$  each): mPGES1<sup>+/+</sup> CTRL, receiving oil as vehicle; mPGES1<sup>+/+</sup> DSS, receiving oil as vehicle and DSS 4% in drinking water; mPGES1<sup>-/-</sup> CTRL, receiving tamoxifen; mPGES1<sup>-/-</sup> DSS, receiving tamoxifen and DSS in drinking water. In order to induce mPGES1 deletion, tamoxifen (Cayman Chemical, Ann Arbor, Michigan, USA) was dissolved in oil and was daily injected (100 mg/kg) via intraperitoneal route for five consecutive days (from day -14 to day -9). Colitis was induced by administrating 4% DSS in drinking water for 4 consecutive days starting from day 0. During this time interval, intestinal permeability and total transit time were daily measured by oral gavage with 0.4 kDa fluorescein-5-(and-6)-sulfonic acid (10 mg/mL) and red carmine dye (60 mg/mL) dissolved in a solution of carboxymethylcellulose 0,5%. At day 4, animals were euthanized and colon was isolated to perform immunohistochemical analysis.

## ***In vivo* Intestinal Permeability Assay**

From day 0 to day 4, intestinal permeability was daily measured by administration of gavage solution (4  $\mu\text{L}/\text{mg}$ ) containing 0.4 kDa fluorescein-5-(and-6)-sulfonic acid. Four hours later, blood was collected from the tail vein and plasma obtained by centrifugation. Fluorescence was detected from 5  $\mu\text{L}$  of plasma on a microtiter plate reader (Varioskan, Thermo Fisher Scientific).

## ***In vivo* Total Transit Time Measurement**

From day 0 to day 4, the intestinal total transit time was measured. After the administration of gavage solution containing red carmine dye, mice were placed individually in the cage. Total transit time is considered the time between the gavage administration and the appearance of the first red stool.

## **Immunohistochemical Staining**

For immunohistochemical staining, colon isolated at day 4 were fixed in paraformaldehyde 4% and embedded in paraffin. Thus, they were cut in 20  $\mu\text{m}$  slices and deparaffinized in xylene and rehydrate in graded alcohol. Antigen retrieval with 0.1 M citrate sodium (pH 6) buffer was performed. Next, slices were incubated for 1 h at RT with PBS containing 0.5% Triton X-100 for tissue permeabilization. Then they were blocked for 2 h at RT with PBS containing 0.5% Triton X-100 and 10% horse and then incubated O/N at  $+4^\circ$  with mouse monoclonal antibody anti-GFAP (1:500 v/v, Santa Cruz Biotechnology, Heidelberg, Germany) and rabbit polyclonal anti-mPGES1 (1:100 v/v, Cayman Chemical). Then, slices were incubated with proper anti-mouse CY-



3 and anti-rabbit CY-5 secondary antibodies (all 1:500; Jackson ImmunoResearch, West Grove, PA, USA) for 3 h at RT and then mounted with ProLong antifade mountant (ThermoFisher Scientific, Waltham, MA, USA). Images were acquired with a digital camera (Olympus DP 50) coupled to a fluorescence microscope (Olympus IX 50).

### **Statistical analysis**

Results were expressed as mean  $\pm$  SEM of experiments. Statistical analysis was performed using parametric one-way analysis of variance (ANOVA) and multiple comparisons were performed by Bonferroni's post hoc test. p values  $<0.05$  were considered significant.

### 3.3 Results

#### DSS administration induces a marked increase in mPGES1 protein expression in myenteric plexi

To test whether the mPGES1 deletion has effectively occurred, an immunohistochemistry staining was performed. mPGES1 protein expression is increased by DSS administration in wild type mice and co-localize with GFAP protein in myenteric plexi when compared to control group, suggesting

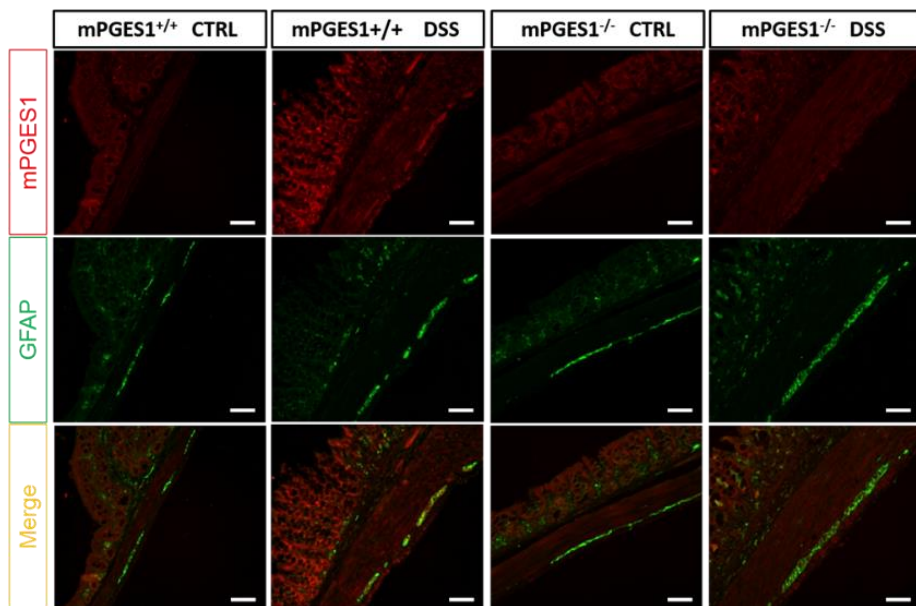


**Figure 3.1.** mPGES1 protein expression is increased after DSS exposure in female wild type mice but not in female mPGES1-S100B-deleted mice. The panel shows mPGES1 (red) and GFAP (green) immunoreactivity in colon sections after DSS exposure in female wild type and mPGES1<sup>-/-</sup> mice. Magnification: 160X. Scale bar: 100  $\mu$ m.

that enteric glia expressed high levels of mPGES1 protein and, consequently, produce a massive PGE<sub>2</sub> release in inflammatory conditions (Figure 3.1-2). As expected, mPGES1 protein expression is not affected by DSS exposure in S100B-mPGES1-deleted mice (Figure 3.1-2). No significant differences between male and female are observed (Figure 3.1-2).

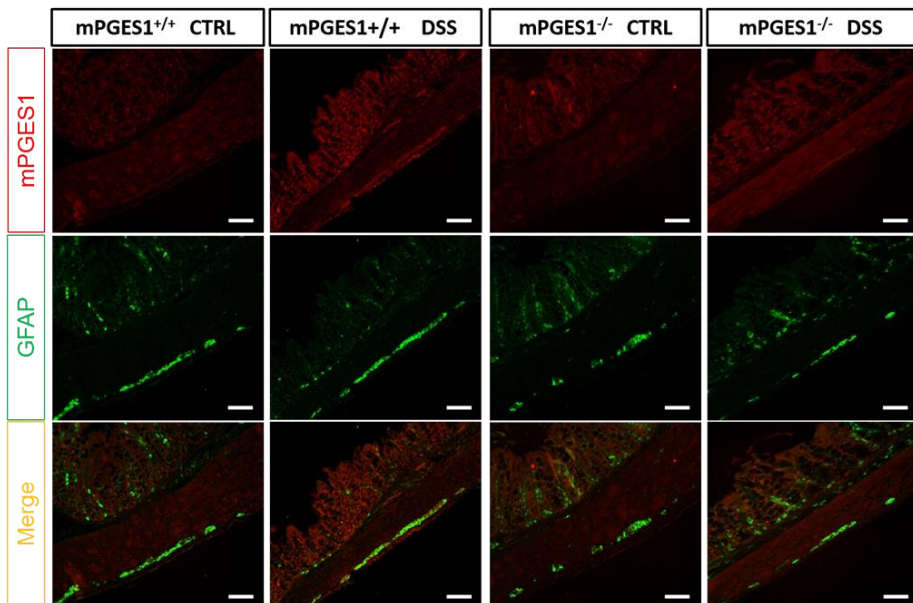


**Figure 3.2.** mPGES1 protein expression is increased after DSS exposure in male wild type mice but not in male mPGES1-S100B-deleted mice. The panel shows mPGES1 (red) and GFAP (green) immunoreactivity in colon sections after DSS exposure in male wild type and mPGES<sup>-/-</sup> mice. Magnification: 160X. Scale bar: 100  $\mu$ m.

**In basal condition, mPGES1 deletion induces an intestinal permeability decrease in female and a transit time increase in male**

Fourteen days after the beginning of mPGES1 deletion by tamoxifen injection, basal effect on intestinal permeability and total transit time were evaluated. Surprisingly, mPGES1 deletion reduced significantly intestinal

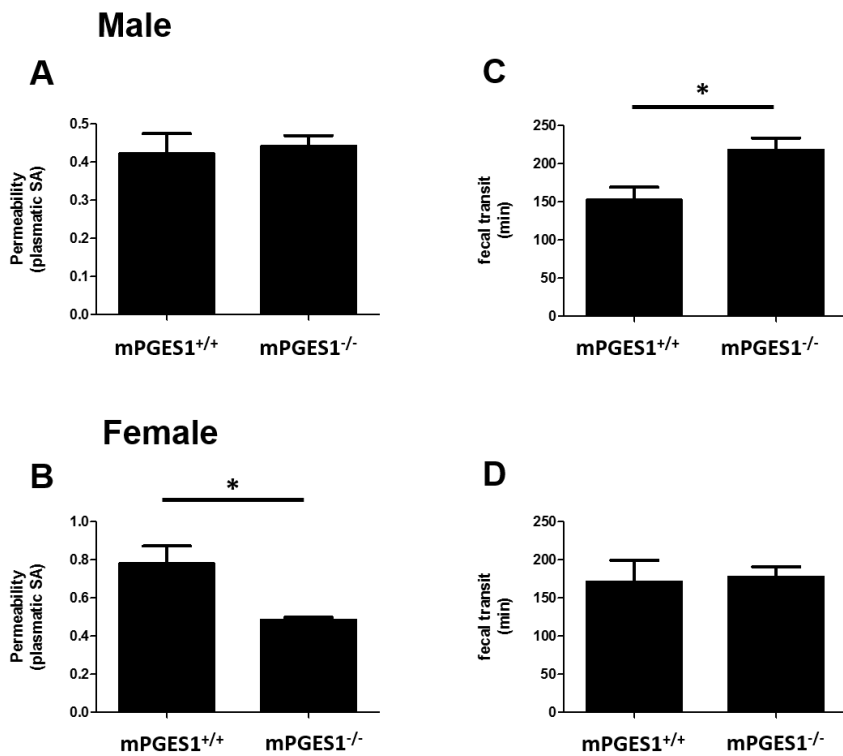


**Figure 3.3.** mPGES1 deletion reduces intestinal permeability in female and increases total transit time in male. Measurements of intestinal permeability performed in (A) male and (B) female wild type and mPGES1<sup>-/-</sup> mice. Measurements of fecal transit measurements performed in (C) male and (D) female wild type and mPGES1<sup>-/-</sup> mice. Results are expressed as mean±SEM of *n* = 16 each group. \* *p*<0.05 versus mPGES1<sup>+/+</sup> mice.

permeability in female ( $p < 0.05$  vs mPGES1<sup>+/+</sup> mice, Figure 3.3 B), whereas no changes were observed in male (Figure 3.3 A). Conversely, total transit time is not affected in mPGES1<sup>-/-</sup> female mice when compared to mPGES1<sup>+/+</sup> female mice (Figure 3.3 D), but it is markedly increased in S100B-mPGES1-deleted male mice ( $p < 0.05$  vs mPGES1<sup>+/+</sup> mice, Figure 3.3 C). These data advance the hypothesis that PGE<sub>2</sub> specifically released by EGCs at physiological conditions may modulate intestinal permeability and motility differently in male and female.

### **mPGES1 deletion did not affect total transit time and permeability increase DSS-induced**

Globally, DSS administration increased significantly intestinal permeability and fecal transit in both male (intestinal permeability:  $p < 0.01$  vs control mPGES1<sup>+/+</sup> mice and  $p < 0.05$  vs mPGES1<sup>-/-</sup> mice; Figure 3.4 A) (fecal transit:  $p < 0.05$  vs mPGES1<sup>+/+</sup> mice; Figure 3.4 C) and female (intestinal permeability:  $p < 0.05$  vs control mPGES1<sup>+/+</sup> mice and  $p < 0.05$  vs mPGES1<sup>-/-</sup> mice; Figure 3.4 B) (fecal transit:  $p < 0.05$  vs control mPGES1<sup>+/+</sup> mice and  $p < 0.05$  vs mPGES1<sup>-/-</sup> mice; Figure 3.4 D), without remarkable differences between wild type mice and S100B-mPGES1-deleted mice, suggesting that glial-derived PGE<sub>2</sub> did not affect DSS effects, at least at day 4 of treatment. The only exception is represented by transit time in male. Here it appears that glial mPGES1 deletion resembles the transit time increase DSS-induced, but actually it is due to the basal effect of glia mPGES1 deletion aforementioned. Indeed, the transit time is already high thus DSS effects cannot be appreciated. Consistently with previous results, in CTRL groups, deletion of glial mPGES1 induced an increase in transit time in mPGES1<sup>-/-</sup> male ( $p < 0.05$  vs control mPGES1<sup>+/+</sup> mice;

Figure 3.4 C) and a significant decrease in permeability in mPGES1<sup>-/-</sup> female (p<0.01 vs control mPGES1<sup>+/+</sup> mice; Figure 3.4 B).

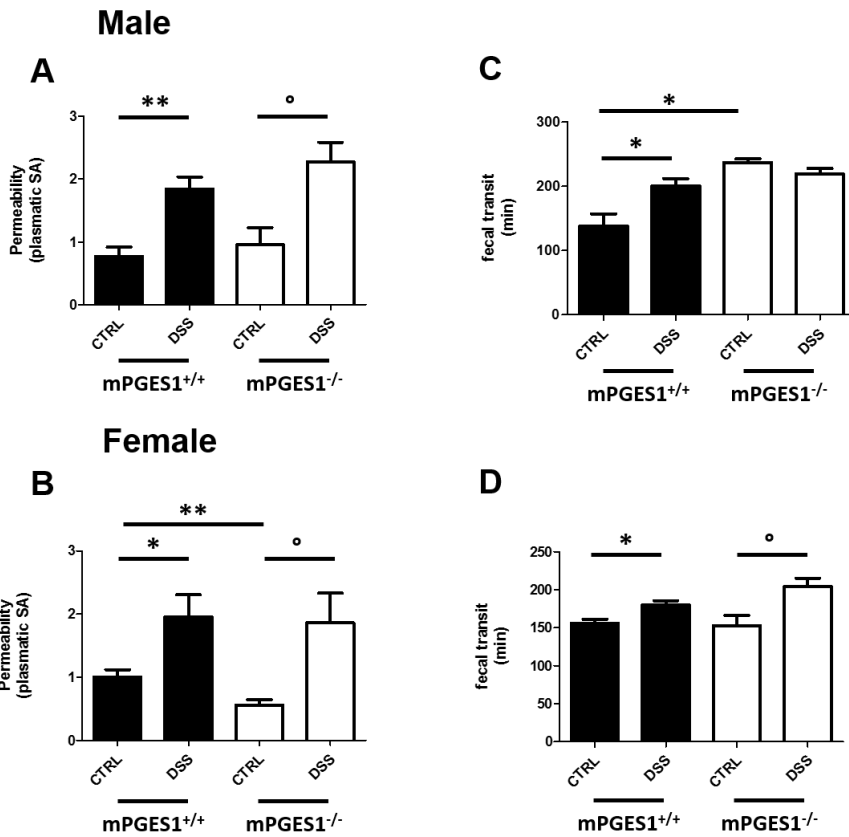


**Figure 3.4.** mPGES1 deletion did not induce any alteration of DSS-induced effects on permeability and fecal transit. Measurements of intestinal permeability performed in (A) male and (B) female wild type and mPGES1<sup>-/-</sup> mice following DSS exposure. Measurements of fecal transit measurements performed in (C) male and (D) female wild type and mPGES1<sup>-/-</sup> mice following DSS exposure. Results are expressed as mean±SEM of *n* = 8 each group. \* p<0.05 and \*\* p<0.01 versus control mPGES1<sup>+/+</sup> mice; ° p<0.05 versus control mPGES1<sup>-/-</sup> mice.

## mPGES1 deletion accelerates DSS effects during colitis development

Since mPGES1 deletion did not affect the effects DSS-induced after 4 day of administration, we investigated functional alterations during colitis development. Interestingly, mPGES1 deletion in DSS-treated mice induces an increase in intestinal permeability starting from day 2 and day 3 from DSS administration in male and female, respectively. Differently, the increase in total transit time, already observed at day 0 in S100B-mPGES1-deleted male DSS-treated mice, remains constant for all the treatment days in comparison with mPGES1<sup>+/+</sup> male animals. Conversely, mPGES1 deletion in female DSS-treated mice did not affect the effects DSS-induced on fecal transit time. Based on these evidences, it can be assumed that glial-derived PGE<sub>2</sub> a preventive effect on delaying DSS activity.

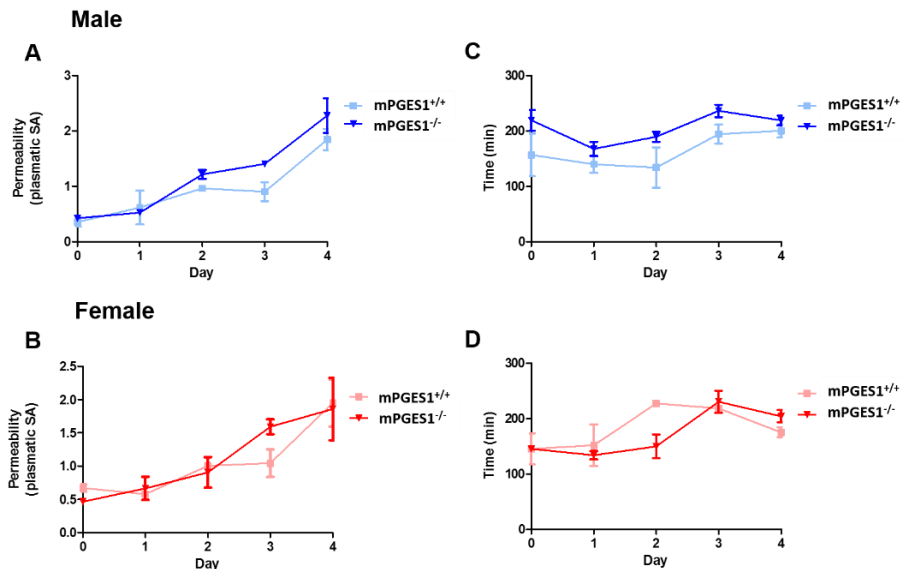


**Figure 3.5.** mPGES1 deletion accelerates DSS-induced effects on permeability and fecal transit. Time course of intestinal permeability DSS-mediated in both (A) male and (B) female. Time course of fecal transit DSS-mediated in both (C) male and (D) female. Results are expressed as mean $\pm$ SEM of  $n = 2$  each group.

### 3.4 Discussion

The present study is focused on the impact displayed by PGE<sub>2</sub> as specific glial mediator in the regulation of intestinal functions. Here we provided for the first time *in vivo* evidences about the effects of PGE<sub>2</sub> specifically released by enteric glia on intestinal permeability and motility through the deletion of mPGES1 in S100B positive cells in both physiological and pathological conditions.

In the last decades, it was well established the ability of enteric glia in modulating homeostasis as well as immunoinflammatory responses of the gastrointestinal tract (Neunlist et al., 2014; Capoccia et al., 2015). A pioneristic study in 1998, investigated the effect of EGCs ablation in a transgenic mice model (Bush et al., 1998). The induction of a fulminant jejuno-ileitis in association with a marked loss in mucosal integrity demonstrated the crucial involvement of enteric glia in the gut pathophysiology (Bush et al., 1998). Since then, a wide range of glial-derived compounds has been identified as responsible for enteric glia activity, including growth factors and arachidonic acid metabolites (Flamant et al., 2011; Van Landeghem et al., 2011; Pochard et al., 2016). Among these factors, it may be possible include PGE<sub>2</sub>, a bioactive lipid belonging to the prostaonoid family able to modulate intestinal permeability. In fact, recent studies showed that PGE<sub>2</sub> via EP4 receptor increased D-mannitol flux and decreased transepithelial resistance in differentiated Caco-2 cells monolayer, in association with a marked reduction in occludin and ZO-1 protein expression (Lejeune et al., 2010; Rodriguez-Lagunas et al., 2010). However, evidences about the activity of PGE<sub>2</sub> specifically released by enteric glia are still missing. To this purpose, we targeted the deletion of terminal enzyme of PGE<sub>2</sub> synthetic pathway mPGES1 in S100B positive through the Cre-lox recombination system in transgenic mice. Surprisingly, important differences in intestinal functions between male and female are observed. In absence of glial-derived PGE<sub>2</sub>, female showed a



significant reduction in intestinal permeability, whereas male did not exhibit any alteration. Conversely, total transit time is not affected by mPGES1 deletion in female but is markedly increased in male. These results suggest a possible physiological regulation of permeability and motility operated by enteric glial cells through the basal production of PGE<sub>2</sub>.

PGE<sub>2</sub> exerts an important inflammatory activity acting as pyrogenic and vasodilator agent (Wallace, 2001). Moreover, it has been demonstrated that PGE<sub>2</sub> induces IL-23 expression promoting, consequentially, cell T activation that can start to produce IL-17 (Sheibanie et al., 2007). Accordingly, high levels of PGE<sub>2</sub> have been detected in experimental model of inflammatory bowel diseases and celiac disease, likewise in colon cancer (Wang and Dubois, 2006; Esposito et al., 2007, 2014). In these pathological conditions it is well accepted that enteric glia is morphological and functional activated and actively participates in the onset and perpetuation of inflammatory states. In particular, enteric glia release S100B at micromolar concentrations that through the activation of RAGE/NF-κB pathway promotes COX-2 protein expression and downstream PGE<sub>2</sub> production (Bianchi et al., 2007; Cirillo et al., 2011). Hence, it can be speculated that PGE<sub>2</sub> act as specific mediator of glial activity also in inflammatory conditions. In our experimental conditions, deletion of mPGES1 did not affect the increase in permeability and total transit time mediated by DSS after 4 days of treatment. Some interesting observations can be made during colitis development. Indeed, the deletion of glial mPGES1 increase significantly intestinal permeability similarly to DSS but after two or three days of treatment. Conversely, it's not surprisingly that total transit is steadily higher in comparison with mPGES1<sup>+/+</sup> male mice, because of the basal effect observed at day 0. Our data suggest that enteric glia may exert a transient protective role by PGE<sub>2</sub> releasing, as observed in previous works. In fact, it has been shown that mPGES1 deficient mice displayed a marked exacerbation of colitis after one day of DSS exposure (Hara et al., 2010). Similar results are reported in EP4 knockout mice and after EP4 agonists administration,

underlying the crucial role of these receptors in mediating PGE<sub>2</sub> effects (Kabashima et al., 2002; Nitta et al., 2002; Montrose et al., 2015). Even though glial-derived PGE<sub>2</sub> exhibit a transient preventive effect in structural barrier integrity, we must consider that this bioactive lipid possesses relevant tumorigenesis activity when persistently released (Nakanishi et al., 2008). The continuous exposure to high levels of PGE<sub>2</sub> in chronic inflammatory states represents an important predisposing factor to colon cancer outcome (Castellone et al., 2005; Nakanishi et al., 2008; Montrose et al., 2015). Indeed, several clinical researches demonstrated that the chronic administration of non-steroidal anti-inflammatory drugs (NSAIDs) are associated with a significant reduction in colon and rectal cancers formation due to COX-2 inhibition and relative PGE<sub>2</sub> release (Ruder et al., 2011; Hamoya et al., 2016). Along this line, a direct *in vivo* evidence has been reported by Kawamori et al showing that PGE<sub>2</sub> weekly administration via intraperitoneal route induces a marked increase in multiplicity and incidence of intestinal adenomas (Kawamori et al., 2003).

In conclusion, the present study underlined the importance of PGE<sub>2</sub> specifically released by enteric glia in the homeostatic functions of intestinal tract. In particular, PGE<sub>2</sub> acts as specific glial mediator in positively modulating total transit time in male and negatively intestinal permeability in female. Moreover glial-derived PGE<sub>2</sub> exerts a transient protective effect on development of colitis DSS-induced. However, based on the implication of PGE<sub>2</sub> in intestinal inflammation and carcinogenesis, our data pave the way to new investigations aimed to clarify the involvement of EGCs in gut diseases through the release of PGE<sub>2</sub> proposing, at the same time, a promising therapeutic strategy of intervention.

### 3.5 References

- Abdo H, Mahe MM, Derkinderen P, Bach-Ngohou K, Neunlist M, Lardeux B. 2012. The omega-6 fatty acid derivative 15-deoxy-Delta(1)(2),(1)(4)-prostaglandin J2 is involved in neuroprotection by enteric glial cells against oxidative stress. *J Physiol* 590:2739–2750.
- Bassotti G, Villanacci V, Antonelli E, Morelli A, Salerni B. 2007. Enteric glial cells: new players in gastrointestinal motility? *Lab Invest* 87:628.
- Bianchi R, Adami C, Giambanco I, Donato R. 2007. S100B binding to RAGE in microglia stimulates COX-2 expression. *J Leukoc Biol* 81:108–118.
- Bush TG, Savidge TC, Freeman TC, Cox HJ, Campbell EA, Mucke L, Johnson MH, Sofroniew M V. 1998. Fulminant Jejuno-Ileitis following Ablation of Enteric Glia in Adult Transgenic Mice. *Cell* 93:189–201.
- Cabarrocas J, Savidge TC, Liblau RS. 2003. Role of enteric glial cells in inflammatory bowel disease. *Glia* 41:81–93.
- Capoccia E, Cirillo C, Gigli S, Pesce M, D’Alessandro A, Cuomo R, Sarnelli G, Steardo L, Esposito G. 2015. Enteric glia: A new player in inflammatory bowel diseases. *Int J Immunopathol Pharmacol* 28:443–451.
- Castellone MD, Teramoto H, Williams BO, Druey KM, Gutkind JS. 2005. Prostaglandin E2 promotes colon cancer cell growth through a Gs-axin-beta-catenin signaling axis. *Science* 310:1504–1510.
- Cirillo C, Sarnelli G, Esposito G, Grosso M, Petruzzelli R, Izzo P, Calì G, D’Armiento FP, Rocco A, Nardone G, Iuvone T, Steardo L, Cuomo R. 2009. Increased mucosal nitric oxide production in ulcerative colitis is mediated in part by the enteroglial-derived S100B protein.

Neurogastroenterol Motil 21:1209-e112.

Cirillo C, Sarnelli G, Esposito G, Turco F, Steardo L, Cuomo R. 2011. S100B protein in the gut: the evidence for enteroglial-sustained intestinal inflammation. *World J Gastroenterol* 17:1261–1266.

Coquenlorge S, Van Landeghem L, Jaulin J, Cenac N, Vergnolle N, Duchalais E, Neunlist M, Rolli-Derkinderen M. 2016. The arachidonic acid metabolite 11 $\beta$ -ProstaglandinF2 $\alpha$  controls intestinal epithelial healing: deficiency in patients with Crohn's disease. *Sci Rep* 6:25203.

Dey I, Lejeune M, Chadee K. 2006. Prostaglandin E2 receptor distribution and function in the gastrointestinal tract. *Br J Pharmacol* 149:611–623.

Esposito G, Capoccia E, Gigli S, Pesce M, Bruzzese E, Alessandro AD, Cirillo C, Cerbo A, Cuomo R, Steardo L, Sarnelli G. 2017. HIV-1 Tat-induced diarrhea evokes an enteric glia-dependent neuroinflammatory response in the central nervous system. *Sci Rep* 7:7735.

Esposito G, Capoccia E, Turco F, Palumbo I, Lu J, Steardo A, Cuomo R, Sarnelli G, Steardo L. 2014. Palmitoylethanolamide improves colon inflammation through an enteric glia/toll like receptor 4-dependent PPAR- $\alpha$  activation. *Gut* 63:1300–12.

Esposito G, Cirillo C, Sarnelli G, De Filippis D, D'Armiento FP, Rocco A, Nardone G, Petruzzelli R, Grosso M, Izzo P, Iuvone T, Cuomo R. 2007. Enteric glial-derived S100B protein stimulates nitric oxide production in celiac disease. *Gastroenterology* 133:918–25.

Flamant M, Aubert P, Rolli-Derkinderen M, Bourreille A, Neunlist MR, Mahe MM, Meurette G, Marteyn B, Savidge T, Galmiche JP, Sansonetti PJ, Neunlist M. 2011. Enteric glia protect against *Shigella flexneri* invasion in intestinal epithelial cells: a role for S-nitrosoglutathione. *Gut* 60:473–484.

- Hamoya T, Fujii G, Miyamoto S, Takahashi M, Totsuka Y, Wakabayashi K, Toshima J, Mutoh M. 2016. Effects of NSAIDs on the risk factors of colorectal cancer: a mini review. *Genes Environ* 38:6.
- Hara S, Kamei D, Sasaki Y, Tanemoto A, Nakatani Y, Murakami M. 2010. Prostaglandin E synthases: Understanding their pathophysiological roles through mouse genetic models. *Biochimie* 92:651–659.
- Jakobsson PJ, Thoren S, Morgenstern R, Samuelsson B. 1999. Identification of human prostaglandin E synthase: a microsomal, glutathione-dependent, inducible enzyme, constituting a potential novel drug target. *Proc Natl Acad Sci USA* 96:7220–7225.
- Kabashima K, Saji T, Murata T, Nagamachi M, Matsuoka T, Segi E, Tsuboi K, Sugimoto Y, Kobayashi T, Miyachi Y, Ichikawa A, Narumiya S. 2002. The prostaglandin receptor EP4 suppresses colitis, mucosal damage and CD4 cell activation in the gut. *J Clin Invest* 109:883–893.
- Kawamori T, Uchiya N, Sugimura T, Wakabayashi K. 2003. Enhancement of colon carcinogenesis by prostaglandin E2 administration. *Carcinogenesis* 24:985–990.
- Van Landeghem L, Chevalier J, Mahe MM, Wedel T, Urvil P, Derkinderen P, Savidge T, Neunlist M. 2011. Enteric glia promote intestinal mucosal healing via activation of focal adhesion kinase and release of proEGF. *Am J Physiol Gastrointest Liver Physiol* 300:G976-87.
- Lejeune M, Leung P, Beck PL, Chadee K. 2010. Role of EP4 receptor and prostaglandin transporter in prostaglandin E2-induced alteration in colonic epithelial barrier integrity. *Am J Physiol Gastrointest Liver Physiol* 299:G1097-105.
- Montrose DC, Nakanishi M, Murphy RC, Zarini S, McAleer JP, Vella AT, Rosenberg DW. 2015. The role of PGE2 in intestinal inflammation and

- tumorigenesis. *Prostaglandins Other Lipid Mediat* 116–117:26–36.
- Nakanishi M, Montrose DC, Clark P, Nambiar PR, Belinsky GS, Claffey KP, Xu D, Rosenberg DW. 2008. Genetic deletion of mPGES-1 suppresses intestinal tumorigenesis. *Cancer Res* 68:3251–3259.
- Neunlist M, Rolli-derkinderen M, Latorre R, Landeghem L Van, Coron E, Derkinderen P, Giorgio R De. 2014. Enteric Glial Cells: Recent Developments and Future Directions. *Gastroenterology* 147:1230–1237.
- Nitta M, Hirata I, Toshina K, Murano M, Maemura K, Hamamoto N, Sasaki S, Yamauchi H, Katsu K. 2002. Expression of the EP4 prostaglandin E2 receptor subtype with rat dextran sodium sulphate colitis: colitis suppression by a selective agonist, ONO-AE1-329. *Scand J Immunol* 56:66–75.
- Park JY, Pillinger MH, Abramson SB. 2006. Prostaglandin E2 synthesis and secretion: the role of PGE2 synthases. *Clin Immunol* 119:229–240.
- Pochard C, Coquenlorge S, Jaulin J, Cenac N, Vergnolle N, Meurette G, Freyssinet M, Neunlist M, Rolli-Derkinderen M. 2016. Defects in 15-HETE Production and Control of Epithelial Permeability by Human Enteric Glial Cells From Patients With Crohn's Disease. *Gastroenterology* 150:168–180.
- Rodriguez-Lagunas MJ, Martin-Venegas R, Moreno JJ, Ferrer R. 2010. PGE2 promotes Ca<sup>2+</sup>-mediated epithelial barrier disruption through EP1 and EP4 receptors in Caco-2 cell monolayers. *Am J Physiol Cell Physiol* 299:C324-34.
- Ruder EH, Laiyemo AO, Graubard BI, Hollenbeck AR, Schatzkin A, Cross AJ. 2011. Non-steroidal anti-inflammatory drugs and colorectal cancer risk in a large, prospective cohort. *Am J Gastroenterol* 106:1340–1350.

- Rühl A, Nasser Y, Sharkey KA. 2004. Enteric glia. *Neurogastroenterol Motil* 16:44–49.
- Savidge TC, Newman P, Pothoulakis C, Ruhl A, Neunlist M, Bourreille A, Hurst R, Sofroniew M V. 2007. Enteric glia regulate intestinal barrier function and inflammation via release of S-nitrosoglutathione. *Gastroenterology* 132:1344–58.
- Sheibanie AF, Yen J-H, Khayrullina T, Emig F, Zhang M, Tuma R, Ganea D. 2007. The proinflammatory effect of prostaglandin E2 in experimental inflammatory bowel disease is mediated through the IL-23-->IL-17 axis. *J Immunol* 178:8138–8147.
- Wallace JL. 2001. Prostaglandin biology in inflammatory bowel disease. *Gastroenterol Clin North Am* 30:971–980.
- Wang D, Dubois RN. 2006. Prostaglandins and cancer. *Gut* 55:115–122.

# ANNEXES

---

## List of Publications

1. Sarnelli, G., Seguella, L., Pesce, M., Lu, J., Gigli, S., Bruzzese, E., Lattanzi, R., D'Alessandro, A., Cuomo, R., Steardo, L., Esposito, G. HIV-1 Tat-induced diarrhea is improved by the PPAR $\alpha$  agonist, palmitoylethanolamide, by suppressing the activation of enteric glia. (2018) *J Neuroinflammation*, Accepted.

2. Pesce, M., D'Alessandro, A., Borrelli, O., Gigli, S., Seguella, L., Cuomo, R., Esposito, G., Sarnelli, G. Endocannabinoid-related compounds in gastrointestinal diseases. (2017) *Journal of Cellular and Molecular Medicine*, 22(2):706-715.

3. Gigli, S., Seguella, L., Pesce, M., Bruzzese, E., D'Alessandro, A., Cuomo, R., Steardo, L., Sarnelli, G., Esposito, G. Cannabidiol restores intestinal barrier dysfunction and inhibits the apoptotic process induced by *Clostridium difficile* Toxin A in Caco-2. (2017) *United European Gastroenterology Journal*, 5 (8): 1108-1115.

4. Esposito, G., Capoccia, E., Gigli, S., Pesce, M., Bruzzese, E., D'Alessandro, A., Cirillo, C., Di Cerbo, A., Cuomo, R., Seguella, L., Steardo, L., Sarnelli, G. HIV-1 Tat-induced diarrhea evokes an enteric glia-dependent neuroinflammatory response in the central nervous system. (2017) *Scientific Reports*, 7: 7735.

5. Esposito, G., Gigli, S., Seguella, L., Nobile, N., D'Alessandro, A., Pesce, M., Capoccia, E., Steardo, L., Cirillo, C., Cuomo, R., Sarnelli, G. Rifaximin, a



non-absorbable antibiotic, inhibits the release of pro-angiogenic mediators in colon cancer cells through a pregnane X receptor-dependent pathway (2016) *International Journal of Oncology*, 49 (2), pp. 639-645.

6. Sarnelli, G., Gigli, S., Capoccia, E., Iuvone, T., Cirillo, C., Seguella, L., Nobile, N., D'Alessandro, A., Pesce, M., Steardo, L., Cuomo, R., Esposito, G. Palmitoylethanolamide Exerts Antiproliferative Effect and Downregulates VEGF Signaling in Caco-2 Human Colon Carcinoma Cell Line Through a Selective PPAR- $\alpha$ -Dependent Inhibition of Akt/mTOR Pathway (2016) *Phytotherapy Research*, 30 (6), pp. 963-970.

7. Sarnelli, G., D'Alessandro, A., Iuvone, T., Capoccia, E., Gigli, S., Pesce, M., Seguella, L., Nobile, N., Aprea, G., Maione, F., De Palma, G.D., Cuomo, R., Steardo, L., Esposito, G. Palmitoylethanolamide modulates inflammation-associated Vascular Endothelial Growth Factor (VEGF) signaling via the Akt/mTOR pathway in a selective peroxisome proliferator-activated receptor alpha (PPAR- $\alpha$ )-dependent manner (2016) *PLoS ONE*, 11 (5), art. no. e0156198.

8. Esposito, G., Nobile, N., Gigli, S., Seguella, L., Pesce, M., d'Alessandro, A., Bruzzese, E., Capoccia, E., Steardo, L., Cuomo, R., Sarnelli, G. Rifaximin improves *Clostridium difficile* toxin A-induced toxicity in Caco-2 cells by the PXR-dependent TLR4/MyD88/NF- $\kappa$ B pathway(2016) *Frontiers in Pharmacology*, 7 (MAY), art. no. 120, DOI: 10.3389/fphar.2016.00120

9. Capoccia, E., Cirillo, C., Gigli, S., Pesce, M., D'Alessandro, A., Cuomo, R., Sarnelli, G., Steardo, L., Esposito, G. Enteric glia: A new player in inflammatory bowel diseases (2015) *International Journal of Immunopathology and Pharmacology*, 28 (4), pp. 443-451. DOI: 10.1177/0394632015599707

RESEARCH

Open Access



# HIV-1 Tat-induced diarrhea is improved by the PPARalpha agonist, palmitoylethanolamide, by suppressing the activation of enteric glia

Giovanni Sarnelli<sup>1\*</sup>, Luisa Seguella<sup>2</sup>, Marcella Pesce<sup>1</sup>, Jie Lu<sup>3</sup>, Stefano Gigli<sup>2</sup>, Eugenia Bruzzese<sup>4</sup>, Roberta Lattanzi<sup>2</sup>, Alessandra D'Alessandro<sup>1</sup>, Rosario Cuomo<sup>1</sup>, Luca Steardo<sup>1,2</sup> and Giuseppe Esposito<sup>2\*</sup>

## Abstract

**Background:** Diarrhea is a severe complication in HIV-1-infected patients with Trans-activator of transcription (HIV-1 Tat) protein being recognized as a major underlying cause. Beside its direct enterotoxic effects, Tat protein has been recently shown to affect enteric glial cell (EGC) activity. EGCs regulate intestinal inflammatory responses by secreting pro-inflammatory molecules; nonetheless, they might also release immune-regulatory factors, as palmitoylethanolamide (PEA), which exerts anti-inflammatory effects by activating PPAR $\alpha$  receptors. We aimed at clarifying whether EGCs are involved in HIV-1 Tat-induced diarrhea and if PEA exerts antidiarrheal activity.

**Methods:** Diarrhea was induced by intracolonic administration of HIV-1 Tat protein in rats at day 1. PEA alone or in the presence of peroxisome proliferator-activated receptor (PPAR) antagonists was given intraperitoneally from day 2 to day 7. S100B, iNOS, NF-kappaB, TLR4 and GFAP expression were evaluated in submucosal plexi, while S100B and NO levels were measured in EGC submucosal plexi lysates, respectively. To verify whether PEA effects were PPAR $\alpha$ -mediated, PPAR $\alpha$ <sup>-/-</sup> mice were also used. After 7 days from diarrhea induction, endogenous PEA levels were measured in submucosal plexi homogenates deriving from rats and PPAR $\alpha$ <sup>-/-</sup> mice.

**Results:** HIV-1 Tat protein induced rapid onset diarrhea alongside with a significant activation of EGCs. Tat administration significantly increased all hallmarks of neuroinflammation by triggering TLR4 and NF-kappaB activation and S100B and iNOS expression. Endogenous PEA levels were increased following HIV-1 Tat exposure in both wildtype and knockout animals. In PPAR $\alpha$ <sup>-/-</sup> mice, PEA displayed no effects. In wildtype rats, PEA, via PPAR $\alpha$ -dependent mechanism, resulted in a significant antidiarrheal activity in parallel with marked reduction of EGC-sustained neuroinflammation.

**Conclusions:** EGCs mediate HIV-1 Tat-induced diarrhea by sustaining the intestinal neuroinflammatory response. These effects are regulated by PEA through a selective PPAR $\alpha$ -dependent mechanism. PEA might be considered as an adjuvant therapy in HIV-1-induced diarrhea.

**Keywords:** HIV-1 Tat protein, EGCs, Diarrhea, Neuroinflammation, PEA

\* Correspondence: [sarnelli@unina.it](mailto:sarnelli@unina.it); [giuseppe.esposito@uniroma1.it](mailto:giuseppe.esposito@uniroma1.it)

<sup>1</sup>Department of Clinical Medicine and Surgery, "Federico II" University of Naples, 80131 Naples, Italy

<sup>2</sup>Department of Physiology and Pharmacology, "Vittorio Erspamer", La Sapienza University of Rome, 00185 Rome, Italy

Full list of author information is available at the end of the article



## Background

The use of combined anti-retroviral therapy against human immunodeficiency virus-type 1 (HIV-1) infection has dramatically improved the survival and prognosis of patients affected by the acquired immunodeficiency syndrome (AIDS) [1]. However, chronic diarrhea is reported in up to 30% of HIV-1-infected patients and significantly contributes to AIDS morbidity [2, 3].

Many of the pathogenic effects of HIV-1 in the gut are caused by the HIV-1 trans-activating factor protein (Tat), a viral protein of 86 aminoacids, which is essential to viral replication [4]. HIV-1 Tat targets enterocytes and induces the expression of many genes regulating cells' survival and growth; but it also affects immune and inflammatory responses, altering the intracellular calcium concentration, inducing epithelial cell apoptosis, and ultimately causing secretory diarrhea [5, 6]. The intestinal epithelial mucosa has been considered for years as the key target in HIV-1 Tat-related enterotoxicity; however, the enteric nervous system (ENS) is now emerging to be also involved [7, 8]. Within the ENS, enteric glial cells (EGCs), together with neurons, cooperate to finely regulate secretion, motility, and blood flow, as well as immune responses [9–11]. EGCs express Toll-like receptors (TLRs), and there is mounting evidence suggesting that they actively participate to the homeostatic immune control of the gut [12]. EGCs are able to secrete pro-inflammatory mediators, interleukins, and enteroglial-released factors [13–15], but they also release a number of protective mediators that sustain epithelial barrier functions [16–18]. Among EGC-derived factors, S100B, a specific glial  $\text{Ca}^{+2}/\text{Zn}^{+2}$ -binding protein, and nitric oxide (NO) deriving from the inducible isoform of nitric oxide synthase (iNOS) expressed by EGCs play a central role during immune-inflammatory responses [14, 19, 20]. We recently demonstrated that glial cells participate to HIV-1 Tat-induced intestinal and neurological pathogenesis [21], but the possibility to pharmacologically modulate Tat-induced secretory diarrhea by inhibiting EGC activation has not been explored yet.

Palmitoylethanolamide (PEA), an endogenous, *on-demand* released N-Acylethanolamide [22–24], exerts immunoregulatory functions targeting EGC activation in ulcerative colitis, with a consistent protection of colonic epithelial mucosa [25]. Different studies have shown that the pharmacological activity of PEA depends on its capacity to selectively bind peroxisome proliferator-activated receptor- $\alpha$  (PPAR $\alpha$ ), a member of a nuclear hormone receptor superfamily of ligand-activated transcription factor [24]. The involvement of and the ability of PEA to protect against HIV-1 Tat-induced diarrhea have never been investigated.

The aims of the present study were to investigate the involvement of EGCs in a rat model of diarrhea induced by the intracolonic administration of HIV-1 Tat, to

characterize the mediators secreted by EGCs activation, and to evaluate the protective effect of PEA, its site, and mechanisms of action, respectively.

## Methods

### Animals and experimental design

Eight-week-old Wistar male rats (Harlan Laboratories, Udine, Italy) and 6-week-old PPAR $\alpha^{-/-}$  mice (Taconic, Germantown, New York, USA) were used for experiments. All procedures were approved by La Sapienza University's Ethics Committee. Animal care was in compliance with the IASP and European Community (EC L358/1 18/12/86) guidelines on the use and protection of animals in experimental research. Rats were randomly divided into the following groups ( $n = 8$  each): non-diarrhea, vehicle group; HIV-1 Tat protein-induced diarrhea group; HIV-1 Tat protein-induced diarrhea group receiving daily PEA 2 and 10 mg/Kg, respectively; HIV-1 Tat protein-induced diarrhea group receiving daily PEA (10 mg/Kg) and selective PPAR $\alpha$  antagonist MK866 (10 mg/Kg) and selective PPAR $\gamma$  antagonist GW9662 (1 mg/Kg), respectively; HIV-1 Tat protein-induced diarrhea group receiving 0.03% *w/v* lidocaine; bisacodyl group (20 mg/Kg) as internal control in some experiments. Analogously, PPAR $\alpha^{-/-}$  mice were randomly divided into the following groups ( $n = 8$  each): non-diarrhea, vehicle group; HIV-1 Tat protein-induced diarrhea group; HIV-1 Tat protein-induced diarrhea group receiving daily PEA 50 and 100 mg/Kg, respectively; HIV-1 Tat protein-induced diarrhea group receiving 0.03% *w/v* lidocaine; bisacodyl group (20 mg/Kg) as internal control in some experiments.

Diarrhea was experimentally induced by intracolonic administration of HIV-1 Tat protein (130 ng/Kg) at day 1. HIV-1 Tat was dissolved in pyrogen-free distilled water and a volume of 400  $\mu\text{l}$  or 40  $\mu\text{l}$  of a 100 ng/ml solution of HIV-1 Tat was injected into the lumen of the rat and PPAR $\alpha^{-/-}$  mice colon (3–4 cm proximal to anus) by using a 24-gauge catheter, respectively. PEA alone, or combined with PPARs antagonists, was given intraperitoneally from day 1 to day 7.

In a subset of experiments, lidocaine hydrochloride monohydrate (Sigma-Aldrich, Milan, Italy, 0.03% *w/v*) dissolved in sterile, pyrogen-free distilled water, was given in a single dose through intracolonic administration at day 1 concomitantly with HIV-1 Tat. In another set of experiments, bisacodyl was administered orally as aqueous solution at day 1 and served as positive internal control. Depending upon the experimental plan, at day 7, animals were euthanatized and colon was isolated to perform macroscopic, histochemical, and biochemical analyses as described below.

### Evaluation of diarrhea

Depending upon the experimental protocol, animals were separated in subgroups and placed separately in cages lined

with filter paper to evaluate diarrhea severity. The individual cages were inspected every 2 h for 16 h, from day 1 to day 7 after HIV 1-Tat intracolonic administration, for the presence of characteristic wet diarrhoeal droppings. Daily defecation frequency and number of unformed water fecal pellets of each animal were assessed and compared with the score from the vehicle group. The data were expressed as a daily mean score (16 h) of diarrhoeal dropping number and total number of fecal pellets/wet spots for defecation frequency within 7 days from diarrhea induction. Evaluation of accumulation of intracolonic fluid was performed using the enteropooling technique according to previously described method [26]. Briefly, enteropooling is defined as the intraluminal accumulation of fluid into the small intestine and corresponds with the fluid already located in the lumen and excreted from the blood. According to the experimental plan, the entire small intestine and colon of rats and PPAR $\alpha^{-/-}$  mice were isolated, taken care to avoid tissue rupture and loss of fluid, by removing the mesentery and connective tissue. To normalize the data, fluid accumulation was expressed as follows:

$$(W_1 - W_2) / W_2 \times 10^{-6}$$

where  $W_1$  is the weight of the intestine after excision and  $W_2$  is the weight of the intestine after expulsion of its content. Water content was measured and compared with the score from vehicle group.

#### Tissue preparation

To isolate submucosal plexi from animals at day 7 after diarrhea induction, we performed a slightly modified method than previously described procedure by Cirillo et al. [14]. Following dissection, colonic segments (approximately 2-cm long) were collected and placed in a cold oxygenated sterile Krebs solution containing (in mM) 117 NaCl, 4.7 KCl, 1.2 MgCl<sub>2</sub>, 6 H<sub>2</sub>O, 1.2 NaH<sub>2</sub>PO<sub>4</sub>, 25 NaHCO<sub>3</sub>, 2.5 CaCl<sub>2</sub>, 2 H<sub>2</sub>O, and 11 glucose under carbogen (5% CO<sub>2</sub>, 95% O<sub>2</sub>) atmosphere equilibrated at pH 7.4. The tissue was longitudinally cut along the mesenteric border, and the submucosal plexus was carefully separated from the mucosal and the muscle layers by microdissection. After removal, submucosal plexi were processed for biochemical and immunofluorescence assays.

#### Protein extraction and western blot analysis

Proteins were extracted from submucosal plexi deriving from rats and PPAR $\alpha^{-/-}$  mice at day 7 after diarrhea induction. The tissue was homogenized in ice-cold hypotonic lysis buffer to obtain cytosolic extracts and underwent electrophoresis through a polyacrilamide minigel. Proteins were transferred into nitrocellulose membrane that were saturated with non-fat dry milk and then incubated with either mouse anti-S100B (Neo-

Marker, Milan, Italy), mouse anti-iNOS, rabbit anti-GFAP, rabbit anti-TLR4, and mouse anti- $\beta$ -actin (all Santa Cruz Biotechnology, Santa Cruz, California, USA). Membranes were then incubated with the specific secondary antibodies conjugated to horseradish peroxidase (Dako, Milan, Italy). Immune complexes were revealed by enhanced chemiluminescence detection reagents (Amersham Biosciences, Milan, Italy). Blots were analyzed by scanning densitometry (GS-700 imaging densitometer; Bio-Rad). Results were expressed as OD (arbitrary units; mm<sup>2</sup>) and normalized on the expression of the housekeeping protein  $\beta$ -actin.

#### Electrophoretic mobility shift assay (EMSA)

EMSA was performed to detect NF-kappaB activation in submucosal plexi obtained from rats and PPAR $\alpha^{-/-}$  mice at day 7 after diarrhea induction. Double-stranded oligonucleotides containing the NF-kappaB recognition sequence for rats (5-CAACGG CAGGGGAATCTCCCTCTCCTT-3) and mice (5-TCAGAGGGGACTTCCGAGAGG-3) were end-labeled with <sup>32</sup>P-ATP. Nuclear extracts were incubated for 15 min with radiolabeled oligonucleotides (2.5–5.0 × 10<sup>4</sup> cpm) in 20 ml reaction buffer containing 2 mg poly dI-dC, 10 mM Tris-HCl (pH 7.5), 100 mM NaCl, 1 mM ethylenediaminetetraacetic acid, 1 mM dl-dithiothreitol, 1 mg/ml bovine serum albumin, and 10% (v/v) glycerol. Nuclear protein-oligonucleotide complexes were resolved by electrophoresis on a 6% non-denaturing polyacrilamide gel in 1 Tris Borate ethylenediaminetetraacetic acid buffer at 150 V for 2 h at 4 °C. The gel was dried and autoradiographed with an intensifying screen at -80 °C for 20 h. Subsequently, the relative bands were quantified by densitometric scanning with Versadoc (Bio-Rad Laboratories) and a computer program (Quantity One Software, Bio-Rad Laboratories). <sup>32</sup>P- $\gamma$ -ATP was from Amersham (Milan, Italy). Poly dI-dC was from Boehringer-Mannheim (Milan, Italy). Oligonucleotide synthesis was performed to our specifications by Tib Molbiol (Boehringer-Mannheim).

#### NO quantification

NO was measured as nitrite (NO<sub>2</sub><sup>-</sup>) accumulation in submucosal plexi homogenates deriving from rats and PPAR $\alpha^{-/-}$  mice at day 7 after diarrhea induction, by a spectrophotometer assay based on the Griess reaction. Briefly, Griess reagent (1% sulphanilamide, 0.1% naphthylethylenediamine in phosphoric acid) was added to an equal volume of supernatant, and the absorbance was measured at 550 nm. Nitrite concentration (nM) was thus determined using a standard curve of sodium nitrite.

#### Enzyme-linked immunosorbent assay for S100B

Enzyme-linked immunosorbent assay (ELISA) for S100B (Biovendor R&D, Brno, Czech Republic) was carried out on submucosal plexi lysates obtained from rats and

PPAR $\alpha^{-/-}$  mice at day 7 after diarrhea induction, according to the manufacturer's protocol. Absorbance was measured on a microtiter plate reader. S100B level was determined using standard curves method.

### Immunofluorescence analysis

Additional experiments were performed using specific isotype antibody controls (Abcam, Cambridge, UK), at the same concentration as the primary antibodies. Tissues were then incubated in the dark with the proper secondary antibody: fluorescein isothiocyanate-conjugated anti-rabbit or Texas Red-conjugated anti-mouse, respectively (both Jackson ImmunoResearch Laboratories, West Grove, PA, USA). Tissues were analyzed with a microscope (Nikon Eclipse 80i), and images were captured by a high-resolution digital camera (Nikon Digital Sight DS-U1).

### Measurement of PEA in rats and mice EGCs

Tissue content of endogenous PEA was measured in submucosal plexi homogenates deriving from both rats and PPAR $\alpha^{-/-}$  mice at day 7 after diarrhea induction. Following isolation of lipidic fraction by tissue homogenates, intracellular PEA concentrations (pmol) were normalized per milligram of extracted lipid fraction and were analyzed by liquid chromatography coupled to tandem mass spectrometry (LC-MS/MS) using a 325-MS LC/MS Triple Quadrupole Mass Spectrometer (Agilent Technologies Italia, Cernusco s/N, Italy) according to literature [27].

### Statistical analysis

Results were expressed as mean  $\pm$  SEM of  $n$  experiments. A statistical analysis was performed using parametric one-way analysis of variance (ANOVA), and multiple comparisons were performed by Bonferroni's post hoc test;  $p$  values  $< 0.05$  were considered significant.

## Results

### Intracolonic administration of HIV-1 Tat induces diarrhea in rats and stimulates the release of endogenous PEA

Intracolonic administration of HIV-1 Tat-induced acute diarrhea, starting from day 1 and lasting up to 7 days post treatment; the severity of which was significantly improved by PEA, in a concentration-dependent fashion and in PPAR $\alpha$ -dependent manner (Fig. 1). Interestingly, the antidiarrheal effect of PEA appeared to be specifically related to HIV-1 Tat administration since PEA treatment failed to significantly inhibit bisacodyl-induced diarrhea, even at the highest dose (Additional file 1).

In order to provide a rationale for the antidiarrheal effect of PEA, we measured its intracellular content in submucosal plexi after 7 days from the induction of the diarrhea. We found that HIV-1 Tat significantly increased the levels of endogenous PEA and that this

increase was significantly inhibited by lidocaine (+147 and -50% vs. vehicle group and HIV-1 Tat group, respectively; all  $p < 0.01$ ; Fig. 2); in rats receiving bisacodyl, the tissue content of PEA was unaffected, likely suggesting that it is dependent by the activation of EGCs.

### HIV-1 Tat induces an inflammatory response through EGC activation that is inhibited by PEA

Administration of HIV-1 Tat induced a significant activation of NF- $\kappa$ B and resulted in an increased expression of GFAP, S100B, TLR4, and iNOS in rat submucosal plexi (Fig. 3, all  $p < 0.001$  vs. vehicle group); significantly, the S100B and nitrite levels were also increased.

PEA treatment significantly reduced HIV-1 Tat-induced NF- $\kappa$ B activation, in a dose-dependent manner (-42 and -58%,  $p < 0.01$  and  $p < 0.001$ ); similarly, the activation of EGCs was inhibited by PEA, with the expression of GFAP (-35 and -69%), S100B (-29 and -65%), TLR4 (-31 and -70%), iNOS (-35 and 74%), and the levels of S100B (-27 and -64%) and nitrite (-30 and -64%) being all significantly reduced ( $p < 0.01$  and  $p < 0.001$ ; at 2 and 10 mg/kg, respectively; Fig. 3). The ability of PEA to reduce HIV-1 Tat-induced EGC activation was significantly inhibited by MK866, but not by GW9662, suggesting that its effect was mediated by PPAR- $\alpha$  rather than by PPAR- $\gamma$ . PEA failed to significantly affect the release of EGC-derived mediators in rats with bisacodyl-induced diarrhea (Fig. 3), and this finding suggests that its effect specifically targets HIV-1 Tat-induced diarrhea by acting on EGC-related activation.

Further supporting the involvement of EGCs, a significantly higher S100B/iNOS expression was observed in the submucosal plexi preparation of HIV-1 Tat-treated rats, compared to vehicle group (+310 and +260%, respectively,  $p < 0.001$ ) (Fig. 4). Treatment with PEA (2-10 mg/kg) reduced the expression of both markers, in a concentration-dependent manner (-28 and -50%, -26 and -40% for S100B and iNOS, respectively;  $p < 0.01$  and  $p < 0.001$  vs. HIV-1 Tat; Fig. 4). Similar to what was reported above, the effect of PEA was inhibited by the presence of the PPAR $\alpha$ -, but not PPAR $\gamma$ -antagonist, while bisacodyl administration failed to modify S100B/iNOS expression (Fig. 4).

### PEA treatment failed to improve HIV-1 Tat-induced diarrhea and EGC-associated neuroinflammation in PPAR $\alpha^{-/-}$ mice

Intracolonic administration of HIV-1 Tat protein induced acute diarrhea in PPAR $\alpha^{-/-}$  mice, similar to what was observed in a subset of wild mice (data not shown) and in rats (Additional file 2); the diarrhea was associated with the increased activation of NF- $\kappa$ B of submucosal enteric glial cells and the upregulation of S100B/iNOS expression (Fig. 5). In line with the results obtained with the PPAR $\alpha$  antagonist, treatment with

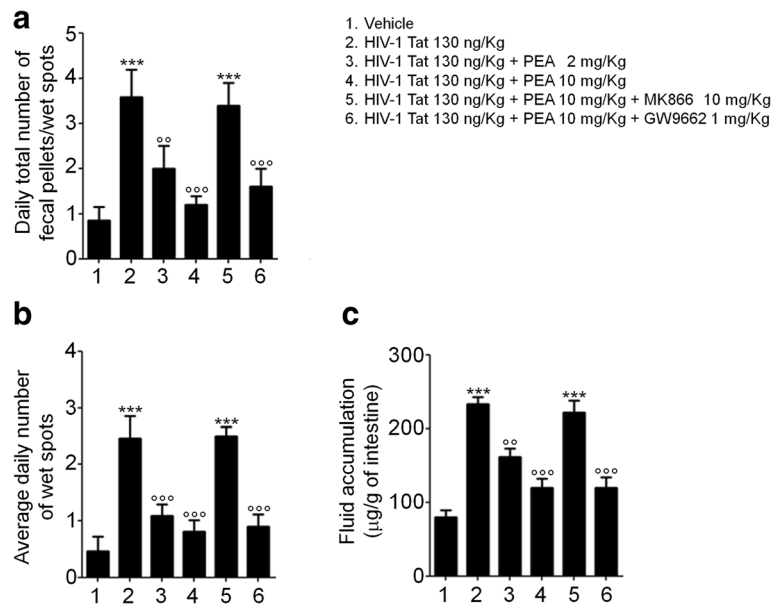


**Fig. 1** Palmitoylethanolamide (PEA) improves diarrheal hallmarks in rats via PPAR $\alpha$  activation. Intracolonic administration of HIV-1 Tat protein (130 ng/Kg) resulted in a significant increase of **a** daily defecation frequency, **b** average daily number of wet spots, and **c** fluid accumulation within 7 days from diarrhea induction. Administration of PEA significantly improved diarrhea in a concentration-dependent manner (at 2 and 10 mg/kg, respectively); the anti-diarrheal activity of PEA was significantly inhibited in the presence of PPAR $\alpha$  antagonist (MK866), whereas PPAR $\gamma$  antagonist (GW9662) had no effect. The results are expressed as mean  $\pm$  SEM of  $n = 5$  experiments. \*\*\* $p < 0.001$  vs. vehicle group; <sup>oo</sup> $p < 0.01$  and <sup>oo</sup> $p < 0.001$  vs. HIV-1 Tat group

PEA, even at highest doses, failed to significantly improve the diarrhea in PPAR $\alpha^{-/-}$  mice and had no effect on the activation of EGCs induced by HIV-1 Tat (Fig. 5).

Bisacodyl treatment was able to induce the diarrhea in PPAR $\alpha^{-/-}$  mice, but was unaffected by the administration of PEA (Fig. 5). Bisacodyl failed to modify the tissue content of endogenous PEA which was, conversely, significantly increased by HIV-1 Tat administration and inhibited by lidocaine (+250% vs. vehicle group, and -55% vs. HIV-1 Tat group, respectively; all  $p < 0.01$ ; Fig. 5).

## Discussion

Secretory diarrhea is a common clinical issue observed in nearly 60–80% of HIV-1 patients, and it is considerably widespread in third-world countries [28]. So far, HIV-1 Tat protein has been identified as the main responsible for the damage of intestinal mucosal, by promoting pro-oxidant and pro-apoptotic-mediated disruption of colonic epithelial cells and consequently the intestinal barrier integrity [5, 29]. More recently, it has been described that HIV-1 Tat protein has an additional effect on the

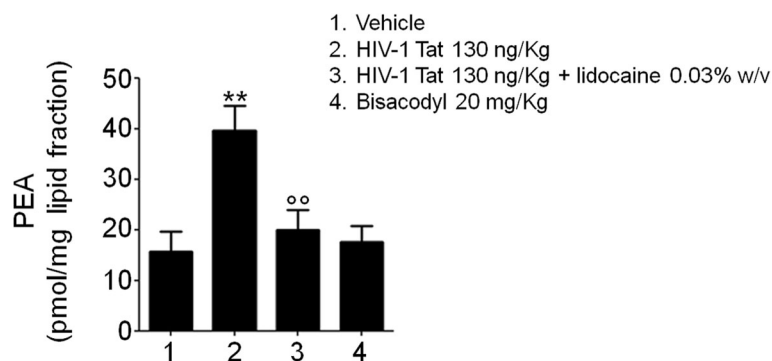
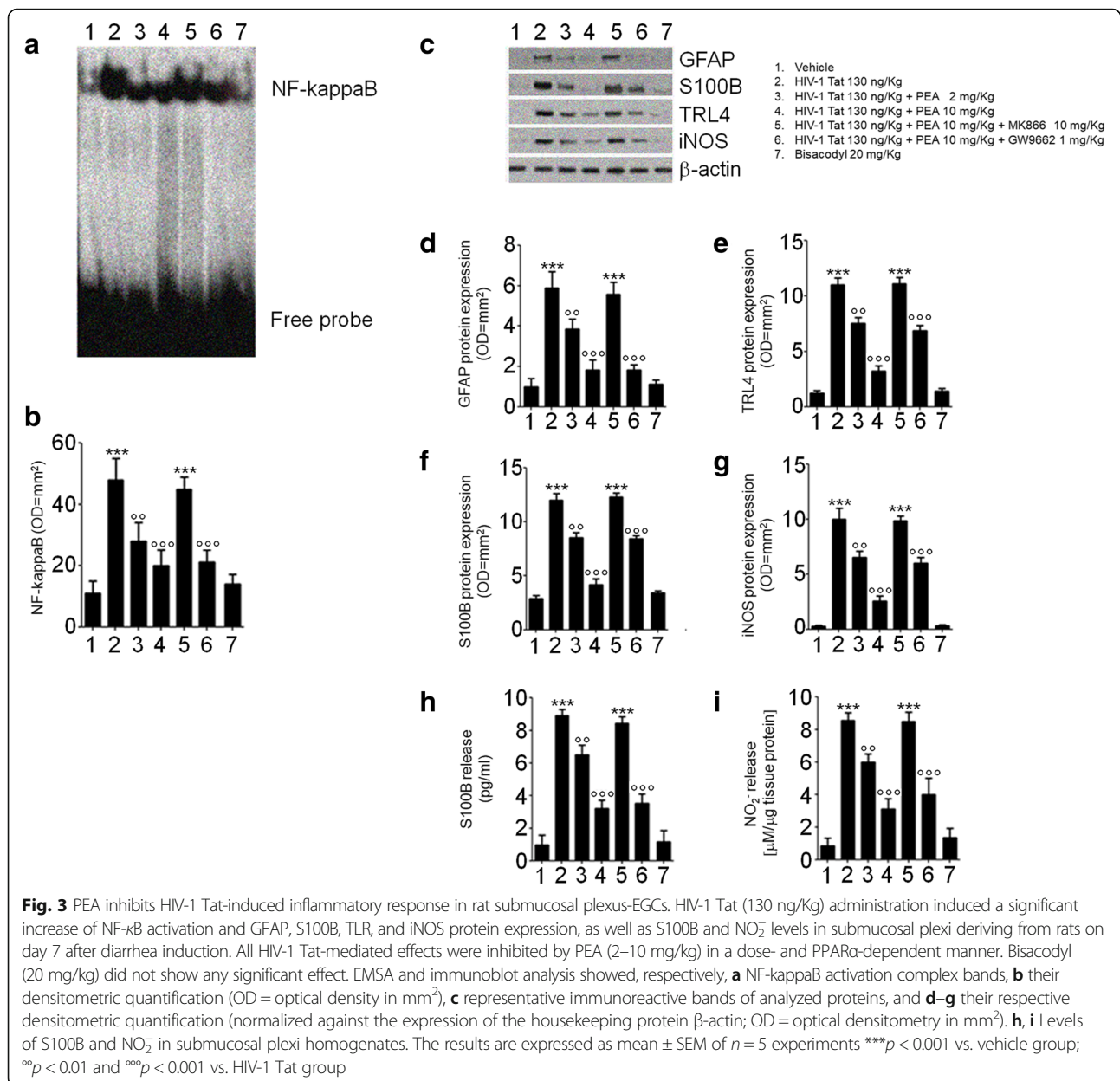


**Fig. 2** HIV-1 Tat administration increases endogenous PEA levels in submucosal plexi EGCs. As a consequence of HIV-1 Tat intracolonic administration, a marked increase of PEA produced in rat submucosal plexi was observed in comparison with vehicle group. Lidocaine (0.03% w/v) counteracted this HIV-1 Tat-induced effect, while bisacodyl treatment did not induce any significant changes in PEA levels. The results are expressed as mean  $\pm$  SEM of  $n = 5$  experiments. \*\* $p < 0.01$  vs. vehicle group; <sup>oo</sup> $p < 0.01$  vs. HIV-1 Tat group



nervous part of the gut, the ENS [7, 21, 30]. This direct action on the nervous system, which regulates many intestinal functions, causes abnormalities in neuronal excitability that, together with the release of pro-inflammatory cytokines in the intestinal milieu, contributes to gut dysfunction described in HIV patients [7].

Our results demonstrate that, beside its effect on enteric neurons, HIV-1 Tat protein also targets EGCs and mediates the overexpression of specific glial markers, as S100B and GFAP, in colonic submucosal plexus with a parallel increase in the expression of iNOS protein and pro-inflammatory signaling molecules (i.e., NO).

These final events occur via activation of the NF-kappaB-mediated cascade and TLR4 activation, two molecular pathways that are linked to each other during EGC activation [25].

The ability of the ENS to modulate virus-induced diarrhea was first reported by Lundgren et al., who showed that the inhibition of enteric nerves excitability was able to significantly inhibit the diarrhea induced by rotavirus [31]. Accordingly, we showed that lidocaine challenge was able to dampen symptoms and biochemical markers indicative for secretory diarrhea, further supporting the role of the ENS, as a whole, in mediating HIV-1 Tat-induced diarrhea. We here show that enteric glia cells take part in mediating the diarrhea induced by viral

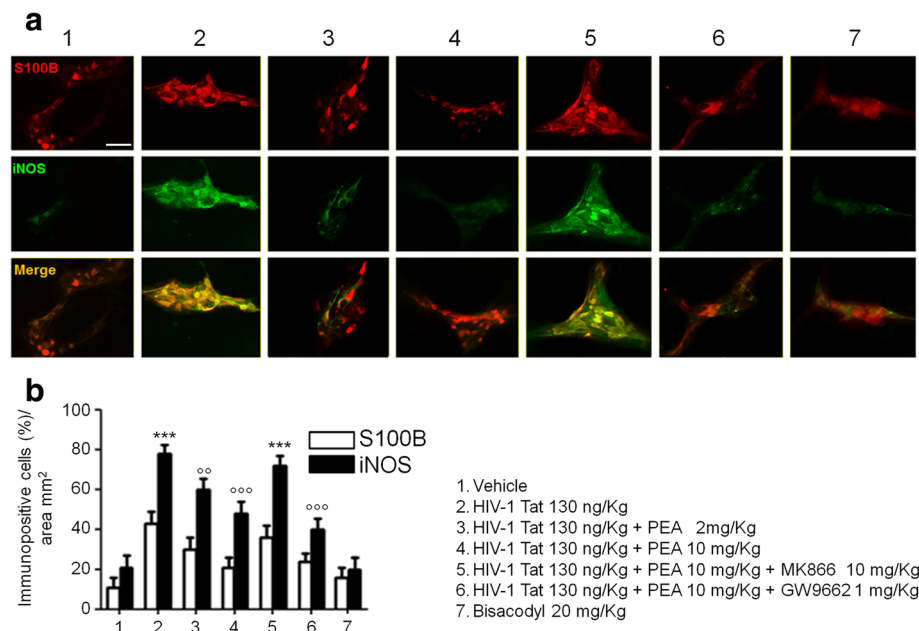


**Fig. 4** PEA reduces S100B/iNOS expression in submucosal plexi of HIV-1 Tat-treated rat. Immunofluorescence analysis showing that HIV-1 Tat (130 ng/Kg) induced a marked increase of S100B and iNOS expression in submucosal plexi that was reduced by PEA through a PPAR $\alpha$ -dependent mechanism. Bisacodyl (20 mg/kg) administration failed to significantly affect S100B/iNOS co-expression. **a** The panel shows S100B (red) and iNOS (green) immunoreactivity and **b** their respective quantification (open and filled bars indicate S100B and iNOS expression, respectively). The results are expressed as mean  $\pm$  SEM of  $n = 5$  experiments. \*\*\* $p < 0.001$  vs. vehicle group;  $^{\circ\circ}p < 0.01$  and  $^{\circ\circ\circ}p < 0.001$  vs. HIV-1 Tat group. Scale bar = 20  $\mu$ m

toxin and that their modulation is able to reduce HIV-1 Tat diarrheagenic effects by inhibiting the overexpression of S100B and iNOS and of the TLR4/NF-kappaB axis, respectively.

Furthermore, supporting the role of EGCs and their activation in HIV-1 Tat diarrhea, we also observed that when the secretory diarrhea was induced by a non-immunological stimulus (i.e., bisacodyl), no significant changes in glial network and markers were noticed.

Furthermore, we evaluated whether PEA was able to decrease glial activation and to improve the diarrhea, respectively. PEA has been recently showed to improve colonic inflammation through EGCs/TLR4-dependent PPAR $\alpha$  activation [25]. Here, we demonstrated that PEA administration significantly and dose-dependently counteracted all diarrheal hallmarks in rodents, as shown by the decrease of stool frequency and weight, and by the rescue of water losses in colonic lumen.

According to our previous reports in human and animal models of intestinal inflammation, we also showed that the anti-diarrheal effect of PEA was selectively mediated by PPAR $\alpha$  receptor activation [25, 32]. In fact, PPAR $\alpha$ , but not PPAR $\gamma$  antagonist, significantly inhibited PEA effects, with this being further confirmed in a transgenic PPAR $\alpha$  knockout model. Though HIV-1 Tat administration in these mice-induced secretory diarrhea, the treatment with PEA, even at high doses, did not evoke any anti-diarrheal effect, likely because the site of action was not expressed.

However, it has to be noted that PPAR $\alpha$  receptor sites are expressed by EGCs, as well as by enteric neurons, supporting that the anti-diarrheagenic effects of PEA are more likely to be the result of its synergistic effects on both neurons and glial cells.

According to our previous results, obtained in an experimental model of colitis [25], PEA was able to dampen EGC activation and the consequent overexpression of S100B and iNOS protein in the submucosal plexus isolated from colon. Moreover, we found that PEA, through the selective PPAR $\alpha$  involvement, blocked the TLR4/NF-kappaB activation in the submucosal plexus of rats with HIV-1 Tat-induced diarrhea. These effects caused a decreased activation of EGCs with the reduction of S100B, GFAP, iNOS, and NO expression in the cell milieu. In PPAR $\alpha^{-/-}$  mice, PEA failed to prevent HIV-1 Tat-induced EGC activation, further confirming that these effects are mediated by PPAR $\alpha$  receptors.

Since its discovery, PEA has been believed to be an endogenous cannabinoid-like lipid able to suppress inflammatory responses in vitro [33]; moreover, PEA has been described to reduce gastrointestinal motility in mice model of colitis [34]. Also, during intestinal inflammation, PEA level increases, most probably as a protective response to mucosal damage [35]. The observation that PEA levels are higher in colonic mucosa of patients with ulcerative colitis and in experimental models of colitis strengths, the hypothesis that this endogenous compound



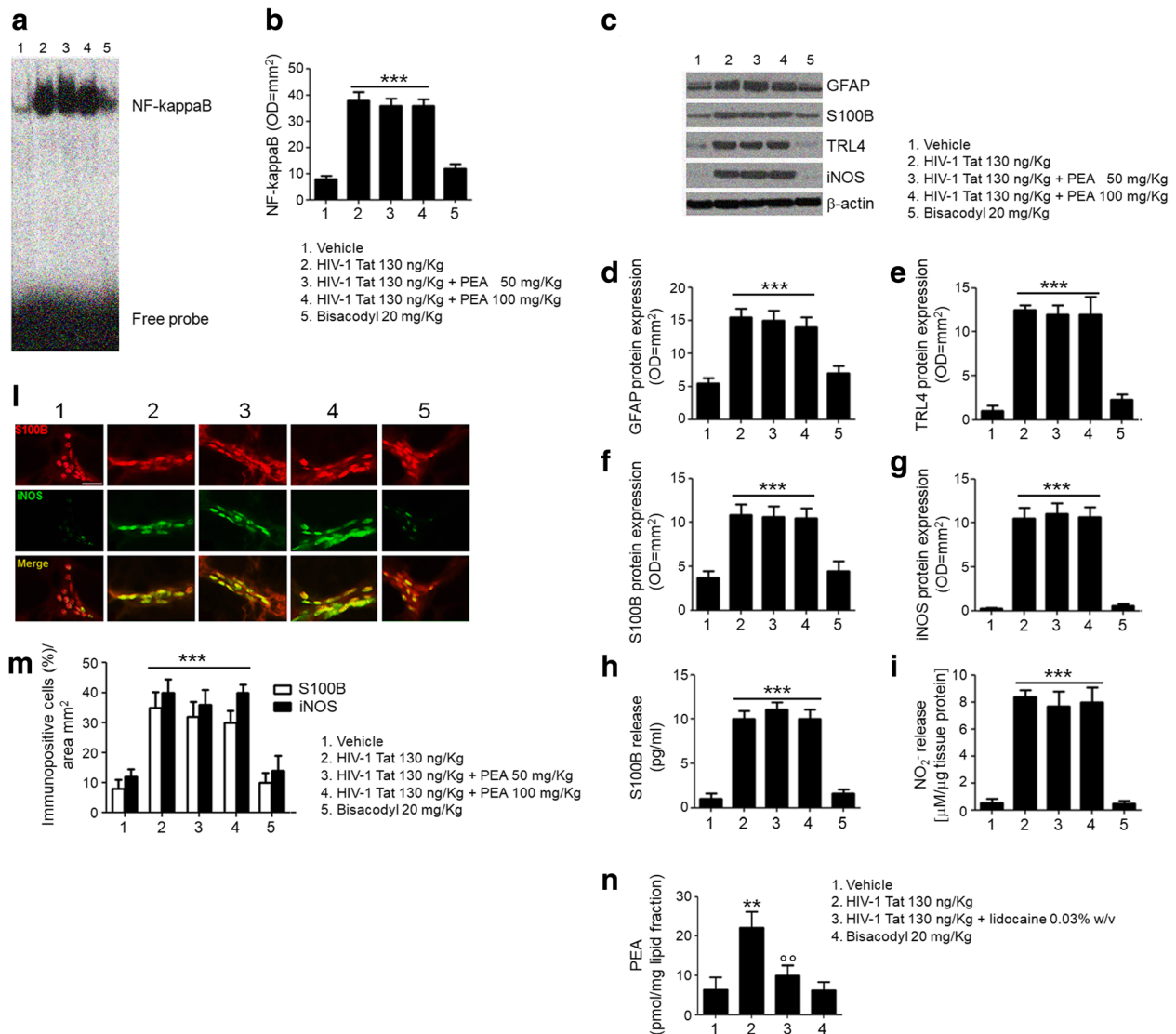


**Fig. 5** PEA fails to counteract submucosal plexus-EGC activation induced by HIV-1 Tat in  $PPAR\alpha^{-/-}$  mice. EMSA analysis showed marked upregulation of NF-kappaB in submucosal plexi at day 7 following HIV-1 Tat administration, compared to vehicle group. PEA was ineffective to reduce NF-kappaB activation in  $PPAR\alpha^{-/-}$  mice, while bisacodyl (20 mg/kg) did not induce NF-kappaB upregulation. **a** Representative NF-kappaB activation complex bands and **b** their densitometric quantification (OD = optical density in mm<sup>2</sup>). HIV-1 Tat significantly increased GFAP, S100B, TLR4, and iNOS protein expression and S100B and NO<sub>2</sub> levels in submucosal plexi isolated from  $PPAR\alpha^{-/-}$  mice in the same experimental conditions. Again, HIV-1 Tat-mediated effects were unaffected by PEA, while bisacodyl did not induce any change in the above investigated parameters. **c** Representative immunoreactive bands of analyzed proteins, **d-g** their respective densitometric quantification (normalized against the expression of the housekeeping protein  $\beta$ -actin; OD = optical densitometry in mm<sup>2</sup>) and **h, i** S100B and NO<sub>2</sub> levels. Immunofluorescence analysis showed an increased S100B/iNOS co-expression in submucosal plexus-EGCs at day 7 after HIV-1 Tat administration, vs. vehicle group. As expected, PEA was unable to counteract HIV-1 Tat activity and bisacodyl did not induce any S100B/iNOS upregulation. **j** S100B (red) and iNOS (green) immunoreactivity with **k** the respective quantification of S100B (open bars) and iNOS (filled bars) expression in the submucosal plexi. **l** HIV-1 Tat caused a marked increase of endogenous PEA content in submucosal plexi vs. vehicle group. Lidocaine inhibited HIV-1 Tat activity, whereas bisacodyl did not produce any alteration in endogenous PEA production. The results are expressed as mean  $\pm$  SEM of  $n = 5$  experiments.  $**p < 0.01$  and  $***p < 0.001$  vs. vehicle group;  $^{\circ}p < 0.01$  and  $^{\circ\circ}p < 0.001$  vs. HIV-1 Tat group. Scale bar = 100  $\mu$ m

may act as “on-demand modulator” of inflammatory processes in the gut [36]. Very interestingly, we found that in our models of HIV-1 Tat-induced diarrhea, the levels of endogenous PEA are significantly increased, while in the

non-immunologic model of diarrhea obtained via bisacodyl administration, they remained unaltered. The fact that the endogenous level of PEA was significantly reduced by lidocaine indicates that, at least in our experimental

conditions, PEA acts specifically by following the immune stimulus (HIV-1 Tat protein), behaving like a regulative ALIAMide and such action is intimately modulated by the ENS, and at least partly mediated by EGC activity.

## Conclusions

Although we cannot definitely rule out the role of enteric neuron dysfunction in mediating these effects, our results indicate that EGCs play a role in HIV-1 Tat-induced diarrhea and highlight the importance of these cells in regulating immune/inflammatory response featuring intestinal disturbance occurring in AIDS infection. We also demonstrated that PEA, by targeting HIV-1 Tat-induced neuroinflammatory responses, significantly modulates the diarrhea and that this occurs through the selective PPAR $\alpha$  involvement. If confirmed by clinical trials in humans, our findings suggest that PEA, given its low cost and toxicological profile [37], might be regarded as promising tool that may integrate the current therapeutic approaches for treating a high-morbidity condition like diarrhea in HIV-infected patients.

## Additional files

**Additional file 1:** PEA failed to inhibit bisacodyl-induced diarrhea in rats. Bisacodyl (20 mg/kg) caused a significant increase of (a) daily defecation frequency, (b) average daily number of wet spots, and (c) fluid accumulation within 7 days from diarrhea induction, vs. vehicle group. PEA (2–10–50 mg/kg) resulted ineffective to exert any anti-diarrheal activity. The results are expressed as mean  $\pm$  SEM of  $n = 5$  experiments. \*\*\* $p < 0.001$  vs. vehicle group. (TIFF 1347 kb)

**Additional file 2:** PEA failed to improve diarrhea course in PPAR $\alpha^{-/-}$  mice. HIV-1 Tat (130 ng/Kg)-induced diarrhea in PPAR $\alpha^{-/-}$  mice, increasing (a) daily defecation frequency, (b) average daily number of wet spots, and (c) fluid accumulation within 7 days from diarrhea induction, vs. vehicle group. PEA (50–100 mg/kg) did not show any significant effect even at highest doses. The results are expressed as mean  $\pm$  SEM of  $n = 5$  experiments. \*\*\* $p < 0.001$  vs. vehicle group. (TIFF 580 kb)

## Abbreviations

AIDS: Acquired immunodeficiency syndrome; ALIAMides: Autacoid local inflammation antagonism amides; ANOVA: Analysis of variance; EDTA: Ethylenediaminetetraacetic acid; EGCs: Enteric glial cells; ELISA: Enzyme-linked immunosorbent assay; EMSA: Electrophoretic mobility shift assay; ENS: Enteric nervous system; GDNF: Glial cell-derived neurotrophic factor; GFAP: Glial fibrillary acidic protein; GSNO: S-nitrosoglutathione; HIV-1: Human immunodeficiency virus-type 1; iNOS: Inducible nitric oxide synthase; LC-MS/MS: Liquid chromatography coupled to tandem mass spectrometry; NO: Nitric oxide; NO $_2^-$ : Nitrite; PEA: Palmitoylethanolamide; PPARs: Peroxisome proliferator-activated receptors; PPAR $\alpha$ : Peroxisome proliferator-activated receptor  $\alpha$ ; PPAR $\alpha^{-/-}$ : Peroxisome proliferator-activated receptor  $\alpha$  knockout; PPAR $\gamma$ : Peroxisome proliferator-activated receptor  $\gamma$ ; Tat: Trans-activating factor protein; TLR4: Toll-like receptor 4; TLRs: Toll-like receptors

## Acknowledgements

Not applicable.

## Funding

G.E. and G.S. were partially funded, respectively, by MIUR (PRIN 2009HLNRL) and La Sapienza University (C26N15YY9F\_ 2015).

## Availability of data and materials

Please contact the authors for data requests.

## Authors' contributions

GS and GE conceived and supervised the project. LS, SG, and AD performed most of the experiments and analyses. MP, RL, and JL helped with the analysis and contributed to the writing and revision of the manuscript. LS performed and contributed to immunofluorescence studies. EB and LSt contributed to the critical revision of the manuscript. All the authors discussed the results and commented on the manuscript. All authors read and approved the final version of the manuscript.

## Ethics approval

All procedures were approved by the local University's Ethics Committee. Animal care was in compliance with the IASP and European Community (EC L358/1 18/12/86) guidelines on the use and protection of animals in experimental research and met stipulations of the guide for the care and use of laboratory animals, as well as recommendations of reduction, refinement, and replacement (known as the 3 Rs).

## Consent for publication

Not applicable

## Competing interests

The authors declare that they have no competing interests.

## Publisher's Note

Springer Nature remains neutral with regard to jurisdictional claims in published maps and institutional affiliations.

## Author details

<sup>1</sup>Department of Clinical Medicine and Surgery, "Federico II" University of Naples, 80131 Naples, Italy. <sup>2</sup>Department of Physiology and Pharmacology, "Vittorio Erispamer", La Sapienza University of Rome, 00185 Rome, Italy. <sup>3</sup>Department of Anatomy, China Medical University, Shenyang, Liaoning Province 110122, People's Republic of China. <sup>4</sup>Department of Translational Medical Science, Section of Pediatrics, University Federico II, 80131 Naples, Italy.

Received: 27 October 2017 Accepted: 9 March 2018

Published online: 24 March 2018

## References

1. Poorolajal J, Hooshmand E, Mahjub H, Esmailnasab N, Jenabi E. Survival rate of AIDS disease and mortality in HIV-infected patients: a meta-analysis. *Public Health*. 2016;139:3–12.
2. Zacharof A. AIDS-related diarrhea—pathogenesis, evaluation and treatment. *Ann Gastroenterol*. 2001;14:22–6.
3. Siddiqui U, Bini EJ, Chandarana K, Leong J, Ramsetty S, Schiliro D, et al. Prevalence and impact of diarrhea on health-related quality of life in HIV-infected patients in the era of highly active antiretroviral therapy. *J Clin Gastroenterol*. 2007;41:484–90.
4. Goldstein G. HIV-1 Tat protein as a potential AIDS vaccine. *Nat Med*. 1996;1:960–4.
5. Buccigrossi V, Laudiero G, Nicastro E, Miele E, Esposito F, Guarino A. The HIV-1 transactivator factor (Tat) induces enterocyte apoptosis through a redox-mediated mechanism. *PLoS One*. 2011;6:e29436.
6. Berni Canani R, Cirillo P, Mallardo G, Buccigrossi V, Secondo A, Annunziato L, et al. Effects of HIV-1 Tat protein on ion secretion and on cell proliferation in human intestinal epithelial cells. *Gastroenterology*. 2003;124:368–76.
7. Ngwainmbi J, De DD, Smith TH, El-Hage N, Fitting S, Kang M, et al. Effects of HIV-1 Tat on enteric neuropathogenesis. *J Neurosci*. 2014;34:14243–51.
8. Galligan JJ. HIV, opiates, and enteric neuron dysfunction. *Neurogastroenterol Motil*. 2015;27:449–54.
9. Aubé A, Cabarrocas J, Bauer J, Philippe D, Aubert P, Doulay F, et al. Changes in enteric neurone phenotype and intestinal functions in a transgenic mouse model of enteric glia disruption. *Gut*. 2006;55:630–8.
10. Nasser Y, Fernandez E, Keenan CM, Ho W, Oland LD, Tibbles LA, et al. Role of enteric glia in intestinal physiology: effects of the gliotoxin fluorocitrate on motor and secretory function. *Am J Physiol Gastrointest Liver Physiol*. 2006;291:G912–27.

11. Capoccia E, Cirillo C, Gigli S, Pesce M, D'Alessandro A, Cuomo R, et al. Enteric glia: a new player in inflammatory bowel diseases. *Int J Immunopathol Pharmacol*. 2015;28:443–51.
12. Barajon I, Serrao G, Arnaboldi F, Opizzi E, Ripamonti G, Balsari A, et al. Toll-like receptors 3, 4, and 7 are expressed in the enteric nervous system and dorsal root ganglia. *J Histochem Cytochem*. 2009;57:1013–23.
13. Turco F, Sarnelli G, Cirillo C, Palumbo I, De Giorgi F, D'Alessandro A, et al. Enteroglia-derived S100B protein integrates bacteria-induced Toll-like receptor signalling in human enteric glial cells. *Gut*. 2014;63:105–15.
14. Cirillo C, Sarnelli G, Turco F, Mango A, Grosso M, Aprea G, et al. Proinflammatory stimuli activates human-derived enteroglia cells and induces autocrine nitric oxide production. *Neurogastroenterol Motil*. 2011;23:e372–82.
15. Ruhl A, Franzke S, Collins SM, Stremmel W. Interleukin-6 expression and regulation in rat enteric glial cells. *Am J Physiol Gastrointest Liver Physiol*. 2001;280:G1163–71.
16. Savidge TC, Newman P, Pothoulakis C, Ruhl A, Neunlist M, Bourreille A, et al. Enteric glia regulate intestinal barrier function and inflammation via release of S-nitrosoglutathione. *Gastroenterology*. 2007;132:1344–58.
17. Zhang DK, He FQ, Li TK, Pang XH, Cui DJ, Xie Q, et al. Glial-derived neurotrophic factor regulates intestinal epithelial barrier function and inflammation and is therapeutic for murine. *J Pathol*. 2010;222:213–22.
18. Van Landeghem L, Mahé MM, Teusan R, Léger J, Guisle I, Houllatte R, et al. Regulation of intestinal epithelial cells transcriptome by enteric glial cells: impact on intestinal epithelial barrier functions. *BMC Genomics*. 2009;10:507.
19. Cirillo C, Sarnelli G, Esposito G, Grosso M, Petruzzelli R, Izzo P, et al. Increased mucosal nitric oxide production in ulcerative colitis is mediated in part by the enteroglia-derived S100B protein. *Neurogastroenterol Motil*. 2009;21:1209–e112.
20. Esposito G, Cirillo C, Sarnelli G, De Filippis D, D'Armiento FP, Rocco A, et al. Enteric glial-derived S100B protein stimulates nitric oxide production in celiac disease. *Gastroenterology*. 2007;133:918–25.
21. Esposito G, Capoccia E, Gigli S, Pesce M, Bruzzese E, Alessandro AD, et al. HIV-1 Tat-induced diarrhea evokes an enteric glia-dependent neuroinflammatory response in the central nervous system. *Sci Rep*. 2017;7:7735.
22. Calignano A, La Rana G, Piomelli D. Antinociceptive activity of the endogenous fatty acid amide, palmitylethanolamide. *Eur J Pharmacol*. 2001;419:191–8.
23. Lambert D, Vandervoort S, Diependaele G, Govaerts S, Robert A. Anticonvulsant activity of N-palmitylethanolamide, a putative endocannabinoid, in mice. *Epilepsia*. 2001;42:321–7.
24. Lo Verme J, Fu J, Astarita G, La Rana G, Russo R, Calignano A, et al. The nuclear receptor peroxisome proliferator-activated receptor- $\alpha$  mediates the anti-inflammatory actions of palmitylethanolamide. *Mol Pharmacol*. 2005;67:15–9.
25. Esposito G, Capoccia E, Turco F, Palumbo I, Lu J, Steardo A, et al. Palmitylethanolamide improves colon inflammation through an enteric glia/toll like receptor 4-dependent PPAR- $\alpha$  activation. *Gut*. 2014;63:1300–12.
26. Ateufack G, Nana Yousseu W, Dongmo Feudjio B, Fonkeng Sama L, Kuiate J, Kamanyi A. Antidiarrheal and in vitro antibacterial activities of leaves extracts of *hibiscus asper*. *Hook f. (malvaceae)*. *Asian J Pharm Clin Res*. 2014;7:130–6.
27. Ghafouri N, Larsson B, Turkina MV, Karlsson L, Fowler CJ, Gerdle BGB. High levels of N-palmitylethanolamide and N-stearylethanolamide in microdialysate samples from myalgic trapezius muscle in women. *PLoS One*. 2011;6:e27257.
28. Weber R. Enteric infections and diarrhea in human immunodeficiency virus-infected persons. *Archives Inter Med*. 1999;159:1473.
29. Nazli A, Chan O, Dobson-belaire WN, Ouellet M, Tremblay MJ, Scott D, et al. Exposure to HIV-1 directly impairs mucosal epithelial barrier integrity allowing microbial translocation. *PLoS Pathog*. 2010;6:e1000852.
30. Fitting S, Ngwainmbi J, Kang M, Khan F a, Stevens DL, Dewey WL, et al. Sensitization of enteric neurons to morphine by HIV-1 Tat protein. *Neurogastroenterol Motil*. 2015;27:468–80.
31. Lundgren O, Peregrin AT, Persson K, Kordasti S, Uhnoo I, Svensson L. Role of the enteric nervous system in the fluid and electrolyte secretion of rotavirus diarrhea. *Science*. 2000;287:491–6.
32. Sarnelli G, Alessandro AD, Iuvone T, Capoccia E, Gigli S, Pesce M, et al. Palmitylethanolamide modulates inflammation-associated vascular endothelial growth factor (VEGF) signaling via the Akt/mTOR pathway in a selective peroxisome proliferator-activated receptor alpha (PPAR- $\alpha$ )-dependent manner. *PLoS One*. 2016;11:e0156198.
33. De Filippis D, Negro L, Vaia M, Cinelli MP, Iuvone T. New insights in mast cell modulation by palmitylethanolamide. *CNS Neurol Disord Drug Targets*. 2013;12:78–83.
34. Capasso R, Izzo AA, Fezza F, Pinto A, Capasso F, Mascolo N, et al. Inhibitory effect of palmitylethanolamide on gastrointestinal motility in mice. *Br J Pharmacol*. 2001;134:945–50.
35. De Filippis D, D'Amico A, Cipriano M, Petrosino S, Orlando P, Di Marzo V, et al. Levels of endocannabinoids and palmitylethanolamide and their pharmacological manipulation in chronic granulomatous inflammation in rats. *Pharmacol Res*. 2010;61:321–8.
36. Costa B, Comelli F, Bettoni I, Colleoni M, Giagnoni G. The endogenous fatty acid amide, palmitylethanolamide, has anti-allodynic and anti-hyperalgesic effects in a murine model of neuropathic pain: involvement of CB(1), TRPV1 and PPARgamma receptors and neurotrophic factors. *Pain*. 2008;139:541–50.
37. Petrosino S, Cristino L, Karsak M, Gaffal E, Ueda N, Tüting T, et al. Protective role of palmitylethanolamide in contact allergic dermatitis. *Allergy*. 2010;65:698–711.

Submit your next manuscript to BioMed Central and we will help you at every step:

- We accept pre-submission inquiries
- Our selector tool helps you to find the most relevant journal
- We provide round the clock customer support
- Convenient online submission
- Thorough peer review
- Inclusion in PubMed and all major indexing services
- Maximum visibility for your research

Submit your manuscript at  
[www.biomedcentral.com/submit](http://www.biomedcentral.com/submit)



## Endocannabinoid-related compounds in gastrointestinal diseases

Marcella Pesce <sup>a, b</sup> , Alessandra D'Alessandro <sup>a</sup>, Osvaldo Borrelli <sup>b</sup>, Stefano Gigli <sup>c</sup>,  
Luisa Seguela <sup>c</sup>, Rosario Cuomo <sup>a</sup>, Giuseppe Esposito <sup>c</sup>, Giovanni Sarnelli <sup>a, \*</sup>

<sup>a</sup> Department of Clinical Medicine and Surgery, 'Federico II' University of Naples, Naples, Italy

<sup>b</sup> Division of Neurogastroenterology & Motility, Great Ormond Street Hospital and University of College (UCL), London, UK

<sup>c</sup> Department of Physiology and Pharmacology 'Vittorio Erspamer', La Sapienza University of Rome, Rome, Italy

Received: May 29, 2017; Accepted: July 23, 2017

### • Introduction

- Endocannabinoid-related compounds
- The endocannabinoid system and the control of gastrointestinal motility
- The endocannabinoid system and the control of visceral sensitivity
- The endocannabinoid system and the control of intestinal inflammation

### • The endocannabinoid system in gut pathophysiology

- The endocannabinoid system and functional dyspepsia
- The endocannabinoid system in irritable bowel syndrome
- The endocannabinoid system in inflammatory bowel disease
- The endocannabinoid system in liver disease
- Endocannabinoids in non-alcoholic fatty liver disease

### • Conclusions

- Conflict of interest

## Abstract

The endocannabinoid system (ECS) is an endogenous signalling pathway involved in the control of several gastrointestinal (GI) functions at both peripheral and central levels. In recent years, it has become apparent that the ECS is pivotal in the regulation of GI motility, secretion and sensitivity, but endocannabinoids (ECs) are also involved in the regulation of intestinal inflammation and mucosal barrier permeability, suggesting their role in the pathophysiology of both functional and organic GI disorders. Genetic studies in patients with irritable bowel syndrome (IBS) or inflammatory bowel disease have indeed shown significant associations with polymorphisms or mutation in genes encoding for cannabinoid receptor or enzyme responsible for their catabolism, respectively. Furthermore, ongoing clinical trials are testing EC agonists/antagonists in the achievement of symptomatic relief from a number of GI symptoms. Despite this evidence, there is a lack of supportive RCTs and relevant data in human beings, and hence, the possible therapeutic application of these compounds is raising ethical, political and economic concerns. More recently, the identification of several EC-like compounds able to modulate ECS function without the typical central side effects of cannabinomimetics has paved the way for emerging peripherally acting drugs. This review summarizes the possible mechanisms linking the ECS to GI disorders and describes the most recent advances in the manipulation of the ECS in the treatment of GI diseases.

**Keywords:** endocannabinoid system • gastrointestinal pathophysiology • functional gastrointestinal disorders • non-alcoholic steatohepatitis • inflammatory bowel disease

## Introduction

*Cannabis sativa* plant is the most commonly used illicit drug for recreational purposes worldwide, with estimated 16 million users in the United States [1, 2]. At present, many patients use cannabis

anecdotally to achieve symptomatic relief from a wide variety of symptoms, commonly of GI origin, particularly nausea and pain [3–5]. The therapeutic efficacy of cannabis in the treatment of GI dysfunction relies on the fact that the GI tract is endowed with cannabinoid receptors and *N*-arachidonylethanolamine (anandamide, AEA) and 2-arachidonoylglycerol (2-AG), their best-characterized endogenous ligands [6, 7]. Together with their synthesizing

\*Correspondence to: Giovanni SARNELLI, M.D., Ph.D.  
E-mail: sarnelli@unina.it

and degrading enzymes, they embody the endocannabinoid system (ECS), a ubiquitous and complex system involved in the control of gut homeostasis. Since first coined in 1995 [8], the term 'endocannabinoids' (ECs) has been enlarged to a number of recently, yet only partially, identified endogenous ligands, such as 2-arachidonoylglycerol ether (noladin ether), *N*-arachidonoyl-dopamine (NADA) and *O*-arachidonylethanolamine (virodhamine) [9]. In recent years, several lipid-derived mediators, closely resembling typical ECs, have been described, raising questions on the different pathophysiological role of these compounds [10–13]. These analogues [namely *N*-linoleylethanolamine (LEA), *N*-oleoylethanolamine (OEA), *N*-palmitoylethanolamine (PEA) and *N*-stearoylethanolamine (SEA)] are structurally related to classical ECs and have been shown to act synergistically, either enhancing the effects of prototypic ECs (the

so-called entourage effect) or displaying unique effects (see the 'Endocannabinoid-related compounds' section). An overview of the principal ECs and of the enzymes responsible for their metabolism is proposed in Figure 1. Different from other transmitters, the ECs and their congeners are not stored in intracytoplasmic vesicles, but synthesized from membrane precursors in an 'on-demand' fashion [13]. After their release into the extracellular space, these short-lived compounds are rapidly removed from membrane transporters and degraded by specific enzymes (Fig. 1) [14]. The ECs are able to exert their multifaceted activities by binding a large number of receptors that have not been fully identified, so far. The best-characterized receptors are cannabinoid receptors 1 and 2 (CB1 and CB2), two G-protein-coupled receptors expressed in both peripheral and central nervous systems, as well as by a number of non-neural

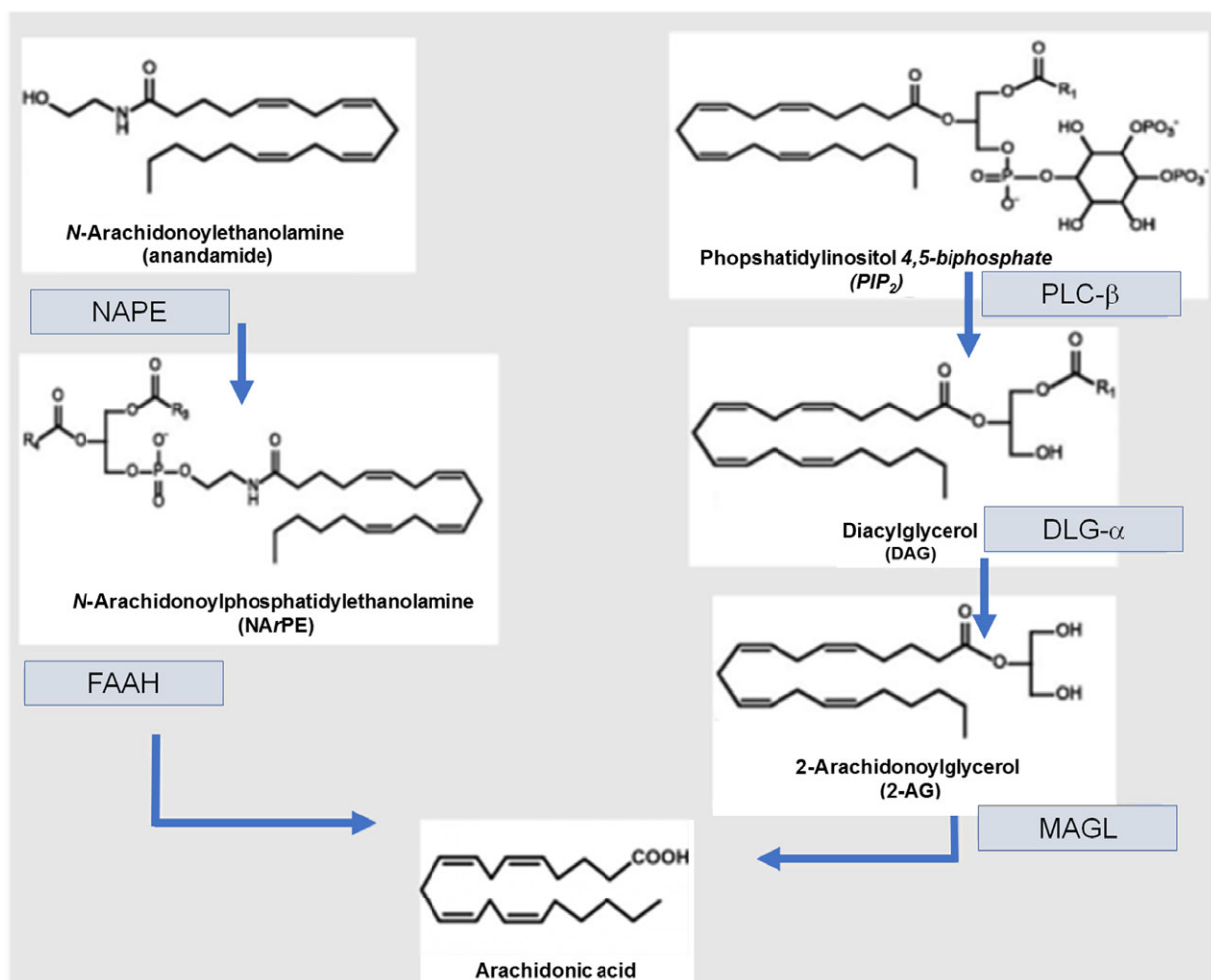


**Fig. 1** Schematic overview of the enzymes involved in EC metabolism. Anandamide (AEA) and 2-acylglycerol (2-AG) are the two best-recognized stereotypical ECs. Both are synthesized by hydrolysis from membrane lipid precursors, namely *N*-arachidonoyl-phosphatidylethanolamine (NArPE) and phosphatidylinositol-4,5-bisphosphate (PIP<sub>2</sub>) for AEA and 2-AG, respectively. Both AEA and 2-AG, after the binding with CB receptors, are rapidly removed by membrane transporters and converted into arachidonic acid by fatty acid amide hydrolase (FAAH) and monoacylglycerol lipase (MAGL), respectively.

cells [6, 15, 16]. CB1 is responsible for the classical psychotropic effects of marijuana and is mainly expressed in the CNS [17]. In the GI tract, CB1 is expressed in both myenteric and submucosal plexuses of the enteric nervous system (ENS), mostly by motoneurons, interneurons and primary afferent neurons but also by epithelial cells [18]. Conversely, CB2 predominantly shows a peripheral distribution, with the highest rate of expression on immune cells [19, 20], but it is also found on enteric neurons [21]. In rodent models, CB2 appears to be expressed by intestinal epithelial cells; however, this evidence has not been confirmed in both other animal models and human beings [22–24]. As mentioned above, ECs and their related compounds exhibit several non-CB1/CB2-mediated effects by binding other receptors with different affinity. The orphan G-protein-coupled receptor 55 (GPR55), identified in 1999, has been proposed as the third CB receptor, and although it has been found in the jejunum, ileum and colon, its distribution has not been extensively studied [25]. One of the best-characterized non-CB receptors for ECs is the transient receptor potential vanilloid type 1 (TRPV1), mainly located on the primary afferent nerve fibres [26]. Originally identified as receptors for the capsaicin [27], TRPV1 receptors are known for being activated by NADA and AEA as effectively as capsaicin [28]. AEA is a full agonist on TRPV1 receptors, but it also exerts indirect effects by binding CB1 [29]. Furthermore, a number of ECs have been shown to bind peroxisome proliferator-activated receptors (PPARs). *In vitro* studies showed that AEA, noladin and virodhamine are receptor agonists to PPAR $\alpha$ , while 2-AG binds to PPAR $\beta/\delta$  [30]. Taken together, the bewildering redundancy of the ECS and the different sites of action of the ECs account for the great variety of actions exhibited by these compounds *in vivo*.

## Endocannabinoid-related compounds

EC-like compounds, such as *N*-acylethanolamides (NAEs), have a close structural resemblance with classical ECs, but display no activity on CB receptors [10, 31, 32]. However, these compounds share some biological activities and similar biosynthetic pathways of those of typical ECs, particularly AEA. AEA synthesis is, indeed, coupled with the formation of PEA, OEA and LEA [10, 33, 34]. Although OEA and PEA do not directly activate cannabinoid receptors, they are thought to indirectly potentiate ECS signalling *via* the ‘entourage effect’ by either competing with stereotypical ECs for enzymatic degradation or increasing their receptor binding affinity [10] (Fig. 2). PEA and OEA are, indeed, both substrates of FAAH, the enzyme responsible for AEA degradation. By either competing with AEA for FAAH or inducing FAAH down-regulation [35, 36], PEA and OEA could reduce AEA catabolism and ultimately increase AEA concentrations. Furthermore, independently of FAAH, PEA and OEA are able to enhance AEA effects at TRPV1 receptors [37, 38]. OEA and PEA can activate, even if with different receptor affinity, PPAR $\alpha$ , the G-protein-coupled receptor GPR119 and the TRPV1 [39–42]. A growing body of evidence has shown that these compounds are involved in the control of a wide variety of functions, including the control of food intake [43, 44], neuroprotection [45] and inhibition of pain and inflammation [46, 47]. PEA levels increase in inflamed tissues, possibly as a protective effect to exert its well-recognized anti-inflammatory and analgesic properties [46]. In biopsies from patients with coeliac disease, levels of both PEA and AEA were increased [48]. It has been shown that by selectively binding PPAR $\alpha$  receptors, PEA is able to down-regulate iNOS expression and nuclear factor- $\kappa$ B (NF $\kappa$ B) activation, and in turn the inflammation in

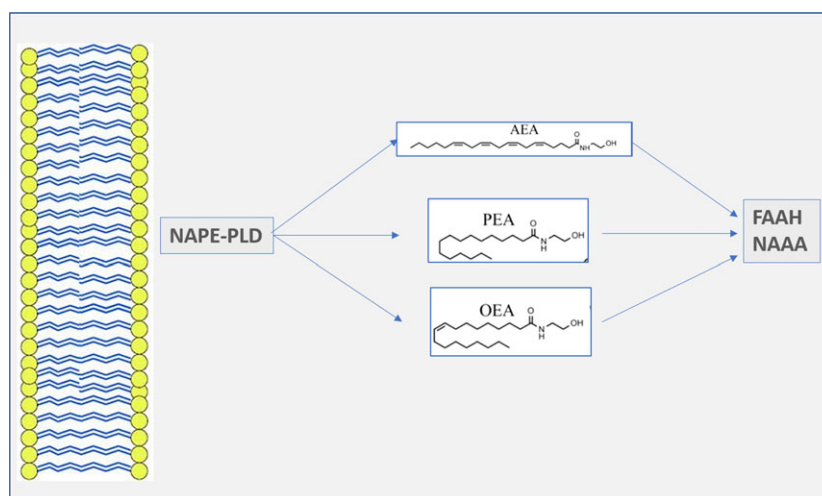


**Fig. 2** Biosynthesis and degradation of *N*-acylethanolamides (NAEs) and possible points of interaction between AEA and its related compounds. Similar to AEA, *N*-palmitoylethanolamine (PEA) and *N*-oleoylethanolamine (OEA) are synthesized by *N*-acylphosphatidylethanolamine-specific phospholipase D (NAPE-PLD) from membrane precursors. Unlike AEA, PEA and OEA exhibit no binding affinity on CB1/CB2 receptors, but they can enhance AEA activity at TRPV1 receptors. PEA and OEA are degraded by either fatty acid amide hydrolase (FAAH) or *N*-acylethanolamine-hydrolysing acid amidase (NAAA). By competing with AEA for FAAH (mainly OEA) or by down-regulating FAAH expression (predominantly PEA), they can increase AEA levels.

a number of chronic inflammatory conditions, including experimental and human models of inflammatory bowel disease (IBD) [49–51]. PEA is indeed able to significantly inhibit the expression of S100B and Toll-like receptor 4 on enteric glial cells, thus reducing inflammation induced by nuclear factor- $\kappa$ B (NF $\kappa$ B) by selectively binding PPAR $\alpha$  receptors [51]. On the contrary, OEA was able to display antinociceptive properties in a PPAR- $\alpha$ -insensitive manner in mice [47].

### **The endocannabinoid system and the control of gastrointestinal motility**

In both animal and human GI tract, the ECs exert marked antipropulsive effects. This result is mainly mediated by the reduction in the release of acetylcholine *via* the activation of presynaptic CB1 [18, 52–54]. However, recent evidence suggests that along with the inhibition of acetylcholine release, the effects of the ECs on GI motility are likely to be related to the inhibition of all the components of the peristaltic reflex. In parallel with the inhibition of the release of acetylcholine, in rat models CB1 agonists were indeed able to significantly inhibit the release of both substance P and VIP, inhibiting, respectively, both the ascending contraction and the descending relaxation of the peristaltic reflex [55–58]. Furthermore, both the deletion of the CB1 gene [55–57] and the pharmacological blockade of these receptors [59–61] displayed prokinetic effects. Altogether, these lines of evidence seem to suggest that ECs are able to significantly reduce smooth muscle contractility, mainly by binding CB1. CB2 does not appear to play a major role in the control of intestinal motility under physiological conditions. However, studies on rodents have shown that intestinal hypermotility due to lipopolysaccharide (LPS) administration was abolished by CB2, but not by CB1 agonists [62]. Hence, in animal models, CB2 agonism is more likely to inhibit intestinal motility in pathophysiological conditions associated with intestinal inflammation and immune activation.

### **The endocannabinoid system and the control of visceral sensitivity**

Undoubtedly, the most documented effect of the ECS is the control of visceral sensitivity and, although empirically grounded, phytocannabinoid-based treatments have been used for centuries in a number of conditions featured by chronic pain. In recent years, several studies have elucidated the molecular mechanism by which ECs are able to reduce visceral sensation and pain. The reduction in visceral sensitivity threshold to colorectal distension was found to be dependent on both CB1 activation and CB2 activation [63–67]. Rousseaux *et al.* have shown that after colorectal distension, orally administered probiotics were able to reduce visceral sensation in rats in a CB2-dependent fashion [68]. Moreover, in pro-inflammatory conditions, AM124 was able to reduce the bradykinin-induced activation of primary afferents

in wild-type but not in CB2-deficient mice [69], further supporting the evidence that CB2 is probably involved in the control of visceral hypersensitivity in inflammatory conditions. In rodents, visceral hypersensitivity due to water avoidance stress was significantly associated with a decreased expression and function of CB1, while a reciprocal increase in TRPV1 expression was found in dorsal root ganglion (DRG) neurons [70]. CB1 and TRPV1 receptors are intimately connected, and CB1 is able to inhibit TRPV1 activity either directly or indirectly through the cyclic AMP–protein kinase A [71]. The treatment of DRG neurons with anandamide, whose levels are increased in psychological stress, was able to reproduce the changes in TRPV1 and CB1 expressions, while administration of CB1 agonist and/or TRPV1 receptor antagonist was able to prevent these effects [70]. Furthermore, injections of corticosteroids were able to increase anandamide expression and to reproduce the reciprocal changes in the expression of CB1 and TRPV1 receptors [70]. Although not completely elucidated, the mechanism underlying the reduced expression of CB1 in chronic stress conditions might rely on increased methylation of the *Cnr1* gene promoter by DNMT1, which results in epigenetic modifications of CB1 expression [72]. Collectively, these findings indicate that the interplay between the cannabinoid and vanilloid signalling pathways may play an important role in stress-induced visceral hyperalgesia [73, 74]. In summary, both CB1 activation and CB2 activation have been linked to the control of visceral sensitivity and stress-induced hyperalgesia in animal models. The antinociceptive effects of CB1 are probably intimately connected to a reciprocal down-regulation of TRPV1 receptors, while CB2 is likely able to counteract the sensitizing effects of inflammatory mediators, such as bradykinin, on peripheral endings of visceral afferents.

### **The endocannabinoid system and the control of intestinal inflammation**

Over the past decade, many lines of evidence highlighting the role of the ECS in intestinal inflammation have been produced in both animal and pre-clinical models [18, 75, 76]. Although genetic studies failed to find any significant association between the polymorphisms in the gene encoding for FAAH and the risk of developing Crohn's disease (CD), homozygosis for the mutation Pro129Thr in FAAH gene was significantly associated with development of fistulas and extra-intestinal manifestations in patients with CD [77]. Also, in patients with ulcerative colitis (UC), the same FAAH genetic variant led to an earlier average onset of the inflammatory disease [77]. Furthermore, in a recent case–control association analysis from a paediatric IBD population, the functional CB2-R63 variant was significantly associated with the risk of developing IBDs and also linked to a more aggressive phenotype in both patients with CD and patients with UC [78]. The pivotal role of the ECS in regulating intestinal inflammation has been confirmed by the evidence that both genetic ablation of FAAH and the pharmacological treatment with

**Table 1** Reported altered expression profile of endocannabinoid system (ECS) in intestinal disease

Clinical condition		AEA	PEA	FAAH	CB1	CB2	Ref.
Ileitis	Mouse	+	=	=	+	+	[54, 74]
Coeliac-like atrophy	Rat	+	+	nd	nd	nd	[48]
Colitis	Mouse	+/-	nd	+/-	nd	nd	[82]
IBD	Human	+/-	*	+/=	+/-	+	[24,62]
Diverticulitis	Human	+	=	nd	=	nd	[75]
FD	Human	nd	nd	nd	+/*	nd	[85]
IBS	Human	nd	*	nd	*	+	[105]
NAFLD/NASH	Human	+	nd	nd	+	*	[116, 117, 120, 121]

+: increase; -: decrease; =: no significant change; nd: not determined; +/-: conflicting results; \*: indirect evidence from administration of agonists/antagonists. IBD: inflammatory bowel disease; FD: functional dyspepsia; IBS: irritable bowel syndrome; NAFLD: non-alcoholic fatty liver disease; NASH: non-alcoholic steatohepatitis.

FAAH inhibitors prevented the development of colitis in rodents [79]. In animal models, these effects are dependent on both CB1 and CB2. CB1 and CB2 agonists are indeed able to significantly reduce experimental colitis, while CB2 antagonists and CB1 knockout mice developed a more severe TNBS-induced colitis [80, 81]. Finally, it has been shown that an increase in AEA levels, induced by inhibitors of the catabolic or reuptake enzymes, significantly attenuates colitis in wild-type mice, but not in CB1- and CB2-deficient mice [82]. In human beings, *ex vivo* studies have demonstrated a significantly increased expression of CB and EC levels in chronic inflammatory conditions, including IBDs, diverticulitis and coeliac disease [48, 74, 75]. An overview of the reciprocal changes in CB receptors and EC level is reported in Table 1. However, both FAAH expression and levels of AEA have been reported to be decreased or increased in colitis from different studies, pointing towards the need for further studies to fully address the role of ECS in the modulation of intestinal inflammation.

## The endocannabinoid system in gut pathophysiology

The homeostatic role of ECS, able to regulate GI functions peripherally and centrally, represents both a blessing and a curse, making it an appealing therapeutic target and, at the same time, a challenge in selectively modulating GI functions without altering the functionality of other organs. We will now discuss in detail the evidence produced on the role of the ECS in GI disorders, namely functional dyspepsia (FD) and irritable bowel syndrome (IBS), two of the main functional gastrointestinal disorders (FGIDs), IBDs and non-alcoholic fatty liver disease (NAFLD). We

will also review the most recent advances in the possible therapeutic exploitation of manipulating ECS in the treatment of these GI disorders.

## The endocannabinoid system and functional dyspepsia

Although only few studies have investigated the potential effects of ECS in FD, there is evidence suggesting that the ECS might be an intriguing target in FD treatment, as it is involved in the modulation of some of the proposed mechanisms underlying FD pathophysiology [83, 84]. In a recent study in patients with FD, Ly *et al.* have demonstrated a sustained increase in CB1 receptor availability in cerebral regions involved in the control of food intake and visceral sensitivity, suggesting for the first time a long-term dysfunction in ECS signalling pathways in FD [85]. However, whether this effect is a consequence of altered visceral sensitivity or of dysregulation in food intake still needs to be clarified. Impaired gastric accommodation, delayed gastric emptying and visceral hypersensitivity have been suggested as the underlying pathophysiological mechanisms of some FD symptoms, such as nausea, early satiety, post-prandial fullness and pain [84, 86, 87]. In experimental animals, CB receptor agonists have been shown to significantly reduce gastric emptying [88, 89]. Similarly, oral administration of dronabinol ( $\Delta^9$ -THC) was able to significantly reduce gastric emptying in human beings [90, 91]. Furthermore, in healthy individuals, administration of a CB1 antagonist (rimonabant) was able to inhibit gastric accommodation, but not affecting gastric sensitivity, suggesting a role of ECS in the control of gastric accommodation [92]. Although further studies are required to fully address the putative role of ECS in FD pathophysiology, the well-recognized orexigenic and antiemetic effects of cannabino-mimetics make the



manipulation of ECS signalling pathway a promising strategy in FD treatment.

### The endocannabinoid system in irritable bowel syndrome

Although the pathophysiology of IBS is still not completely understood, gut motility impairment, visceral hyperalgesia, low-grade inflammation and gut–brain axis alterations have all been associated with symptoms onset [93]; hence, the ECS may represent a new therapeutic target. As ECs are known to decrease GI motility [94, 95], dronabinol, a derivative of THC, has been tested in patients affected by diarrhoea-predominant IBS (IBS-D) showing variable results. It has been shown that this compound was effective in decreasing the colonic transit but not colonic sensitivity, and this effect was limited to those patients carrying CB1 receptor polymorphism rs806378 [96, 97]. Moreover, as the activation of CB1 may reduce GI transit, the use of its antagonist may be used to increase stool frequency in constipation-predominant IBS (IBS-C). Actually, a selective CB1 antagonist, namely rimonabant (SR141716A), was able to increase colonic motility in mice [61]. Interestingly, also the inhibition of the 2-AG synthesizer DAGL using orlistat was found to normalize stool frequency in a mouse model of chronic constipation, without affecting basal motility [98]. In addition, several lines of evidence suggested that the increase in CB1 activity might lead to a reduction in visceral sensitivity [66, 99–101]. Esfandyari *et al.* have tested the efficacy of dronabinol in visceral sensitivity in a randomized, double-blind, placebo-controlled trial showing its ability to increase colonic compliance and relaxation *in vivo* [90]. However, a further study failed to find significant difference in terms of rectal compliance between dronabinol and placebo [97]. This discrepancy may be due to a different expression of CB1 in colon and rectum. Finally, several studies revealed that the ECS also participates in immune response, mainly reducing the production of inflammatory cytokines. Given the evidence for a role of low-grade inflammation in IBS, ECs may also improve IBS symptoms by decreasing the inflammatory response [102–104]. All these lines of evidence confirm that the ECS may represent a new therapeutic target in IBS; however, the risk of adverse effect still limits the use of ECs in treating FGIDs. Therefore, EC-like compounds able to modulate ECS signalling with a good safety profile and, more importantly, without central side effects appear as promising candidates in IBS treatment. Recently, a multi-centre randomized, double-blind, placebo-controlled study has shown the efficacy of orally administered PEA in decreasing the pain severity in patients with IBS. The authors found a significantly increased expression of mast cells and CB2 in IBS, while the levels of OEA were significantly reduced. Furthermore, orally administered PEA significantly improved the pain severity in these patients; however, the authors concluded that it was less obvious whether this effect was dependent on the ECS-induced modulation of visceral hyperalgesia or on mast cell stabilization; hence, further studies evaluating the relation between ECs, inflammation and IBS are needed [105].

### The endocannabinoid system in inflammatory bowel disease

The lines of evidence showing the involvement of ECs in the regulation of inflammatory and immune response in the digestive tract inevitably promoted research on the role of ECs in IBD. The first evidence came from CB1 and CB2 knockout mice that showed a higher susceptibility to chemically induced colitis, suggesting that ECs play a key protective role against chronic inflammation [81, 106]. Moreover, *in vitro* studies showed that AEA and other CB1 agonists promote wound closure in human colonic epithelium and hence might improve mucosal healing in patients with IBD [22]. Furthermore, *in vitro* experiments showed that anandamide and 2-AG increased intestinal permeability when apically administered on Caco-2 cells, and an *in vivo* study in obese mice, a model of leaky gut, showed that the CB1 antagonist rimonabant was able to reduce plasmatic LPS level, confirming the role of ECs in regulating gut permeability [107–109]. Interestingly, further studies have revealed that while CB1 mainly mediates the effects of ECs in a physiological setting, CB2 seems to assume a prevalent role during inflammatory process. Indeed, immunohistochemical studies showed that during inflammatory flares, the expression of CB2, but not of CB1, is modified and amplified [24, 62]. This evidence is very intriguing as CB2 agonists may represent a new therapeutic strategy in IBD, acting directly and specifically on inflamed tissue, thus reducing central adverse effects. Finally, a protective effect of PEA has been demonstrated in human biopsies from patients with active UC, suggesting that exogenous administration of EC-like amides may improve mucosal healing in patients with IBD [51]. As NAEs are already available for treating neuropathic pain, showing a good efficacy and safety profile, further clinical trials to evaluate the therapeutic role of these compounds are clearly required.

### The endocannabinoid system in liver disease

Liver plays a major role in human homeostasis with numerous functions, including regulation of lipid and carbohydrate metabolism, plasma protein synthesis, hormone production and detoxification. The emerging role of ECs in homeostasis and lipid metabolism led several authors to investigate the interactions between the ECS and liver functions in normal and pathological conditions. The cannabinoid receptors are widely distributed on both hepatocytes and cholangiocytes, as on Kupffer and stellate cells, and their expression is modified during liver injury [110–113]. In particular, it was found that the ECS is involved in hepatic haemodynamic, cellular regeneration, liver fibrosis and lipid metabolism. As known, liver haemodynamic dysregulation plays a central role in cirrhosis, indeed portal hypertension and systemic vasodilation are involved in all major cirrhotic complications, such as ascites, variceal bleeding, liver-related cardiomyopathy and increased risk of cardiovascular events [114, 115]. Remarkably, the hypotensive effects of ECs, mainly mediated *via* CB1 activation,

have been associated with cirrhosis-induced vasodilation, and increased levels of AEA have been found in peripheral blood of patients with cirrhosis [116, 117]. In rodent models of cirrhosis, the administration of CB1 antagonist was found to decrease ascites and ameliorate sodium balance, and CB1 was shown to contribute to cardiac contractility alterations related to liver cardiomyopathy, suggesting that CB1 antagonists might be used to improve cardiovascular activity in cirrhosis [118, 119]. ECs have also been associated with fibrosis progression in HCV-infected patients, suggesting a profibrotic activity of ECs. Indeed, CB1 stimulation promotes the activity of myofibroblasts and stellate cells, likely *via* an increased TGF- $\beta$  production [120, 121]. On the contrary, CB2 activation seems to play a protective role against fibrosis, promoting regeneration of liver cells after acute injury. Indeed, selective CB2 agonists have been found to slow fibrosis in a rat model of cirrhosis, and CB2<sup>-/-</sup> knockout mice are more sensitive to acute liver injury, showing a low regenerative response [122, 123]. In summary, although ECs may worsen cirrhosis progression and complications mainly *via* CB1 activation, specific CB2 agonists might slow liver fibrotic evolution.

## Endocannabinoids in non-alcoholic fatty liver disease

The emblematic role of ECS in metabolic syndrome and obesity is already known; indeed, the CB1 antagonist rimonabant has been proposed in obesity treatment due to its beneficial effects on both body-weight and lipid profile. However, the neuropsychiatric adverse effects have limited the clinical use of this compound. Non-alcoholic fatty liver disease (NAFLD) and non-alcoholic steatohepatitis (NASH) are strongly associated with metabolic syndrome, representing the 'liver response' to obesity, dyslipidaemia and altered carbohydrate metabolism. As ECs play a key role in liver lipid metabolism, a great interest is raised on effects of ECs on fatty liver diseases [124]. Cannabinoid receptors are involved in hepatic lipogenesis, inducing specific transcriptional factors, such as SREBPs (sterol regulatory element-binding proteins). Indeed in

a mouse model with a selective deletion of hepatic CB1, a significant reduction in lipid storage during high-fat diet has been observed [125]. Intriguingly, also lipid profile and insulin resistance were improved; however, no effects on BMI have been registered in this murine model, suggesting that other mechanisms are involved in bodyweight regulation [125]. Altogether, these lines of evidence support the role of ECs in hepatic steatosis and fibrotic progression, opening the possibility of new therapeutic options in treatment of NAFLD and NASH; in particular, the efficacy and safety of the CB1 antagonist rimonabant are currently under investigation in a phase III clinical trial for treatment of NASH.

## Conclusions

In the last years, accumulating lines of evidence have pointed out the homeostatic role of the ECS in regulating intestinal motility, sensitivity and inflammation. An impairment of ECS signalling has been suggested to play a key role in several gastrointestinal disorders, such as FGIDs, IBDs and liver diseases. Even if conflicting results have been produced *in vivo*, convincing evidence suggests that pharmacological manipulation of this multifaceted system might provide new therapeutic options in treating GI diseases. The complexity and the redundancy of ECS make the manipulation of this complex system an appealing target for therapeutic purposes, although the possibility of central side effects strongly limited the current use of these compounds in clinical settings. Using peripherally acting drugs with no affinity on central cannabinoid receptors is an intriguing strategy, and as PEA formulations are already available for the treatment of chronic pain, further *in vivo* studies to test the clinical efficacy of these compounds are strongly warranted.

## Conflict of interest

The authors have no conflicting interests to declare.

## References

1. **United Nations Office on Drugs and Crime.** World Drug Report 2015 (United Nations publication, Sales No. E.15.XI.6). Available at [http://www.unodc.org/documents/wdr2015/World\\_Drug\\_Report\\_2015.pdf](http://www.unodc.org/documents/wdr2015/World_Drug_Report_2015.pdf).
2. **Degenhardt L, Ferrari AJ, Calabria B, et al.** The global epidemiology and contribution of cannabis use and dependence to the global burden of disease: results from the GBD 2010 study. *PLoS ONE*. 2013; 8: e76635.
3. **Russo EB.** History of cannabis and its preparations in saga, science, and sobriquet. *Chem Biodivers*. 2007; 4: 1614–48.
4. **Campbell FA, Tramèr MR, Carroll D, et al.** Are cannabinoids an effective and safe treatment option in the management of pain? A qualitative systematic review *BMJ*. 2001; 323: 13–6.
5. **Ware MA, Adams H, Guy GW.** The medicinal use of cannabis in the UK: results of a nationwide survey. *Int J Clin Pract*. 2005; 59: 291–5.
6. **Devane WA, Hanus L, Breuer A, et al.** Isolation and structure of a brain constituent that binds to the cannabinoid receptor. *Science*. 1992; 258: 1946–9.
7. **Sugiura T, Kondo S, Sukagawa A, et al.** 2-Arachidonoylglycerol: a possible endogenous cannabinoid receptor ligand in brain. *Biochem Biophys Res Commun*. 1995; 215: 89–97.
8. **Di Marzo V, Fontana A.** Anandamide, an endogenous cannabinomimetic eicosanoid: 'killing two birds with one stone'. *Prostaglandins Leukot Essent Fatty Acids*. 1995; 53: 1–11.
9. **Di Marzo V.** The endocannabinoid system: its general strategy of action, tools for its pharmacological manipulation and potential therapeutic exploitation. *Pharmacol Res*. 2009; 60: 77–84.
10. **Lambert DM, Di Marzo V.** The palmitoylethanolamide and oleamide enigmas: are these two fatty acid amides cannabinomimetic? *Curr Med Chem*. 1999; 6: 757–73.
11. **Lambert DM, Muccioli GG.** Endocannabinoids and related N-acyl ethanolamines in the control of appetite and energy

- metabolism: emergence of new molecular players. *Curr Opin Clin Nutr Metab Care*. 2007; 10: 735–44.
12. **Di Marzo V, Wang J.** *The Endocannabinoidome: The World of Endocannabinoids and Related Mediators*. Amsterdam: Elsevier; 2015. ISBN 978-0-12-420126-2.
  13. **Piomelli D, Giuffrida A, Calignano A, et al.** The endocannabinoid system as a target for therapeutic drugs. *Trends Pharmacol Sci*. 2000; 21: 218–24.
  14. **Fezza F, Bari M, Florio R, et al.** Endocannabinoids, related compounds and their metabolic routes. *Molecules*. 2014; 19: 17078–106.
  15. **Matsuda LA, Lolait SJ, Brownstein MJ, et al.** Structure of a cannabinoid receptor and functional expression of the cloned cDNA. *Nature*. 1990; 346: 561–4.
  16. **Munro S, Thomas KL, Abu-Shaar M.** Molecular characterization of a peripheral receptor for cannabinoids. *Nature*. 1993; 365: 61–5.
  17. **Howlett AC, Barth F, Bonner TI, et al.** International Union of Pharmacology. XXVII. Classification of cannabinoid receptors. *Pharmacol Rev*. 2002; 54: 161–202.
  18. **Izzo AA, Camilleri M.** Emerging role of cannabinoids in gastrointestinal and liver diseases: basic and clinical aspects. *Gut*. 2008; 57: 1140–55.
  19. **Izzo AA.** The cannabinoid CB(2) receptor: a good friend in the gut. *Neurogastroenterol Motil*. 2007; 19: 704–8.
  20. **Pacher P, Mechoulam R.** Is lipid signaling through cannabinoid 2 receptors part of a protective system? *Prog Lipid Res*. 2011; 50: 193–211.
  21. **Kano M, Ohno-Shosaku T, Hashimoto-dani Y, et al.** Endocannabinoid-mediated control of synaptic transmission. *Physiol Rev*. 2009; 89: 309–80.
  22. **Wright KL, Rooney N, Feeney M, et al.** Differential expression of cannabinoid receptors in the human colon: cannabinoids promote epithelial wound healing. *Gastroenterology*. 2005; 129: 437–53.
  23. **Buckley NE, Hansson S, Harta G, et al.** Expression of the CB1 and CB2 receptor messenger RNAs during embryonic development in the rat. *Neuroscience*. 1998; 82: 1131–49.
  24. **Marqu ez L, Su arez J, Iglesias M, et al.** Ulcerative colitis induces changes on the expression of the endocannabinoid system in the human colonic tissue. *PLoS ONE*. 2009; 4: e6893.
  25. **Brown AJ.** Novel cannabinoid receptors. *Br J Pharmacol*. 2007; 152: 567–75.
  26. **Ross RA.** Anandamide and vanilloid TRPV1 receptors. *Br J Pharmacol*. 2003; 140: 790–801.
  27. **Caterina MJ, Schumacher MA, Tominaga M, et al.** The capsaicin receptor: a heat-activated ion channel in the pain pathway. *Nature*. 1997; 389: 816–24.
  28. **Huang SM, Bisogno T, Trevisani M, et al.** An endogenous capsaicin-like substance with high potency at recombinant and native vanilloid VR1 receptors. *Proc Natl Acad Sci USA*. 2002; 99: 8400–5.
  29. **Ryskamp DA, Redmon S, Jo AO, et al.** TRPV1 and endocannabinoids: emerging molecular signals that modulate mammalian vision. *Cells*. 2014; 3: 914–38.
  30. **Pertwee RG, Howlett AC, Abood ME, et al.** International Union of Basic and Clinical Pharmacology. LXXIX. Cannabinoid receptors and their ligands: beyond CB(1) and CB(2). *Pharmacol Rev*. 2010; 62: 588–631.
  31. **Sheskin T, Hanus L, Slager J, et al.** Structural requirements for binding of anandamide-type compounds to the brain cannabinoid receptor. *J Med Chem*. 1997; 40: 659–67.
  32. **Griffin G, Tao Q, Abood ME.** Cloning and Pharmacological Characterization of the Rat CB2 Cannabinoid Receptor. *J Pharmacol Exp Ther*. 2000; 292: 886–94.
  33. **Ben-Shabat S, Fride E, Sheskin T, et al.** An entourage effect: inactive endogenous fatty acid glycerol esters enhance 2-arachidonoyl-glycerol cannabinoid activity. *Eur J Pharmacol*. 1998; 353: 23–31.
  34. **Mechoulam R, Fride E, Di Marzo V.** Endocannabinoids. *Eur J Pharmacol*. 1998; 359: 1–18.
  35. **Fowler CJ, Jonsson KO, Tiger G.** Fatty acid amide hydrolase, biochemistry, pharmacology, and therapeutic possibilities for an enzyme hydrolyzing anandamide, 2-arachidonoylglycerol, palmitoylethanolamide, and oleamide. *Biochem Pharmacol*. 2001; 62: 517–26.
  36. **Di Marzo V, Melck D, Orlando P.** Palmitoylethanolamide inhibits the expression of fatty acid amide hydrolase and enhances the anti-proliferative effect of anandamide in human breast cancer cells. *Biochem J*. 2001; 358: 249–55.
  37. **De Petrocellis L, Davis JB, Di Marzo V.** Palmitoylethanolamide enhances anandamide stimulation of human vanilloid VR1 receptors. *FEBS Lett*. 2001; 506: 253–6.
  38. **Borrelli F, Izzo AA.** Role of acylethanolamides in the gastrointestinal tract with special reference to food intake and energy balance. *Best Pract Res Clin Endocrinol Metab*. 2009; 23: 33–49.
  39. **Ho W-SV, Barrett DA, Randall MD.** 'Entourage' effects of N-palmitoylethanolamide and N-oleoylethanolamide on vasorelaxation to anandamide occur through TRPV1 receptors. *Br J Pharmacol*. 2008; 155: 837–46.
  40. **LoVerme J, La Rana G, Russo R, et al.** The search for the palmitoylethanolamide receptor. *Life Sci*. 2005; 77: 1685–98.
  41. **Capasso R, Matias I, Lutz B, et al.** Fatty acid amide hydrolase controls mouse intestinal motility *in vivo*. *Gastroenterology*. 2005; 129: 941–51.
  42. **Matias I, Gonthier MP, Petrosino S, et al.** Role and regulation of acylethanolamides in energy balance: focus on adipocytes and beta-cells. *Br J Pharmacol*. 2007; 152: 676–90.
  43. **Matias I, Di Marzo V.** Endocannabinoids and the control of energy balance. *Trends in Endocrinol Metab*. 2007; 18: 27–37.
  44. **Williams CM, Kirkham TC.** Anandamide induces overeating: mediation by central cannabinoid (CB1) receptors. *Psychopharmacology*. 1999; 143: 315–7.
  45. **Ahn EH, Kim DW, Shin MJ, et al.** Pep-1-PEA-15 protects against toxin-induced neuronal damage in a mouse model of Parkinson's disease. *Biochim Biophys Acta*. 2014; 1840: 1686–700.
  46. **Lo Verme J, Fu J, Astarita G, et al.** The nuclear receptor peroxisome proliferator-activated receptor- $\alpha$  mediates the anti-inflammatory actions of palmitoylethanolamide. *Mol Pharmacol*. 2005; 67: 15–9.
  47. **Suard'az M, Estivill-Torru's G, Goicoechea C, et al.** Analgesic properties of oleoylethanolamide (OEA) in visceral and inflammatory pain. *Pain*. 2007; 133: 99–110.
  48. **D'Argenio G, Petrosino S, Gianfrani C, et al.** Overactivity of the intestinal endocannabinoid system in celiac disease and in methotrexate-treated rats. *J Mol Med*. 2007; 85: 523–30.
  49. **Lowin T, Apitz M, Anders S, et al.** Anti-inflammatory effects of N-acylethanolamines in rheumatoid arthritis synovial cells are mediated by TRPV1 and TRPA1 in a COX-2 dependent manner. *Arthritis Res Ther*. 2015; 17: 321.
  50. **Impellizzeri D, Ahmad A, Bruschetta G, et al.** The anti-inflammatory effects of palmitoylethanolamide (PEA) on endotoxin-induced uveitis in rats. *Eur J Pharmacol*. 2015; 15: 28–35.
  51. **Esposito G, Capoccia E, Turco F, et al.** Palmitoylethanolamide improves colon inflammation through an enteric glia/toll like receptor 4-dependent PPAR- $\alpha$  activation. *Gut*. 2014; 63: 1300–12.

52. **Mulè F, Amato A, Baldassano S, et al.** Involvement of CB1 and CB2 receptors in the modulation of cholinergic neurotransmission in mouse gastric reparations. *Pharmacol Res.* 2007; 56: 185–92.
53. **Croci T, Manara L, Aureggi G, et al.** *In vitro* functional evidence of neuronal cannabinoid CB1 receptors in human ileum. *Br J Pharmacol.* 1998; 125: 1393–5.
54. **Manara L, Croci T, Guagnini F, et al.** Functional assessment of neuronal cannabinoid receptors in the muscular layers of human ileum and colon. *Dig Liver Dis.* 2002; 34: 262–9.
55. **Yucec B, Sibaev A, Broedl U, et al.** Cannabinoid type 1 receptor modulates intestinal propulsion by an attenuation of intestinal motor responses within the myenteric part of the peristaltic reflex. *Neurogastroenterol Motil.* 2007; 19: 744–53.
56. **Aviello G, Romano B, Izzo AA.** Cannabinoids and gastrointestinal motility: animal and human studies. *Eur Rev Med Pharmacol Sci.* 2008; 1(Suppl): 81–93.
57. **Sibaev A, Yucec B, Kemmer M, et al.** Cannabinoid-1 (CB1) receptors regulate colonic propulsion by acting at motor neurons within the ascending motor pathways in mouse colon. *Am J Physiol Gastrointest Liver Physiol.* 2008; 296: G119–28.
58. **Grider JR, Mahavadi S, Li Y, et al.** Modulation of motor and sensory pathways of the peristaltic reflex by cannabinoids. *Am J Physiol Gastrointest Liver Physiol.* 2009; 297: G539–49.
59. **Colombo G, Agabio R, Lobina C, et al.** Cannabinoid modulation of intestinal propulsion in mice. *Eur J Pharmacol.* 1998; 344: 67–9.
60. **Izzo AA, Mascolo N, Tonini M, et al.** Modulation of peristalsis by cannabinoid CB(1) ligands in the isolated guinea-pig ileum. *Br J Pharmacol.* 2000; 129: 984–90.
61. **Pinto L, Izzo AA, Cascio MG, et al.** Endocannabinoids as physiological regulators of colonic propulsion in mice. *Gastroenterology.* 2002; 123: 227–34.
62. **Duncan M, Mouihate A, Mackie K, et al.** Cannabinoid CB2 receptors in the enteric nervous system modulate gastrointestinal contractility in lipopolysaccharide treated rats. *Am J Physiol Gastrointest Liver Physiol.* 2008; 295: G78–87.
63. **Sanson M, Bueno L, Fioramonti J.** Involvement of cannabinoid receptors in inflammatory hypersensitivity to colonic distension in rats. *Neurogastroenterol Motil.* 2006; 18: 949–56.
64. **Fioramonti J, Bueno L.** Role of cannabinoid receptors in the control of gastrointestinal motility and perception. *Expert Rev Gastroenterol Hepatol.* 2008; 2: 385–97.
65. **Kikuchi A, Ohashi K, Sugie Y, et al.** Pharmacological evaluation of a novel cannabinoid 2 (CB2) ligand, PF-03550096, *in vitro* and *in vivo* by using a rat model of visceral hypersensitivity. *J Pharmacol Sci.* 2008; 106: 219–24.
66. **Brusberg M, Arvidsson S, Kang D, et al.** CB1 receptors mediate the analgesic effects of cannabinoids on colorectal distension-induced visceral pain in rodents. *J Neurosci.* 2009; 29: 1554–64.
67. **Ravnefjord A, Brusberg M, Kang D, et al.** Involvement of the transient receptor potential vanilloid 1 (TRPV1) in the development of acute visceral hyperalgesia during colorectal distension in rats. *Eur J Pharmacol.* 2009; 611: 85–91.
68. **Rousseaux C, Thuru X, Gelot A, et al.** *Lactobacillus acidophilus* modulates intestinal pain and induces opioid and cannabinoid receptors. *Nat Med.* 2007; 13: 35–7.
69. **Hillsley K, McCaul C, Aerssens J, et al.** Activation of the cannabinoid 2 (CB2) receptor inhibits murine mesenteric afferent nerve activity. *Neurogastroenterol Motil.* 2007; 19: 769–77.
70. **Hong S, Zheng G, Wu X, et al.** Corticosterone mediates reciprocal changes in CB1 and TRPV1 receptors in primary sensory neurons in the chronically stressed rat. *Gastroenterology.* 2011; 140: 627–37. e4.
71. **Bhave G, Zhu W, Wang H, et al.** cAMP-dependent protein kinase regulates desensitization of the capsaicin receptor (VR1) by direct phosphorylation. *Neuron.* 2002; 35: 721–31.
72. **Hong S, Zheng G, Wiley JW.** Epigenetic regulation of genes that modulate chronic stress-induced visceral pain in the peripheral nervous system. *Gastroenterology.* 2015; 148: 148–57.
73. **Hong S, Fan J, Kemmerer ES, et al.** Reciprocal changes in vanilloid (TRPV1) and endocannabinoid (CB1) receptors contribute to visceral hyperalgesia in the water avoidance stressed rat. *Gut.* 2009; 58: 202–10.
74. **Izzo AA, Sharkey KA.** Cannabinoids and the gut: new developments and emerging concepts. *Pharmacol Ther.* 2010; 126: 21–38.
75. **Guagnini F, Valenti M, Mukenge S, et al.** Neural contractions in colonic strips from patients with diverticular disease: role of endocannabinoids and substance P. *Gut.* 2006; 55: 946–53.
76. **Schicho R, Storr M.** Targeting the endocannabinoid system for gastrointestinal diseases: future therapeutic strategies. *Expert Rev Clin Pharmacol.* 2010; 3: 193–207.
77. **Storr M, Emmerdinger D, Diegelmann J, et al.** The role of fatty acid hydrolase gene variants in inflammatory bowel disease. *Aliment Pharmacol Ther.* 2009; 29: 542–51.
78. **Strisciungio C, Bellini G, Miele E, et al.** Cannabinoid Receptor 2 Functional Variant Contributes to the Risk for Pediatric Inflammatory Bowel Disease. *J Clin Gastroenterol.* 2016; [Epub ahead of print].
79. **Sařaga M, Mokrowiecka A, Zakrzewski PK, et al.** Experimental colitis in mice is attenuated by changes in the levels of endocannabinoid metabolites induced by selective inhibition of fatty acid amide hydrolase (FAAH). *J Crohns Colitis.* 2014; 8: 998–1009.
80. **Storr M, Emmerdinger D, Diegelmann J, et al.** The cannabinoid 1 receptor (CNR1) 1359 G/A polymorphism modulates susceptibility to ulcerative colitis and the phenotype in Crohn's disease. *PLoS ONE.* 2010; 5: e9453.
81. **Massa F, Marsicano G, Hermann H, et al.** The endogenous cannabinoid system protects against colonic inflammation. *J Clin Invest.* 2004; 113: 1202–9.
82. **D'Argenio G, Valenti M, Scaglione G, et al.** Up-regulation of anandamide levels as an endogenous mechanism and a pharmacological strategy to limit colon inflammation. *FASEB J.* 2006; 20: 568–70.
83. **Tack J, Bisschops R, Sarnelli G.** Pathophysiology and treatment of functional dyspepsia. *Gastroenterology.* 2004; 127: 1239–55.
84. **Sarnelli G, Vandenberghe J, Tack J.** Visceral hypersensitivity in functional disorders of the upper gastrointestinal tract. *Dig Liver Dis.* 2004; 36: 371–6.
85. **Ly HG, Ceccarini J, Weltens N, et al.** Increased Cerebral Cannabinoid-1 Receptor Availability Is a Stable Feature of Functional Dyspepsia: A [18 F]MK-9470 PET Study. *Psychother Psychosom.* 2015; 84: 149–58.
86. **Tack J, Piessevaux H, Coulie B, et al.** Role of impaired gastric accommodation to a meal in functional dyspepsia. *Gastroenterology.* 1998; 115: 1346–1352.
87. **Tack J, Caenepeel P, Fischler B, et al.** Symptoms associated with hypersensitivity to gastric distention in functional dyspepsia. *Gastroenterology.* 2001; 121: 526–35.
88. **Calignano A, La Rana G, Makrivanis A, et al.** Inhibition of intestinal motility by

- anandamide, an endogenous cannabinoid. *Eur J Pharmacol.* 1997; 340: R7–8.
89. **Izzo AA, Capasso R, Pinto L, et al.** Effect of vanilloid drugs on gastrointestinal transit in mice. *Br J Pharmacol.* 2001; 132: 1411–6.
  90. **Esfandiyari T, Camilleri M, Busciglio I, et al.** Effects of a cannabinoid receptor agonist on colonic motor and sensory functions in humans: a randomized, placebo-controlled study. *Am J Physiol Gastrointest Liver Physiol.* 2007; 293: G137–45.
  91. **Esfandiyari T, Camilleri M, Ferber I, et al.** Effect of a cannabinoid agonist on gastrointestinal transit and postprandial satiation in healthy human subjects: a randomized, placebo-controlled study. *Neurogastroenterol Motil.* 2006; 18: 831–8.
  92. **Ameloot K, Janssen P, Scarpellini E, et al.** Endocannabinoid control of gastric sensorimotor function in man. *Aliment Pharmacol Ther.* 2010; 31: 1123–31.
  93. **Drossman DA.** Functional gastrointestinal disorders: history, pathophysiology, clinical features and Rome IV. *Gastroenterology.* 2016; doi: 10.1053/j.gastro.2016.02.032. [Epub ahead of print].
  94. **Reichenbach ZW, Shey R.** Cannabinoids and GI disorders: endogenous and exogenous. *Curr Treat Options Gastroenterol.* 2016; 14: 14461–77.
  95. **Hornby PJ, Prouty SM.** Involvement of cannabinoid receptors in gut motility and visceral perception. *Br J Pharmacol.* 2004; 141: 1335–45.
  96. **Wong BD, Camilleri M, Busciglio I, et al.** Pharmacogenetics trial on a cannabinoid agonist shows reduced fasting colonic motility in patients with non-constipated irritable bowel syndrome. *Gastroenterology.* 2011; 141: 1638–47.
  97. **Wong BD, Camilleri M, Eckert D, et al.** Randomized pharmacodynamics and pharmacogenetics trial on dronabinol effects on colon transit in irritable bowel syndrome-diarrhea. *Neurogastroenterol Motil.* 2012; 24: 358–e169.
  98. **Bashashati M, Nasser Y, Keenan C, et al.** Inhibiting endocannabinoid biosynthesis: a novel approach to the treatment of constipation. *Br J Pharmacol.* 2015; 172: 3099–111.
  99. **Fichna J, Wood JT, Papanastasiou M, et al.** Endocannabinoid and cannabinoid-like fatty acid amine levels correlate with pain-related symptom in patient with IBS-D and IBS-C: a pilot study. *PLoS ONE.* 2013; 8: e85073.
  100. **Duncan M, Davison JS, Sharkey KA** Review article: endocannabinoids and their receptors in the enteric nervous system. *Aliment Pharmacol Ther.* 2005; 22: 667–83.
  101. **Booker L, Naidu PS, Razdan RK, et al.** Evaluation of prevalent phytocannabinoids in the acetic acid model of visceral nociception. *Drug Alcohol Depend.* 2009; 105: 42–7.
  102. **Barbara G, De Giorgio R, Stanghellini V, et al.** A role for inflammation in irritable bowel syndrome? *Gut.* 2002; 51: i41–4.
  103. **Hirota A, Eikichi I, Kazuhiko N.** Low-grade inflammation plays a pivotal role in gastrointestinal dysfunction in irritable bowel syndrome. *World J Gastrointest Pathophysiol.* 2010; 1: 97–105.
  104. **Greisen WE, Turner H.** Immunoreactive effects of cannabinoids: considerations for therapeutic use of cannabinoid receptor agonists and antagonists. *Int Immunopharmacol.* 2010; 10: 547–55.
  105. **Barbara G, Cremon C, Bellacosa L, et al.** Randomized Placebo-Controlled Multicenter Study on the effect of palmitoylethanolamide and polydatin on immune activation in patients with irritable bowel syndrome. *Gastroenterology.* 2014. 146, Issue 5, Supp 1, Page S–124.
  106. **Engel MA, Kellermann CA, Burnat G, et al.** Mice lacking cannabinoid CB1-CB2 receptors or both receptors show increased susceptibility to TNBS-induced colitis. *J Physiol Pharmacol.* 2010; 61: 89–97.
  107. **Alhamoruni A, Lee AC, Wright KL, et al.** Pharmacological effects of cannabinoids on Caco2 cells culture model of intestinal permeability. *J Pharmacol Exp Ther.* 2010; 335: 92–102.
  108. **Muccioli GG, Naslain D, Bäckhed F, et al.** The endocannabinoid system links gut microbiota to adipogenesis. *Mol Syst Biol.* 2010; 6: 392.
  109. **Alhamoruni A, Wright KL, Larvin M, et al.** Cannabinoids mediate opposing effects on inflammation-induced intestinal permeability. *Br J Pharmacol.* 2012; 165: 2598–610.
  110. **Xu X, Liu Y, Hung S, et al.** Overexpression of cannabinoid receptors CB1 and CB2 correlates with improved prognosis of patients with hepatocellular carcinoma. *Cancer Genet Cytogenet.* 2006; 171: 31–8.
  111. **Mukhopadhyay B, Liu J, Osei-Hyiaman D, et al.** Transcriptional regulation of cannabinoid receptor-1 expression in the liver by retinoic acid acting via retinoic acid receptor-gamma. *J Biol Chem.* 2010; 285: 19002–11.
  112. **Floreani A, Lazzari R, Macchi V, et al.** Hepatic expression of endocannabinoid receptors and their novel polymorphisms in primary biliary cirrhosis. *J Gastroenterol.* 2009; 45: 68–76.
  113. **Tam J, Liu J, Mukhopadhyay B, et al.** Endocannabinoids and liver disease. *Hepatology.* 2011; 53: 346–355.
  114. **Møller S, Henriksen JH.** Cirrhotic cardiomyopathy: a pathophysiological review of circulatory dysfunction in liver disease. *Heart.* 2002; 87: 9–15.
  115. **Rockey D.** The cellular pathogenesis of portal hypertension: stellate cell contractility, endothelin, and nitric oxide. *Hepatology.* 1997; 25: 1.
  116. **Balkai S, Jarai Z, Wagner JA, et al.** Endocannabinoids acting at vascular CB1 receptors mediated the vasodilated state in advanced liver cirrhosis. *Nat Med.* 2001; 7: 827–32.
  117. **Caraceni P, Viola A, Piscitelli Giannone F, et al.** Circulating and hepatic endocannabinoids and endocannabinoids-related molecules in patients with cirrhosis. *Liver Int.* 2010; 30: 816–25.
  118. **Domenicali M, Caraceni P, Giannone F, et al.** Cannabinoid type 1 receptor antagonism delays ascites formation in rats with cirrhosis. *Gastroenterology.* 2009; 137: 341–9.
  119. **Gaskari SA, Homar H, Lee SS.** Therapy insight: cirrhotic cardiomyopathy. *Nat Clin Pract Gastroenterol Hepatol.* 2006; 3: 329–37.
  120. **Teixeira-Clerc F, Julien B, Grenard P, et al.** CB1 cannabinoid receptor antagonism: a new strategy for the treatment of liver fibrosis. *Nat Med.* 2006; 12: 671–6.
  121. **Hezod C, Roudot-Thoraval F, Nguyen S, et al.** Daily cannabis smoking as a risk factor for progression of fibrosis in chronic hepatitis C. *Hepatology.* 2005; 42: 63–71.
  122. **Munoz-Luque J, Ros J, Fernandez-Varo G, et al.** Regression of fibrosis after chronic stimulation of cannabinoid CB2 receptor in cirrhotic rats. *J Pharmacol Exp Ther.* 2008; 324: 475–83.
  123. **Lotersztajn S, Teixeira-Clerc F, Julien B, et al.** CB2 receptors as a new therapeutic target for liver diseases. *Br J Pharmacol.* 2008; 153: 286–9.
  124. **Caraceni P, Domenicali M, Giannone F, et al.** The role of the endocannabinoid system in liver diseases. *Best Pract Res Clin Endocrinol Metab.* 2009; 23: 65–77.
  125. **Osei-Hyiaman D, Liu J, Zhou L, et al.** Hepatic CB1 receptor is required for development of diet-induced steatosis, dyslipidemia, and insulin and leptin resistance in mice. *J Clin Invest.* 2008; 118: 3160–3169.

# Cannabidiol restores intestinal barrier dysfunction and inhibits the apoptotic process induced by *Clostridium difficile* toxin A in Caco-2 cells

Stefano Gigli<sup>1</sup>, Luisa Seguella<sup>1</sup>, Marcella Pesce<sup>2</sup>, Eugenia Bruzzese<sup>3</sup>,  
Alessandra D'Alessandro<sup>2</sup>, Rosario Cuomo<sup>2</sup>, Luca Steardo<sup>1</sup>,  
Giovanni Sarnelli<sup>2</sup> and Giuseppe Esposito<sup>1</sup>

## Abstract

**Background:** *Clostridium difficile* toxin A is responsible for colonic damage observed in infected patients. Drugs able to restore *Clostridium difficile* toxin A-induced toxicity have the potential to improve the recovery of infected patients. Cannabidiol is a non-psychotropic component of *Cannabis sativa*, which has been demonstrated to protect enterocytes against chemical and/or inflammatory damage and to restore intestinal mucosa integrity.

**Objective:** The purpose of this study was to evaluate (a) the anti-apoptotic effect and (b) the mechanisms by which cannabidiol protects mucosal integrity in Caco-2 cells exposed to *Clostridium difficile* toxin A.

**Methods:** Caco-2 cells were exposed to *Clostridium difficile* toxin A (30 ng/ml), with or without cannabidiol ( $10^{-7}$ – $10^{-9}$  M), in the presence of the specific antagonist AM251 ( $10^{-7}$  M). Cytotoxicity assay, transepithelial electrical resistance measurements, immunofluorescence analysis and immunoblot analysis were performed in the different experimental conditions.

**Results:** *Clostridium difficile* toxin A significantly decreased Caco-2 cells' viability and reduced transepithelial electrical resistance values and RhoA guanosine triphosphate (GTP), bax, zonula occludens-1 and occludin protein expression, respectively. All these effects were significantly and concentration-dependently inhibited by cannabidiol, whose effects were completely abolished in the presence of the cannabinoid receptor type 1 (CB1) antagonist, AM251.

**Conclusions:** Cannabidiol improved *Clostridium difficile* toxin A-induced damage in Caco-2 cells, by inhibiting the apoptotic process and restoring the intestinal barrier integrity, through the involvement of the CB1 receptor.

## Keywords

*Clostridium difficile*, cannabinoids, cannabidiol, *Clostridium difficile* toxin A, intestinal permeability

Received: 31 October 2016; accepted: 15 February 2017

## Introduction

*Clostridium difficile* infection (CDI) is responsible for the pseudomembranous colitis, a serious pathological condition of the large intestine, characterised by massive inflammation and bleeding.<sup>1</sup> It is known that *Clostridium difficile* produces two enterotoxins, named *Clostridium difficile* toxin A and B (TcdA and TcdB, respectively) that, in turn, are responsible for the extensive colonic mucosal damage, causing severe diarrhoea, colitis, shock and death in most severe cases.<sup>2,3</sup> TcdA is the major cause of *Clostridium difficile* enterotoxicity. TcdA is a glucosyltransferase, that once internalised

<sup>1</sup>Department of Physiology and Pharmacology, La Sapienza University of Rome, Rome, Italy

<sup>2</sup>Department of Clinical Medicine and Surgery, University of Naples 'Federico II', Naples, Italy

<sup>3</sup>Department of Translational Medical Science, University of Naples 'Federico II', Naples, Italy

### Corresponding author:

Giovanni Sarnelli, Department of Clinical Medicine and Surgery, University of Naples 'Federico II', Naples, Italy.

Email: sarnelli@unina.it

into the host cell via receptor-mediated endocytosis, inactivates small GTPases.<sup>4</sup> Among these proteins, RhoA, a small GTPase member of the Rho subfamily that is a critical regulator of actin cytoskeleton and tight junction assembly, is the primary target of TcdA.<sup>5</sup> TcdA-induced inactivation of RhoA results in the transition from guanosine triphosphate (GTP)-bound form (active) to guanosine diphosphate (GDP)-bound form (inactive), leading to an alteration of cellular structure and tight junction integrity, and consequently to increased epithelial barrier permeability; this process is also sustained by the acute inflammation of colonic mucosa and contributes to the leaky gut and massive ions' secretion.<sup>6</sup> Due to its role in the mucosal homeostasis and functions, the targeting of RhoA may represent an innovative pharmacological strategy for the treatment of CDI.

In the last decade, cannabinoids extracted from the marijuana plant (*Cannabis sativa*) and synthetic cannabinoids have shown numerous beneficial effects on gastrointestinal (GI) functions.<sup>7</sup> Non-psychotropic phytocannabinoid cannabidiol (CBD) is one of the most interesting compounds, since it exerts a wide range of beneficial pharmacological actions on GI functions, ranging from antioxidant to antiinflammatory activities.<sup>8,9</sup> Unlike psychoactive cannabinoids such as tetrahydrocannabinol (THC), CBD has little binding affinity to cannabinoid receptors (either CB1 and CB2); whereas, by acting on peroxisome proliferator-activated receptor gamma (PPAR $\gamma$ )<sup>10</sup> and 5-hydroxytryptamine (5HT)-1A receptors,<sup>11</sup> it displays antiinflammatory and antioxidant effects.<sup>12</sup> Unlike other phytocannabinoids, CBD has been shown to act as a non-competitive negative allosteric modulator of CB1 receptors.<sup>13</sup> Notably, CBD is able to restore in vitro intestinal permeability increased by ethylenediaminetetraacetic acid (EDTA) or pro-inflammatory stimuli.<sup>14,15</sup> So far, no evidence has been produced about the putative protective role exerted by CBD in CDI. To further this aim, the present study was addressed at evaluating the in vitro effects of CBD on TcdA-induced apoptosis in Caco-2 cells and at investigating the effects of CBD and its mechanism of action.

## Materials and methods

### Materials

The experiments were performed in human Caucasian colon adenocarcinoma (Caco-2) cells that have been shown to be a good model to address TcdA toxicity in vitro.<sup>16</sup> Caco-2 cells were purchased from European Collection of Cell Cultures (ECACC, Public Health England, Porton Down, Salisbury, UK). Cell medium, chemicals and reagents used for

cell culture, and TcdA were obtained from Sigma-Aldrich (St. Louis, Missouri, USA). Instruments, reagents, and materials used for Western blot analysis were obtained from Bio-Rad Laboratories (Milan, Italy). CBD and AM251 (CB1 receptor antagonist) were purchased from Tocris Cookson, Inc. (Ballwin, Missouri, USA). The antibodies rabbit anti-zonula occludens-1 (ZO-1), rabbit anti-occludin, rabbit anti-bax and rabbit anti-glyceraldehyde-3-phosphate dehydrogenase (GAPDH) antibodies were procured from Cell Signalling Technology (Danvers, Massachusetts, USA). Mouse anti-ZO-1 antibody was purchased from Santa Cruz Biotechnology (Santa Cruz, California, USA). Mouse monoclonal antibody anti-active RhoA by New East Bioscience (Pennsylvania, USA) has been used. Fluorescein isothiocyanate-conjugated anti-rabbit antibody and Texas red conjugated anti-mouse antibody were purchased from Abcam (Cambridge, UK) and horseradish peroxidase (HRP) was obtained from Dako (Milan, Italy).

### Cell culture and experimental conditions

Caco-2 cells were grown at 37°C with 5% CO<sub>2</sub> in Dulbecco's modified Eagle's medium (DMEM) in addition with 10% foetal bovine serum (FBS), 1% penicillin-streptomycin, 2mM L-glutamate, and 1% non-essential amino acids. Caco-2 cells were plated at a density of  $1 \times 10^6$  cells/well in six-well plates and incubated for 24 h. Every 24–48 h the medium was replaced with fresh medium to confluence. After reaching confluence, the cells were washed three times with phosphate-buffered saline (PBS), detached with trypsin/EDTA, plated in six-well plates some containing and on polyethylene-terephthalate (PET) filter inserts (Falcon Becton-Dickinson, 0.4 mm pore diameter, area 4.21 cm<sup>2</sup>, pore density  $2 \pm 0.2 \times 10^6$ /cm<sup>2</sup>) to measure the transepithelial electrical resistance (TEER), and allowed to adhere for an appropriate time. Caco-2 cells were randomly divided into the following groups: vehicle, 30 ng/ml TcdA, 30 ng/ml TcdA plus CBD at  $10^{-9}$ ,  $10^{-8}$  and  $10^{-7}$  M CBD and 30 ng/ml TcdA plus  $10^{-7}$  M CBD plus  $10^{-7}$  M CB1 receptor antagonist AM251. The concentrations of CBD and AM251 were selected on the basis of previous reports<sup>14,15</sup> and our preliminary experiments (Supplementary Material, Figure 1, data not shown); in brief, cells were treated with different concentrations of CBD and/or AM251 for 24 h and then incubated at 37°C in the presence of TcdA for 24 h.

### TEER

Caco-2 (TEER) was measured using the EVOM volt-ohm meter (World Precision Instruments Germany,

Berlin, Germany) according to the method described by Wells and colleagues.<sup>17</sup>

In brief, cells were used for experimentation between 14–21 days and each epithelial cell layer with a TEER value greater than  $1000 \Omega \times \text{cm}^2$ , was considered to have tight adhesion. At this point, cell monolayers were treated according to experimental protocol described above and TEER measurements were performed at different time points (2, 3, 5, 7, 12, 18 and 24 h, respectively). TEER values were measured at a current of 20 mA, corrected for background, resistance value without cells, and normalised by multiplying the determined resistance by effective membrane growth area,  $4.71 \text{ cm}^2$ .

$$\text{TEER} (\Omega \times \text{cm}^2) = (\text{Total resistance} - \text{blank resistance}) (\Omega) \times \text{Area} (\text{cm}^2)$$

### Cytotoxicity assay

The 3-[4,5-dimethylthiazol-2-yl]-2,5 diphenyltetrazolium bromide (MTT) assay was used to determine Caco-2 cell proliferation and survival.<sup>18</sup> At least ( $5 \times 10^4$  cells/well) were plated in 96-well plates and allowed to adhere for 3 h. Then DMEM was replaced with fresh medium and then cells were treated according to the different experimental protocols (see above). After 24 h, 25  $\mu\text{l}$  MTT (5 mg/ml MTT in DMEM) was added to the cells and the mixture was incubated for further 3 h at 37°C. Subsequently, the cells were lysed and the dark blue crystals were solubilised using a 100  $\mu\text{l}$  solution containing 50% N,N-dimethylformamide and 20% (w/v) sodium dodecyl sulphate (SDS) (pH 4.5). The optical density (OD) of each well was determined using a microplate spectrophotometer equipped with a 620 nm filter (PerkinElmer, Inc.; Waltham, Massachusetts, USA).

### Western blot analysis

Twenty-four hours after treatment, the cells ( $1 \times 10^6$ /well) were washed with ice-cold PBS, were harvested into Separate Eppendorf tubes for different treatment groups and collected by centrifugation at 180 g for 10 min at 4°C. The cell pellet, obtained after centrifugation, was re-suspended in 100  $\mu\text{l}$  ice-cold hypotonic lysis buffer (10 mM 4-(2-hydroxyethyl)-1-piperazineethanesulfonic acid (HEPES), 1.5 mM  $\text{MgCl}_2$ , 10 mM KCl, 0.5 mM phenylmethylsulphonyl fluoride, 1.5  $\mu\text{g}/\text{ml}$  soybean trypsin inhibitor, 7  $\mu\text{g}/\text{ml}$  pepstatin A, 5  $\mu\text{g}/\text{ml}$  leupeptin, 0.1 mM benzamide and 0.5 mM dithiothreitol (DTT)) and incubated on ice for an additional 15 min.

The suspension was rapidly passed through a syringe needle five to six times to lyse the cells and then

centrifuged for 15 min at  $13,000 \times g$  to obtain the cytoplasmic fraction. The cytoplasmic fraction proteins were used to determine the protein concentration with Bradford assay and mixed with non-reducing gel loading buffer (50 mM Tris (hydroxymethyl) aminomethane (Tris), 10% SDS, 10% glycerol, 2 mg bromophenol/ml) at a 1:1 ratio. The solutions were then boiled for 3 min, centrifugated at 10,000 g for 10 min and 50  $\mu\text{g}$  of each homogenate was used for electrophoresis using 12% discontinuous polyacrylamide mini gels. Proteins were then transferred to nitrocellulose membranes that were saturated by incubation with 10% non-fat dry milk in 1X PBS overnight at 4°C and then incubated with rabbit anti-ZO-1 (1:1000), rabbit anti-occludin (1:1000), mouse anti-active RhoA (1:1000), rabbit anti-bax (1:1000) and rabbit anti-GAPDH (1:1000) antibodies. After being extensively washed in TBS 1X with 0.1% Tween 20, membranes were then incubated for 2 h at room temperature with the specific secondary antibodies conjugated to HRP anti-mouse (1:2000) or anti-rabbit (1:3000). Immune complexes were identified by enhanced chemiluminescence detection reagents (Amersham Biosciences, Milan, Italy) and the blots were analysed by scanning densitometry (GS-700 Imaging 143 Densitometer; Bio-Rad, Segrate, Italy). Results are expressed as OD; (arbitrary units; mm<sup>2</sup>) and normalised against the expression of the house-keeping protein GAPDH.

### Immunofluorescence

For these experiments, Caco-2 cells were cultured onto coverslips until confluence, and then treated according to the different above-described protocols. Cells were then fixed for 30 min in 4% formaldehyde, washed with ice-cold PBS and permeabilised with 0.3% Triton-X100 in PBS for one hour. Subsequently, 2% bovine serum albumin (BSA) was used to block the nonspecific binding sites. The cells were then incubated overnight with mouse anti-ZO-1 (1:100), or rabbit anti-occludin antibody (1:100), following PBS washing and further incubated in the dark for half an hour with the appropriate secondary antibody (fluorescein isothiocyanate (FITC)-conjugated anti-rabbit or Texas red conjugated anti-mouse). After final PBS washing, the cells were analysed using a microscope (Nikon Eclipse 80i), and images were captured with a high-resolution digital camera (Nikon Digital Sight DS-U1). Texas Red was excited at a wavelength of 568 nm and collected through a long pass filter (590LP). FITC was excited with a wavelength of 488 nm and collected with a narrow band filter (515–540BP). Texas Red and FITC were assigned to the red and green channels respectively of the generated RGB channel image.



## Statistical analysis

Results are expressed as mean  $\pm$  standard error of the mean (SEM) of four or five experiments and each experiment was performed in triplicate. Statistical analysis was performed using parametric one-way analysis of variance (ANOVA) and Bonferroni's post-hoc test was used for multiple comparisons. Values of  $p < 0.05$  were considered significant.

## Results

### CBD affects TcdA-induced damage of epithelial barrier integrity and restores the expression of ZO-1 and occludin

TEER measurements were performed to evaluate the effect of CBD ( $10^{-7}$ ,  $10^{-8}$  and  $10^{-9}$  M) alone, or in the presence of CB1 antagonist AM251, on epithelial barrier integrity of Caco-2 cells layers exposed to TcdA (30 ng/ml) for 24 h.

As shown in Figure 1(a), TcdA exposure induced a significant and time-dependent reduction of TEER (by  $-35$ ,  $-46$ ,  $-57$ ,  $-69$ ,  $-78$ ,  $-81$  and  $-86\%$ , at 2, 3, 5, 7, 12, 18 and 24 h, respectively;  $p < 0.01$  at 2 h and  $p < 0.001$  at all other time-points). Starting from 2 h after toxin challenge, the effect of TcdA on electrical resistance was significantly and concentration-dependently counteracted by CBD treatment (Figure 1(a)); TEER values at 2, 3, 5, 7, 12, 18 and 24 h were indeed significantly increased by 15, 33, 56, 73, 119, 133 and 225% in CBD  $10^{-9}$  M-treated cells ( $p = ns$  at 2 h and  $p < 0.01$  at all other time-points), while CBD  $10^{-8}$  M and CBD  $10^{-7}$  M treatments yield to a significant increase of TEER values by 31, 52, 90, 133, 219, 239, 361%, and 38, 65, 114, 193, 300, 372 and 538%, respectively ( $p < 0.01$  at 2 and 3 h and  $p < 0.001$  at all other time points for CBD  $10^{-8}$  M;  $p < 0.01$  at 2, 3 and 5 h and  $p < 0.001$  at all other time-points for CBD  $10^{-7}$  M).

Interestingly, the effect of CBD on the TcdA-induced TEER reduction was completely abolished in the presence of the CB1 antagonist, AM251 ( $p < 0.01$ , Figure 1(a)).

Immunofluorescence analysis, showed that  $10^{-7}$  M CBD, markedly reversed the TcdA-induced decrease of both occludin and ZO-1 co-expression in cultured cells, thus restoring the epithelial barrier architecture (Figure 1(b)). This finding was confirmed by quantitative analysis showing that TcdA-reduced expression of occludin and ZO-1 ( $0.3 \pm 0.1$  and  $0.2 \pm 0.1$  vs  $1.0 \pm 0.1$  fold-change in the vehicle group, respectively; all  $p < 0.001$ ) was significantly and concentration dependently restored by CBD at the doses of  $10^{-9}$  M (occludin:  $2.1 \pm 0.2$  vs  $1.0 \pm 0.3$  fold-change in TcdA-treated cells,  $p < 0.01$ ; ZO-1:  $2.6 \pm 0.5$  vs  $1.0 \pm 0.5$  fold-change in

TcdA-treated cells,  $p < 0.05$ ),  $10^{-8}$  M (occludin:  $2.6 \pm 0.3$  vs  $1.0 \pm 0.3$  fold-change in TcdA-treated cells,  $p < 0.001$ ; ZO-1:  $4.4 \pm 0.4$  vs  $1.0 \pm 0.5$  fold-change in TcdA-treated cells,  $p < 0.001$ ) and  $10^{-7}$  M (occludin:  $3.1 \pm 0.3$  vs  $1.0 \pm 0.3$  fold-change in TcdA-treated cells,  $p < 0.001$ ; ZO-1:  $5.5 \pm 0.5$  vs  $1.0 \pm 0.5$  fold-change in TcdA-treated cells,  $p < 0.001$ ) (Figure 1(c) and (d)). Once again, AM251 significantly inhibited the CBD-mediated rescue of ZO-1 and occludin proteins (all  $p < 0.001$ ) (Figure 1(b)–(d)).

### CBD inhibits TcdA-induced apoptosis and cells' toxicity

As shown in Figure 2(a), a significant decrease in Caco-2 cell viability was observed at 24 h following the TcdA challenge ( $-70\%$  as compared to vehicle group assumed as 100% viable cells,  $p < 0.001$ ). Under the same experimental conditions, CBD caused a significant and concentration-dependent inhibition of TcdA-induced cytotoxicity, resulting in an increased cells' viability (by 61, 133 and 328% at  $10^{-9}$ ,  $10^{-8}$  and  $10^{-7}$  M, respectively, vs TcdA group ( $p < 0.05$ ,  $p < 0.01$  and  $p < 0.001$ , respectively)).

Exposure to TcdA significantly reduced the expression of RhoA GTP ( $0.2 \pm 0.1$  vs  $1.0 \pm 0.3$  fold-change in the vehicle group,  $p < 0.001$ ) and increased the expression of the pro-apoptotic Bax protein ( $10.5 \pm 1.2$  vs  $1.0 \pm 0.5$  fold-change in the vehicle group,  $p < 0.001$ ) (Figure 2(b) and (c)); these effects were significantly restored by CBD, that at  $10^{-9}$ ,  $10^{-8}$  and  $10^{-7}$  M increased the expression of RhoA GTP ( $1.8 \pm 0.4$ ,  $3.3 \pm 0.5$  and  $4.5 \pm 0.5$  vs  $1.0 \pm 0.3$  fold-change in TcdA-treated cells;  $p < 0.05$ ,  $p < 0.001$  and  $p < 0.001$ , respectively) and decreased the expression of Bax ( $0.7 \pm 0.1$ ,  $0.6 \pm 0.1$  and  $0.2 \pm 0.1$  vs  $1.0 \pm 0.1$  fold-change in TcdA-treated cells;  $p < 0.05$ ,  $p < 0.001$  and  $p < 0.001$ ) (Figure 2(b) and (c)). As shown for the TcdA-impaired barrier function the protective effects of CBD on cells toxicity were completely abolished in the presence of AM251 (all  $p < 0.001$ ) (Figure 2(a)–(c)).

## Discussion

CDI is one of the main causes of nosocomial diarrhoea and it is responsible for pseudomembranous colitis. An annual incidence of  $\sim 450,000$  cases in the USA has been estimated, turning CDI into a very important sanitary emergency,<sup>19</sup> since it is associated with significant morbidity, 5% infection-related mortality and an overall mortality of 13–20%.<sup>3,20</sup> There is an urgent need for new drugs able to improve CDI outcome, maximising the recovery of patients.

Due to its ability to inhibit Rho GTP activation,<sup>4,21</sup> TcdA has been postulated as the main enterotoxin

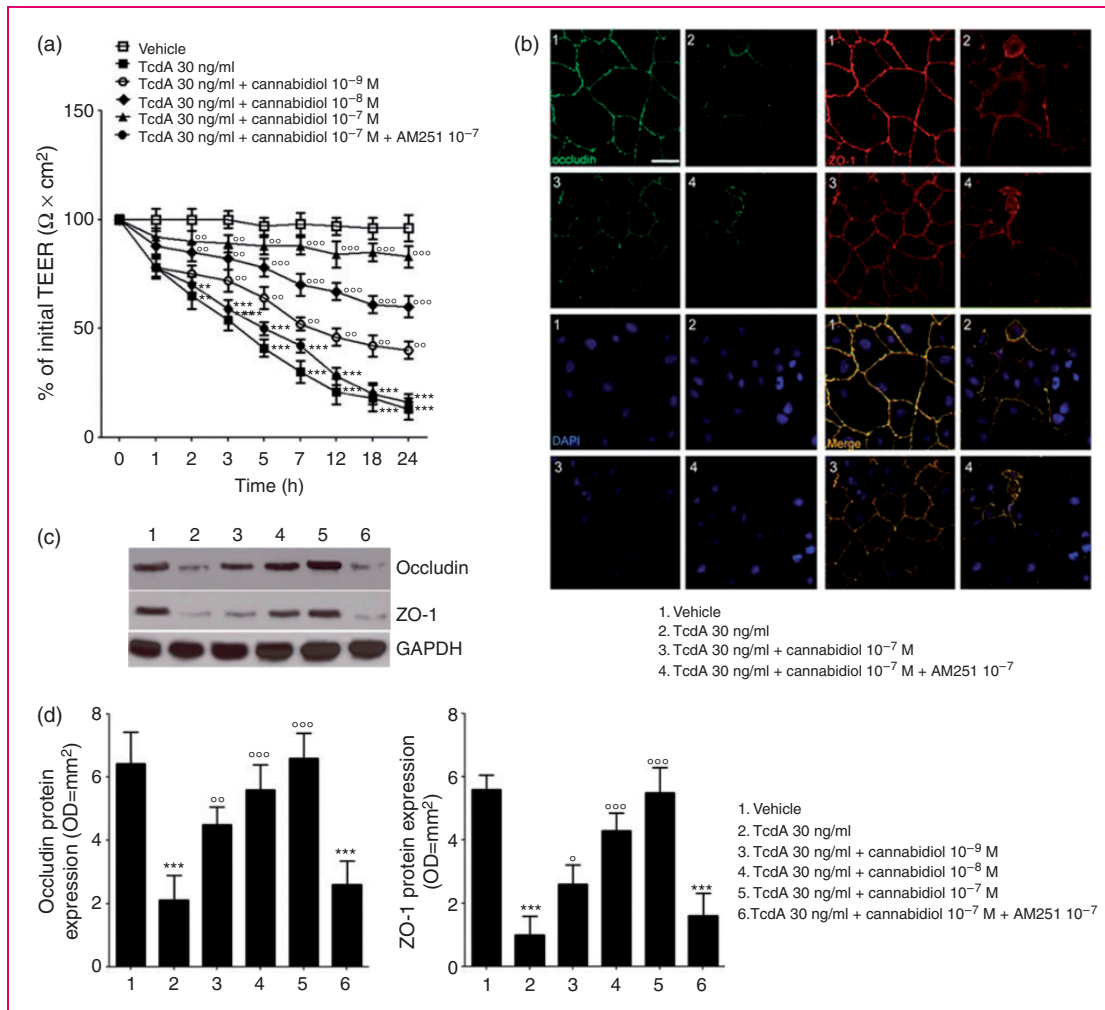


**Figure 1.** Effect of cannabidiol (CBD) on transepithelial electrical resistance (TEER) and barrier integrity of *Clostridium difficile* toxin A (TcdA)-exposed Caco-2 cells. (a) 24 h Time course TEER changes following treatment ( $n = 4$ ); (b) immunofluorescent staining showing the effects of TcdA on zonula occludens-1 (ZO-1) and occludin co-expression at 24 h. Nuclei were stained by DAPI (scalebar = 25  $\mu\text{m}$ ); (c) immunoreactive bands corresponding to ZO-1 and occludin expression at 24 h following the TcdA challenge; (d) relative densitometric analysis of immunoreactive bands (arbitrary units normalised against the expression of the housekeeping glyceraldehyde-3-phosphate dehydrogenase (GAPDH) protein;  $n = 5$ ). Results are expressed as mean  $\pm$  standard error of the mean (SEM) of experiments performed in triplicate. \*\*\* $p < 0.001$  and \*\* $p < 0.01$  vs vehicle group;  $\circ\circ\circ p < 0.001$ ,  $\circ\circ p < 0.01$  and  $\circ p < 0.05$  vs TcdA group. DAPI (4',6-diamidino-2-phenylindole).

involved in gut mucosal disruption,<sup>5,22</sup> leaky gut and loss of cell-to-cell integrity, leading to massive apoptosis.<sup>23,24</sup> The inhibition of TcdA effects might thus represent the key for a targeted therapy of CDI.

In this perspective, cannabinoids might display a wide range of protective effects on the GI epithelial barrier, due to their antiinflammatory, anticancer and antioxidant properties.<sup>25,26</sup> Among the almost 113 active phytocannabinoids isolated from *Cannabis sativa* plant, CBD is one of the most interesting compounds considered for medical use, as different clinical reports showed its almost complete lack of side effects in humans.<sup>27</sup> Remarkably, CBD is a non-psychotropic cannabinoid (unlike  $\Delta^9$ -THC) and does not interfere

with psychomotor learning and psychological functions.<sup>28</sup>

In this study we have demonstrated, for the first time, that CBD is able to preserve mucosal integrity and to reduce cellular permeability in in vitro cultured Caco-2 cells, counteracting the effects of TcdA. CBD, indeed, caused a concentration-dependent increase of transepithelial resistance, significantly preventing the enterotoxin-evoked damage. Moreover, CBD caused a marked inhibition of cell death in TcdA-exposed cells, due to a concentration-dependent up-regulation of both occludin and ZO-1 protein, two of the main cell-to-cell tight junction proteins.<sup>29</sup> Furthermore, CBD caused a significant RhoA GTP rescue that raised in

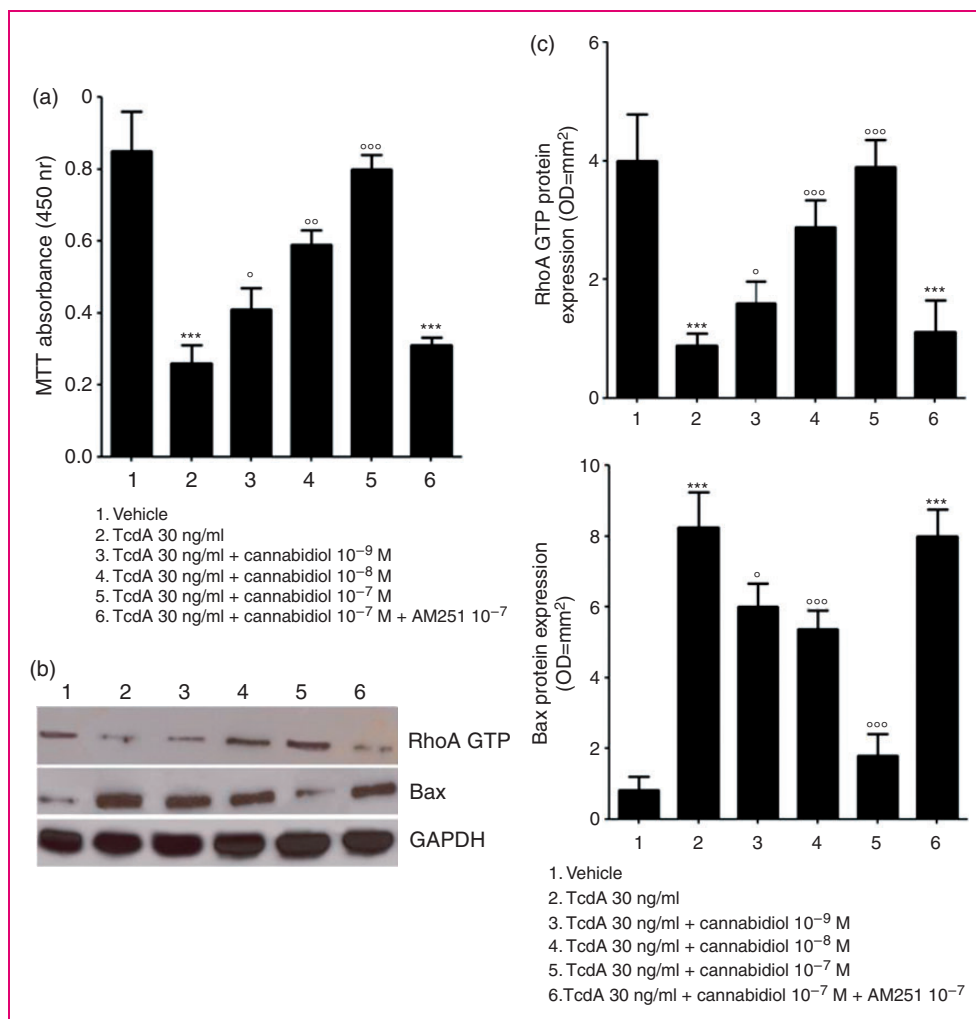


**Figure 2.** Effect of cannabidiol (CBD) on *Clostridium difficile* toxin A (TcdA)-induced cells toxicity and apoptosis. (a) 3-[4,5-Dimethylthiazol-2-yl]-2,5 diphenyltetrazolium bromide (MTT) cell viability absorbance at 24 h ( $n = 5$ ); (b) immunoreactive bands corresponding to RhoA GTP and Bax expression at 24 h following the TcdA challenge; (c) relative densitometric analysis of immunoreactive bands (arbitrary units normalised against the expression of the housekeeping glyceraldehyde-3-phosphate dehydrogenase (GAPDH) protein;  $n = 5$ ). Results are expressed as mean  $\pm$  standard error of the mean (SEM) of experiments performed in triplicate. \*\*\* $p < 0.001$  and vs vehicle group; °°° $p < 0.001$ , °° $p < 0.01$  and ° $p < 0.05$  vs TcdA group. GTP: guanosine triphosphate.

parallel with the inhibition of pro-apoptotic Bax protein expression; these combined effects likely account for the restoration of the TcdA-induced intestinal barrier dysfunction and apoptosis.

CBD effects were, at least partially, mediated by critical involvement of the CB-1 receptor, since they were almost completely abolished in the presence of the specific CB-1 receptor antagonist AM251.

Although different receptors have been proposed to mediate CBD activity,<sup>11,30</sup> it has been postulated that CBD may represent a non-competitive negative allosteric modulator of CB1 receptors.<sup>13</sup> Consequently, the presence of a specific CB1 antagonist markedly impairs CBD activity, as previously demonstrated by different studies.<sup>14,15</sup> Accordingly, CBD was able to

contain cellular damage in the in vitro model of mucosal disruption, as it occurs in our experimental conditions. Our results indicated that CBD is able to increase RhoA GTP expression, via the selective involvement of CB-1 receptors. However, CBD exhibits both antioxidant and anti-inflammatory properties, labelled as generic neuroprotective functions,<sup>30</sup> mediated by a number of different pathways and cellular effectors, that have been only partially recognised so far. These so-called 'entourage' effects are not to be excluded a priori when considering the potential therapeutic effects of this compound in CDI.

One can speculate that this entourage activity might synergistically cooperate with CB-1 dependent negative allosteric modulation, further enhancing the protective

effects on gut epithelial cells; preventing the cytotoxic effects of reactive oxygen species products and pro-inflammatory cytokines,<sup>31,32</sup> released in the mucosa following TcdA stimulus.

In recent decades, CBD has been proposed as an effective therapeutic option in a variety of GI pathologies, ranging from inflammatory bowel disease<sup>8</sup> to colon cancer,<sup>33</sup> inflammatory hypermotility in mice<sup>34</sup> and intestinal sepsis.<sup>35</sup> The results of our preliminary report indicate that CBD might be an intriguing candidate in CDI treatment, as well.

Although to be confirmed in vivo, the multifaceted activities exerted by CBD might prevent the cytotoxic damage in CDI and from a translational standpoint, given its lack of any significant toxic effect in humans, may ideally represent an effective adjuvant treatment in this high-mortality and morbidity rate condition.

## Conclusion

*Clostridium difficile* infection is the leading cause of hospital-acquired diarrhoea and pseudomembranous colitis. *Clostridium difficile*-Toxin A significantly affects enterocytes permeability leading to apoptosis and colonic mucosal damage. In the present study, we showed that Cannabidiol, a non-psychoactive component of *Cannabis sativa* significantly inhibit the apoptosis rate in TcdA-exposed cells and restores barrier function by a significant RhoA GTP rescue. We also provide evidence that the effects of Cannabidiol are mediated by CB-1 receptor. Given the absence of any significant toxic effect in humans, cannabidiol may ideally represent an effective adjuvant treatment for *Clostridium difficile*-associated colitis.

### *Knowledge on this subject:*

1. *Clostridium difficile* infection is the leading cause of hospital-acquired diarrhoea and pseudomembranous colitis
2. *Clostridium difficile*-Toxin A is responsible for extensive colonic mucosal damage and altered barrier function
3. Cannabidiol is a non-psychoactive component of *Cannabis sativa* with potent anti-inflammatory activities on the gastrointestinal tract

### *What are the significant and/or new findings of this study?*

1. *Clostridium difficile*-Toxin A significantly affects enterocytes permeability and apoptosis
2. Cannabidiol caused a marked inhibition of apoptosis in TcdA-exposed cells and restores barrier function by a significant RhoA GTP rescue

3. The protective effects of Cannabidiol are mediated by CB-1 receptor
4. Given the absence of any significant toxic effect in humans, cannabidiol may ideally represent an effective adjuvant treatment for *Clostridium difficile*-associated colitis

## Declaration of conflicting interests

None declared.

## Funding


This research received no specific grant from any funding agency in the public, commercial, or not-for-profit sectors.

## References

1. McFarland LV, Surawicz CM, Rubin M, et al. Recurrent *Clostridium difficile* disease: Epidemiology and clinical characteristics. *Infect Control Hosp Epidemiol* 1999; 20: 43–50.
2. Rupnik M, Wilcox MH and Gerding DN. *Clostridium difficile* infection: New developments in epidemiology and pathogenesis. *Nat Rev Microbiol* 2009; 7: 526–536.
3. Leffler DA and Lamont JT. *Clostridium difficile* infection. *N Engl J Med* 2015; 372: 1539–1548.
4. Voth DE, Ballard JD, Studi D, et al. *Clostridium difficile* toxins: Mechanism of action and role in disease. *Clin Microbiol Rev* 2005; 18: 247–263.
5. Sun X, Savidge T and Feng H. The enterotoxicity of *Clostridium difficile* toxins. *Toxins* 2010; 2: 1848–80.
6. Kelly CP and Lamont JT. *Clostridium difficile* infection. *Annu Rev Med* 1998; 49: 375–390.
7. Borrelli F, Aviello G, Romano B, et al. Cannabidiol, a safe and non-psychoactive ingredient of the marijuana plant *Cannabis sativa*, is protective in a murine model of colitis. *J Mol Med* 2009; 87: 1111–1121.
8. De Filippis D, Esposito G, Cirillo C, et al. Cannabidiol reduces intestinal inflammation through the control of neuroimmune axis. *PLoS One* 2011; 6: e28159.
9. Izzo A and Sharkey K. Cannabinoids and the gut: New developments and emerging concepts. *Pharmacol Ther* 2010; 126: 21–38.
10. O'Sullivan SE and Kendall D. Cannabinoid activation of peroxisome proliferator-activated receptors: Potential for modulation of inflammatory disease. *Immunobiology* 2010; 215: 611–616.
11. Mishima K, Hayakawa K, Abe K, et al. Cannabidiol prevents cerebral infarction via a serotonergic 5-hydroxytryptamine<sub>1A</sub> receptor-dependent mechanism. *Stroke* 2005; 36: 1077–1082.
12. Hampson AJ, Grimaldi M, Axelrod J, et al. Cannabidiol and (-)D<sub>9</sub>-tetrahydrocannabinol are neuroprotective antioxidants. *PNAS* 1998; 95: 8268–8273.
13. Laprairie RB, Bagher AM, Kelly ME, et al. Cannabidiol is a negative allosteric modulator of the cannabinoid CB<sub>1</sub> receptor. *Brit J Pharmacol* 2015; 172: 4790–4805.

14. Alhamoruni A, Lee AC, Wright KL, et al. Pharmacological effects of cannabinoids on the Caco-2 Cell culture model of intestinal permeability. *J Pharmacol Exp Ther* 2010; 335: 92–102.
15. Alhamoruni A, Wright KL, Larvin M, et al. Cannabinoids mediate opposing effects on inflammation-induced intestinal permeability. *Brit J Pharmacol* 2012; 165: 2598–2610.
16. Esposito G, Nobile N, Gigli S, et al. Rifaximin improves clostridium difficile toxin A-induced toxicity in Caco-2 cells by the PXR-dependent TLR4/MyD88/NF- $\kappa$ B pathway. *Front Pharmacol* 2016; 7: 1–8.
17. Wells CL, Westerlo E, Jechorek RP, et al. Cytochalasin-induced actin disruption of polarized enterocytes can augment internalization of bacteria. *Infect Immun* 1998; 66: 2410–2419.
18. Mosmann T. Rapid colorimetric assay for cellular growth and survival: Application to proliferation and cytotoxicity assays. *J Immunol Methods* 1983; 65: 55–63.
19. Lessa FC, Mu Y, Bamberg WM, et al. Burden of Clostridium difficile infection in the United States. *N Engl J Med* 2015; 372: 825–834.
20. Lofgren ET, Cole SR, Weber DJ, et al. Hospital-acquired Clostridium difficile infections: Estimating all-cause mortality and length of stay. *Epidemiology* 2014; 25: 570–575.
21. Just I, Wilm M, Selzer J, et al. The enterotoxin from Clostridium difficile (ToxA) monoglucosylates the rho proteins. *J Biol Chem* 1995; 270: 13932–13936.
22. Nusrat A, Madara JL and Parkos CA. Clostridium difficile toxins disrupt epithelial barrier function by altering membrane microdomain localization of tight junction proteins. *Infect Immun* 2001; 69: 1329–1336.
23. Gerhard R, Nottrott S, Schoentaube J, et al. Glucosylation of Rho GTPases by Clostridium difficile toxin A triggers apoptosis in intestinal epithelial cells. *J Med Microbiol* 2008; 57: 765–770.
24. Brito GAC, Fujji J, Carneiro-filho BA, et al. Mechanism of Clostridium difficile toxin A – induced apoptosis in T84 cells. *J Infect Dis* 2002; 186: 1438–1447.
25. Esposito G, Ligresti A, Izzo A, et al. The endocannabinoid system protects rat glioma cells against HIV-1 Tat protein-induced cytotoxicity. Mechanism and regulation. *J Biol Chem* 2002; 277: 50348–50354.
26. Scuderi C, Filippis D De, Iuvone T, et al. Cannabidiol in medicine: A review of its therapeutic potential in CNS disorders. *Phytother Res* 2009; 602: 597–602.
27. Mechoulam R and Hanus L. Cannabidiol: An overview of some chemical and pharmacological aspects. Part I: Chemical aspects. *Chem Phys Lipids* 2002; 121: 35–43.
28. Bergamaschi MM, Queiroz RHC, Zuardi AW, et al. Safety and side effects of cannabidiol, a Cannabis sativa constituent. *Curr Drug Saf* 2011; 6: 237–249.
29. Hartsock A and Nelson WJ. Adherens and tight junctions: Structure, function and connections to the actin cytoskeleton. *Biochim Biophys Acta* 2008; 1778: 660–669.
30. Esposito G, Scuderi C, Valenza M, et al. Cannabidiol reduces A $\beta$ -induced neuroinflammation and promotes hippocampal neurogenesis through PPAR $\gamma$  involvement. *PLoS One* 2011; 6: e28668.
31. Frädriich C, Beer L-A and Gerhard R. Reactive oxygen species as additional determinants for cytotoxicity of Clostridium difficile Toxins A and B. *Toxins* 2016; 8: 1–12.
32. Kim JM, Kim JS, Jung HC, et al. Differential expression and polarized secretion of CXC and CC chemokines by human intestinal epithelial cancer cell lines in Response to Clostridium difficile Toxin A. *Microbiol Immunol* 2002; 46: 333–342.
33. Aviello G, Romano B, Borrelli F, et al. Chemopreventive effect of the non-psychoactive phytocannabinoid cannabidiol on experimental colon cancer. *J Mol Med* 2012; 90: 925–934.
34. Capasso R, Borrelli F, Aviello G, et al. Cannabidiol, extracted from Cannabis sativa, selectively inhibits inflammatory hypermotility in mice. *Brit J Pharmacol* 2008; 154: 1001–1008.
35. De Filippis D, Iuvone T, D’Amico A, et al. Effect of cannabidiol on sepsis-induced motility disturbances in mice: Involvement of CB receptors and fatty acid amide hydrolase. *Neurogastroenterol Motil* 2008; 20: 919–927.

# SCIENTIFIC REPORTS



OPEN

## HIV-1 Tat-induced diarrhea evokes an enteric glia-dependent neuroinflammatory response in the central nervous system

Giuseppe Esposito<sup>1</sup>, Elena Capoccia<sup>1</sup>, Stefano Gigli<sup>1</sup>, Marcella Pesce<sup>2</sup>, Eugenia Bruzzese<sup>3</sup>, Alessandra D'Alessandro<sup>2</sup>, Carla Cirillo<sup>4</sup>, Alessandro di Cerbo<sup>5</sup>, Rosario Cuomo<sup>2</sup>, Luisa Seguella<sup>1</sup>, Luca Steardo<sup>1</sup> & Giovanni Sarnelli<sup>2</sup>

Despite the effectiveness of combined anti-retroviral therapy, human immunodeficiency virus (HIV) infected-patients frequently report diarrhea and neuropsychological deficits. It is claimed that the viral HIV-1 Trans activating factor (HIV-1 Tat) protein is responsible for both diarrhea and neurotoxic effects, but the underlying mechanisms are not known. We hypothesize that colonic application of HIV-1 Tat activates glial cells of the enteric nervous system (EGCs), leading to a neuroinflammatory response able to propagate to the central nervous system. We demonstrated that HIV-1 Tat-induced diarrhea was associated with a significant activation of glial cells within the colonic wall, the spinal cord and the frontal cortex, and caused a consistent impairment of the cognitive performances. The inhibition of glial cells activity by lidocaine, completely abolished the above-described effects. These observations point out the role of glial cells as putative effectors in HIV-1 Tat-associated gastrointestinal and neurological manifestations and key regulators of gut-brain signaling.

The involvement of the gastrointestinal tract is a major clinical feature in patients with acquired immunodeficiency syndrome (AIDS) and represents one of the main causes of morbidity and mortality related to the disease<sup>1</sup>. Despite the effectiveness of the combined anti-retroviral therapy, diarrhea is frequently reported by human immunodeficiency virus (HIV) infected-patients, with the viral HIV-1 Trans activating factor protein (Tat) being identified as one of the main pathogenic mechanism<sup>2</sup>. In over fifty percent of HIV-infected adults, cognitive problems and significant neuropsychological deficits have been demonstrated as well, even in the absence of HIV-replication<sup>3</sup>. These observations suggest that most of the HIV-related pathological conditions may be related to HIV-1 Tat toxicity, rather than to the virus *per se*<sup>4</sup>.

In the gut, HIV-1 Tat induces diarrhea by altering enterocytes intracellular calcium concentration, and this results in the secretory diarrhea and the cellular damage<sup>5</sup>. However, HIV-1 Tat also affects the function of the enteric nervous system (ENS) and this further amplifies the intestinal dysfunction<sup>6</sup>. *In vitro* experiments indicate that HIV-1 Tat is able to increase the excitability of cultured enteric neurons and to stimulate the release of proinflammatory cytokines, probably through the activation of enteric glia cells<sup>7,8</sup>. Conversely, in the CNS, a more direct involvement of glial cells in mediating HIV-1 Tat-induced effects has been observed<sup>9</sup>; indeed, HIV-1 Tat-overexpression in astrocytes results in a significant upregulation of the glial fibrillary acidic protein (GFAP), with astrogliosis and an increased release of proinflammatory cytokines<sup>9</sup>.

These observations point out the role of glial cells as pivotal targets and potential effectors in HIV-1 Tat-associated gastrointestinal and neurological manifestations<sup>4,6,8</sup>.

In particular, enteric glial cells (EGCs) are involved in the maintenance of gut homeostasis by their ability to reinforce the epithelial barrier function<sup>10-13</sup>, and, more recently, they have been identified to regulate intestinal

<sup>1</sup>Department of Physiology and Pharmacology, "La Sapienza" University of Rome, Rome, Italy. <sup>2</sup>Department of Clinical Medicine and Surgery, Section of Gastroenterology, University of Naples "Federico II", Naples, Italy.

<sup>3</sup>Department of Translational Medical Science, Section of Pediatrics, University of Naples "Federico II", Naples, Italy.

<sup>4</sup>Laboratory for Enteric Neuroscience (LENS), TARGID, University of Leuven, Leuven, Belgium. <sup>5</sup>Department of Biomedical Science, "G. D'Annunzio" University, Chieti, Italy. Correspondence and requests for materials should be addressed to G.E. (email: [giuseppe.esposito@uniroma1.it](mailto:giuseppe.esposito@uniroma1.it)) or G.S. (email: [sarnelli@unina.it](mailto:sarnelli@unina.it))

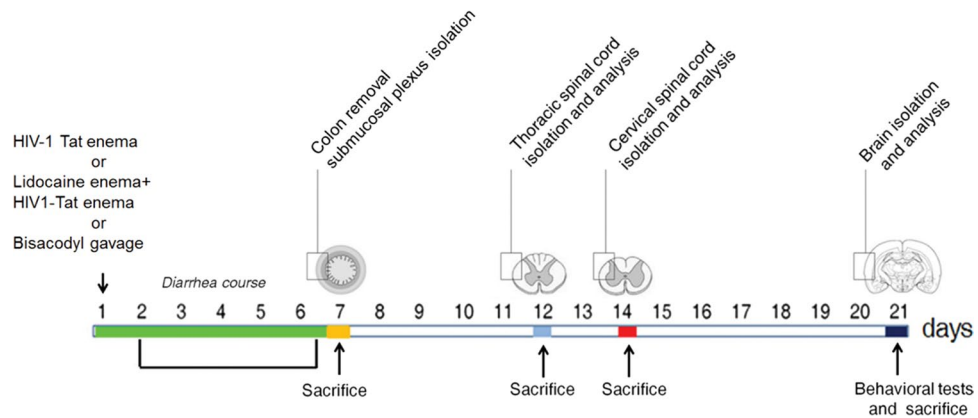


**Figure 1.** Schematic representation of rats-induced diarrhea. Diagram showing the induction of diarrhea by a single intracolonic administration of HIV-1 Tat, alone or in the presence of lidocaine, or by a single dose of bisacodyl, and the time schedule for measurements on enteric, or central nervous system glia cells.

inflammatory responses<sup>14–16</sup> and to mediate host-pathogen interactions<sup>17</sup>. The involvement of EGCs in mediating the effects of HIV-1 Tat in the colon has never been investigated so far.

Collectively, these results provide the rationale for our hypothesis that is to demonstrate, in a rat model of intracolonic administration, the involvement of EGCs in HIV-1 Tat-induced diarrhea and to verify: i) if and how the activation of the enteric glia cells modulates the diarrhea, ii) if EGC-activation is localized at the intestinal level, or it is associated with a signaling to the CNS iii) to characterize the pathway by which HIV-1 Tat signaling propagates from the periphery to the brain, and iv) to correlate these events with cognitive impairment.

## Results

### Intracolonic HIV-1 Tat administration induces diarrhea and activates an enteric glia-mediated neuroinflammatory response.

The study protocol is summarized in the Fig. 1. Intracolonic application of HIV-1 Tat induced an acute onset diarrhea lasting for  $7 \pm 3$  days; the severity and duration of diarrhea were significantly inhibited by the concomitant application of lidocaine (Supplementary Figure 1). EMSA analysis showed that nuclear NF- $\kappa$ B was significantly increased in the submucosal plexi-lysates of HIV-1 Tat treated animals (Fig. 2a and b), and this was associated with a significantly higher expression of EGCs' markers like GFAP, S100B, TLR-4 and iNOS (Fig. 2c and d); similarly, the release of S100B and nitrite production were significantly increased (Fig. 2e and f). Lidocaine application prevented HIV-1 Tat induced NF- $\kappa$ B activation, down-regulated the expression of GFAP, S100B, TLR-4 and iNOS, and reduced the release of S100B and nitrite; no significant differences were instead observed between bisacodyl-treated and control animals (Fig. 2a–f).

To further demonstrate that the effects induced by HIV-1 Tat were specific and evoked the activation of EGCs, immunofluorescence analysis carried on isolated submucosal plexi revealed an up-regulation of S100B and iNOS, and both were significantly inhibited by lidocaine treatment (Fig. 3); no significant changes in S100B and iNOS protein expression were instead observed in rats with bisacodyl-induced diarrhea. These results suggest that HIV-1 Tat-induced diarrhea was at least partially mediated by the activation of submucosal EGCs that, once activated, mediate a local neuroinflammatory response.

### HIV-1 Tat-induced EGCs activation triggers the upregulation of GFAP and S100B in spinal cord and frontal cortex glial cells through the expression of Connexin43.

In order to verify whether HIV-1 Tat-induced glia activation was localized at the intestinal level or associated with a signaling to the CNS, we evaluated the late onset activation of glia cells at different levels of the spinal cord and the frontal cortex. After 12, 14 and 21 days from HIV-1 Tat administration, the expression of GFAP mRNA was significantly increased in the thoracic, cervical spinal cord and brain frontal cortex, respectively (Fig. 4a and b).

Such activation was characterized by a time-dependent significant overexpression of Connexin43 (Cx43), likely mediating cell-to-cell connection. Indeed, immunofluorescence analysis showed that in HIV-1 Tat-treated animals a higher percentage of Cx43 and S100B expressing cells was observed in the submucosal plexus, the spinal cord and the frontal cortex as compared to control rats, respectively (Fig. 5). Interestingly, when HIV-1 Tat was administered in the presence of lidocaine, both the upregulation of GFAP mRNA and the expression of Cx43/S100B in all the analyzed areas were significantly reduced (Figs 4 and 5); similar findings were observed in bisacodyl-treated rats (Figs 4 and 5). These results suggest that modulation of HIV-1 Tat-induced diarrhea by lidocaine inhibits enteric glia activation and prevents cell-to cell signaling from the gastrointestinal tract to the CNS.

### HIV-1 Tat-induced gliosis is associated with a neuroinflammatory response in the spinal cord and brain cortex.

Similarly to what observed in the submucosal plexus, immunofluorescence analysis revealed that, 12, 14 and 21 days after HIV-1 Tat administration, the expression of S100B and iNOS was significantly increased in the thoracic and cervical spinal cord, and in the frontal cortex, respectively (Fig. 6). Once again, application of lidocaine was able to significantly inhibit this response, while in the bisacodyl-treated

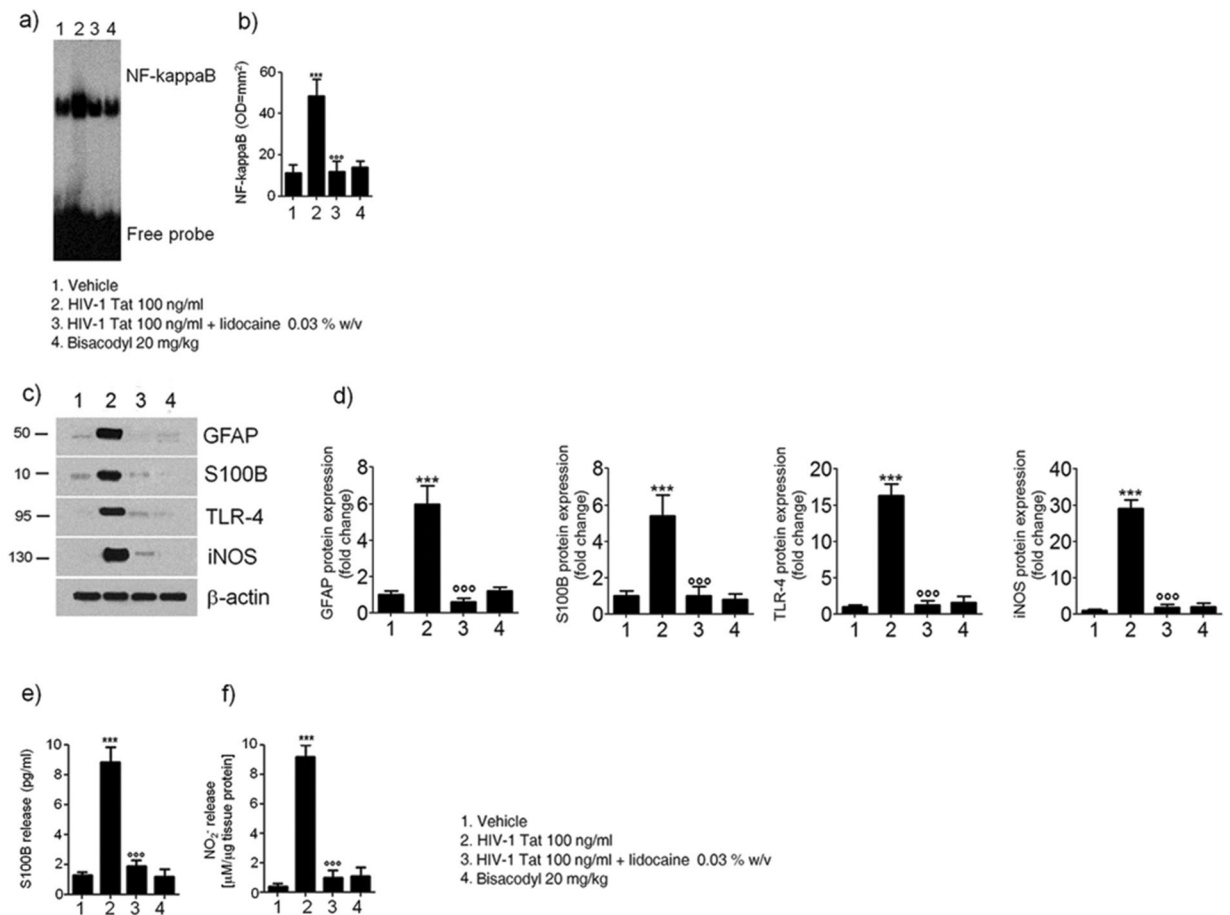


**Figure 2.** (a,b) EMSA analysis showing that intracolonic administration of HIV-1 Tat (100 ng/ml) induced a marked increase of NF-kappaB expression in EGCs nuclear extracts versus vehicle group. The administration of lidocaine significantly reduced HIV-1 Tat-induced NF-kappaB activation, whereas bisacodyl failed to induce any significant effect on NF-kappaB activation. (a) The panel shows representative NF-kappaB activation complex bands and (b) their densitometric quantification (OD = optical density in mm<sup>2</sup>). (c,d) HIV-1 Tat treatment caused a marked increase of GFAP, S100B, TLR-4 and iNOS protein expression in submucosal plexus lysates, as compared to vehicle group and this effect was significantly inhibited by lidocaine; to note that bisacodyl also failed to induce any significant effect. (c) The panel shows representative immunoreactive bands of analyzed proteins and (d) their respective levels expressed as fold change. (e,f) In the medium of submucosal plexi lysates obtained from HIV-1 Tat treated rats a significant increase of NO<sub>2</sub><sup>-</sup> and S100B was observed in comparison with vehicle group and such effect was counteracted by lidocaine; again, bisacodyl had no effect on treated animals. Results are expressed as mean ± SEM; \*\*\*p < 0.001 vs all other groups; °°°p < 0.001 vs HIV-1 Tat group; n = 6 for each group.

animals S100B and iNOS expression was similar to control rats (Fig. 6). As late consequence of submucosal enteric and spinal cord glia activation a significant increase of NF-kappaB expression was observed in the nuclear extracts obtained from brain frontal cortex homogenates of HIV-1 Tat-treated animals (Fig. 7a and b); this increase was associated with a parallel raise of GFAP, S100B, TLR4 and iNOS expression and of S100B release and nitrite production (Fig. 7c–f).

In rats receiving lidocaine all the above-described findings were completely abolished, while bisacodyl treatment did not yield to any significant variation compared to vehicle group (Fig. 7); these results suggest that the inhibition of EGCs–HIV-1 Tat induced signaling was able to prevent the late onset activation of glial cells in the frontal cortex and to inhibit the related neuroinflammatory response.

**HIV-1 Tat-induced neuroinflammatory brain responses led to a cognitive dysfunction.** In HIV-patients minimally impaired neuropsychological and behavior functions have been described even in the absence of viral replication<sup>3</sup>. In order to get new insights into the pathophysiological role of the intestinal-HIV-1 Tat in the decline of cognitive functions we investigated the memory skills of treated rats by the object recognition test. We found that, 21 days after HIV-1 Tat administration, there were no significant differences in the time spent exploring the novel object versus the known one, likely indicating a mild cognitive dysfunction (Supplementary Figure 2). Conversely, in rats treated by lidocaine a significant increase of the recognition index was observed,



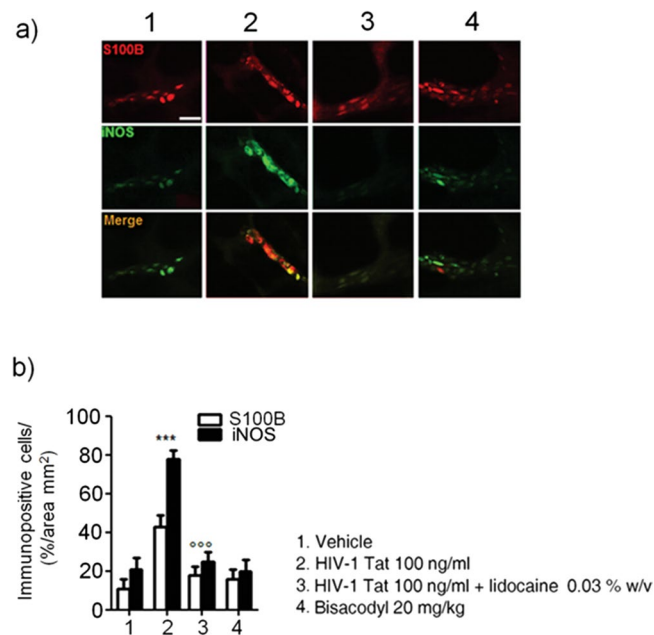


**Figure 3.** Intracolonic administration of HIV-1 Tat (100 ng/ml) yields to a marked activation of submucosal plexus-EGCs, as shown by the immunofluorescence analysis showing a significant increase of S100B and iNOS protein co-expression. **(a)** The panel shows iNOS (green) and S100B (red) immunoreactivity with **(b)** the respective quantification of iNOS (filled bars) and S100B (open bars) expression in the EGCs; both lidocaine pretreatment and bisacodyl administration failed to significantly affect S100B/iNOS expression. Results are expressed as mean  $\pm$  SEM; \*\*\* $p$  < 0.001 vs all other groups; °°° $p$  < 0.001 vs HIV-1 Tat group. Scale bar: 20  $\mu$ m.

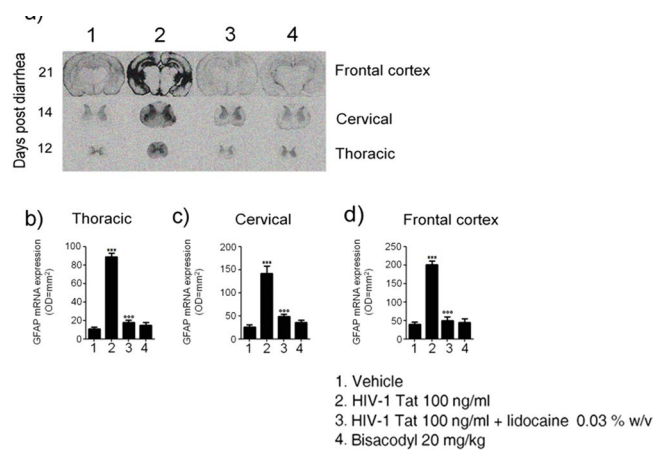


**Figure 4.** **(a)** *In situ* hybridization analysis of thoracic and cervical spinal cord, and frontal cortex showing GFAP mRNA expression at day 12, 14 and 21 after diarrhea induction, respectively. **(b–d)** Quantitative analysis revealed that administration of HIV-1 Tat protein caused a significant increase of GFAP mRNA expression in all the analyzed areas compared, as compared to both vehicle or lidocaine group, while bisacodyl yields to no significant change. (Results are expressed as mean  $\pm$  SEM; \*\*\* $p$  < 0.001 vs all other groups; °°° $p$  < 0.001 vs HIV-1 Tat group; OD = optical density in mm<sup>2</sup>; n = 5 for each group).

while the lack of any significant effect on memory tasks observed in the bisacodyl group indicates that the cognitive/memory dysfunction was dependent by HIV-1 Tat exposure, rather than being related to diarrhea *per se*.

## Discussion

Diarrhea is present in nearly 60–80% of HIV-infected patients, and although it is more common in third-world countries, but it is also a frequent clinical feature despite the effectiveness of combined anti-retroviral therapy<sup>18</sup>.

So far, the HIV-1 Tat protein has been identified as the main responsible for the mucosal damage in the gut. This viral protein induces the pro-oxidative- and pro-apoptotic-mediated disruption of epithelial cells in the

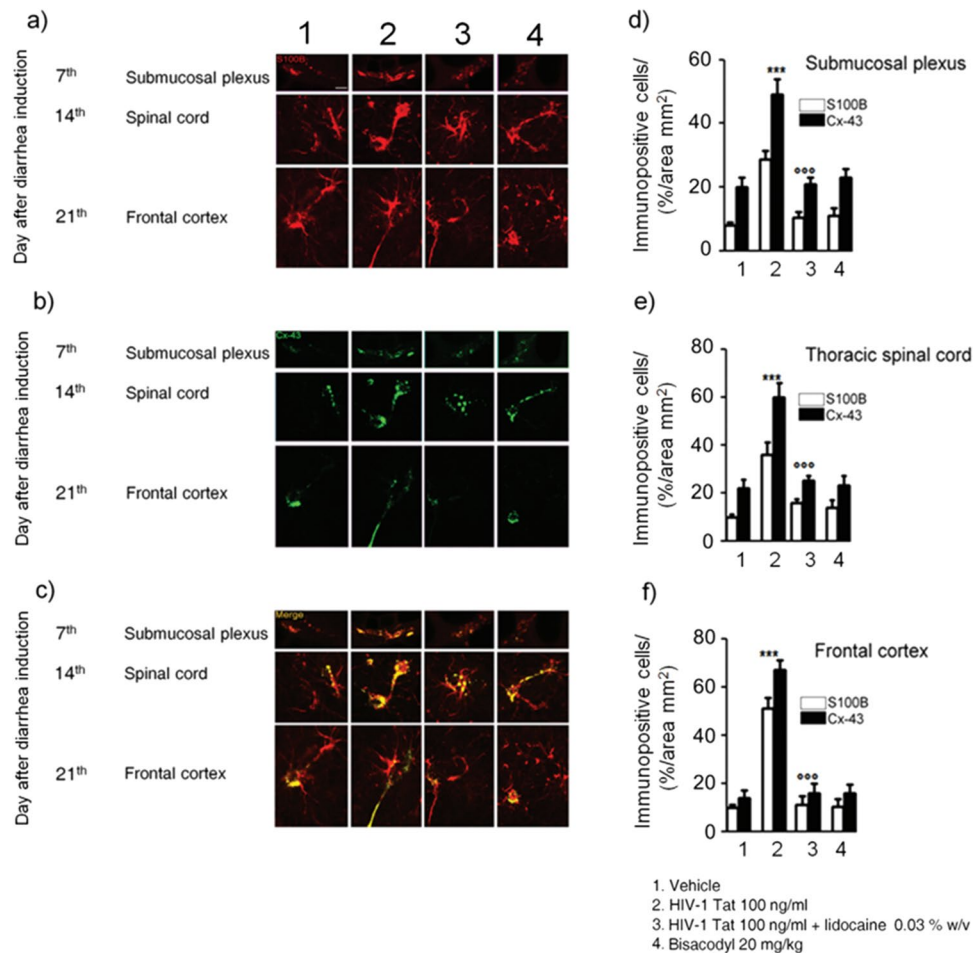


**Figure 5.** (a–c) Intracolonic administration of HIV-1 Tat caused a marked increase of Cx-43 (green) protein expression in S100B-positive cells (red) in the submucosal plexus, spinal cord and frontal cortex, respectively. (d–f) Quantitative analysis revealed that administration of lidocaine significantly reduced Cx-43 expression on S100B-positive cells of HIV-1 Tat group, whereas bisacodyl did not produce any change in Cx-43 expression compared to vehicle group (S100B (open bars) and Cx-43 (filled bars) expression in the analyzed areas. \*\*\* $p < 0.001$  vs all other groups; °°° $p < 0.001$  vs HIV-1 Tat group. Scale bars: 20  $\mu$ m;  $n = 6$  for each group.

colon, thus disrupting the intestinal barrier<sup>19</sup>. More recently, it has been described that HIV-1 Tat protein has an additional effect on the nerve part of the gut, the ENS. This direct action on the nerve system, which regulates many intestinal functions, causes abnormalities in neuronal excitability, that together with the release of pro-inflammatory cytokines in the intestinal milieu, contributes to gut dysfunction described in patients with HIV<sup>6–8</sup>.

Here we demonstrate that beside its effect on enteric neurons, HIV-1 Tat protein targets also EGCs<sup>20</sup>. Specifically, when applied into the colon, HIV-1 Tat triggers the activation of submucosal EGCs with the overexpression of glial proteins, namely S100B and GFAP. Activation of EGC was accompanied by the switch-on of the molecular pathway leading to the induction and release of pro-inflammatory factors, like iNOS protein and NO. These final events occur via the activation of the NF-kappaB-mediated cascade and TLR4 activation, two pathways that are linked each other during inflammation-related EGC activation<sup>16</sup>.

As shown in a pioneering study by Lundgren *et al.*<sup>21</sup>, the selective pharmacological modulation of the ENS, by using local anesthetics such as lidocaine, is able to inhibit the of rotavirus-induced diarrhea in mice. Accordingly, here we confirmed the role of the ENS in HIV-1 Tat-induced diarrhea too, since the co-administration of lidocaine reduced all the symptoms and biochemical markers indicative for secretory diarrhea.

Although we cannot definitely rule out the role of enteric neurons dysfunction in mediating this effect, the observation that, lidocaine suppresses EGC activation, is strongly supported by the inhibition of S100B and iNOS overexpression together with the suppression of TLR-4/NF-kappaB axis. Further in support of this evidence, there is the observation that when secretory diarrhea was induced by a non-immunological stimulus like bisacodyl, no significant changes in glial network and markers were observed, confirming that gliosis does not represent an unspecific feature of diarrhea, but that this is specifically involved in HIV-1 Tat-induced secretory diarrhea.

A gut-brain connection has been identified over the last years and increasing data support the hypothesis that in certain circumstances the gut may be the “entrance door” by which bacteria, prion proteins, viruses or their neurotoxic proteins may migrate to the brain to finally cause damage in the CNS<sup>22,23</sup>. For example, the injection of

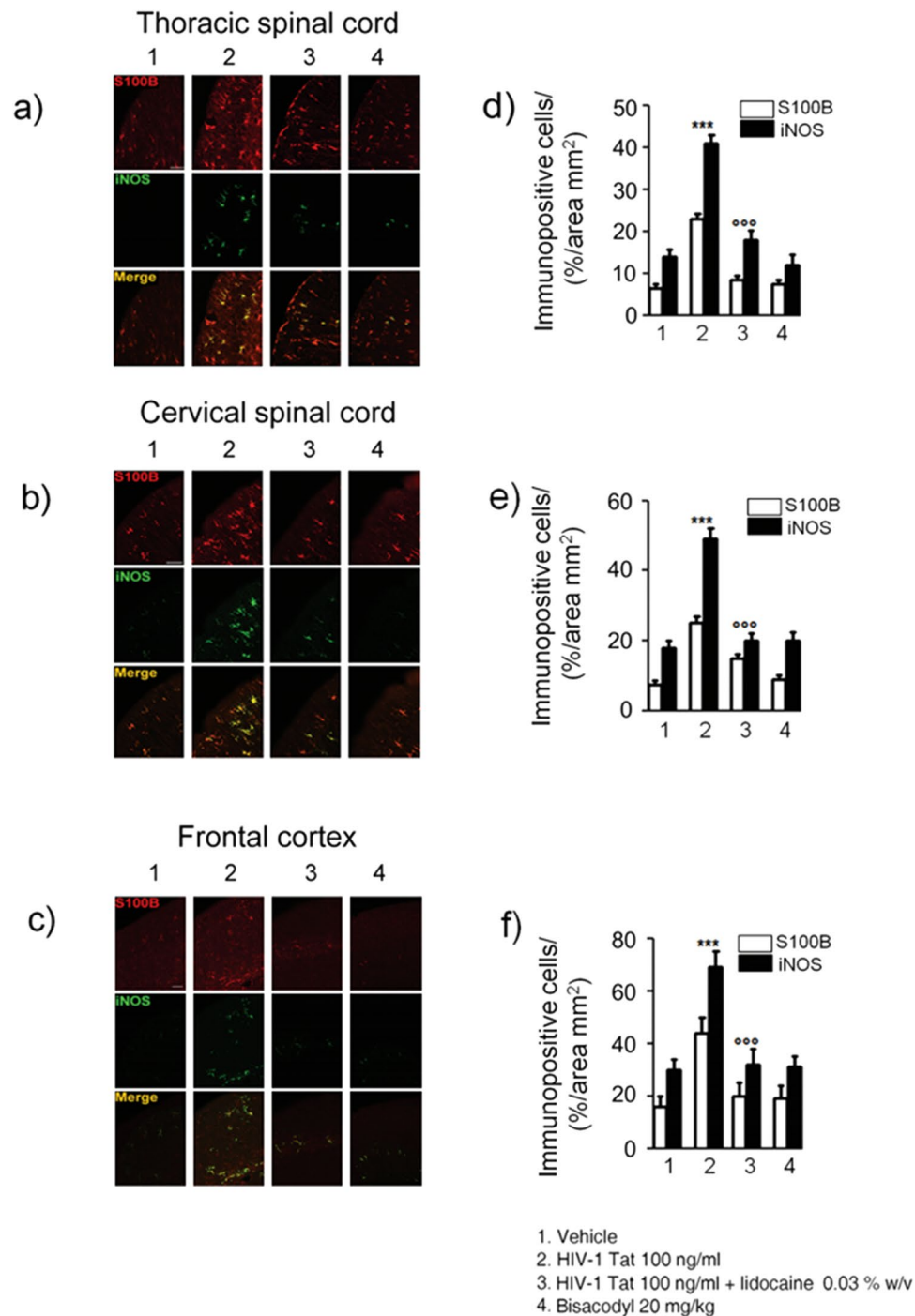


**Figure 6.** Intracolonic administration of HIV-1 Tat induced glial activation in the (a) thoracic and (b) cervical spinal cord and (c) frontal cortex at day 12, 14 and 21 after diarrhea induction, respectively. (a–c) Immunofluorescence analysis showed that iNOS (green) and S100B (red) co-expression was increased in the spinal cord and frontal of HIV-1 Tat treated rats. (d–f) Quantitative analysis showed that HIV-1 Tat-induced upregulation of iNOS (filled bars) and S100B (open bars) was significantly inhibited by lidocaine treatment. Results are expressed as mean  $\pm$  SEM; \*\*\* $p < 0.001$  vs all other groups; °°° $p < 0.001$  vs HIV-1 Tat group. Scale bars: 100  $\mu$ m;  $n = 6$  for each group.

formalin in the rat colonic wall induced c-Fos expression in the myenteric plexus, the spinal cord and the brain-stem, in a retrograde way<sup>24</sup>, similarly, in a model of intestinal inflammation associated with the post-operative ileus, the increased expression of cyclooxygenase-2 leads to cFos activation in the spinal cord via the ascending nerve pathways<sup>25</sup>.

In our setting we demonstrated that the local application of HIV-1 Tat by determining the activation of EGCs in the colonic submucosal plexi is able to trigger a neuroinflammatory response that propagates to the CNS.

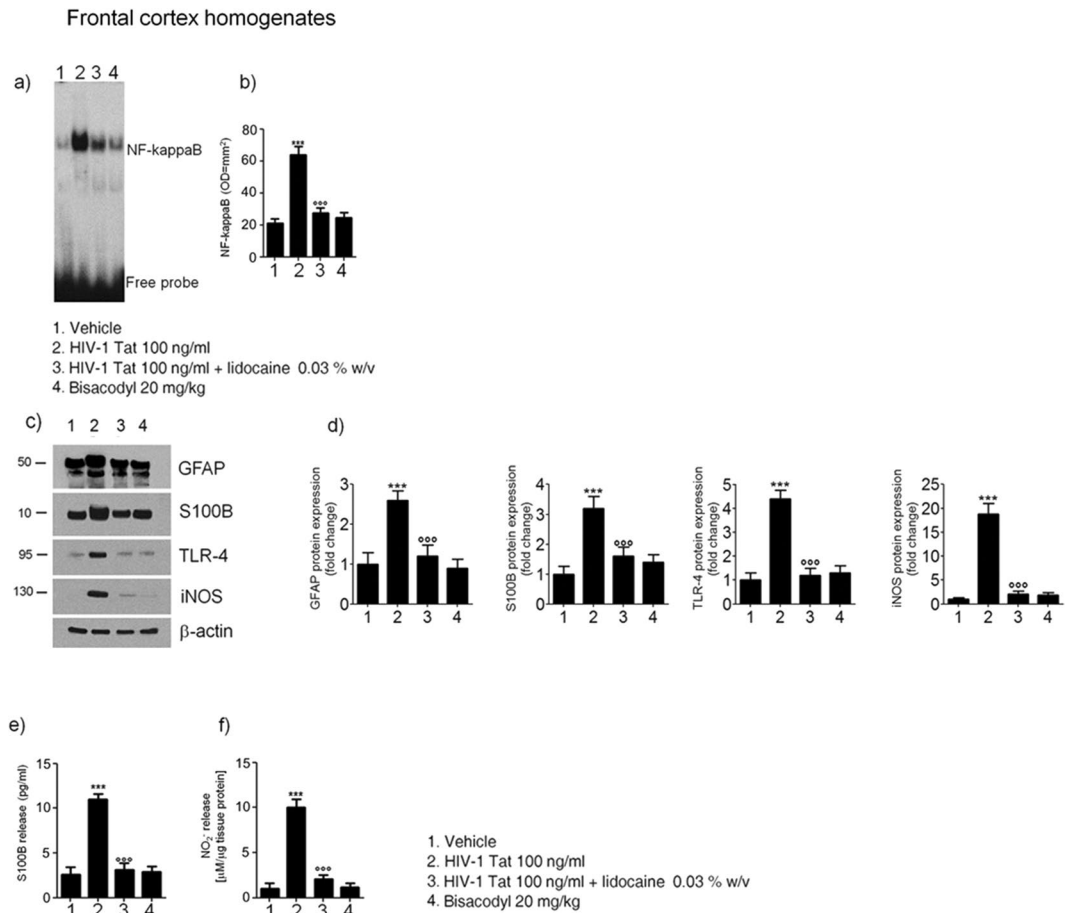


**Figure 7.** Effect of HIV-1 Tat treatment on NF-kappaB activation in the nuclear extracts of frontal cortex and astrocytes activation. **(a)** The panel shows representative NF-kappaB activation complex bands in the different groups of rats. **(b)** The quantitative analysis revealed that intracolonic HIV-1 Tat administration yields to a significant increase of NF-kappaB, as compared to vehicle, lidocaine, or bisacodyl groups (OD = optical density in mm<sup>2</sup>). **(c)** HIV-1 Tat caused a marked increase of GFAP, S100B, TLR-4 and iNOS protein expression in the frontal cortex homogenates of treated rats. **(d)** Quantitative analysis revealed that HIV-1 Tat induced a significantly higher expression of GFAP, S100B, TLR-4 and iNOS, than lidocaine, or bisacodyl groups. **(e,f)** In the medium of frontal cortex homogenates deriving from HIV-1 Tat group a significant increase of NO<sub>2</sub><sup>-</sup> and S100B was also observed as compared to the other groups. (Results are expressed as mean ± SEM; \*\*\*p < 0.001 vs all other groups; °°°p < 0.001 vs HIV-1 Tat group; n = 6 for each group).

Indeed, after the induction of the diarrhea, a time dependent propagation and a significant up-regulation of GFAP mRNA and protein were observed in the thoracic and cervical spinal cord, and in the brain cortex, respectively. Further confirming the spreading of glial activation from the ENS to the CNS glia, a significant overexpression of the TLR-4/NF-kappaB pathway and an increased expression of GFAP, S100B and iNOS protein were also measured up to two weeks after the induction of the diarrhea. Interestingly, EGCs HIV-1 Tat-induced response and the related propagation from the gut to the brain were significantly blocked by lidocaine. Although we did not provide a detailed analysis of the mechanism beyond the effect of lidocaine, previous reports suggest that this may be dependent by its ability to inhibit voltage-gated Na<sup>+</sup> channels on glia cells, thus preventing cells' activation, or, alternatively, by its ability to reduce the induced glia-mediated inflammatory signaling pathways<sup>26,27</sup>.

Further supporting the concept that the colonic HIV-1 Tat application represents a specific stimuli for EGCs triggering and the spread of activation of glia cells outside the gut there is also the observation that the protein was virtually absent in the CNS (see Supplementary Figure 3). Furthermore, the absence of any signs of glial activation in the brain of bisacodyl-treated rats reinforces the hypothesis that pathologic signals lifting from the enteric to the CNS glia are due to the selective priming of EGC by HIV-1 Tat protein, rather than to the diarrhea *per se*.

In the attempt to explain how EGCs and CNS astrocytes communicate during HIV-1 Tat-induced diarrhea, we tested the involvement of the gap junction protein Cx43, that is involved in cell-to-cell communication, and whose expression is profoundly regulated by inflammation and dependent by intracellular Ca<sup>2+</sup><sup>28-30</sup>. The expression of Cx43 in S100B-positive cells was significantly up-regulated in the submucosal plexi of HIV-1 Tat treated rats, and, more interestingly, an increased expression of Cx43 was also observed in S100B expressing glia cells of the spinal cord and frontal cortex, respectively. Again, the pretreatment with lidocaine yields to an overall and significant

inhibition of HIV-1 Tat-induced Cx-43/S100B overexpression, suggesting that the inhibition of the priming stimuli in the colon is able to block the glia-mediated signaling from the gut to the central nervous system.

We finally evaluated whether the late onset of neuropathological features in the brain due to HIV-1 Tat treatment could affect the cognitive performances in our experimental models. Behavior tests showed that rats with HIV-1 Tat-induced diarrhea presented a significant worsening of mnemonic/cognitive performances, as assessed by the object recognition test. Although our study is limited because we did not evaluate the putative neurodegeneration associated with HIV-1 Tat induced glia-mediated neuroinflammation, our findings are coherent with both clinical and *in vitro* data showing a significant cognitive decline in HIV-infected even in the absence of viral replication, or an astrocytes-mediated neuronal degeneration, respectively<sup>3</sup>.

In conclusion, our study demonstrates that a single colonic application of HIV-1 Tat induces an acute diarrhea that is at least partially modulated by the activation of glia cells in the submucosal plexus. This local response is able to trigger and activate glia cells in the spinal cord and brain cortex through the expression of Cx43, that results in an inflammatory reaction in the brain and that is associated with a significant cognitive decline in treated rats.

## Methods

**Animals and experimental design.** Eight-weeks-old Wistar male rats (Harlan Laboratories, Udine, Italy) were used for experiments. All procedures were approved by La Sapienza University's Ethics Committee. Animal care was in compliance with the IASP and European Community (EC L358/1 18/12/86) guidelines on the use and protection of animals in experimental research. Rats were randomly divided into the following groups: vehicle, HIV-1 Tat, lidocaine plus HIV-1 Tat, and bisacodyl.

HIV-1 Tat (1–86) was chemically synthesized by a step-by-step solid phase peptide synthesis according to our previously described protocol<sup>31</sup>. In brief, the protein was dissolved in pyrogen-free distilled water and a volume of 400  $\mu$ l of a 100 ng/ml solution of HIV-1 Tat was injected into the lumen of the rat colon, 3–4 cm proximal to anus by using a 24 gauge catheter; an equivalent volume of apyrogenic distilled water was administered into the colon of the vehicle group. In a subset of animals HIV 1-Tat was administered immediately after a 400  $\mu$ l of a 0.03% w/v solution of lidocaine hydrochloride monohydrate (Sigma-Aldrich, Milan, Italy; catalog number L5647) dissolved in sterile and pyrogen-free distilled water. Immediately after the enema, rats were kept in a vertical position for 5–10 min to avoid leakage of the instilled intracolonic solutions and animals were all held in a gentle manner to minimize any stress. In another group of animals a single dose of bisacodyl (20 mg/Kg) (Sigma-Aldrich, Milan, Italy; catalog number B1390) was administered orally by gavage. The study protocol is summarized in the Fig. 1 and depending upon the scheduled experimental plan, animals were euthanized and colon, thoracic and cervical spinal cord and brain were isolated to perform immunofluorescence, *in situ* hybridization and biochemical/molecular analyses as described below.

**Diarrhea evaluation.** Depending on the experimental protocol, animals were separated in subgroups and placed separately in cages lined with filter paper that was changed every 2 h. The severity of the diarrhea was assessed every 2 h for 16 hours from day 1 to day 7. Frequency of defecation and number of the wet spot were recorded and compared with the score of the vehicle group. Evaluation of accumulation of intracolonic fluid was performed using the enteropooling technique according to Ateufack *et al.*<sup>32</sup>. Briefly, enteropooling is defined as the intraluminal accumulation of fluid into the small intestine and corresponds with the fluid already located in the lumen and excreted from the blood. Depending upon the experimental plan, the last portion of colon rats was isolated, taking care to avoid tissue rupture and loss of fluid, removing the mesentery and connective tissue. To normalize the data, fluid accumulation was expressed as follows:

$$(W_1 - W_2)/W_2 \times 10^{-6}$$

where  $W_1$  is the weight of the colon after excision and  $W_2$  is the weight of the colon after expulsion of its content. Water content was measured and compared with the score from the vehicle group.

**Tissue preparations.** To study the effects of HIV 1-Tat-mucosal challenge on enteric glia cells, 2 cm colonic segments were used to prepare submucosal plexus by carefully removing the mucosal and the muscle layers, according to a slightly modified previously reported method<sup>33</sup>. On completion of the study 12 or 14 days after HIV 1-Tat administration, the left ventricle was cannulated and perfused with saline, and, after the removal of the vertebral column and the spinal cord; coded sections from spinal cervical and thoracic segments (C2–C6 and T4 to T8, respectively) were isolated and processed for biochemical or immunofluorescence assays. In a subset of animals, brain was isolated and processed for biochemical assays; part of the brain cortex was also isolated and processed to isolate astrocytes according to our previously reported methods<sup>34, 35</sup>.

**Protein extraction and western blot analysis.** Proteins were extracted from both submucosal plexi and brain astrocytes, obtained from rats at day 7 and 21 after diarrhea induction, respectively. Cellular extracts were homogenized in ice-cold hypotonic lysis buffer to obtain cytosolic extracts and underwent electrophoresis through a polyacrilamide minigel. Proteins were transferred into nitrocellulose membrane that was saturated with non-fat dry milk and then incubated with either mouse anti-S100B (Neo-Marker, Milan, Italy; catalog number MA1-25005), mouse anti-inducible Nitric Oxide Synthase (iNOS), rabbit anti-GFAP, mouse anti-TLR4, and mouse anti- $\beta$ -actin (all from Abcam, Cambridge, UK; catalog numbers ab49999, ab7260, ab30667 and ab8226, respectively). In another set of supplementary experiments, specific mouse anti-HIV-1 Tat (Biolegend, San Diego, CA, USA; catalog number MMS-116P) was used. Membranes were then incubated with the specific secondary goat anti-mouse and goat anti-rabbit antibodies conjugated to horseradish peroxidase (HRP) (Dako, Milan, Italy;

catalog number P0447 and P0448). Immune complexes were revealed by enhanced chemiluminescence detection reagents (Amersham Biosciences, Milan, Italy; catalog number RPN2108). Blots were analyzed by scanning densitometry (Versadoc, Bio-Rad Laboratories) and results expressed as relative fold change and normalized on the expression of the housekeeping protein  $\beta$ -actin.

**Electrophoretic mobility shift assay (EMSA).** EMSA was performed to detect NF- $\kappa$ B activation in both submucosal plexi and brain astrocytes. Double stranded oligonucleotides containing the NF- $\kappa$ B recognition sequence for rats (5-CAACGG CAGGGGAATCTCCCTCTCCTT-3) were end-labelled with  $^{32}$ P- $\gamma$ -ATP (Amersham, Milan, Italy). Nuclear extracts were incubated for 15 min with radiolabeled oligonucleotides ( $2.5$ – $5.0 \times 10^4$  cpm) in 20 ml reaction buffer containing 2 mg poly dI-dC, 10 mM Tris-HCl (pH 7.5), 100 mM NaCl, 1 mM EDTA, 1 mM dl-dithiothreitol, 1 mg/ml bovine serum albumin, 10% (v/v) glycerol. Nuclear protein-oligonucleotide complexes were resolved by electrophoresis on a 6% non-denaturing polyacrylamide gel in 1 Tris Borate EDTA buffer at 150 V for 2 hrs at 4 °C. The gel was dried and autoradiographed with an intensifying screen at  $-80$  °C for 20 hrs. Subsequently, the relative bands were quantified by densitometric scanning with Versadoc (Bio-Rad Laboratories) and a computer programme (Quantity One Software, Bio-Rad Laboratories)<sup>25</sup>. P- $\gamma$ -ATP was from Amersham (Milan, Italy; catalog number PB10168). Poly dI-dC was from Boehringer-Mannheim (Milan, Italy; catalog number 1219847). Oligonucleotide synthesis was performed to our specifications by Tib Molbiol (Boehringer-Mannheim).

**Nitric oxide quantification.** Nitric oxide (NO) was measured as nitrite ( $\text{NO}_2^-$ ) accumulation in submucosal plexi and brain astrocytes homogenates, by a spectrophotometer assay based on the Griess reaction. Briefly, Griess reagent (1% sulphanilamide, 0.1% naphthylethylenediamine in  $\text{H}_3\text{PO}_4$ ) was added to an equal volume of plasma or supernatant and the absorbance was measured at 550 nm. Nitrite concentration (nM) was thus determined using a standard curve of  $\text{NaNO}_2$ .

**Enzyme-linked immunosorbent assay for S100B.** Enzyme-linked immunosorbent assay (ELISA) for S100B (Biovendor R&D, Brno, Czech Republic; catalog number RD192090100R) was carried out on both submucosal plexi and brain astrocytes lysates, according to the manufacturer's protocol. Absorbance was measured on a microtitre plate reader. S100B level was determined using standard curves method.

**Immunofluorescence analysis.** Submucosal plexi preparations were fixed for 30 minutes in ice-cold 4% paraformaldehyde, washed with PBS 1X then blocked with bovine serum albumin, and then incubated in a mixture containing a mouse anti-S100B (1:200 dil v/v; Neo-Marker, Milan, Italy; catalog number MA1-25005) and a rabbit anti-iNOS (1:100 dil. v/v; Abcam, Cambridge, UK; catalog number ab49999). Tissues were then washed ( $3 \times 10$  min) with PBS and incubated for 2 h at room temperature, with a mixture of anti-rabbit fluorescein isothiocyanate-conjugated (Abcam, Cambridge, UK; catalog number ab6717) and anti-mouse Texas Red-conjugated (Abcam, Cambridge, UK; catalog number ab6787), respectively.

Tissue sections (15  $\mu\text{m}$ ) of thoracic and cervical spinal cord and frontal cortex were isolated from rats at days 12, 14 and 21, respectively. Slices were fixed for 30 minutes in ice-cold 4% paraformaldehyde, washed with PBS 1X then blocked with bovine serum albumin. Sections were then stained with mouse anti-S100B (1:200 dil v/v) and rabbit anti-Cx43 (1:300 v/v; Cell Signaling Technology, Danvers, USA; catalog number 3512) or rabbit anti-iNOS antibody (1:100 v/v;). Appropriate negative controls were carried out by omitting primary antibodies. To test any non-specific antigen-binding sites, additional experiments were performed using specific isotype antibody controls (Abcam, Cambridge, UK), at the same concentration as the primary antibodies. Slices were then incubated in the dark with the proper secondary antibody: fluorescein isothiocyanate-conjugated anti-rabbit (Abcam, Cambridge, UK; catalog number ab6717) or Texas Red-conjugated anti-mouse (Abcam, Cambridge, UK; catalog number ab6787), respectively. Slices were analysed with a microscope (Nikon Eclipse 80i), and images were captured by a high-resolution digital camera (Nikon Digital Sight DS-U1).

**In situ hybridization.** Tissue sections of thoracic and cervical spinal cord and frontal cortex were isolated from rats at day 12, 14 and 21, respectively. Sections were fixed in ice-cold 4% paraformaldehyde for 20 min, rinsed in PBS, quenched for 15 min in 1%  $\text{H}_2\text{O}_2$  methanol solution, rinsed in PBS, quenched for 8 min in 0.2 M HCl, rinsed in PBS, treated with proteinase K 20  $\mu\text{g}/\text{ml}$  (Roche Molecular Diagnostics, Milan, Italy; catalog number 03 115 887 001) in 50 mM Tris-HCl, 5 mM ethylene diamine tetra acetic acid (EDTA) (pH 8.0) for 10 min, rinsed in PBS, fixed in ice-cold 4% paraformaldehyde, incubated for 10 min in 0.1 M triethanolamine (pH 8.0) to which 1.2 ml acetic anhydride was added dropwise, rinsed in PBS, washed with 0.9% NaCl for 5 min, dehydrated in graded series of ethanol and air-dried. Hybridization was carried out in 100  $\mu\text{l}$  of hybridization buffer containing specific sense or antisense<sup>28</sup> S-labelled riboprobe for glial fibrillary acidic protein (GFAP; 70,000–100,000 c.p.m./ $\mu\text{l}$ ). Hybridization buffer consisted of 50% deionized formamide, 20 mM Tris-HCl (pH 8.0), 0.3 M NaCl, 5 mM EDTA (pH 8.0), 10% dextran sulphate (Sigma, Milan, Italy; catalog number 51227), 0.02% Ficoll 400 (Sigma; catalog number F2637), 0.02% polyvinylpyrrolidone (PVP 40; Sigma; catalog number PVP40), 0.02% bovine serum albumin (BSA; Sigma; catalog number A2153), 0.5  $\text{mg ml}^{-1}$  tRNA (Roche Molecular Diagnostics; catalog number 109500), 0.2  $\text{mg}/\text{ml}$  fragmented herring sperm DNA and 200 mM dithiothreitol. Before applying to the tissue the hybridization cocktail was denatured for 2 min at 95 °C. Slides were incubated overnight at 54 °C in a humidified chamber. Four high-stringency washes were carried out at 62 °C with 5X saline sodium citrate (SSC)/0.05% Tween-20, then with 50% formamide/2X SSC/0.05% Tween-20, with 50% formamide/1X SSC/0.05% Tween-20 and finally with 0.1X SSC/0.05% Tween-20. Slides were dehydrated in graded ethanol series, air-dried and exposed to Biomax MR film (Scientific Imaging Systems, NY, USA). GFAP mRNA expression was

semi-quantified by densitometric scanning of the Biomax film with a GS 700 imaging densitometer (Bio-Rad Laboratories, CA, USA) and a computer programme (Molecular Analyst, IBM, Milan, Italy).

**Object recognition test.** The object recognition (OR) test is commonly used to assess the behavioral function in rodents<sup>36, 37</sup>. The test is carried on in two steps: a first session (acquisition) and a second session (test). The animal is faced with two similar objects during the first session, and then one of the two objects is replaced by a new object (novel) during the second session. The amount of time taken to explore the new object provides an index of the recognition memory. In our setting, the object recognition test was performed in an open-field arena of black Plexiglas (50 cm × 40 cm × 63 cm). Depending upon the experiments, and before their sacrifice, rats underwent a 8 min acquisition trial, during which the animal was placed in the open field in presence of two identical objects (namely A, that were a cube or a ball) and located at 15 cm from the arena wall (acquisition task); at the end of the exploration time, animals were returned to their respective cages for 3 hours. After the retention interval, the rats were placed back into the box and exposed to the known object A and to a novel object B for further 8 min (test task). The objects were placed in the same locations as the previous ones. The position of the novel object was randomly chosen to avoid preferences not based on novelty. Exploratory behavior was considered with the animal directing its nose toward the object closely (<2 cm) and the amount of time spent exploring each of the two objects. To measure recognition memory, a recognition index was calculated as the amount of time exploring the familiar object (TA) or the novel object (TB) in according with the formula:

$$[TA \text{ or } TB / (TA + TB)] \times 100$$

In the acquisition and retention trials, if the exploration time was <30 s and < 15 seconds, respectively, the rats were excluded from the trial.

**Data analysis.** All values are expressed as the mean ± SEM. Statistical differences were determined to be significant at  $P < 0.05$ . The specific tests used are described in the figure legends. All analyses were performed using GraphPad Prism software (GraphPad Software, Inc., CA USA). The investigators were not blinded to allocation during experiments and outcome assessment.

## References

- Weber, R. Enteric Infections and Diarrhea in Human Immunodeficiency Virus-Infected Persons. *Arch Intern Med.* 159–1473 (1999).
- Goldstein, G. HIV-1 Tat protein as a potential AIDS vaccine. *Nat Med* **1**, 960–964 (1996).
- Simioni, S., Cavassini, M. & Annoni, J.-M. *et al.* Cognitive dysfunction in HIV patients despite long-standing suppression of viremia. *AIDS* **24**, 1243–1250 (2010).
- Bagashev, A. & Sawaya, B. E. Roles and functions of HIV-1 Tat protein in the CNS: an overview. *Viral J* **10**, 358 (2013).
- Canani, R. B., Cirillo, P. & Mallardo, G. *et al.* Effects of HIV-1 Tat protein on ion secretion and on cell proliferation in human intestinal epithelial cells. *Gastroenterology* **124**, 368–76 (2003).
- Ngwainmbi, J., De, D. D. & Smith, T. H. *et al.* Effects of HIV-1 Tat on enteric neuropathogenesis. *J Neurosci* **34**, 14243–51 (2014).
- Fitting, S., Ngwainmbi, J. & Kang, M. *et al.* Sensitization of enteric neurons to morphine by HIV-1 Tat protein. *Neurogastroenterol Motil* **27**, 468–80 (2015).
- Galligan, J. J. HIV, opiates, and enteric neuron dysfunction. *Neurogastroenterol Motil* **27**, 449–54 (2015).
- Nookala, A. R. & Kumar, A. Molecular mechanisms involved in HIV-1 Tat-mediated induction of IL-6 and IL-8 in astrocytes. *J Neuroinflammation* **11**, 214 (2014).
- Bassotti, G., Villanacci, V. & Antonelli, E. *et al.* Enteric glial cells: new players in gastrointestinal motility? *Lab Invest* **87**, 628–32 (2007).
- Savidge, T. C., Sofroniew, M. V. & Neunlist, M. Starring roles for astroglia in barrier pathologies of gut and brain. *Lab Invest* **87**, 731–6 (2007).
- Sharkey, K. A. Emerging roles for enteric glia in gastrointestinal disorders. *J Clin Invest* **125**, 918–925 (2015).
- Landeghem, L., Van Mahé, M. M. & Teusan, R. *et al.* Regulation of intestinal epithelial cells transcriptome by enteric glial cells: impact on intestinal epithelial barrier functions. *BMC Genomics* **10**, 507 (2009).
- Barajon, I., Serrao, G. & Arnaboldi, F. *et al.* Toll-like receptors 3, 4, and 7 are expressed in the enteric nervous system and dorsal root ganglia. *J Histochem Cytochem* **57**, 1013–23 (2009).
- Espósito, G., Cirillo, C. & Sarnelli, G. *et al.* Enteric glial-derived S100B protein stimulates nitric oxide production in celiac disease. *Gastroenterology* **133**, 918–25 (2007).
- Espósito, G., Capoccia, E. & Turco, F. *et al.* Palmitoylethanolamide improves colon inflammation through an enteric glia/toll like receptor 4-dependent PPAR- $\alpha$  activation. *Gut* **63**, 1300–12 (2014).
- Turco, F., Sarnelli, G. & Cirillo, C. *et al.* Enteroglial-derived S100B protein integrates bacteria-induced Toll-like receptor signalling in human enteric glial cells. *Gut* **63**, 105–15 (2014).
- Zacharof, A. AIDS-Related diarrhea—pathogenesis, evaluation and treatment. *Ann Gastroenterol* **14**, 22–26 (2007).
- Buccigrossi, V., Laudiero, G. & Nicastro, E. *et al.* The HIV-1 transactivator factor (Tat) induces enterocyte apoptosis through a redox-mediated mechanism. *PLoS One* **6**, e29436 (2011).
- Cabarrocas, J., Savidge, T. C. & Liblau, R. S. Role of enteric glial cells in inflammatory bowel disease. *Glia* **41**, 81–93 (2003).
- Lundgren, O., Peregrin, A. T., Persson, K. *et al.* Role of the Enteric Nervous System in the Fluid and Electrolyte Secretion of Rotavirus Diarrhea. **287**, 491–496 (2000).
- Foster, J. & McVey Neufeld, K.-A. Gut-brain axis: how the microbiome influences anxiety and depression. *Trends Neurosci* **36**, 305–12 (2013).
- Luna, R. A. & Foster, J. A. Gut brain axis: diet microbiota interactions and implications for modulation of anxiety and depression. *Curr Opin Biotechnol* **32**, 35–41 (2015).
- Miampamba, M. & Sharkey, K. A. c-Fos expression in the myenteric plexus, spinal cord and brainstem following injection of formalin in the rat colonic wall. *J Auton Nerv Syst* **77**, 140–151 (1999).
- Tjwa, E. T., Bradley, J. M. & Keenan, C. M. *et al.* Interleukin-1 $\beta$  activates specific populations of enteric neurons and enteric glia in the guinea pig ileum and colon. *Am J Physiol Gastrointest Liver Physiol* **1**, 1268–1276 (2003).
- Craner, M. J., Damarjian, T. G. & Liu, S. *et al.* Sodium channels contribute to microglia/macrophage activation and function in EAE and MS. *Glia* **49**, 220–9 (2005).

27. Yuan, T., Li, Z. & Li, X. *et al.* Lidocaine attenuates lipopolysaccharide-induced inflammatory responses in microglia. *J Surg Res* **192**, 150–162 (2014).
28. McClain, J., Grubisic, V. & Fried, D. *et al.* Ca<sup>2+</sup> responses in enteric glia are mediated by connexin-43 hemichannels and modulate colonic transit in mice. *Gastroenterology* **146**, 497–507 (2014).
29. Lurtz, M. M. & Louis, C. F. Intracellular calcium regulation of connexin43. *Am J Physiol Cell Physiol* **293**, C1806–13 (2007).
30. Brown, I. A., McClain, J. L., Watson, R. E. *et al.* Enteric glia mediate neuron death in colitis through purinergic pathways that require connexin-43 and nitric oxide. *Cell Mol Gastroenterol Hepatol.* **2**(1), 77–91 (Jan 1 2016).
31. Esposito, G., Ligresti, A. & Izzo, A. *et al.* The endocannabinoid system protects rat glioma cells against HIV-1 Tat protein-induced cytotoxicity. Mechanism and regulation. *J Biol Chem* **277**, 50348–54 (2002).
32. Ateufack, G., Nana Yousseu, W. & Dongmo Feudjio, B. *et al.* Antidiarrheal and *in vitro* antibacterial activities of leaves extracts of *hibiscus asper. hook. f.* (malvaceae). *Asian J Pharm Clin Res* **7**, 130–136 (2014).
33. Sarnelli, G., DeGiorgio, R. & Gentile, F. *et al.* Myenteric neuronal loss in rats with experimental colitis: role of tissue transglutaminase-induced apoptosis. *Dig Liver Dis* **41**, 185–93 (2009).
34. Esposito, G., Sarnelli, G. & Capoccia, E. *et al.* Autologous transplantation of intestine-isolated glia cells improves neuropathology and restores cognitive deficits in  $\beta$  amyloid-induced neurodegeneration. *Sci Rep* **6**, 22605 (2016).
35. Scuderi, C., Esposito, G. & Blasio, A. *et al.* Palmitoylethanolamide counteracts reactive astrogliosis induced by  $\beta$ -amyloid peptide. *J Cell Mol Med* **15**, 2664–74 (2011).
36. Leger, M., Quiedeville, A. & Bouet, V. *et al.* Object recognition test in mice. *Nat Protoc* **8**, 2531–7 (2013).
37. Grayson, B., Leger, M. & Piercy, C. *et al.* Assessment of disease-related cognitive impairments using the novel object recognition (NOR) task in rodents. *Behav Brain Res* **285**, 176–93 (2015).

## Acknowledgements

G.E. and R.C. were partially funded by MIUR (PRIN 2009HLNNRL). C.C. is a post-doctoral fellow of the Fonds voor Wetenschappelijk Onderzoek (FWO, Belgium).

## Author Contributions

G.E. and G.S. conceived and supervised the project. E.C., S.G. and G.E. performed most of the experiments and analyses. C.C., E.B., M.P., A.D. and A.d. helped with the analysis and contributed to the writing and revision of the manuscript. L.S. performed and contributed to immunofluorescence studies. R.C. and L.S. contributed to the critical revision of the manuscript. All the authors discussed the results and commented on the manuscript.

## Additional Information

**Supplementary information** accompanies this paper at doi:[10.1038/s41598-017-05245-9](https://doi.org/10.1038/s41598-017-05245-9)

**Competing Interests:** The authors declare that they have no competing interests.

**Publisher's note:** Springer Nature remains neutral with regard to jurisdictional claims in published maps and institutional affiliations.



**Open Access** This article is licensed under a Creative Commons Attribution 4.0 International License, which permits use, sharing, adaptation, distribution and reproduction in any medium or format, as long as you give appropriate credit to the original author(s) and the source, provide a link to the Creative Commons license, and indicate if changes were made. The images or other third party material in this article are included in the article's Creative Commons license, unless indicated otherwise in a credit line to the material. If material is not included in the article's Creative Commons license and your intended use is not permitted by statutory regulation or exceeds the permitted use, you will need to obtain permission directly from the copyright holder. To view a copy of this license, visit <http://creativecommons.org/licenses/by/4.0/>.

© The Author(s) 2017



# Rifaximin, a non-absorbable antibiotic, inhibits the release of pro-angiogenic mediators in colon cancer cells through a pregnane X receptor-dependent pathway

GIUSEPPE ESPOSITO<sup>1\*</sup>, STEFANO GIGLI<sup>1\*</sup>, LUISA SEGUELLA<sup>1</sup>, NICOLA NOBILE<sup>1</sup>,  
ALESSANDRA D'ALESSANDRO<sup>2</sup>, MARCELLA PESCE<sup>2</sup>, ELENA CAPOCCIA<sup>1</sup>, LUCA STEARDO<sup>1</sup>,  
CARLA CIRILLO<sup>3</sup>, ROSARIO CUOMO<sup>2</sup> and GIOVANNI SARNELLI<sup>2</sup>

<sup>1</sup>Department of Physiology and Pharmacology, 'Vittorio Erspamer', La Sapienza University of Rome, I-00185 Rome;

<sup>2</sup>Department of Clinical Medicine and Surgery, 'Federico II' University of Naples, I-80131 Naples, Italy;

<sup>3</sup>Laboratory for Enteric NeuroScience (LENS), Translational Research Center for Gastrointestinal Disorders (TARGID), University of Leuven, 3000 Leuven, Belgium

Received February 22, 2016; Accepted March 3, 2016

DOI: 10.3892/ijo.2016.3550

**Abstract.** Activation of intestinal human pregnane X receptor (PXR) has recently been proposed as a promising strategy for the chemoprevention of inflammation-induced colon cancer. The present study was aimed at evaluating the effect of rifaximin, a non-absorbable antibiotic, in inhibiting angiogenesis in a model of human colorectal epithelium and investigating the role of PXR in its mechanism of action. Caco-2 cells were treated with rifaximin (0.1, 1.0 and 10.0  $\mu$ M) in the presence or absence of ketoconazole (10  $\mu$ M) and assessed for cell proliferation, migration and expression of proliferating cell nuclear antigen (PCNA). The release of vascular endothelial growth factor (VEGF) and nitric oxide (NO), expression of Akt, mechanistic target of rapamycin (mTOR), p38 mitogen activated protein kinases (MAPK), nuclear factor  $\kappa$ B (NF- $\kappa$ B) and metalloproteinase-2 and -9 (MMP-2 and -9) were also evaluated. Treatment with rifaximin 0.1, 1.0 and 10.0  $\mu$ M caused significant and concentration-dependent reduction of cell proliferation, cell migration and PCNA expression in the Caco-2 cells vs. untreated cells. Treatment downregulated

VEGF secretion, NO release, VEGFR-2 expression, MMP-2 and MMP-9 expression vs. untreated cells. Rifaximin treatment also resulted in a concentration-dependent decrease in the phosphorylation of Akt, mTOR, p38MAPK and inhibition of hypoxia-inducible factor 1- $\alpha$  (HIF-1 $\alpha$ ), p70S6K and NF- $\kappa$ B. Ketoconazole (PXR antagonist) treatment inhibited these effects. These findings demonstrated that rifaximin causes PXR-mediated inhibition of angiogenic factors in Caco-2 cell line and may be a promising anticancer tool.

## Introduction

Colorectal cancer (CRC) represents one of the major causes of morbidity and mortality throughout the world and is the third most common form of human cancer worldwide (1,2). Like other forms of cancer, CRC is characterized by angiogenesis, which is a crucial event in promoting cancer growth, progression and metastasis (3). Among the various signaling molecules involved in the angiogenic process, vascular endothelial growth factor (VEGF) and nitric oxide (NO) are thought to be the key signaling molecules responsible for neo-vascularization (4-6). Once hypersecreted, VEGF binds to its type 2 receptor (VEGFR-2) and mediates the regulation of different pathways in the target cells, mainly the phosphatidylinositol 3-kinase (PI3K)/protein kinase B (Akt)/mammalian target of rapamycin (mTOR) pathway (7,8) and the phospho-p38 mitogen activated protein kinase (MAPK)-dependent activation of nuclear factor  $\kappa$ B (NF- $\kappa$ B) (9,10). Activation of the NF- $\kappa$ B and Akt/mTOR pathways increases the levels of the inducible nitric oxide synthase (iNOS) isoform, leading to the release and accumulation of nitric oxide (NO) that acts as a pro-angiogenic stimulus on the blood vessels and favors neo-vascularization in solid tumors (5,11). Thus, targeting the angiogenic and mitogenic pathways is a rational and potentially effective strategy in the treatment of CRC (12).

Rifaximin is a semi-synthetic antibiotic largely used for the treatment of travelers' diarrhea and hepatic encephalopathy (13,14). It is poorly absorbed on oral administration (15)

---

*Correspondence to:* Dr Giovanni Sarnelli, Department of Clinical Medicine and Surgery, 'Federico II' University of Naples, Via Pansini 5, I-80131 Naples, Italy  
E-mail: sarnelli@unina.it

Dr Giuseppe Esposito, Department of Physiology and Pharmacology 'Vittorio Erspamer', La Sapienza University of Rome, Piazzale Aldo Moro 5, I-00185 Rome, Italy  
E-mail: giuseppe.esposito@uniroma1.it

\*Contributed equally

**Key words:** angiogenesis, Caco-2 cell line, nitric oxide, pregnane X receptor, rifaximin, vascular endothelial growth factor

and as such has an optimum safety profile. Apart from its antibiotic potential, rifaximin has also been studied for its anti-inflammatory effects; several studies have highlighted the anti-inflammatory potential of rifaximin, which is mainly attributed to the inhibition of the NF- $\kappa$ B signaling and NO release via activation of intestinal human pregnane X (PXR) receptors (16,17).

The aim of the present study was to explore the anti-proliferative and anti-migration effects of rifaximin, and to evaluate the possible control of the angiogenic mediator release by rifaximin using a human intestinal epithelial cell line to model the intestinal barrier. The effect of rifaximin on VEGF and NO signaling and the mechanisms involved were also investigated.

## Materials and methods

Caco-2 cells were purchased from the European Collection of Cell Cultures (ECACC, Public Health England Porton Down, Salisbury, UK). Cell medium, drugs and reagents for cell culture were purchased from Sigma-Aldrich (St. Louis, MO, USA), unless otherwise specified. Instruments, reagents and materials for western blot analysis were obtained from Bio-Rad Laboratories (Milan, Italy). Rifaximin and ketoconazole were purchased from Tocris Cookson, Inc. (Ballwin, MO, USA). Mouse anti-total Akt, rabbit monoclonal anti-phospho-Akt (Ser473), rabbit polyclonal anti-phospho-mTOR (pSer2448), rabbit polyclonal anti-total p70S6K, rabbit polyclonal anti-phospho-p70S6K (Thr421/Ser424, Thr389) and rabbit monoclonal anti-VEGF receptor were purchased from Cell Signaling Technology (Euroclone, Pero, Milan, Italy). Rabbit polyclonal anti-total mTOR was purchased from Abcam (Cambridge, UK); mouse monoclonal anti-hypoxia-inducible factor 1- $\alpha$  (HIF1- $\alpha$ ) was purchased from Sigma-Aldrich (Milan, Italy); rabbit polyclonal anti-matrix metalloproteinase-2 and 9 (MMP-2 and MMP-9) and mouse anti- $\beta$ -actin were purchased from Santa Cruz Biotechnology (Santa Cruz, CA, USA). Polyclonal rabbit anti-mouse immunoglobulin G was procured from Dako (Glostrup, Denmark),  $^{32}$ P- $\gamma$ -ATP from Amersham Biosciences (Milan, Italy), poly(deoxyinosinic-deoxycytidylic acid (poly(dI-dC)), from Boehringer Mannheim (Milan, Italy) and horseradish peroxidase (HRP) from Dako (Milan, Italy). Chemiluminescence detection reagents were purchased from Amersham Biosciences and custom oligonucleotides were synthesized by TIB Molbiol (Boehringer-Mannheim, Mannheim, Germany).

**Cell culture.** Caco-2 cells were cultured in 6-well plates in Dulbecco's modified Eagle's medium (DMEM) containing 10% fetal bovine serum (FBS), 1% penicillin-streptomycin, 2 mM L-glutamate and 1% non-essential amino acids. A total of  $1 \times 10^6$  cells/well were plated and incubated for 24 h. Upon reaching confluence, the cells were washed three times with phosphate-buffered saline (PBS), detached with trypsin/ethylene diamine tetraacetic acid (EDTA), plated in 10-cm diameter petri dishes and allowed to adhere for 24 h. Subsequently, DMEM was replaced with fresh medium and cells were treated for 72 h with increasing concentrations of rifaximin (0.1, 1.0 and 10.0  $\mu$ M) dissolved in ultrapure and pyrogen-free sterile vehicle in the presence or absence of the PXR antagonist ketoconazole (10 mM) at different time-points

depending upon the experiments. Rifaximin and ketoconazole concentrations were selected based on the data from the available literature (16,18) and the pilot experiments (data not shown) that helped in identifying the lowest effective concentrations.

**Western blot analysis.** Protein expression in the Caco-2 cells was evaluated by western blot analysis. After the different treatments, cells ( $1 \times 10^6$ ) were harvested, washed twice with ice-cold PBS and centrifuged at  $180 \times g$  for 10 min at 4°C. The cell pellet obtained after centrifugation was re-suspended in 100  $\mu$ l ice-cold hypotonic lysis buffer (10 mM HEPES, 1.5 mM  $MgCl_2$ , 10 mM KCl, 0.5 mM phenylmethylsulphonyl fluoride, 1.5  $\mu$ g/ml soybean trypsin inhibitor, 7  $\mu$ g/ml pepstatin A, 5  $\mu$ g/ml leupeptin, 0.1 mM benzamidine and 0.5 mM DTT). To lyse the cells, the suspension was rapidly passed through a syringe needle five to six times and then centrifuged for 15 min at  $13,000 \times g$  to obtain the cytoplasmic fraction. The cytoplasmic fraction proteins were mixed with non-reducing gel loading buffer [50 mM Tris, 10% sodium dodecyl sulphate (SDS), 10% glycerol, 2 mg bromophenol/ml] at a 1:1 ratio, boiled for 3 min and centrifuged at  $10,000 \times g$  for 10 min. The protein concentration was determined using the Bradford assay and 50  $\mu$ g of each sample was electrophoresed on a 12% discontinuous polyacrylamide mini-gel. Proteins were then transferred onto nitrocellulose membranes that had been saturated by incubation with 10% non-fat dry milk in 1X PBS overnight at 4°C with the following antibodies: total Akt (1:1,000), phospho-Akt (1:2,000), total mTOR (1:1,000), phospho-mTOR (1:1,000), total p70S6K (1:1,000), phospho-p70S6K (1:1,000), anti-HIF-1 $\alpha$  (1:500), anti-iNOS (1:1,000), anti-VEGFR-2 (1:1,000), anti-MMP-2 (1:1,000), anti-MMP-9 (1:1,000), anti-phospho-p38 (1:1,000), and anti- $\beta$ -actin protein expression was performed on total protein fractions of homogenates. Membranes were then incubated with the specific secondary antibodies conjugated to HRP. Immune complexes were identified by enhanced chemiluminescence detection reagents and blots were analyzed by scanning densitometry (GS-700 imaging densitometer; Bio-Rad Laboratories). Results were expressed as optical density (OD) (arbitrary units;  $mm^2$ ) and normalized against the expression of the housekeeping protein  $\beta$ -actin.

**Electrophoretic mobility shift assay.** Electrophoretic mobility shift assay (EMSA) was performed to detect NF- $\kappa$ B activation in Caco-2 cells. Briefly, 10 mg of the cell extracts were incubated in a binding buffer (8 mM HEPES, pH 7.0, 10% glycerol, 20 mM KCl, 4 mM  $MgCl_2$ , 1 mM sodium pyrophosphate) containing 1.0 mg of poly(dI-dC) and  $^{32}$ P- $\gamma$  end-labeled probe with the following sequence: i) 5' AAC TCC GGG AAT TTC CCT GGC CC 3' and ii) 5' GGG CCA GGG AAA TTC CCG GAG TT 3'. Nuclear extracts were incubated for 15 min with radiolabelled oligonucleotides (2.5-5.0  $\times 10^4$  cpm) in 20 ml reaction buffer containing 2 mg poly(dI-dC), 10 mM Tris-HCl (pH 7.5), 100 mM NaCl, 1 mM EDTA, 1 mM DL-dithiothreitol, 1 mg/ml bovine serum albumin (BSA) and 10% (v/v) glycerol. Nuclear protein-oligonucleotide complexes were resolved by electrophoresis on a 6% non-denaturing polyacrylamide gel in a Tris-borate-EDTA buffer at 150 V for 2 h at 4°C. The gel was dried and autoradiographed with an intensifying screen at -80°C for 20 h. The relative bands were

quantified by densitometric scanning using VersaDoc (Bio-Rad Laboratories) and a computer program (Quantity One Software; Bio-Rad Laboratories).

**Nitric oxide quantification.** NO was measured as nitrite (NO<sub>2</sub>) accumulation in the homogenates derived from Caco-2 cells by a spectrophotometric assay based on the Griess reaction. Griess reagent (1% sulphanilamide in H<sub>2</sub>O plus 0.1% naphthyl ethylenediamine in H<sub>3</sub>PO<sub>4</sub>) was added to an equal volume of supernatant and the absorbance was measured at 550 nm. Nitrite concentration (nM) was determined using a standard curve of NaNO<sub>2</sub>.

**Cell proliferation assay.** Cell proliferation was evaluated by performing a 3-[4,5-dimethylthiazol-2-yl]-2,5-diphenyl tetrazolium bromide (MTT) assay (19). Caco-2 cells (5x10<sup>4</sup>) were plated in 96-well plates and allowed to adhere for 3 h. DMEM was then replaced with fresh medium and the cells were untreated or treated with increasing concentrations of rifaximin (0.1, 1 and 10 μM) in the presence or absence of ketoconazole (10 mM). After 48 h, 25 μl MTT (5 mg/ml MTT in DMEM) was added to the cells and the mixture was incubated for further 3 h at 37°C. Cells were then lysed and the dark blue crystals were solubilized using a 125 μl solution containing 50% N,N-dimethyl formamide and 20% (w/v) SDS (pH 4.5). The OD of each well was determined using a Perkin-Elmer, Inc. (Waltham, MA, USA) microplate spectrophotometer equipped with a 620-nm filter. Cell proliferation in response to treatment was calculated using the following equation: Cell proliferation at 48 h (%) = (OD treated/OD untreated) x 100.

**Wound healing assay.** The wound healing assay was performed as previously described by Renault-Mihara and colleagues, with some modifications (20). Briefly, Caco-2 cells were plated on a 6-well plate and allowed to adhere to the surface of the wells. The cells were then scratched using a 200-μl sterile pipette tip, washed with PBS and incubated with rifaximin (0.1-10 μM) for 48 h. After incubation, the cells were again washed twice with PBS and fixed with 4% paraformaldehyde for 30 min. The cells were washed three times with PBS and photographed in a bright field using a Nikon Eclipse 80 (Nikon Instruments Europe, Kingston, UK) microscope equipped with a high-resolution digital camera (Nikon Digital Sight DS-U1; Nikon Corp.). The percentage of migration was calculated by counting the number of cells that migrated into scratched areas compared with cells that stayed in the peripheral areas.

**Enzyme-linked immunosorbent assay.** Enzyme-linked immunosorbent assay (ELISA) for mouse VEGF (Abcam, Cambridge, UK) was carried out on Caco-2 cell supernatant at 24-h post treatment, according to the manufacturer's protocol. Absorbance was measured on a microtiter plate reader. VEGF levels were determined using the standard curve method.

**Proliferating cell nuclear antigen immunofluorescence.** Caco-2 cells were plated onto glass slide chambers coated with poly-D-lysine (3x10<sup>4</sup> cells/well) and incubated for 24 h in the presence of rifaximin with or without ketoconazole.

After the treatment, cells were washed with PBS-Triton 0.1% (T-PBS), fixed in 4% paraformaldehyde and then incubated in 10% BSA/0.1% T-PBS solution for 90 min and for 1 h with a 10% BSA/0.1% T-PBS solution of anti-proliferating cell nuclear antigen (PCNA) antibody 1:100 (Abcam) for immunostaining. Finally, the cells were incubated for 1 h in the dark with fluorescein isothiocyanate conjugated anti-rabbit antibody 1:100 (Abcam). Nuclei were stained using Hoechst stain (1:5,000) (Sigma-Aldrich) and images were captured using a camera (Nikon digital sight DS-U1) connected to a microscope (Nikon eclipse 80i; Nikon Instruments Europe). The analysis of RGB intensity was performed using NIH software and quantification of PCNA<sup>+</sup> proliferating cells was expressed as % of PCNA<sup>+</sup> expressing cells per selected area (1 mm<sup>2</sup>).

**Statistical analysis.** Results were expressed as mean ± SEM of n=4 experiments in triplicate. Statistical analysis was performed using parametric one way analysis of variance (ANOVA) and multiple comparisons were performed using Bonferroni's post hoc test. P-values <0.05 were considered to indicate a statistically significant result.

## Results

**Cell proliferation in Caco-2 cells.** The effect of rifaximin treatment on cell proliferation and PCNA expression is shown in Fig. 1. Rifaximin 0.1, 1 and 10 μM caused a significant and concentration-dependent reduction in Caco-2 cell proliferation (-25, -40 and -68% vs. untreated cells; Fig. 1A), and this effect was inhibited by ketoconazole. Similarly, the expression of PCNA was reduced in a concentration-dependent manner by rifaximin 0.1, 1 and 10 μM (-29, -53 and -76% vs. untreated cells; Fig. 1B and C) and completely abolished by ketoconazole.

**Cell migration, VEGF secretion, and VEGFR-2, MMP-2 and MMP-9 expression.** The wound healing assay was used to evaluate the effect of rifaximin on Caco-2 cell migration. As indicated in panel 1 of Fig. 2A, untreated Caco-2 cells were able to invade and fully recolonize the scratched area within 48 h of treatment. In contrast, the migration of cells treated with rifaximin 0.1, 1 and 10 μM was significantly reduced in a concentration-dependent manner (-18, -30 and -46%, vs. untreated cells) (Fig. 2B). Also, the distances between the borders of the wound were significantly different compared to those measured in the untreated cells (Fig. 2A, panels 2, 3 and 4). The anti-migratory effect of rifaximin was completely counteracted by ketoconazole (Fig. 2A, panel 5).

As shown in Fig. 2, incubation with rifaximin 0.1, 1 and 10 μM resulted in a significant downregulation of pro-angiogenic mediators released at 48 h, causing a significant and concentration-dependent decrease of both VEGF secretion and NO release (-32, -45 -72 and -40, -69 and -87%, respectively, vs. untreated cells) (Fig. 2C and D). Similarly, rifaximin incubation significantly reduced the expression of VEGFR-2 and iNOS protein (-33 -58, -65 and -40, -69, -78%, respectively, vs. untreated cells) (Fig. 2E-G). Moreover, the treatment caused a significant and concentration-dependent inhibition of PXR-mediated MMP-2 and MMP-9 protein expression (-25,

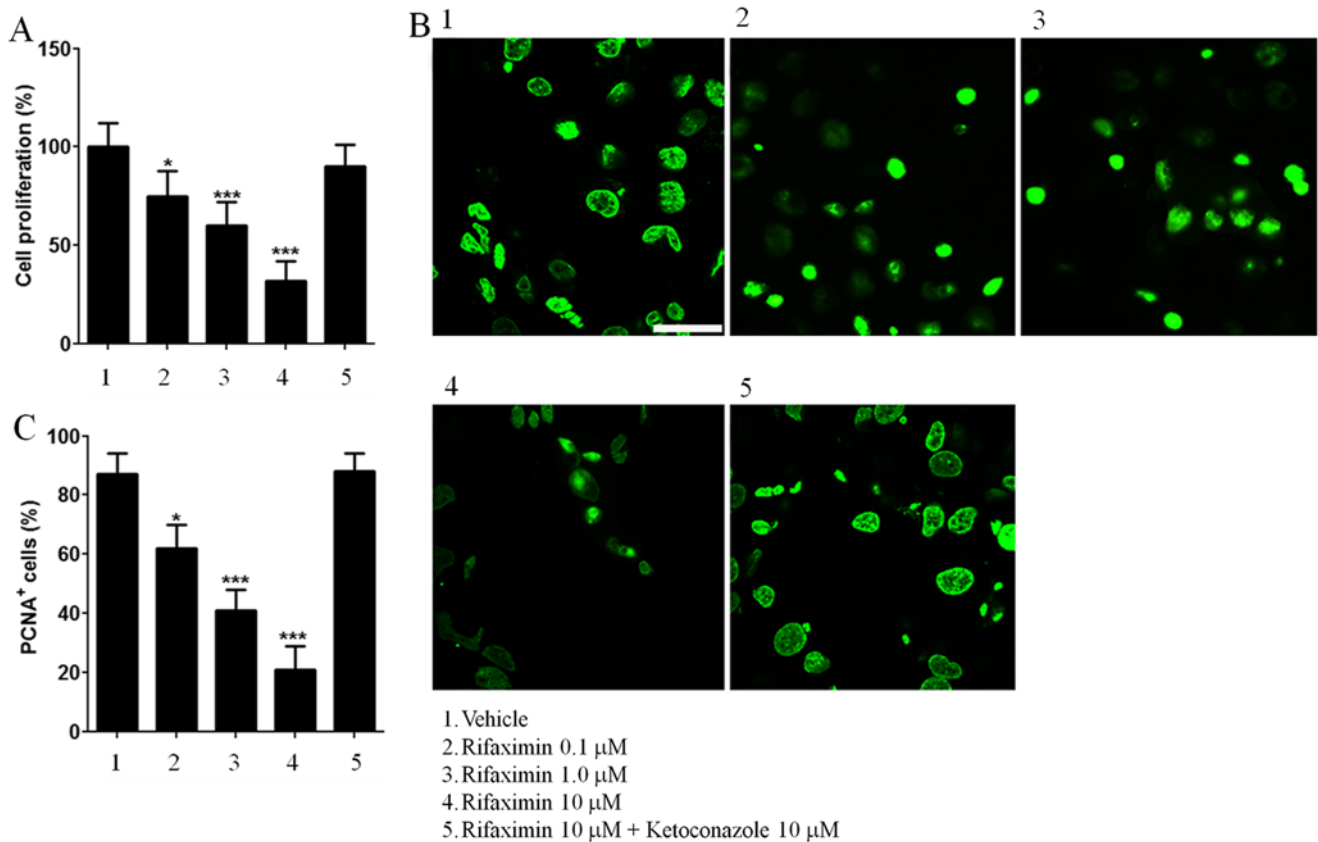


Figure 1. Rifaximin (0.1–10  $\mu$ M) exerts antiproliferative effects on Caco-2 cell line through a PXR-dependent selective involvement. (A) MTT analysis showing the effect of rifaximin plus ketoconazole (10  $\mu$ M) on Caco-2 cell proliferation; (B) immunofluorescence analysis of PCNA<sup>+</sup> positive Caco-2 cells; and (C) relative quantification in Caco-2 cells exposed to rifaximin in the presence or absence of ketoconazole (10  $\mu$ M) (scale bar, 50  $\mu$ m). Results are expressed as mean  $\pm$  SEM of n=5 experiments performed in triplicate. \*\*\*P<0.001; \*\*P<0.01 and \*P<0.05 vs. untreated Caco-2 cells.

-62, -87 and -38, -56 and -78%, respectively, vs. untreated cells) (Fig 2E, H and I).

#### *Akt/mTOR/p70S6K/HIF-1 $\alpha$ and p38MAPK/NF- $\kappa$ B expression.*

In order to further characterize the mechanisms underlying the effect of rifaximin, the involvement of the Akt/mTOR/p70S6K pathway was evaluated. Treatment with rifaximin 0.1, 1 and 10  $\mu$ M resulted in a PXR-mediated and concentration-dependent decrease in Akt phosphorylation (-50 -75 and -86% vs. untreated cells) and a significant reduction in the phosphorylation rates of mTOR (-38, -56 and -78% vs. untreated cells). Inhibition of p70S6K (-27, -55 and -85% vs. untreated cells; Fig. 3A–D) was also seen at 24 h after rifaximin 0.1, 1 and 10  $\mu$ M treatment. Rifaximin also caused a significant and concentration-dependent decrease in HIF-1 $\alpha$  (-65, -82 and -92% vs. untreated cells); this effect was counteracted by ketoconazole. Rifaximin 0.1, 1 and 10  $\mu$ M significantly blocked p38MAPK-phosphorylation (-24, -62 and -71% vs. untreated cells; Fig 3F and G) and inhibited NF- $\kappa$ B nuclear activation (-29, -55 and -61% vs. untreated cells; Fig. 3H and I) as seen by EMSA analysis; inhibition was significantly reversed by ketoconazole treatment.

#### Discussion

In the present study, rifaximin caused a concentration-dependent reduction of Caco-2 cell proliferation and expression

of PCNA vs. untreated cells. The migration of cells and the expression of VEGF, VEGFR-2, NOS and iNOS were also reduced in a concentration-dependent manner after treatment. Rifaximin significantly blocked p38MAPK-phosphorylation, inhibited NF- $\kappa$ B nuclear activation and p70S6K in Caco-2 cells. Moreover, MMP-2 and MMP-9 levels, Akt phosphorylation, mTOR phosphorylation and HIF-1 $\alpha$  expression were also reduced in a concentration-dependent manner.

PCNA is a marker of cell division and its overexpression is associated with malignancy, infiltration of the vasculature and tumor metastasis (21). It is considered to be a biomarker of colorectal cancer (22). In this study, rifaximin caused a progressive reduction of Caco-2 cell proliferation and downregulated PCNA expression, thus, confirming its antiproliferative effect. This effect was counteracted by the selective PXR antagonist ketoconazole, suggesting a PXR-dependent control of carcinoma cell growth rate.

The results of the present study also showed that rifaximin effectively prevented the release of pro-angiogenic mediators in Caco-2 cells and reduced the levels of VEGF, NO, VEGFR and iNOS. Rifaximin-induced p38MAPK/NF- $\kappa$ B inhibition and reduction in HIF-1 $\alpha$  levels were significantly reversed by ketoconazole, further confirming the involvement of PXR. HIF-1 $\alpha$  is a transcriptional modulator of pro-angiogenic factor release and its expression is increased upon activation of the Akt/mTOR pathway (23). Based on the results of the present study, it can be stated that rifaximin acted at the

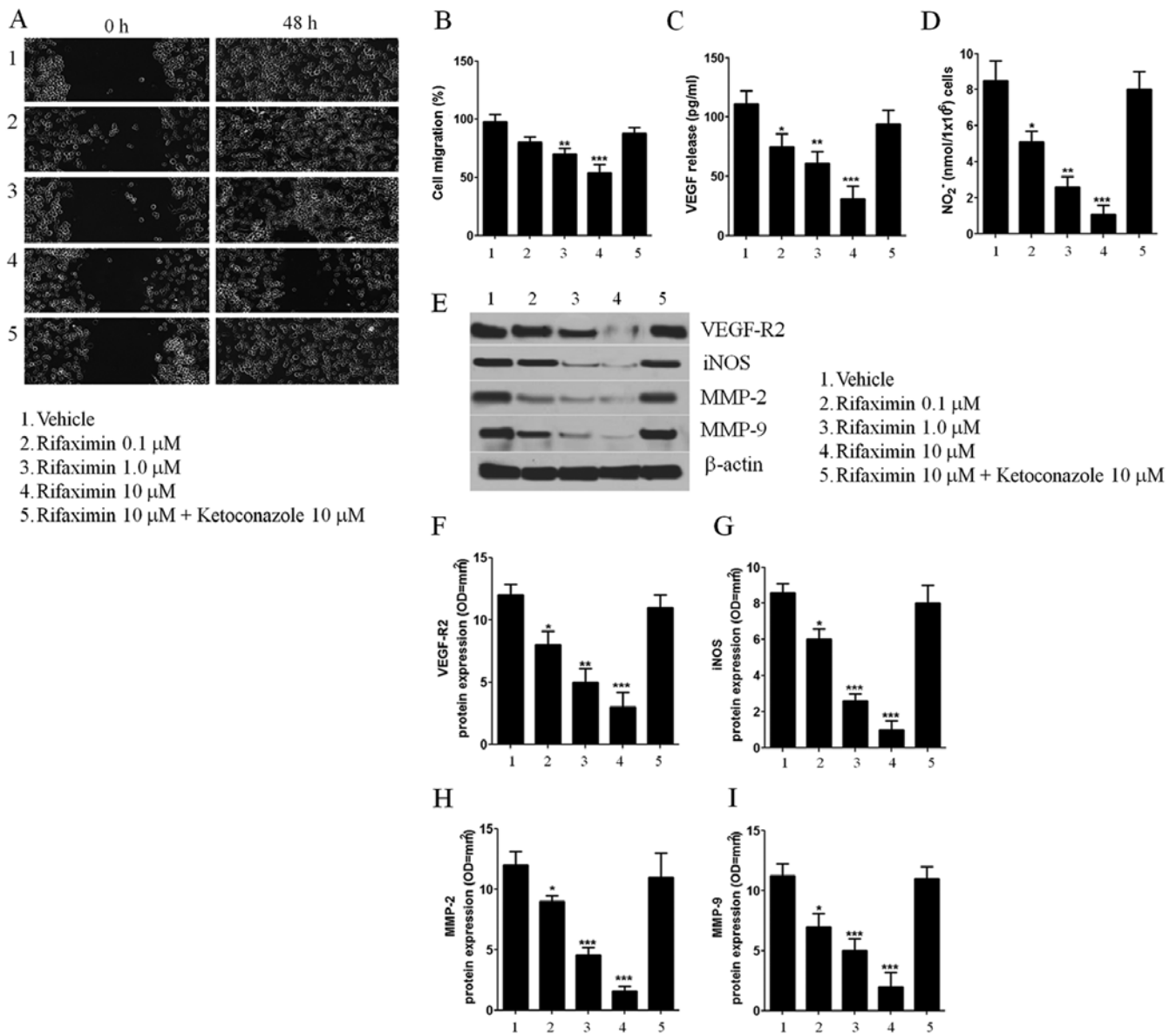


Figure 2. The anti-migration and anti-angiogenic effect of rifaximin in Caco-2 cells depends on PXR-dependent activation. (A) Wound healing assay showing the effect of rifaximin on Caco-2 cell migration *in vitro*. Bright field microscopy indicated that rifaximin inhibited Caco-2 cell migration in a concentration- and PXR-dependent manner (scale bar, 200  $\mu$ m); (B) quantification of cell migration (%); (C and D) rifaximin concentration-dependently inhibited pro-angiogenic release of VEGF and NO by a PXR-dependent pathway; (E) rifaximin inhibited VEGFR-2, iNOS, MMP-2 and MMP-9 protein expression in a concentration-dependent manner; and (F-I) densitometric analysis and relative quantification of corresponding immunoreactive bands for VEGFR-2, iNOS, MMP-2 and MMP-9 (normalized against the expression of the housekeeping protein  $\beta$ -actin). Results are expressed as mean  $\pm$  SEM of n=5 experiments performed in triplicate \*\*\*P<0.001; \*\*P<0.01 and \*P<0.05 vs. untreated Caco-2 cells.

PXR site and further inhibited the release of VEGF and NO by negatively interfering with both p38MAPK/NF- $\kappa$ B and p-Akt/p-mTOR-dependent signaling pathways. Specifically, rifaximin markedly reduced the phosphorylation of Akt, mTOR and p70S6K proteins in Caco-2 cells, leading to inhibition of HIF-1 $\alpha$  and blocking of the p38MAPK/ERK phosphorylation signaling pathway, reducing the activation of NF- $\kappa$ B. Also, rifaximin resulted in a significant and PXR-dependent decrease in the expression of MMP-2 and MMP-9 in Caco-2 cells. MMPs are involved in the growth and metastasis of cancer, specifically by promoting angiogenesis, degrading the matrix barriers and causing cell migration and proliferation (24). Thus, inhibition of MMP-2 and MMP-9 by rifaximin might be responsible for the observed reduction in the migration of Caco-2 cells *in vitro*.

Additionally, inhibition of both NO and VEGF secretion by rifaximin may be responsible for the consistent reduction of both iNOS and VEGFR expression in the experimental setting. Cheng *et al* (16) studied the anti-inflammatory effect of rifaximin in a colitis model and showed that rifaximin acted on human PXR and caused NF- $\kappa$ B inhibition. Another study demonstrated that rifaximin induced specific activation of PXR in PXR-humanized mice and mediated the inflammation, cancer cell proliferation and pro-apoptotic events in colon cancer (25). The results from the present study are in line with these reports and further show that rifaximin is a potent inhibitor of the release of angiogenic mediators.

One of the greatest advantages of this antibiotic is its poor oral absorption and an optimum safety profile (23,26); the

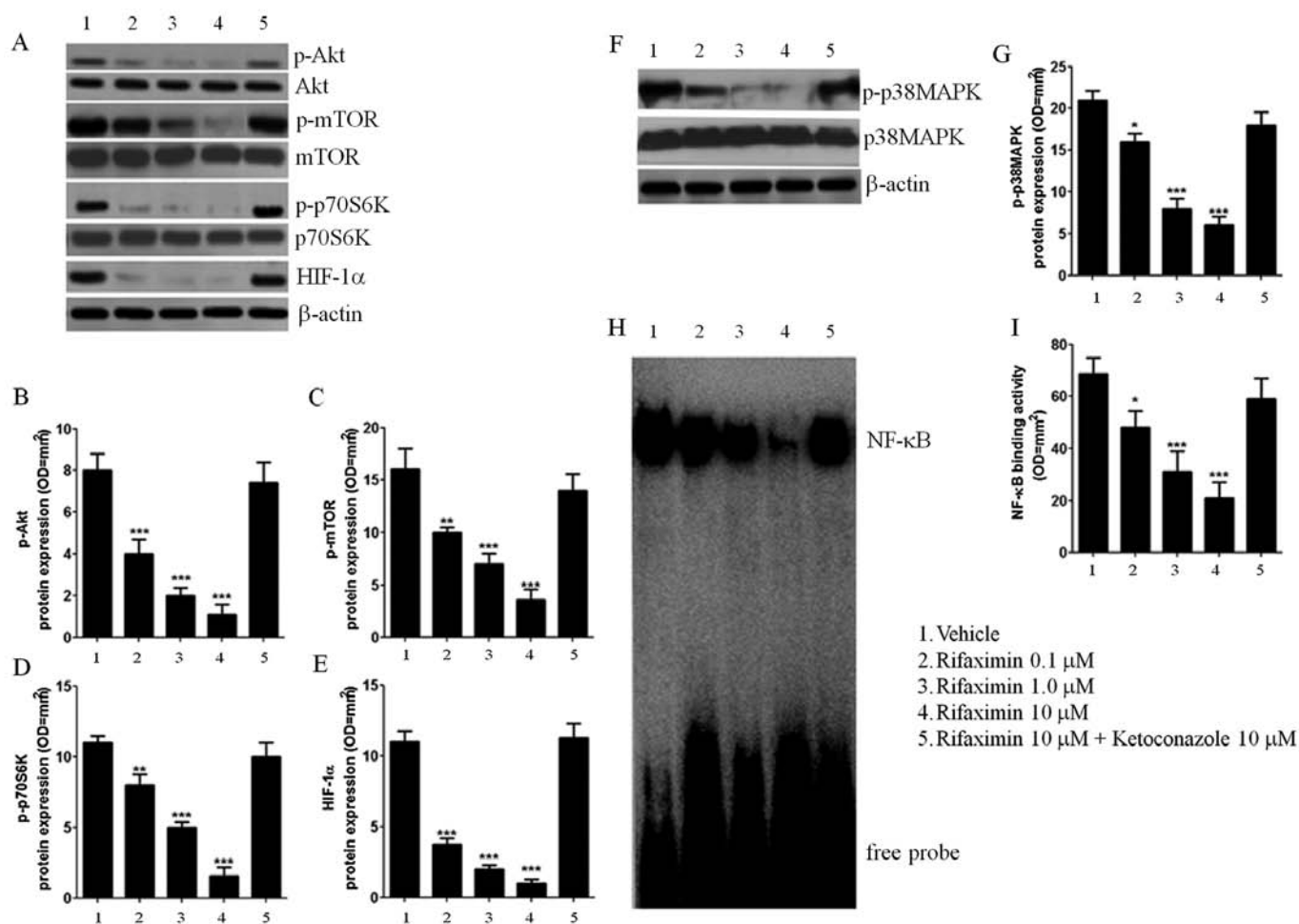


Figure 3. Rifaximin (0.1-10  $\mu$ M) downregulated Akt/mTOR and p38MAPK/NF- $\kappa$ B pathways through a PXR-dependent mechanism. (A) Immunoblot of phosphorylated/unphosphorylated Akt, mTOR, p70S6K and HIF-1 $\alpha$  protein bands; (B-E) relative densitometric analysis (normalized against the expression of the housekeeping protein  $\beta$ -actin) showing the effects of rifaximin, given alone or in the presence of ketoconazole (10  $\mu$ M), on the expression of Akt, mTOR and p70S6K phosphorylated proteins and HIF-1 $\alpha$  pro-angiogenic modulator in Caco-2 cells, (F) rifaximin inhibited p38MAPK phosphorylation as seen by immunoblot and EMSA analysis; (H) relative NF- $\kappa$ B activation in a concentration- and PXR-dependent manner; and (G-I) relative densitometric analysis of p38 MAPK and NF- $\kappa$ B bands (normalized against the expression of the housekeeping protein  $\beta$ -actin). Results are expressed as mean  $\pm$  SEM of n=5 experiments performed in triplicate. \*\*\*P<0.001 and \*P<0.05 vs. untreated Caco-2 cells.

unabsorbed drug stays in the gut, specifically in the colon, long enough to locally exert its effects without any adverse events.

Anti-angiogenic approaches in the treatment of colon cancer have been extensively studied in the past decade, following US Food and Drug Administration approval of the first anti-VEGF monoclonal antibody, bevacizumab (27,28). Despite their indisputable advantages as anticancer therapy, anti-angiogenic compounds are limited by the complexity of the converging pro-angiogenic pathways responsible for the neo-vascularization process that makes angiogenesis in cancer difficult to control, especially when the tumor starts developing and metastasizing. This limits the use of anti-VEGF drugs, unless they are used in combination with traditional chemotherapy (29-31). Drugs capable of interfering with the different steps of the pro-angiogenic and proliferative processes in cancer cells are of special interest in an attempt to identify an effective treatment. The results of the present study indicate that rifaximin efficiently mediates the synergic inhibition of multiple converging pathways involved in the growth of cancer cells, pro-angiogenic mediator release and tissue remodeling/

invasion that could markedly increase the efficacy of the anti-cancer therapy in CRC, when used in combination with VEGF inhibitors. Based on the promising results seen with rifaximin *in vitro*, further *in vivo* studies investigating a possible multi-therapeutic approach with rifaximin plus traditional VEGF inhibitors in CRC are warranted.

#### Acknowledgements

The authors would like to thank Nishad Parkar of Springer Healthcare Communications for providing English and scientific editing of the manuscript before submission. This medical writing assistance was funded by Alfa Wasserman. C.C. is post-doctoral fellow of the Fonds voor Wetenschappelijk Onderzoek (FWO, Belgium).

#### References

- Boyle P and Langman JS: ABC of colorectal cancer: Epidemiology. *BMJ* 321: 805-808, 2000.

2. Haggard FA and Boushey RP: Colorectal cancer epidemiology: Incidence, mortality, survival, and risk factors. *Clin Colon Rectal Surg* 22: 191-197, 2009.
3. Carmeliet P and Jain RK: Angiogenesis in cancer and other diseases. *Nature* 407: 249-257, 2000.
4. Scaldaferrri F, Vetrano S, Sans M, Arena V, Straface G, Stigliano E, Repici A, Sturm A, Malesci A, Panes J, *et al*: VEGF-A links angiogenesis and inflammation in inflammatory bowel disease pathogenesis. *Gastroenterology* 136: 585-595.e585, 2009.
5. Ambs S, Merriam WG, Bennett WP, Felley-Bosco E, Ogunfusika MO, Oser SM, Klein S, Shields PG, Billiar TR and Harris CC: Frequent nitric oxide synthase-2 expression in human colon adenomas: Implication for tumor angiogenesis and colon cancer progression. *Cancer Res* 58: 334-341, 1998.
6. Lala PK and Chakraborty C: Role of nitric oxide in carcinogenesis and tumour progression. *Lancet Oncol* 2: 149-156, 2001.
7. Karar J and Maity A: PI3K/AKT/mTOR pathway in angiogenesis. *Front Mol Neurosci* 4: 51, 2011.
8. Pratheeshkumar P, Sreekala C, Zhang Z, Budhraj A, Ding S, Son YO, Wang X, Hitron A, Hyun-Jung K, Wang L, *et al*: Cancer prevention with promising natural products: Mechanisms of action and molecular targets. *Anticancer Agents Med Chem* 12: 1159-1184, 2012.
9. Gee E, Milkiewicz M and Haas TL: p38 MAPK activity is stimulated by vascular endothelial growth factor receptor 2 activation and is essential for shear stress-induced angiogenesis. *J Cell Physiol* 222: 120-126, 2010.
10. Olsson AK, Dimberg A, Kreuger J and Claesson-Welsh L: VEGF receptor signalling - in control of vascular function. *Nat Rev Mol Cell Biol* 7: 359-371, 2006.
11. Cianchi F, Cortesini C, Fantappiè O, Messerini L, Schiavone N, Vannacci A, Nistri S, Sardi I, Baroni G, Marzocca C, *et al*: Inducible nitric oxide synthase expression in human colorectal cancer: Correlation with tumor angiogenesis. *Am J Pathol* 162: 793-801, 2003.
12. Reinacher-Schick A, Pohl M and Schmiegel W: Drug insight: Antiangiogenic therapies for gastrointestinal cancers - focus on monoclonal antibodies. *Nat Clin Pract Gastroenterol Hepatol* 5: 250-267, 2008.
13. Mullen KD, Sanyal AJ, Bass NM, Poordad FF, Sheikh MY, Frederick RT, Bortey E and Forbes WP: Rifaximin is safe and well tolerated for long-term maintenance of remission from overt hepatic encephalopathy. *Clin Gastroenterol Hepatol* 12: 1390-1397.e1392, 2014.
14. de la Cabada Bauche J and Dupont HL: New developments in traveler's diarrhea. *Gastroenterol Hepatol (NY)* 7: 88-95, 2011.
15. Calanni F, Renzulli C, Barbanti M and Viscomi GC: Rifaximin: Beyond the traditional antibiotic activity. *J Antibiot (Tokyo)* 67: 667-670, 2014.
16. Cheng J, Shah YM, Ma X, Pang X, Tanaka T, Kodama T, Krausz KW and Gonzalez FJ: Therapeutic role of rifaximin in inflammatory bowel disease: Clinical implication of human pregnane X receptor activation. *J Pharmacol Exp Ther* 335: 32-41, 2010.
17. Mencarelli A, Renga B, Palladino G, Claudio D, Ricci P, Distrutti E, Barbanti M, Baldelli F and Fiorucci S: Inhibition of NF- $\kappa$ B by a PXR-dependent pathway mediates counter-regulatory activities of rifaximin on innate immunity in intestinal epithelial cells. *Eur J Pharmacol* 668: 317-324, 2011.
18. Kota BP, Tran VH, Allen J, Bebawy M and Roufogalis BD: Characterization of PXR mediated P-glycoprotein regulation in intestinal LS174T cells. *Pharmacol Res* 62: 426-431, 2010.
19. Mosmann T: Rapid colorimetric assay for cellular growth and survival: Application to proliferation and cytotoxicity assays. *J Immunol Methods* 65: 55-63, 1983.
20. Renault-Mihara F, Beuvon F, Iturriz X, Canton B, De Bouard S, Léonard N, Mouhamad S, Sharif A, Ramos JW, Junier MP, *et al*: Phosphoprotein enriched in astrocytes-15 kDa expression inhibits astrocyte migration by a protein kinase C delta-dependent mechanism. *Mol Biol Cell* 17: 5141-5152, 2006.
21. Guzińska-Ustymowicz K, Pryczynicz A, Kemon A and Czyżewska J: Correlation between proliferation markers: PCNA, Ki-67, MCM-2 and antiapoptotic protein Bcl-2 in colorectal cancer. *Anticancer Res* 29: 3049-3052, 2009.
22. Yang HB, Hsu PI, Chan SH, Lee JC, Shin JS and Chow NH: Growth kinetics of colorectal adenoma-carcinoma sequence: An immunohistochemical study of proliferating cell nuclear antigen expression. *Hum Pathol* 27: 1071-1076, 1996.
23. Cacciottolo TM, Kingdon A and Alexander GJ: Rifaximin is largely safe and well tolerated but caution is necessary when taken with statins. *Clin Gastroenterol Hepatol* 12: 1765, 2014.
24. Cathcart J, Pulkoski-Gross A and Cao J: Targeting matrix metalloproteinases in cancer: Bringing new life to old ideas. *Genes Dis* 2: 26-34, 2015.
25. Cheng J, Fang ZZ, Nagaoka K, Okamoto M, Qu A, Tanaka N, Kimura S and Gonzalez FJ: Activation of intestinal human pregnane X receptor protects against azoxymethane/dextran sulfate sodium-induced colon cancer. *J Pharmacol Exp Ther* 351: 559-567, 2014.
26. Hirota SA: Understanding the molecular mechanisms of rifaximin in the treatment of gastrointestinal disorders: A focus on the modulation of host tissue function. *Mini Rev Med Chem* 16: 206-217, 2015.
27. Li J and Saif MW: Current use and potential role of bevacizumab in the treatment of gastrointestinal cancers. *Biologics* 3: 429-441, 2009.
28. Giantonio BJ, Catalano PJ, Meropol NJ, O'Dwyer PJ, Mitchell EP, Alberts SR, Schwartz MA and Benson AB III; Eastern Cooperative Oncology Group Study E3200: Bevacizumab in combination with oxaliplatin, fluorouracil, and leucovorin (FOLFOX4) for previously treated metastatic colorectal cancer: Results from the Eastern Cooperative Oncology Group Study E3200. *J Clin Oncol* 25: 1539-1544, 2007.
29. Hurwitz HI, Fehrenbacher L, Hainsworth JD, Heim W, Berlin J, Holmgren E, Hambleton J, Novotny WF and Kabbinavar F: Bevacizumab in combination with fluorouracil and leucovorin: An active regimen for first-line metastatic colorectal cancer. *J Clin Oncol* 23: 3502-3508, 2005.
30. Jain RK: Normalizing tumor vasculature with anti-angiogenic therapy: A new paradigm for combination therapy. *Nat Med* 7: 987-989, 2001.
31. Huber PE, Bischof M, Jenne J, Heiland S, Peschke P, Saffrich R, Gröne HJ, Debus J, Lipson KE and Abdollahi A: Trimodal cancer treatment: Beneficial effects of combined antiangiogenesis, radiation, and chemotherapy. *Cancer Res* 65: 3643-3655, 2005.

# Palmitoylethanolamide Exerts Antiproliferative Effect and Downregulates VEGF Signaling in Caco-2 Human Colon Carcinoma Cell Line Through a Selective PPAR- $\alpha$ -Dependent Inhibition of Akt/mTOR Pathway

Giovanni Sarnelli,<sup>1†</sup> Stefano Gigli,<sup>2†</sup> Elena Capoccia,<sup>2</sup> Teresa Iuvone,<sup>3</sup> Carla Cirillo,<sup>4</sup> Luisa Seguella,<sup>2</sup> Nicola Nobile,<sup>2</sup> Alessandra D'Alessandro,<sup>1</sup> Marcella Pesce,<sup>1</sup> Luca Steardo,<sup>2</sup> Rosario Cuomo<sup>1</sup> and Giuseppe Esposito<sup>2\*</sup>

<sup>1</sup>Department of Clinical Medicine and Surgery, 'Federico II' University of Naples, Naples, Italy

<sup>2</sup>Department of Physiology and Pharmacology 'Vittorio Erspamer', La Sapienza University of Rome, Rome, Italy

<sup>3</sup>Department of Pharmacy, University of Naples Federico II, Naples, Italy

<sup>4</sup>Laboratory for Enteric NeuroScience (LENS), Translational Research Center for Gastrointestinal Disorders (TARGID), University of Leuven, Leuven, Belgium

**Palmitoylethanolamide (PEA) is a nutraceutical compound that has been demonstrated to improve intestinal inflammation. We aimed at evaluating its antiproliferative and antiangiogenic effects in human colon adenocarcinoma Caco-2 cell line. Caco-2 cells were treated with increasing concentrations of PEA (0.001, 0.01 and 0.1  $\mu$ M) in the presence of peroxisome proliferator-activated receptor- $\alpha$  (PPAR- $\alpha$ ) or PPAR- $\gamma$  antagonists. Cell proliferation was evaluated by performing a MTT assay. Vascular endothelial growth factor (VEGF) release was estimated by ELISA, while the expression of VEGF receptor and the activation of the Akt/mammalian target of rapamycin (mTOR) pathway were evaluated by western blot analysis. PEA caused a significant and concentration-dependent decrease of Caco-2 cell proliferation at 48 h. PEA administration significantly reduced in a concentration-dependent manner VEGF secretion and VEGF receptor expression. Inhibition of Akt phosphorylation and a downstream decrease of phospho-mTOR and of p-p70S6K were observed as compared with untreated cells. PPAR- $\alpha$ , but not PPAR- $\gamma$  antagonist, reverted all effects of PEA. PEA is able to decrease cell proliferation and angiogenesis. The antiangiogenic effect of PEA depends on the specific inhibition of the Akt/mTOR axis, through the activation of PPAR- $\alpha$  pathway. If supported by *in vivo* models, our data pave the way to PEA co-administration to the current chemotherapeutic regimens for colon carcinoma. Copyright © 2016 John Wiley & Sons, Ltd.**

**Keywords:** Palmitoylethanolamide (PEA); Caco-2 human adenocarcinoma cell line; angiogenesis; proliferation.

## INTRODUCTION

Angiogenesis is the formation of new blood vessels from pre-existing ones and is a key step in the growth, progression and metastasis formation of many form of cancers, including colorectal cancer (CRC) (Tanigawa *et al.*, 1997; Yoshimura *et al.*, 2004). CRC represents one of the major causes of morbidity and mortality throughout the world (Haggard and Boushey, 2009) and is estimated to be the third most common type of human cancer in Western countries (Boyle and Langman, 2000; Ferlay *et al.*, 2015). Different pro-angiogenic signaling molecules are able to promote tumor progression. Among these, vascular endothelial growth factor (VEGF) is a pivotal secreted factor that stimulates cancer neovascularization interacting with specific receptors, named

VEGF-R1 and 2 (Carmeliet and Jain, 2000; McMahon, 2000). The mammalian target of rapamycin (mTOR) is a protein kinase of the PI3K/Akt signaling pathway involved in the control of cell proliferation, survival, mobility and angiogenesis. Impaired regulation of mTOR pathway has been described in many human cancers, including CRC (Cantley, 2002; Vivanco and Sawyers, 2002). For this reason, mTOR pathway is considered an important target for the development of new anticancer chemotherapeutics (Fasolo and Sessa, 2008) for CRC (Zhang *et al.*, 2009). When Akt is phosphorylated, a subsequent phosphorylation of mTOR is observed. As a result, phosphorylated mTOR regulates the p70S6K phosphorylation and activation (Chen and Fang, 2002). Such pathway downstream leads to VEGF secretion and is not only a crucial network able to coordinate cell proliferation, growth, differentiation and survival but also a crucial step leading to angiogenesis in neoplastic and non-neoplastic processes (Li *et al.*, 2008).

Natural products have been always seen as an interesting source of active therapeutic agents, including anticancer agents (Arumuggam *et al.*, 2015). Cancer prevention by natural products has become an integral

\* Correspondence to: Giuseppe Esposito, Department of Physiology and Pharmacology 'Vittorio Erspamer', La Sapienza University of Rome, Rome, Italy.

E-mail: giuseppe.esposito@uniroma1.it

<sup>†</sup>These authors equally contributed to the manuscript



part of cancer control, and plant-derived molecules have been thus regarded as potential novel leads for developing antiangiogenic drugs (Kuttan *et al.*, 2011; Pratheeshkumar *et al.*, 2012). Palmitoylethanolamide (PEA) is an endogenous N-acyl ethanolamide, acting as an 'on demand' autacoid local antiinflammatory amide (ALIA)-amide involved in many pathophysiological processes ranging from pain control, neuroprotection and antiinflammatory response (Calignano *et al.*, 2001; Lambert *et al.*, 2001; Levi-Montalcini *et al.*, 1996; LoVerme *et al.*, 2005a). Although PEA is synthesized and metabolized by different animal cell types, it is commonly considered a nutraceutical compound (Keppel Hesselink *et al.*, 2014) because it is abundantly present in plants (Coulon *et al.*, 2012; Kim *et al.*, 2010) particularly in peanuts or fenugreek seeds and soybean lecithin (Kuehl *et al.*, 1957). Several evidences show that PEA is a 'promiscuous' molecule (Di Marzo *et al.*, 2001; LoVerme *et al.*, 2005b; Pertwee *et al.*, 2010), whose specific molecular mechanism of action has not been completely clarified yet. Together with the inhibition of mast cell degranulation (Aloe *et al.*, 1993), a number of its possible molecular targets have been indeed described, including the transient receptor potential vanilloid receptor type 1 (TRPV1) channel, the orphan G-protein coupled receptor (GPR55) and the nuclear peroxisome proliferator-activated receptor- $\alpha$  (PPAR- $\alpha$ ) (LoVerme *et al.*, 2005a), which has been demonstrated to mediate most of the pharmacologic effects of this compound (D'Agostino *et al.*, 2009; Scuderi *et al.*, 2011).

Because of its multi-faceted activity, PEA has been considered a very interesting molecule because it is able to exert antiproliferative (Keppel Hesselink, 2013a) and antiangiogenic effects (Cipriano *et al.*, 2015). Many of these properties are a consequence of its well-known antiinflammatory activity, as seen, for instance, in granuloma formation (De Filippis *et al.*, 2010), in colitis (Alhouayek *et al.*, 2015; Borrelli *et al.*, 2015) and in *in vitro* amyloid-beta induced neuroinflammation (Scuderi *et al.*, 2011). Although PEA has been recognized to exert cytostatic effects in melanoma and breast cancer models (Di Marzo *et al.*, 2001; Hamtiaux *et al.*, 2012) to date, no proofs about antiangiogenic and antiproliferative activities of PEA in human CRC cells have been provided yet.

Given this background, the present research aimed at evaluating the antiproliferative and antiangiogenic effects of PEA administration in human colon adenocarcinoma Caco-2 cell line; moreover, we examined PEA efficacy in modulating VEGF signaling, *via* the Akt/mTOR pathway. Finally, we aimed at confirming/excluding the involvement of PPAR- $\alpha$  activation in determining PEA pharmacological activity.

## MATERIALS AND METHODS

**Materials.** Caco-2 cells were purchased from European Collection of Cell Cultures (ECACC, Public Health England Porton Down, Salisbury, UK). Cell medium, substances and reagents for cell cultures were all purchased from Sigma-Aldrich (St. Louis, MO, USA), unless otherwise stated. Instruments, reagents and materials for western blot analysis were obtained from Bio-Rad

Laboratories (Milan, Italy). PEA, as well as PPAR antagonists GW9662 and MK 866, was purchased from Tocris Cookson, Inc. (Ballwin, MO, USA). Mouse anti-total Akt, rabbit monoclonal anti-phospho-Akt (Ser<sup>473</sup>), rabbit polyclonal anti-phospho-mTOR (pSer<sup>2448</sup>), rabbit polyclonal anti-total p70S6K, rabbit polyclonal anti-phospho-p70S6K (Thr<sup>421</sup>/Ser<sup>424</sup>, Thr<sup>389</sup>) and rabbit monoclonal anti-VEGF receptor were purchased from Cell Signaling Technology (Euroclone, Pero, MI, Italy). Rabbit polyclonal anti-total mTOR was from Abcam (Cambridge, UK); mouse monoclonal anti-HIF-1 $\alpha$  was purchased from Sigma Aldrich (MI, Italy); rabbit polyclonal anti-matrix metalloprotease-2 (MMP-2) and mouse anti- $\beta$ -actin were from Santa Cruz Biotechnology (Santa Cruz, California, USA). Polyclonal rabbit anti-mouse IgG from Dako (Glostrup, Denmark).

## Methods

**Cell culture.** Caco-2 cells obtained from ECACC (Public Health England Porton Down, Salisbury, UK) were cultured in 6-well plate in DMEM containing 10% fetal bovine serum (FBS), 1% penicillin-streptomycin, 2 mM L-glutamate and 1% non-essential aminoacids to confluence. A total of  $1 \times 10^6$  cells/well were plated and incubated for 24 h. After reaching confluence, the cells were washed three times with phosphate-buffered saline (PBS), detached with trypsin/EDTA, plated in 10-cm diameter petri dish and allowed to adhere for 24 h. Subsequently, DMEM was replaced with fresh medium, and the cells were untreated or treated with increasing concentrations of PEA (0.001, 0.01 and 0.1  $\mu$ M) dissolved in ultrapure and pyrogen-free sterile vehicle in the presence or absence of 3  $\mu$ M MK866 or 9 nM GW9662, a PPAR- $\alpha$  and PPAR- $\gamma$  antagonist, respectively. PEA and relative PPAR antagonist concentrations were selected according to the results of a previous published researches (Scuderi *et al.*, 2011), and pilot experiments aimed at identifying the lowest effective concentration (data not shown).

**Western blot.** Protein expression in the Caco-2 cells was evaluated by performing a western blot analysis. Following treatments, cells ( $1 \times 10^6$ ) were harvested, washed twice with ice-cold PBS and centrifuged at  $180 \times g$  for 10 min at 4°C. The cell pellet was resuspended in 100  $\mu$ L ice-cold hypotonic lysis buffer (10 mM HEPES, 1.5 mM MgCl<sub>2</sub>, 10 mM KCl, 0.5 mM phenylmethylsulphonyl fluoride, 1.5  $\mu$ g/mL soybean trypsin inhibitor, 7  $\mu$ g/mL pepstatin A, 5  $\mu$ g/mL leupeptin, 0.1 mM benzamidine and 0.5 mM dithiothreitol). To lyse the cells, the suspension was rapidly passed through a syringe needle five to six times prior to centrifugation for 15 min at  $13,000 \times g$  to obtain the cytoplasmic fraction. The cytosolic fraction proteins were mixed with non-reducing gel loading buffer (50 mM Tris, 10% SDS, 10% glycerol, 2 mg bromophenol/mL) at a 1:1 ratio, boiled for 3 min and centrifuged at  $10,000 \times g$  for 10 min. The protein concentration was determined using a Bradford assay, and equivalent quantities (50  $\mu$ g) of each sample were electrophoresed on a 12% discontinuous polyacrylamide minigel. Subsequently, the proteins were transferred onto nitrocellulose membranes that had been saturated by incubation with 2.5% non-fat

dry milk in 1× PBS overnight at 4 °C with the following antibodies: total Akt, phosphor-Akt, total mTOR, phosphor-mTOR, total p70S6K, phosphor-p70S6K, anti-VEGF-R and anti-HIF-1 $\alpha$ , and  $\beta$ -actin protein expression was performed on total protein fractions of homogenates. Equivalent amounts (50  $\mu$ g) of each homogenate underwent electrophoresis through a polyacrilamide minigel. Proteins were then transferred onto nitrocellulose membrane that were saturated by incubation with 10% non-fat dry milk in 1× PBS overnight at 4 °C and then incubated, according the experimental protocols with mouse anti-total Akt (1:1000 v/v, Cell Signaling Technology, Euroclone, Pero, MI, Italy), rabbit monoclonal anti-phospho-Akt (Ser<sup>473</sup>) (1:2000 v/v, Cell Signaling Technology, Euroclone, Pero, MI, Italy), rabbit polyclonal anti-total mTOR (1:1000 Abcam, Cambridge, UK), rabbit polyclonal anti-phospho-mTOR (pSer<sup>2448</sup>) (1:1000 v/v, Cell Signaling Technology, Euroclone, Pero, MI, Italy), rabbit polyclonal anti-total p70S6K (1:1000 v/v) and rabbit polyclonal anti-phospho-p70S6K (Thr<sup>421</sup>/Ser<sup>424</sup>, Thr<sup>389</sup>) (1:1000 v/v, Cell Signaling Technology, Euroclone, Pero, MI, Italy), rabbit monoclonal anti-VEGF receptor (1:1000 v/v, Cell Signaling Technology, Euroclone, Pero, MI, Italy), mouse monoclonal anti-HIF1 $\alpha$  (1:500 v/v, Sigma Aldrich, MI, Italy) and mouse anti- $\beta$ -actin (1:2000 v/v) (Santa Cruz Biotechnology, Santa Cruz, California, USA) rabbit polyclonal anti-MMP-2 (1:2000 v/v) (Santa Cruz Biotechnology, Santa Cruz, California, USA). Membranes were then incubated with the specific secondary antibodies conjugated to horseradish peroxidase (Dako, Milan, Italy). Immune complexes were revealed by enhanced chemiluminescence detection reagents (Amersham Biosciences, Milan, Italy). Blots were analyzed by scanning densitometry (GS-700 imaging densitometer; Bio-Rad). Results were expressed as optical density (arbitrary units; mm<sup>2</sup>) and normalized on the expression of the housekeeping protein  $\beta$ -actin.

*Enzyme-linked immunosorbent assay for VEGF.* Enzyme-linked immunosorbent assay for human VEGF (Abcam, Cambridge, UK) was carried out with Caco-2 cell supernatant after treatments at 24 h according to the manufacturer's protocol. Absorbance was measured on a microtiter plate reader. VEGF levels were thus determined using standard curves' method.

*Cell proliferation assay.* Cell proliferation was evaluated by performing a 3-[4,5-dimethylthiazol-2-yl]-2,5-diphenyltetrazolium bromide (MTT) assay (Mosmann, 1983). In brief, Caco-2 cells ( $5 \times 10^4$ ) were plated in 96-well plates and allowed to adhere for 24 h. After that, DMEM was replaced with fresh medium, and the cells were untreated or treated with increasing concentrations of PEA (0.001, 0.01 and 0.1  $\mu$ M) dissolved in ultrapure and pyrogen-free sterile vehicle in the presence or absence of 3  $\mu$ M MK866 or 9 nM GW9662. After 48 h, 25  $\mu$ L MTT (5 mg/mL MTT in DMEM) was added to the cells, and the mixture was incubated for an additional 3 h at 37 °C. Subsequently, the cells were lysed, and the dark blue crystals were solubilized using a 125- $\mu$ L solution containing 50% N,N-dimethylformamide and 20% (w/v) sodium dodecylsulfate (pH 4.5). The OD of each well was

determined using a PerkinElmer, Inc. (Waltham, MA, USA) microplate spectrophotometer equipped with a 620-nm filter. Cell proliferation in response to treatments was calculated using the following equation: Cell proliferation at 48 h (%) = (OD treated/OD untreated)  $\times$  100.

*Immunodetection of incorporation of BrdU.* Caco-2 cells ( $1 \times 10^5$ ) were plated onto cover glass in DMEM medium and grown to ~60% confluence for 24 h. Cells were then untreated or treated for 24 h with PEA (0.001, 0.01 and 0.1  $\mu$ M) dissolved in ultrapure and pyrogen-free sterile vehicle in the presence or absence of 3  $\mu$ M MK866 or 9 nM GW9662 and then labeled for the following 4 h with 1010  $\mu$ M 5'-bromo-2'-deoxyuridine (BrdU). After labeling, the cells were washed twice with PBS and fixed in ice-cold 1% paraformaldehyde. Fixed cells were washed with PBS to remove the organic solvent. The FITC-labeled anti-BrdU antibody, diluted with PBS buffer containing 0.1% Triton X-100, was used to measure BrdU incorporation by fluorescence microscopy. Cover glasses were thus analyzed with a microscope (Nikon Eclipse 80i by Nikon Instruments Europe), and images were captured at 10 $\times$  magnification by a high-resolution digital camera (Nikon Digital Sight DS-U1). Quantification of BrdU<sup>+</sup> incorporation after treatments was thus expressed as % of BrdU<sup>+</sup> expressing cells per selected area (1 mm<sup>2</sup>).

*Wound healing assay.* A wound healing assay using the Caco-2 cells was performed as described previously, with a number of modifications (Renault-Mihara *et al.*, 2006). Briefly, the cells ( $5 \times 10^5$  cells/well) were plated on a 6-well plate and incubated for 24 h in DMEM supplemented with 5% FBS, 2 mM glutamine, 100 U/mL penicillin and 100  $\mu$ g/mL streptomycin in a humidified atmosphere of 5% CO<sub>2</sub> and 95% air at a temperature of 37 °C. The cell layer was scratched using a 200- $\mu$ L sterile pipette tip; then, cells were washed with PBS three times and untreated or incubated with PEA (0.001, 0.01 and 0.1  $\mu$ M) dissolved in ultrapure and pyrogen-free sterile vehicle in the presence or absence of 3  $\mu$ M MK866 or 9 nM GW9662 for 48 h. The Caco-2 cells were washed twice with PBS and fixed with 4% paraformaldehyde for 30 min. In order to facilitate cell counting, the nucleus of the Caco-2 cells was stained with Hoechst 33258 (Invitrogen Life Technologies, Carlsbad, CA, USA) for 5 min at RT. The cells were subsequently washed three times with PBS, and images were captured using a Nikon Eclipse 80 microscope equipped with a high-resolution digital camera (Nikon Digital Sight DS-U1; Nikon Instruments, Inc.). The percentage of migration was calculated by counting the number of cells that had migrated into scratched areas compared with the number of cells that had remained in the peripheral areas.

*Statistical analysis.* Results are expressed as the mean  $\pm$  standard error (SEM) of the mean of *n* experiments. Statistical analyses were performed using one-way analysis of variance, and multiple comparisons were performed using a Bonferroni *post hoc* test. *p* < 0.05 was considered to indicate a statistically significant difference.

## RESULTS

### PEA inhibited Caco-2 cell proliferation through a PPAR- $\alpha$ selective activation

PEA (Fig. 1A) (0.001–0.1  $\mu$ M) administration caused a significant and concentration-dependent (–30, –40 and –58%, respectively vs untreated) decrease of Caco-2 cell proliferation at 48 h in comparison with untreated cells, assumed as 100% proliferation rate (Fig. 1B). PEA effect was counteracted by the presence of PPAR- $\alpha$  selective antagonist MK866, while remained unaffected in the presence of the PPAR- $\gamma$  antagonist GW9662 (Fig. 1B). In order to further confirm this anti-proliferative effect, we tested effect of PEA on BrdU incorporation into the DNA. We observed that PEA (0.001–0.1  $\mu$ M) in a concentration-dependent fashion was able to significantly reduce BrdU<sup>+</sup> cell staining (–25, –48.5 and –72.4% vs untreated cells, respectively) and that this effect was almost completely inhibited by the presence of the PPAR- $\alpha$  but not by the PPAR- $\gamma$  antagonist (Fig. 1C, D).

### PEA inhibited Caco-2 cell migration and reduced VEGF secretion and VEGF receptor and MMP-2 expression.

The wound healing assay was used to evaluate the effect of PEA treatment on Caco-2 cell migration. As indicated in Fig. 2A, panel 1, untreated Caco-2 cells were able to invade and fully recolonize the scratched area within 48 h, while the migration of cells treated with 0.001, 0.01 and 0.1  $\mu$ M PEA was significantly impaired in a concentration-dependent manner (–14, –35 and –78%, respectively vs untreated cells) (Fig. 2B). This

was further confirmed by the fact that the distance between the borders of the wound significantly differs as compared with that measured in the untreated cells group (Fig. 2A, panels 2, 3 and 4). According to the previously obtained results, the antimigratory effect of PEA effect was almost completely abolished by the co-administration of PPAR- $\alpha$  selective but not by PPAR- $\gamma$  receptor antagonist (Fig. 2A panel 5 and 6). Together with this antimigratory effect, PEA incubation resulted in a significant down-regulation of pro-angiogenic effectors, reducing in a concentration-dependent manner both VEGF secretion (–27, –50 and –65% respectively vs untreated) and VEGF receptor expression (–28, –66 and –81% vs untreated cells) (Fig. 2C, D, and E respectively). Moreover, PEA caused a significant and concentration-dependent inhibition of the breakdown of extracellular matrix through a marked and PPAR- $\alpha$ -mediated MMP-2 protein expression decrease in the same experimental conditions (–25, –48 and –83% respectively vs untreated cells) (Fig. 2D, F respectively).

### Antiproliferative effects of PEA and its downregulation of pro-angiogenic mediators depend via Akt/mTOR/p70S6K and HIF-1 $\alpha$ pathway inhibition

In order to better understand the molecular mechanisms at the basis of the antiangiogenic effect of PEA, we evaluated the effect of this ALIA-mide on the Akt/mTOR/p70S6K pathway. PEA caused a PPAR- $\alpha$  and concentration-dependent decrease of Akt phosphorylation (–20, –40 and –65% vs untreated) that was accompanied with a consequent reduction of phospho-mTOR (–23, –73 and –81% vs untreated) and downstream inhibition of p-p70S6K (–34, –58 and –80% respectively vs untreated) at 24 h (Fig. 3A, B). HIF-1 $\alpha$  is a key transcriptional

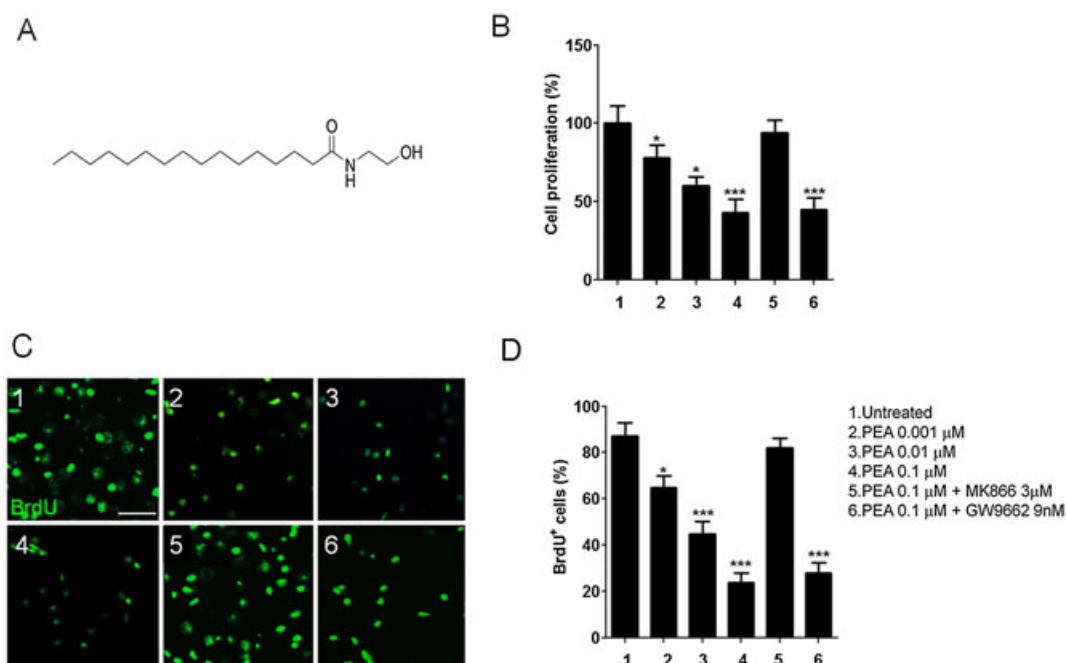


**Figure 1.** Palmitoylethanolamide exerts anti-proliferative effects on Caco-2 cell line. (A) Chemical structure of PEA. (B) MTT analysis showing the effect of PEA (0.001–0.1  $\mu$ M) in the presence of PPAR- $\alpha$  or PPAR- $\gamma$  antagonists MK866 (3  $\mu$ M) and GW9662 (9 nM) on Caco-2 cell proliferation rate at 48 h. (C) Immunofluorescence analysis of BrdU<sup>+</sup> incorporating Caco-2 cells and (D) relative quantification in Caco-2 cells exposed to PEA (0.001–0.1  $\mu$ M) in the presence or absence of MK866 (3  $\mu$ M) and GW9662 (9 nM) (scale bar: 20  $\mu$ m). Results are expressed as mean  $\pm$  SEM of  $n = 4$  experiments performed in triplicate. \*\*\* $p < 0.001$  and \* $p < 0.05$  versus untreated Caco cells.

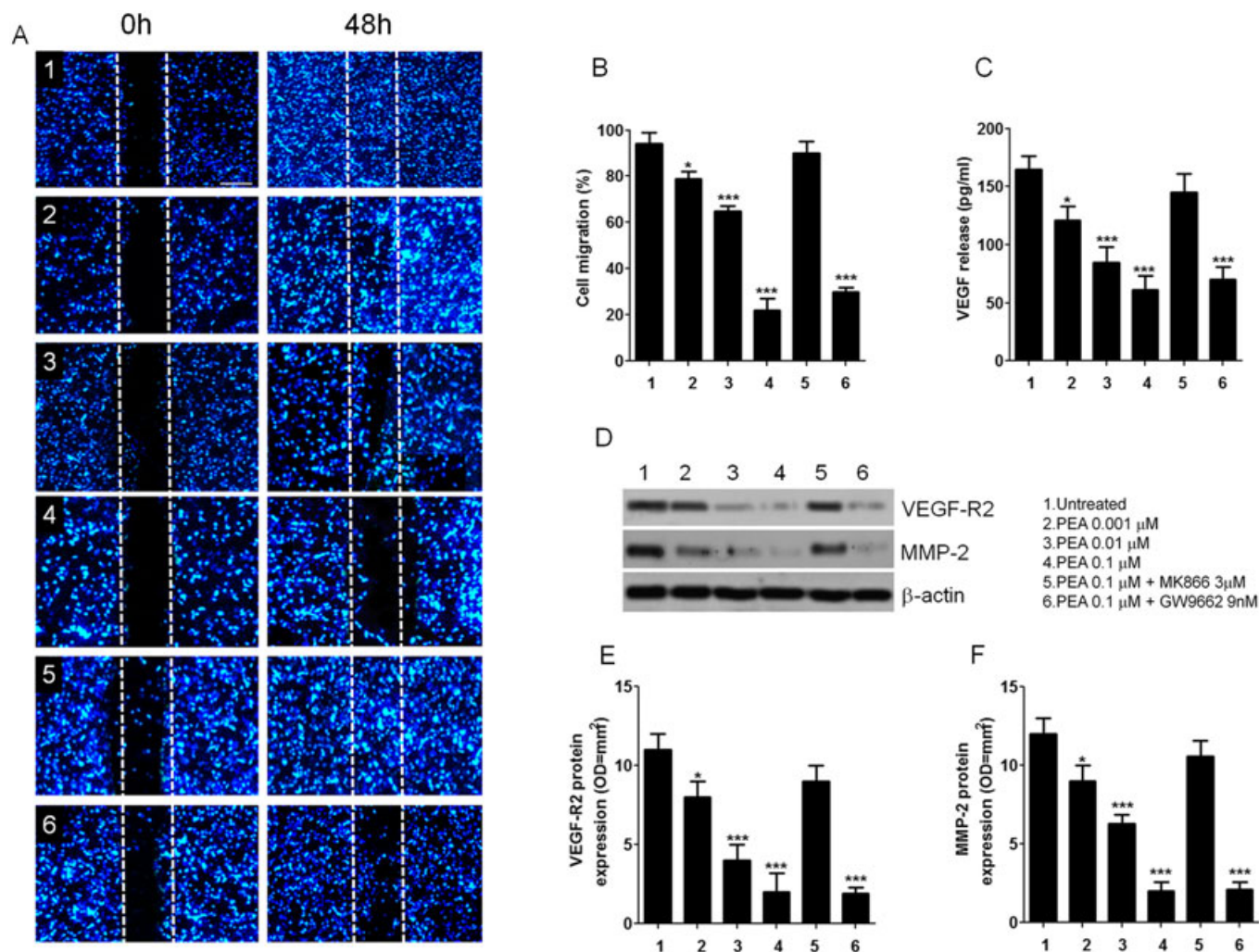


**Figure 2.** Anti-migration and anti-angiogenic effect *in vitro* of PEA in Caco-2 cell line. (A) Wound healing assay demonstrating the effect of PEA on Caco-2 migration *in vitro*. Hoechst staining of cell nuclei indicates that PEA inhibits the migration of Caco-2 cells in a PPAR- $\alpha$  and concentration-dependent manner (scale bar, 200  $\mu$ m). (B) Quantification of cell migration (%). (C) PEA concentration-dependently reduces pro-angiogenic release of VEGF secretion by Caco-2 cells at 24 h through a PPAR- $\alpha$  selective involvement. In the same conditions, western blot bands indicate that (D) PEA reduces both VEGF-R2 and MMP-2 protein expression and PEA (0.1  $\mu$ M) effect is abolished by MK866 (3  $\mu$ M) selective but not by GW9662 (9 nM) co-administration. (E–F) Densitometric analysis and relative quantification of corresponding immunoreactive bands for VEGF-R2 and MMP-2 (arbitrary units normalized on the expression of the housekeeping protein  $\beta$ -actin). Results are expressed as mean  $\pm$  SEM of  $n = 5$  experiments performed in triplicate. \*\*\* $p < 0.001$  and \* $p < 0.05$  versus untreated Caco-2 cells.

modulator of pro-angiogenic factor release, as VEGF. Although its activation has been generally detected *in vitro* following hypoxia conditions, HIF-1 $\alpha$  is commonly increased in colitis whereas it is increased by Akt/mTOR pathway activation (25). PEA caused a significant and dose-dependent decrease of HIF-1 $\alpha$  expression (–28, –52 and 87% respectively vs untreated), and this effect was strictly dependent on the selective PPAR- $\alpha$  involvement, as well (Fig. 3A, B).

## DISCUSSION

Notwithstanding the complex redundancy of different molecular pathways involved in cancer development, the Akt/mTOR axis induction has been focused as one of the most important network regulating both cell proliferation and function during angiogenesis. Impaired regulation of this pathway has been thus considered pivotal in the development and progression of many types of cancer, including colonic adenocarcinoma.

Akt/mTOR pathway activation is downstream accompanied with signals promoting resistance to apoptosis, altered tissue remodeling and metastasis formation (Guertin and Sabatini, 2007). In particular, following Akt/mTOR/p70S6K axis induction, HIF-1 $\alpha$  expression is observed (Liu *et al.*, 2006; Shaw and Cantley, 2006; Zhou *et al.*, 2007), and this protein directly enhances VEGF secretion that, in turn, acts as a powerful pro-angiogenic effector in colon epithelial cells and strongly promotes colon carcinoma progression (Son *et al.*, 2013). VEGF binding at VEGF-R2 is downstream followed by a complex molecular network, including ERK, JNK, PI3K, Akt, P70S6K and p38MAPK that subsequently promote proliferation, migration and tube formation of endothelial cells (Ferrara *et al.*, 2003), converging to massive neovascularization. The results of the present study indicate that PEA exerts a marked anti-proliferative and antiangiogenic effect on cultured human colon carcinoma Caco-2 cell line through a PPAR- $\alpha$ -dependent inhibition of Akt/mTOR pathway. Our results showed that PEA, in a concentration-dependent manner, caused a progressive reduction of

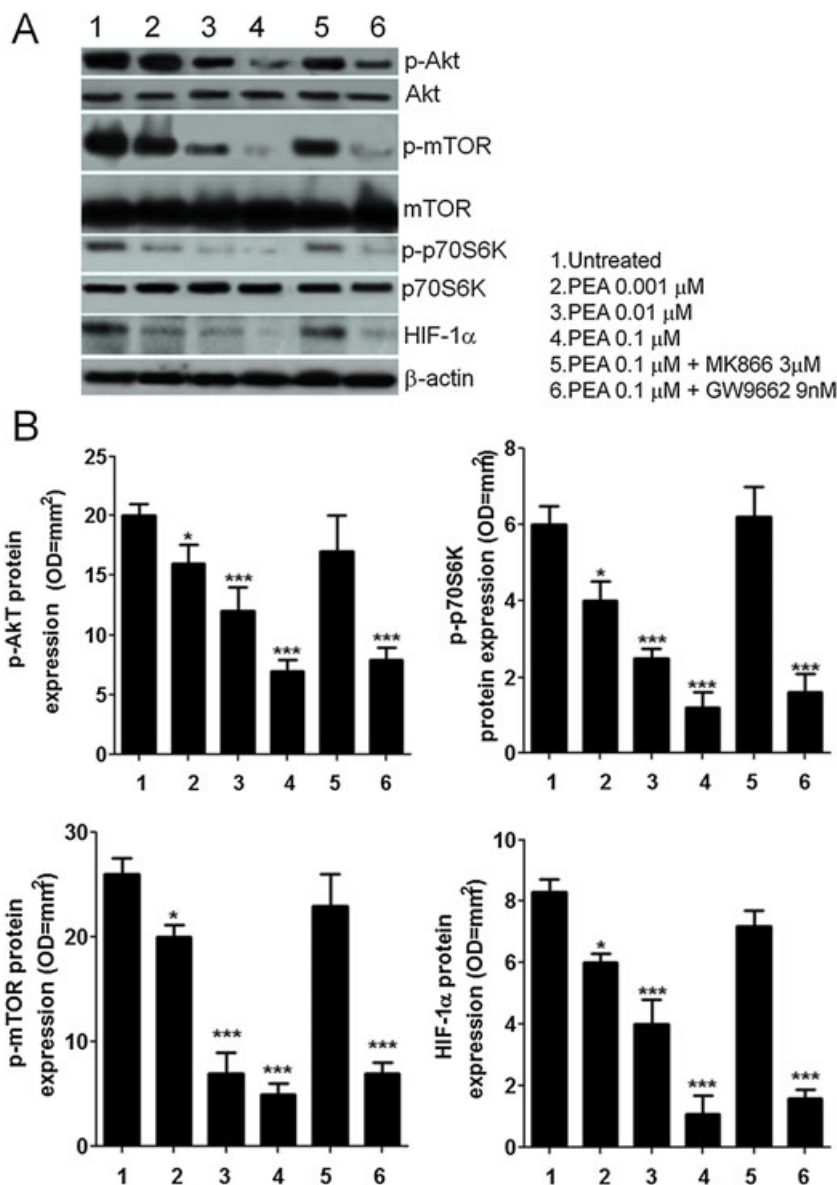


**Figure 3.** PEA downregulates Akt/mTOR pathway through a PPAR- $\alpha$ -dependent mechanism. (A) Immunoblot referred to phosphorylated/unphosphorylated Akt, mTOR, p70S6K and HIF-1 $\alpha$  protein bands and (B) relative densitometric analysis (arbitrary units normalized on the expression of the housekeeping protein  $\beta$ -actin) showing the effects of PEA (0.001–0.1  $\mu$ M), given alone or in the presence of MK866 (3  $\mu$ M) or GW 9662 (9 nM), on the expression of Akt, mTOR and p70S6K phosphorylated proteins and HIF-1 $\alpha$  pro-angiogenic modulator in Caco-2 cell line. Results are expressed as mean  $\pm$  SEM of  $n = 5$  experiments performed in triplicate. \*\*\* $p < 0.001$  and \* $p < 0.05$  versus untreated Caco-2 cells.

Caco-2 cell proliferation percentage by MTT assay. Such effect was counteracted by selective PPAR- $\alpha$  but not by PPAR- $\gamma$  antagonists, and these results were in line with a significant reduction of BrdU staining of PEA-treated versus untreated Caco-2 cells, suggesting a PPAR- $\alpha$ -mediated control of tumoral cell growth. Also, PEA reduced the activation of pro-angiogenic pathways by inhibiting the Akt/mTOR signaling pathway. Our study demonstrates that PEA, in a PPAR- $\alpha$  selective and concentration-dependent manner, significantly reduced phosphorylation of Akt, mTOR and p70S6 proteins in Caco-2 cells, leading to downstream inhibition of HIF-1 $\alpha$ . PEA caused a significant inhibition of VEGF secretion and markedly reduced VEGF receptor expression. Moreover, in the same experimental conditions, PEA caused a significant and PPAR- $\alpha$ -dependent decrease of MMP-2 expression, leading to a marked decrease of Caco-2 cells migration *in vitro* as demonstrated by the wound healing test results.

As largely demonstrated in the last decade, PPARs are nuclear hormone receptors that control many cellular processes (Berger and Moller, 2002; Michalik *et al.*, 2004) including tumor growth and malignancy (Dubois *et al.*, 1998; Ikawa *et al.*, 2001). We previously demonstrated that PEA is an endogenous compound showing anti-inflammatory properties in experimental-induced colitis and in cultured ulcerative colitis specimens through a selective PPAR- $\alpha$ -dependent mechanism (Esposito *et al.*, 2014). This aspect is of considerable interest, because PPAR- $\gamma$  rather than PPAR- $\alpha$  receptor has been considered a possible target for anticancer drugs in the treatment of colorectal carcinoma (Han and Roman, 2007; Huin *et al.*, 2002).

Despite this, functional studies suggested that PPAR- $\alpha$  activation reduced epithelial proliferation with no effect on apoptosis or necrosis. Different studies support a central role for PPAR- $\alpha$  activation in preventing neoplastic transformation and growth, especially in colon

cancer (Jackson *et al.*, 2003). It has been in fact demonstrated that bezafibrate, a PPAR- $\alpha$  ligand, inhibited the formation of azoxymethane-induced aberrant crypt *foci* in rats (Tanaka *et al.*, 2001). Moreover, PPAR- $\alpha$  activation by omega-3 fatty acids resulted in a reduced CRC progression in animals (Nakagawa *et al.*, 1997; Takahashi *et al.*, 1994), and it caused a decrease in cell proliferation in patients affected by familial adenomatous polyposis (Anti *et al.*, 1992). The results of our study demonstrated that selective targeting of PPAR- $\alpha$  receptors is a key step in mediating the antiproliferative and antiangiogenic effect displayed by PEA in cultured human colon carcinoma cells. Moreover, antiangiogenic properties of PEA have been also demonstrated in different conditions featured by chronic inflammation, such as granuloma formation (De Filippis *et al.*, 2010), reactive gliosis following A $\beta$  stimulus *in vitro* and colitis (Esposito *et al.*, 2014; Scuderi *et al.*, 2011). Although the antiproliferative and antiangiogenic activity of PEA involves the Akt/mTOR axis, we cannot reasonably exclude other possible mechanisms by which this endogenous ALA-mide might exert its control on cancer growth and neovascularization. PEA is indeed able to block the p38MAPK/ERK signaling pathway and may consequently markedly inhibit NF-kappaB activation resulting in an antiinflammatory (Esposito *et al.*, 2014) and antiproliferative activity in colonic mucosa. Because of the complexity and redundancy of different pathways involved in colon cancer proliferation and angiogenesis, a combined and multi-step targeting of different signaling molecules may be ideally required, when developing new chemotherapeutic drugs. Although PPAR- $\alpha$  receptor is now recognized as the main pharmacological target of PEA, the multi-faceted activity displayed by this

compound might endorse the antiproliferative effects of other signaling pathways, including the vanilloid and the endocannabinoid systems (Velasco *et al.*, 2016). Hence, PEA-mediated synergic blockage of converging pathways leading to cancer cell growth, angiogenesis and tissue remodeling/invasion significantly increases the efficacy of potential anticancer compounds.

PEA is a safe compound and possesses a widely known pharmacological and toxicological profile; moreover, it can be easily prescribed as it has been already introduced in clinical practice as food for special medical purposes in chronic inflammatory conditions and chronic pain states. Because of its abundant concentration in different plants and phytotherapeutics, PEA has been regarded with particular interest as a dietetic component with cytoprotective properties against neuropathic pain states, including chemotherapy-induced neuropathy (Keppel Hesselink, 2013b; Truini *et al.*, 2011).

Although PEA activity in colon carcinoma models *in vivo* is yet to be confirmed, PEA may represent in the future perspective as an intriguing pharmacological tool able to counteract cell proliferation, angiogenesis and tissue remodeling that negatively impact on colon cancer prognosis. Apart from its neuroprotective and analgesic properties, our data showing PEA intrinsic tumorostatic effects strongly support its co-administration to the current colon carcinoma chemotherapeutic protocols.

### Conflict of Interest

Authors have no conflict of interest to declare.

### REFERENCES

- Alhouayek M, Bottemanne P, Subramanian KV, *et al.* 2015. N-Acylethanolamine-hydrolyzing acid amidase inhibition increases colon N-palmitoylethanolamine levels and counteracts murine colitis. *FASEB J* **29**(2): 650–661. DOI:<http://dx.doi.org/10.1096/fj.14-255208>.
- Aloe L, Leon A, Levi-Montalcini R. 1993. A proposed autacoid mechanism controlling mastocyte behaviour. *Agents Actions* **39**: C145–C147.
- Anti M, Marra G, Armelao F, *et al.* 1992. Effect of omega-3 fatty acids on rectal mucosal cell proliferation in subjects at risk for colon cancer. *Gastroenterology* **103**: 883–891.
- Arumuggam N, Bhowmick NA, Rupasinghe HPV. 2015. A review: phytochemicals targeting JAK / STAT signaling and IDO expression in cancer. *Phytother Res* **29**: 805–817.
- Berger J, Moller DE. 2002. The mechanisms of action of PPARs. *Annu Rev Med* **53**: 409–435.
- Borrelli F, Romano B, Petrosino S, *et al.* 2015. Palmitoylethanolamide, a naturally occurring lipid, is an orally effective intestinal anti-inflammatory agent. *Tables of Links. Br J Pharmacol* **172**: 142–158. DOI:<http://dx.doi.org/10.1111/bph.12907>.
- Boyle P, Langman JS. 2000. ABC of colorectal cancer: epidemiology. *BMJ* **321**(7264): 805–808.
- Calignano A, La Rana G, Piomelli D. 2001. Antinociceptive activity of the endogenous fatty acid amide, palmitoylethanolamide. *Eur J Pharmacol* **419**(2–3): 191–198. DOI:[http://dx.doi.org/10.1016/S0014-2999\(01\)00988-8](http://dx.doi.org/10.1016/S0014-2999(01)00988-8).
- Cantley LC. 2002. The phosphoinositide 3-kinase pathway. *Science* **296**(5573): 1655–1657. DOI:<http://dx.doi.org/10.1126/science.296.5573.1655>.
- Carmeliet P, Jain RK. 2000. Angiogenesis in cancer and other diseases. *Nature* **407**: 249–257.
- Chen J, Fang Y. 2002. A novel pathway regulating the mammalian target of rapamycin (mTOR) signaling. *Biochem Pharmacol* **64**(7): 1071–1077. DOI:[http://dx.doi.org/10.1016/S0006-2952\(02\)01263-7](http://dx.doi.org/10.1016/S0006-2952(02)01263-7).
- Cipriano M, Esposito G, Negro L, *et al.* 2015. Palmitoylethanolamide regulates production of pro-angiogenic mediators in a model of beta amyloid-induced astrogliosis *in vitro*. *CNS Neurol Disord Drug Targets* **14**(7): 828–837.
- Coulon D, Faure L, Salmon M, Wattelet V, Bessoule J-J. 2012. N-Acylethanolamines and related compounds: aspects of metabolism and functions. *Plant Sci* **184**: 129–140. DOI:<http://dx.doi.org/10.1016/j.plantsci.2011.12.015>.
- D'Agostino G, La Rana G, Russo R, *et al.* 2009. Central administration of palmitoylethanolamide reduces hyperalgesia in mice via inhibition of NF-kappaB nuclear signalling in dorsal root ganglia. *Eur J Pharmacol* **613**(1–3): 54–59. DOI:<http://dx.doi.org/10.1016/j.ejphar.2009.04.022>.
- De Filippis D, D'Amico A, Cipriano M, *et al.* 2010. Levels of endocannabinoids and palmitoylethanolamide and their pharmacological manipulation in chronic granulomatous inflammation in rats. *Pharmacol Res* **61**(4): 321–328. DOI:<http://dx.doi.org/10.1016/j.phrs.2009.11.005>.
- Di Marzo V, Melck D, Orlando P, *et al.* 2001. Palmitoylethanolamide inhibits the expression of fatty acid amide hydrolase and enhances the anti-proliferative effect of anandamide in human breast cancer cells. *Biochem J* **255**: 249–255.
- Dubois RN, Gupta R, Brockman J, Reddy BS, Krakow SL, Lazar MA. 1998. The nuclear eicosanoid receptor, PPAR  $\gamma$ , is aberrantly expressed in colonic cancers. *Carcinogenesis* **19**(1): 49–53.
- Esposito G, Capocchia E, Turco F, *et al.* 2014. Palmitoylethanolamide improves colon inflammation through an enteric glia/toll like receptor 4-dependent PPAR- $\alpha$  activation. *Gut* **63**(8): 1300–1312. DOI:<http://dx.doi.org/10.1136/gutjnl-2013-305005>.
- Fasolo A, Sessa C. 2008. mTOR inhibitors in the treatment. *Exp Opin Investig Drugs* **17**(11): 1717–1734.

- Ferlay J, Soerjomataram I, Dikshit R, *et al.* 2015. Cancer incidence and mortality worldwide: sources, methods and major patterns in GLOBOCAN 2012. *Int J Cancer* **136**(5): E359–E386. DOI:<http://dx.doi.org/10.1002/ijc.29210>.
- Ferrara N, Gerber H-P, LeCouter J. 2003. The biology of VEGF and its receptors. *Nat Med* **9**(6): 669–676. DOI:<http://dx.doi.org/10.1038/nm0603-669>.
- Guertin DA, Sabatini DM. 2007. Defining the role of mTOR in cancer. *Cancer Cell* **12**(1): 9–22. DOI:<http://dx.doi.org/10.1016/j.ccr.2007.05.008>.
- Hagggar FA, Boushey RP. 2009. Colorectal cancer epidemiology: incidence, mortality, survival, and risk factors. *Clinics Colon Rect Surg* **22**(4): 191–197. DOI:<http://dx.doi.org/10.1055/s-0029-1242458>.
- Hamtiaux L, Masquelier J, Muccioli GG, *et al.* 2012. The association of N-palmitoylethanolamine with the FAAH inhibitor URB597 impairs melanoma growth through a supra-additive action. *BMC Cancer* **12**(1): 92. DOI:<http://dx.doi.org/10.1186/1471-2407-12-92>.
- Han S, Roman J. 2007. Peroxisome proliferator-activated receptor gamma: a novel target for cancer therapeutics? *Anticancer Drugs* **18**(3): 237–244. DOI:<http://dx.doi.org/10.1097/CAD.0b013e328011e67d>.
- Huin C, Schohn H, Hatier R, *et al.* 2002. Expression of peroxisome proliferator-activated receptors alpha and gamma in differentiating human colon carcinoma Caco-2 cells. *Biol Cell* **94**(1): 15–27. DOI:[http://dx.doi.org/10.1016/S0248-4900\(01\)01178-9](http://dx.doi.org/10.1016/S0248-4900(01)01178-9).
- Ikawa H, Kameda H, Kamitani H, *et al.* 2001. Effect of PPAR activators on cytokine-stimulated cyclooxygenase-2 expression in human colorectal carcinoma cells. *Exp Cell Res* **267**(1): 73–80. DOI:<http://dx.doi.org/10.1006/excr.2001.5233>.
- Jackson L, Wahli W, Michalik L, *et al.* 2003. Potential role for peroxisome proliferator activated receptor (PPAR) in preventing colon cancer. *Gut* **52**: 1317–1323.
- Keppel Hesselink JM. 2013a. Clinical neurorestorative effects of palmitoylethanolamide due to inhibition of inhibition of NF-kappaB? *J Neuroinflammation* **10**: 92.
- Keppel Hesselink JMK. 2013b. Palmitoylethanolamide: a useful adjunct in chemotherapy providing analgesia and neuroprotection. *Chemotherapy* **2**: 121. DOI:<http://dx.doi.org/10.4172/2167-7700.1000121>.
- Keppel Hesselink JM, Kopsky DJ, Witkamp RF. 2014. Palmitoylethanolamide (PEA)—“promiscuous” anti-inflammatory and analgesic molecule at the interface between nutrition and pharma. *PharmaNutrition* **2**(1): 19–25. DOI:<http://dx.doi.org/10.1016/j.phanu.2013.11.127>.
- Kim S-C, Chapman KD, Blancaflor EB. 2010. Fatty acid amide lipid mediators in plants. *Plant Sci* **178**(5): 411–419. DOI:<http://dx.doi.org/10.1016/j.plantsci.2010.02.017>.
- Kuehl FA Jr, Jacob TA, Ganley OH, Ormond REMM. 1957. The identification of N-(2-hydroxyethyl)-palmitate as naturally occurring anti-inflammatory agent. *J Am Soc* **78**(20): 5577–5578.
- Kuttan G, Pratheeshkumar P, Manu KA, Kuttan R. 2011. Inhibition of tumor progression by naturally occurring terpenoids. *Pharm Biol* **49**(10): 995–1007. DOI:<http://dx.doi.org/10.3109/13880209.2011.559476>.
- Lambert DM, Govaerts SJ, Robert AR. 2001. Anticonvulsant activity of N-palmitoylethanolamide, a putative endocannabinoid, in mice. *Epilepsia* **42**(3): 321–327.
- Levi-Montalcini R, Skaper SD, Toso RD, Petrelli L, Leon A, Levi R. 1996. Nerve growth factor: from neurotrophin to neurokin. *Trends Neurosci* **19**: 514–520.
- Li WEI, Tan D, Zhang Z, Liang JJ, Brown RE. 2008. Activation of Akt-mTOR-p70S6K pathway in angiogenesis in hepatocellular carcinoma. *Oncol Rep* **20**: 713–719. DOI:<http://dx.doi.org/10.3892/or>.
- Liu L-Z, Hu X-W, Xia C, *et al.* 2006. Reactive oxygen species regulate epidermal growth factor-induced vascular endothelial growth factor and hypoxia-inducible factor-1alpha expression through activation of AKT and P70S6K1 in human ovarian cancer cells. *Free Rad Biol Med* **41**(10): 1521–1533. DOI:<http://dx.doi.org/10.1016/j.freeradbiomed.2006.08.003>.
- LoVerme J, Fu J, Astarita G, *et al.* 2005a. The nuclear receptor peroxisome proliferator-activated receptor-alpha mediates the anti-inflammatory actions of palmitoylethanolamide. *Mol Pharmacol* **67**(1): 15–19. DOI:<http://dx.doi.org/10.1124/mol.104.006353.dyshev>.
- LoVerme J, La Rana G, Russo R, Calignano A, Piomelli D. 2005b. The search for the palmitoylethanolamide receptor. *Life Sci* **77**(14): 1685–1698. DOI:<http://dx.doi.org/10.1016/j.lfs.2005.05.012>.
- McMahon G. 2000. VEGF receptor signaling in tumor angiogenesis. *Oncologist* **5**(suppl 1): 3–10.
- Michalik L, Desvergne B, Wahli W. 2004. Peroxisome-proliferator-activated receptors and cancers: complex stories. *Nat. Rev Cancer* **4**(1): 61–70. DOI:<http://dx.doi.org/10.1038/nrc1254>.
- Mosmann T. 1983. Rapid colorimetric assay for cellular growth and survival: application to proliferation and cytotoxicity assays. *J Immunol Methods* **65**(1–2): 55–63.
- Nakagawa T, Ishikawa C, Iwahoril Y, *et al.* 1997. Inhibitory effects of docosahexaenoic acid on colon carcinoma 26 metastasis to the lung. *Br J Cancer* **75**(5): 650–655.
- Pertwee RG, Howlett AC, Abood ME, *et al.* 2010. International Union of Basic and Clinical Pharmacology . LXXIX . Cannabinoid Receptors and Their Ligands : Beyond CB 1 and CB 2. *Pharmacol Rev* **62**(4): 588–631. DOI:<http://dx.doi.org/10.1124/pr.110.003004.588>.
- Pratheeshkumar P, Sreekala C, Zhang Z, *et al.* 2012. Cancer prevention with promising natural products: mechanisms of action and molecular targets. *Anticancer Agents Med Chem* **12**(10): 1159–1184. DOI:<http://dx.doi.org/10.2174/187152012803833035>.
- Renault-Mihara F, Beuvon F, Iturrioz X, *et al.* 2006. Phosphoprotein enriched in astrocytes-15 kDa expression inhibits astrocyte migration by a protein kinase C-dependent mechanism. *Mol Biol Cell* **17**: 5141–5152. DOI:<http://dx.doi.org/10.1091/mbc.E05>.
- Scuderi C, Esposito G, Blasio A, *et al.* 2011. Palmitoylethanolamide counteracts reactive astrogliosis induced by  $\beta$ -amyloid peptide. *J Cell Mol Med* **15**(12): 2664–2674. DOI:<http://dx.doi.org/10.1111/j.1582-4934.2011.01267.x>.
- Shaw RJ, Cantley LC. 2006. Ras, PI(3)K and mTOR signalling controls tumour cell growth. *Nature* **441**(7092): 424–430. DOI:<http://dx.doi.org/10.1038/nature04869>.
- Son MK, Jung KH, Hong S-W, *et al.* 2013. SB365, Pulsatilla saponin D suppresses the proliferation of human colon cancer cells and induces apoptosis by modulating the AKT/mTOR signalling pathway. *Food Chem* **136**(1): 26–33. DOI:<http://dx.doi.org/10.1016/j.foodchem.2012.07.096>.
- Takahashi M, Minamoto T, Yamashita N, Kato T, Yazawa K, Esumi H. 1994. Effect of docosahexaenoic acid on azoxymethane-induced colon carcinogenesis in rats. *Cancer Lett* **83**(1–2): 177–184. DOI:[http://dx.doi.org/10.1016/0304-3835\(94\)90316-6](http://dx.doi.org/10.1016/0304-3835(94)90316-6).
- Tanaka T, Kohno H, Yoshitani S. 2001. Ligands for peroxisome proliferator-activated receptors  $\alpha$  and  $\gamma$  inhibit chemically induced colitis and formation of aberrant crypt foci in rats 1. *Cancer Res* **61**: 2424–2428.
- Tanigawa N, Amaya H, Matsumura M, Lu C, Kitaoka A, Matsuyama K. 1997. Advances in brief tumor angiogenesis and mode of metastasis in patients with colorectal cancer. *Cancer Res* **57**: 1043–1046.
- Truini A, Biasiotta A, Di Stefano G, *et al.* 2011. Palmitoylethanolamide restores myelinated-fibre function in patients with chemotherapy-induced painful neuropathy. *CNS Neurol Disord Drug Targets* **10**(8): 916–920.
- Velasco G, Hernández-Tiedra S, Dávila D, Lorente M. 2016. The use of cannabinoids as anticancer agents. *Progr Neuropsychopharmacol Biol Psychiatry* **64**: 259–266. DOI:<http://dx.doi.org/10.1016/j.pnpbp.2015.05.010>.
- Vivanco I, Sawyers CL. 2002. The phosphatidylinositol 3-kinase AKT pathway in human cancer. *Nat Rev Cancer* **2**(7): 489–501. DOI:<http://dx.doi.org/10.1038/nrc839>.
- Yoshimura H, Dhar DK, Kohno H, *et al.* 2004. Prognostic impact of hypoxia-inducible factors 1 alpha and 2 alpha in colorectal cancer patients : correlation with tumor angiogenesis and cyclooxygenase-2 expression. *Clin Cancer Res* **10**: 8554–8560.
- Zhang Y-J, Dai Q, Sun D-F, *et al.* 2009. mTOR signaling pathway is a target for the treatment of colorectal cancer. *Ann Surg Oncol* **16**(9): 2617–2628. DOI:<http://dx.doi.org/10.1245/s10434-009-0555-9>.
- Zhou Q *et al.* 2007. Reactive oxygen species regulate insulin-induced VEGF and HIF-1alpha expression through the activation of p70S6K1 in human prostate cancer cells. *Carcinogenesis* **28**(1): 28–37. DOI:<http://dx.doi.org/10.1093/carcin/bgl085>.

---

## SUPPORTING INFORMATION

---

Additional supporting information may be found in the online version of this article at the publisher's web site.

RESEARCH ARTICLE

# Palmitoylethanolamide Modulates Inflammation-Associated Vascular Endothelial Growth Factor (VEGF) Signaling via the Akt/mTOR Pathway in a Selective Peroxisome Proliferator-Activated Receptor Alpha (PPAR- $\alpha$ )-Dependent Manner

Giovanni Sarnelli<sup>1\*</sup>, Alessandra D'Alessandro<sup>1</sup>, Teresa Iuvone<sup>2</sup>, Elena Capoccia<sup>3</sup>, Stefano Gigli<sup>3</sup>, Marcella Pesce<sup>1</sup>, Luisa Seguela<sup>3</sup>, Nicola Nobile<sup>3</sup>, Giovanni Aprea<sup>1</sup>, Francesco Maione<sup>1</sup>, Giovanni Domenico de Palma<sup>1</sup>, Rosario Cuomo<sup>1</sup>, Luca Steardo<sup>3</sup>, Giuseppe Esposito<sup>3\*</sup>

**1** Department of Clinical Medicine and Surgery, University of Naples Federico II, Naples, Italy, **2** Department of Pharmacy, University of Naples Federico II, Naples, Italy, **3** Department of Physiology and Pharmacology 'Vittorio Erspamer', La Sapienza University of Rome, Rome, Italy

\* [sarnelli@unina.it](mailto:sarnelli@unina.it) (GS); [giuseppe.esposito@uniroma1.it](mailto:giuseppe.esposito@uniroma1.it) (GE)



click for updates

**OPEN ACCESS**

**Citation:** Sarnelli G, D'Alessandro A, Iuvone T, Capoccia E, Gigli S, Pesce M, et al. (2016) Palmitoylethanolamide Modulates Inflammation-Associated Vascular Endothelial Growth Factor (VEGF) Signaling via the Akt/mTOR Pathway in a Selective Peroxisome Proliferator-Activated Receptor Alpha (PPAR- $\alpha$ )-Dependent Manner. *PLoS ONE* 11 (5): e0156198. doi:10.1371/journal.pone.0156198

**Editor:** Sujit Basu, Ohio State University, UNITED STATES

**Received:** February 23, 2016

**Accepted:** May 10, 2016

**Published:** May 24, 2016

**Copyright:** © 2016 Sarnelli et al. This is an open access article distributed under the terms of the [Creative Commons Attribution License](https://creativecommons.org/licenses/by/4.0/), which permits unrestricted use, distribution, and reproduction in any medium, provided the original author and source are credited.

**Data Availability Statement:** All relevant data are within the paper and its Supporting Information files.

**Funding:** The authors have no support or funding to report.

**Competing Interests:** The authors have declared that no competing interests exist.

## Abstract

### Background and Aim

Angiogenesis is emerging as a pivotal process in chronic inflammatory pathologies, promoting immune infiltration and prompting carcinogenesis. Ulcerative Colitis (UC) and Crohn's Disease (CD) represent paradigmatic examples of intestinal chronic inflammatory conditions in which the process of neovascularization correlates with the severity and progression of the diseases. Molecules able to target the angiogenesis have thus the potential to synergistically affect the disease course. Beyond its anti-inflammatory effect, palmitoylethanolamide (PEA) is able to reduce angiogenesis in several chronic inflammatory conditions, but no data about its anti-angiogenic activity in colitis have been produced, yet.

### Methods

The effects of PEA on inflammation-associated angiogenesis in mice with dextran sulphate sodium (DSS)-induced colitis and in patients with UC were assessed. The release of Vascular Endothelial Growth Factor (VEGF), the hemoglobin tissue content, the expression of CD31 and of phosphatidylinositol 3-kinase/Akt/mammalian-target-of-rapamycin (mTOR) signaling axis were all evaluated in the presence of different concentrations of PEA and concomitant administration of PPAR- $\alpha$  and - $\gamma$  antagonists.



## Results

Our results demonstrated that PEA, in a selective peroxisome proliferator activated receptor (PPAR)- $\alpha$  dependent mechanism, inhibits colitis-associated angiogenesis, decreasing VEGF release and new vessels formation. Furthermore, we demonstrated that the mTOR/Akt axis regulates, at least partly, the angiogenic process in IBD and that PEA directly affects this pathway.

## Conclusions

Our results suggest that PEA may improve inflammation-driven angiogenesis in colonic mucosa, thus reducing the mucosal damage and potentially affecting disease progression and the shift towards the carcinogenesis.

## Introduction

Angiogenesis is the process of new vessels development from preexisting vasculature in adult tissues and it is emerging as pivotal in the pathogenesis and progression of chronic inflammatory pathologies [1–4].

There is evidence that angiogenesis contributes to a significant dysfunction of vessel architectures, promotes the recruitment of pro-inflammatory cells, and results in a progressive loss of the epithelial integrity [5,6]. Inflammatory bowel diseases (IBD), such as Crohn's disease (CD) and ulcerative colitis (UC) are paradigmatic examples of chronic inflammatory diseases in which angiogenesis-related factors affect diseases' progression and severity [5–8].

A variegated class of signaling molecules/cytokines, involved in inflammation and tissue remodeling processes, co-promotes angiogenesis, such as nitric oxide (NO) or prostaglandins (PGs), but a prominent role has been identified for Vascular Endothelial Growth Factor A (VEGF). This mediator, through the activation of a complex signaling network, yields to neovascularization, worsening tissue damage and promoting the carcinogenic drift [9–10]. In keeping with this, the inhibition of angiogenic process may represent a potential therapeutic target in IBDs, acting on both inflammation and carcinogenic risk [11,12].

Although the release of VEGF is regulated by different molecular pathways, the upstream activation of phosphatidylinositol 3-kinase/Akt/mammalian target of rapamycin (mTOR) signaling axis (Akt/mTOR pathway) has been recognized as pivotal in VEGF-related neovascularization. Indeed, the activation of this pathway determines also the overexpression of the Hypoxia-Inducible Factor (HIF)-1 $\alpha$ , a specific transcriptional factor, which, in turn, further increases the release of VEGF [12,13]. This complex network, is physiologically induced by hypoxia in order to guarantee the appropriate tissue oxygenation, stimulating vessels formation, however a pathological over-activation of this pathway has been also described in different inflammatory diseases and several tumors [14,15].

Palmitoylethanolamide (PEA) is an N-acylethanolamide (NAE), structurally and functionally related to anandamide (AEA), with anti-inflammatory and analgesic activities. The anti-inflammatory effect of PEA depends on its ability to activate peroxisome proliferator activated receptor (PPAR)- $\alpha$ , a member of nuclear hormone receptor superfamily of ligand activated transcription factors [16,17]. In both mice and human colitis, PEA has been reported to decrease the release of several pro-inflammatory cytokines [18–20], and there are data suggesting that PEA also exerts a significant anti-angiogenic activity in other chronic inflammatory

conditions [21, 22]. However, we recently demonstrated that PEA is able to directly reduce the release of pro-angiogenic factors in an “*in vitro*” model of colon cancer cells [23]. The potential anti-angiogenic activity of PEA during colitis has never been reported, yet. With the present study we aimed to evaluate the ability of PEA to reduce the inflammation-related angiogenesis in the colon of mice with dextran sulphate sodium (DSS)-induced colitis and in UC patients, and to characterize its mechanisms of action.

## Materials and Methods

### Animals and experimental design

Six-weeks-old wild-type (WT) male CD-1 mice (Harlan Laboratories, Udine, Italy) were used for experiments. All procedures on mice were approved by La Sapienza University's Ethics Committee. Animal care was in compliance with the IASP and European Community (EC L358/1 18/12/86) guidelines on the use and protection of animals in experimental research. Animals were randomly divided into six groups (n = 10 per group): non-colitic control group; colitic group; colitic group receiving PEA 2 and 10 mg/kg, [24, 25]; colitic group receiving PEA (10 mg/kg) and selective PPAR- $\alpha$  antagonist MK866 (10 mg/kg); colitic group receiving PEA and selective PPAR- $\gamma$  antagonist GW9662 (1 mg/kg) [26]. Two internal control groups (n = 5 per group) were also considered: colitic group receiving PPAR- $\alpha$  or PPAR- $\gamma$  antagonist; non-colitic group receiving daily PEA 10 mg/kg. Immunohistochemistry was performed on five groups, excluding colitic group receiving the lowest dosage of PEA.

Colitis was induced by administrating 4% DSS (MP Biomedicals, Solon, Ohio, USA) in drinking water for six consecutive days. PEA alone, or combined with PPAR antagonists, was given by intraperitoneal administration from day 2 to 6 and then animals were sacrificed at day 7 by carbon dioxide inhalation followed by cervical dislocation. Colons were isolated to perform histochemical and biochemical analyses as described below.

In order to further confirm the involvement of PPAR- $\alpha$  in mediating the effects of PEA, additional sets of experiment were conducted in six-weeks-old wild-type PPAR- $\alpha$  null (KO) mice (Taconic, Germantown, New York, USA), that were divided in the following groups: vehicle; colitic; colitic receiving daily PEA 10, 50 or 100 mg/kg, n = 5 for each group, respectively.

### Cultured human intestinal biopsies

The experimental group comprised 10 patients with a new diagnose of UC (4 women; age range 21–58 years; endoscopic MAYO score >2) and 5 control subjects (3 men; age range 42–60 years; absence of gastrointestinal symptoms) undergoing colonoscopy for colon cancer screening. Exclusion criteria were history of cancer, use of 5-aminosalicylic acid, immunosuppressant, anti-platelet and anti-coagulant drugs. Also patients suffering from cardiovascular, renal or respiratory comorbidities were excluded. All subjects received and signed an informed consent and the Federico II University Ethical committee approved the protocol.

Four mucosal biopsies from the sigmoid region of UC patients and two biopsies from the same site of controls were collected and cultured in FBS-supplemented Dulbecco Modified Eagle's Medium (DMEM) at 37°C in 5% CO<sub>2</sub>/95% air. All biopsies were cultured for 24 hours, with or without PEA at the following concentrations 0,001, 0,01, 0,1  $\mu$ M [27]. Biopsies were then homogenized and analyzed by western blot as described below. PFA-fixed samples were used for immunohistochemistry, this analysis was only performed on biopsies stimulated with the highest dosage of PEA (0,1  $\mu$ M).

## Protein extraction and western blot analysis

Mice and human specimens were homogenized in ice-cold hypotonic lysis buffer and protein concentration was determined using Bio-Rad protein assay kit (Bio-Rad, Milan, Italy). Analysis of total Akt, phosphor-Akt, total mTOR, phosphor-mTOR, total p70S6K, phosphor-p70S6K, anti-VEGF-R, anti-EGF receptor, anti-HIF1 $\alpha$  and  $\beta$ -actin protein expression was performed on total protein fractions of homogenates. Equivalent amounts of homogenates (50  $\mu$ g) underwent electrophoresis through a polyacrilamide minigel. Proteins were then transferred onto nitrocellulose membranes that were saturated by incubation with 10% nonfat dry milk in 1 $\times$  PBS overnight at 4°C and then incubated, according to the experimental protocols with: mouse anti-total Akt (1:1000 v/v, Cell signaling technology, Euroclone, Pero, MI, Italy); rabbit monoclonal anti phosphor-Akt (Ser<sup>473</sup>), (1:2000 v/v, Cell signaling technology, Euroclone, Pero, MI, Italy); rabbit polyclonal anti total mTOR (1:1000, Abcam, Cambridge, UK); rabbit polyclonal anti phosphor-mTOR (pSer<sup>2448</sup>) (1:1000 v/v, Cell signaling technology, Euroclone, Pero, MI, Italy); rabbit polyclonal anti total p70S6K (1:1000 v/v Cell Signaling Technology, Euroclone, Pero, MI, Italy); and rabbit polyclonal anti-phosphor-p70S6K (Thr421/Ser424, Thr389); (1:1000 v/v, Cell Signaling Technology, Euroclone, Pero, MI, Italy); rabbit monoclonal anti-VEGF receptor (1:1000 v/v, Cell Signaling Technology, Euroclone, Pero, MI, Italy); rabbit polyclonal anti-EGF receptor (1:1000 v/v, Abcam, Cambridge, UK); mouse monoclonal anti-HIF1 $\alpha$  (1:500 v/v, Sigma Aldrich, MI, Italy) and mouse anti- $\beta$ -actin (1:2000 v/v, Santa Cruz Biotechnology, Santa Cruz, California, USA). Membranes were then incubated with the specific secondary antibodies conjugated to horseradish peroxidase (HRP) (Dako, Milan, Italy). Immune complexes were revealed by enhanced chemiluminescence detection reagents (Amersham Biosciences, Milan, Italy). Blots were analyzed by scanning densitometry (GS-700 imaging densitometer; Bio-Rad). Results were expressed as OD (arbitrary units; mm<sup>2</sup>) and normalized on the expression of the housekeeping protein  $\beta$ -actin.

## Enzyme-linked immunosorbent assay for VEGF and EGF

Enzyme-linked immunosorbent assay (ELISA) for VEGF (Abcam, Cambridge, UK) was carried out on mice and human specimens supernatants according to the manufacturer's protocol. Absorbance was measured on a microtitre plate reader. In a subset of experiments an ELISA for EGF (Abcam, Cambridge, UK) was also carried out on plasma of PPAR- $\alpha$  null (KO) mice; VEGF and EGF levels were thus determined using standard curves method.

## Immunohistochemistry

Mice and human specimens were fixed in buffered formalin, embedded in paraffin and cut into 5 $\mu$ m-thick serial sections. According to manufacturer's instructions, after heat-mediated antigen retrieval, the tissue was formaldehyde fixed and blocked with serum. The tissue was incubated with the primary antibody anti CD31 (1:50 v/v, Abcam, Cambridge, UK) for 20 minutes. After three 5-min washes, the secondary antibody was added and the samples were incubated at room temperature for 20 min. The streptavidin-HRP detection system (Chemicon Int., Temecula, CA, USA) was added and samples were incubated at room temperature. After three 5-min washes, 50  $\mu$ L of chromogen was added and the reaction terminated after 1 min in water. Sections were then counterstained with haematoxylin eosin at room temperature. Negative controls were performed by omitting primary antibody. Slides were thus analyzed with a microscope (Nikon Eclipse 80i by Nikon Instruments Europe), and images were captured at 20X magnification by a high-resolution digital camera (Nikon Digital Sight DS-U1). The amount of vascularization in each colon section was quantified as a percentage of tissue area

immunopositive for CD31 at a 20X magnification in 6 regions, each amounting to a 0,20- mm<sup>2</sup> area, and expressed as vessel density of (%).

## Haemoglobin content measurement

As previously demonstrated, hemoglobin content measurement represents an appropriate method for the detection and quantification of angiogenesis in tissues [28,29]. Mice and human colonic specimens were collected and weighted, samples were then homogenized in 1 × PBS. After centrifugation at 2500 × g for 20 min at 4°C, the supernatants were further centrifuged at 5000 × g for 30 min, and hemoglobin concentration in the supernatant was determined spectrophotometrically at 450 nm by the hemoglobin assay kit (Sigma Aldrich, MI, Italy). Values were expressed as mg haemoglobin/g of wet weight.

## Statistical analysis

Results were expressed as mean±SD of n experiments. Statistical analysis was performed using parametric one-way analysis of variance (ANOVA) and multiple comparisons were performed by Bonferroni's posthoc test; p values <0.05 were considered significant.

## Results

### Mice DSS-induced colitis is associated with an increase of angiogenesis that is inhibited by Palmitoylethanolamide

In mice with DSS-induced colitis, bloody diarrhea together with loss of body weight and increase of spleen size were observed from day 4 until the sacrifice. As expected, the immune infiltrate and the inflammatory mediators (NO, PGE<sub>2</sub> and TNF $\alpha$ ) were also significantly increased in treated mice (data not shown).

Hemoglobin tissue content and the expression of CD31, a blood vessel endothelial marker, were evaluated to detect the effect of PEA on angiogenesis. The hemoglobin content was significantly increased in mice with DSS-induced colitis compared to controls (36,6±2 vs 11,6±1,6 mgHb/gr tissue; p<0,0001), but such increase was significantly reduced in mice receiving PEA (2 and 10 mg/kg) in a dose-dependent fashion (-36% and -60%, respectively; all p<0,001, [Fig 1A](#)). Co-administration of the PPAR- $\alpha$  antagonist, MK866, but not PPAR- $\gamma$  antagonist, GW966, significantly reverted the effects of PEA on hemoglobin content, likely indicating the selective involvement of PPAR- $\alpha$  ([Fig 1A](#)).

A significant higher density of CD31 positive cells was also observed in the inflamed mucosa of DSS-treated mice compared to controls, and, in line with the above described results, this was significantly inhibited by PEA in PPAR- $\alpha$  dependent mechanism ([Fig 1B](#)).

In order to evaluate whether VEGF regulates the inflammatory-related angiogenesis in mice colitis and if PEA may directly affect this specific pathway, we assessed the release of VEGF and the expression of its receptor (VEGF-R). As expected, in DSS-treated mice the release of VEGF was significantly higher than in controls, and this was associated with an increased expression of VEGF-R (18,7±6,2 vs 137,5±14 pg/mL and 1,25±0,5 vs 5,27±0,7 OD\*mm<sup>2</sup>, respectively; all p<0,0001; [Fig 1C and 1D](#)). Again, the administration of PEA (2 and 10 mg) significantly inhibited the release of VEGF and the expression of its receptor in a dose-dependent manner (-32 and -72%, -33 and -66% vs DSS-treated mice, respectively; all p<0,001, [Fig 1C and 1D](#)), and this effect was significantly affected by MK866, but not by GW9662, co-administration ([Fig 1C and 1D](#)).

In [Fig 2](#) it is summarized that PEA failed to induce any significant effect in DSS-treated PPAR- $\alpha$  null mice, further supporting the specific involvement of PPAR- $\alpha$ .

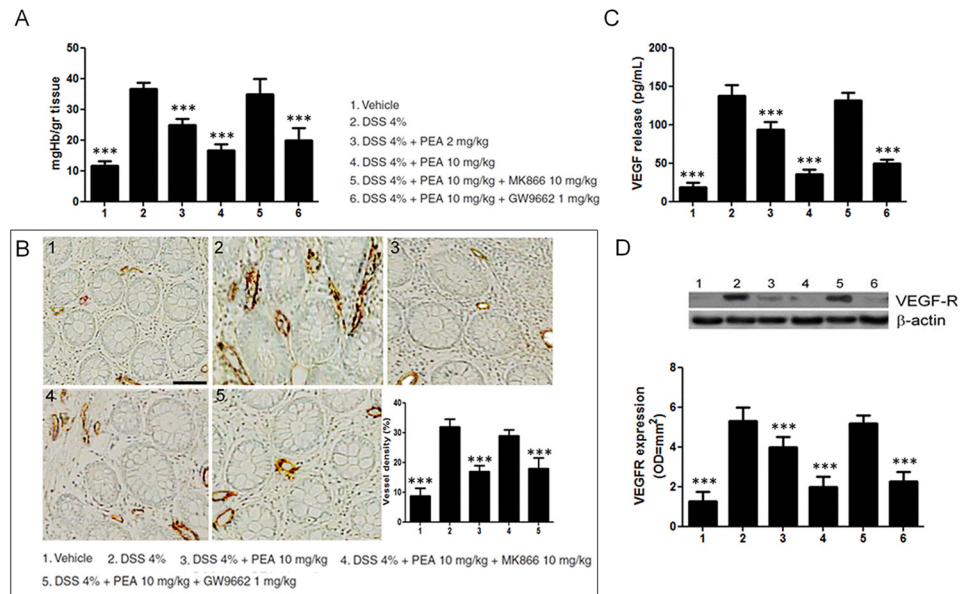


**Fig 1. Palmitoylethanolamide (PEA) inhibits colitis-associated angiogenesis in mice.** (A) DSS-induced colitis caused a significant increase of Hb-content in colonic mucosa, PEA is able to reduce, in a dose-dependent fashion, the Hb-content in colitis mice; this effect persisted in presence of PPAR $\gamma$  antagonist (GW9662) while it was nullified by PPAR $\alpha$  antagonist (MK866). (B) Immunohistochemical images showing the expression of CD31 on untreated mice colonic mucosa (panel 1), DSS-treated mice colonic mucosa (panel 2), DSS-treated mice colonic mucosa in presence of PEA (10 mg/Kg) alone (panel 3), PEA (10 mg/Kg) plus MK866 10 mg/Kg (panel 4), and PEA (10 mg/Kg) plus GW9662 1 mg/Kg (panel 5). Magnification 20X; scale bar: 100 $\mu$ m. The graph summarizes the relative quantification of CD31 expression (%) on mice colonic mucosa in the same experimental groups, showing the reduction of CD31 expression in colitic mice after PEA administration, except for the group also treated with the antagonist of PPAR $\alpha$ . (C) VEGF release resulted increase in DSS-treated mice and it was significantly reduced by PEA treatment in a PPAR $\alpha$  dependent manner. (D) Western blot analysis and relative densitometric analysis (arbitrary units normalized on the expression of housekeeping protein  $\beta$ -actin) of VEGF-receptor (VEGF-R) expression, showing similar results to VEGF release. Results are expressed as mean $\pm$ SD. \* $p$ <0.05, \*\* $p$ <0.01 and \*\*\* $p$ <0.001 versus DSS-treated mice.

doi:10.1371/journal.pone.0156198.g001

## Palmitoylethanolamide inhibits the angiogenesis in the mucosa of patients with UC

In order to verify the effect of PEA in the context of human colonic inflammation we performed the same experimental protocol on mucosal biopsies from UC patients. As previously reported [6,28,29], in the mucosa of UC patients the concentration of hemoglobin was higher than in controls (43 $\pm$ 6 vs 11,8 $\pm$ 3 mgHb/g tissue  $p$ <0,001, Fig 2A) and challenge with PEA induced a significant reduction of at hemoglobin content, in a dose dependent manner (-33, -55 and -67%, for 0,001, 0,01 and 0,1  $\mu$ M respectively; all  $p$ <0.01, Fig 2A). Similarly to what observed in the inflamed colon of mice, 0,1  $\mu$ M of PEA were also able to significantly reduce the number of CD31 positive cells in the mucosa of patients with UC (-50%;  $p$ <0,001, Fig 2B).

As compared to control biopsies, the release of VEGF and the expression of its receptor were also significantly increased in the mucosa from UC patients (191,6 $\pm$ 12 vs 41,6 $\pm$ 8 pg/mL and 10 $\pm$ 0,8 vs 0,5 $\pm$ 0,1 OD\*mm<sup>2</sup>, respectively; all  $p$ <0,001, Fig 2C and 2D). Again, the challenge with PEA was demonstrated to induce a significant and dose-dependent reduction of both VEGF release and VEGFR expression (-37, -53 and -70%, and -30, -50 and -70%, for 0,001, 0,01 and 0,1  $\mu$ M respectively; all  $p$ <0,001, Fig 2C and 2D). Similarly to what observed in the mice all the above described effects of PEA were dependent by PPAR- $\alpha$  since co-

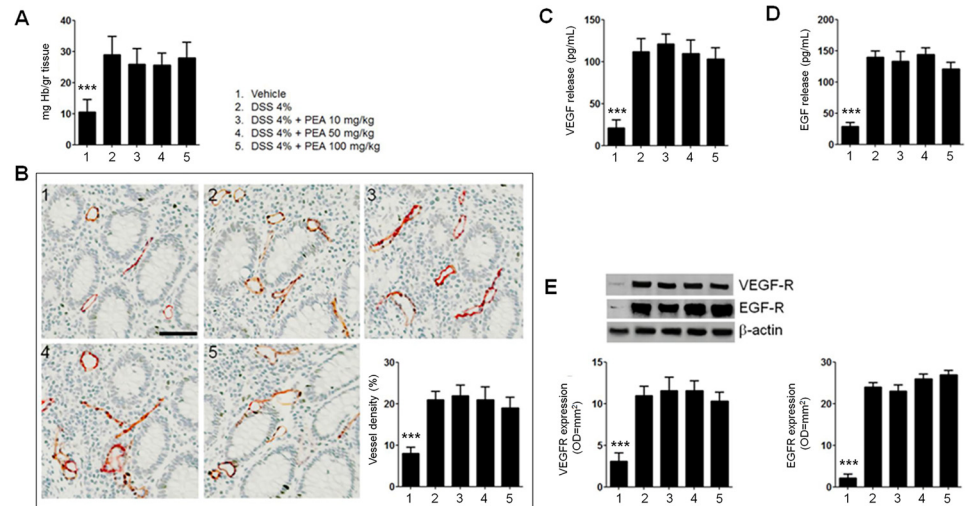


**Fig 2. PEA had no effects on colitis-associated angiogenesis in PPAR $\alpha$  null (KO) mice.** (A) DSS-induced colitis caused a significant increase of Hb-content in colonic mucosa compared to untreated group, PEA at different concentrations (10–100 mg/kg) did not show any effect on the Hb-content in colitis PPAR $\alpha$  (KO) mice. (B) Immunohistochemical images showing the expression of CD31 on untreated (panel 1), DSS-treated (panel 2), and DSS-treated mice in presence of PEA (10 mg/Kg) (panel 3), PEA (50 mg/Kg) (panel 4) and PEA (100 mg/Kg) (panel 5). Magnification 20X; scale bar: 100 $\mu$ m. The graph summarizes the relative quantification of CD31 expression on mice colonic mucosa in each respective group of mice, and shows the lack of any significant effect of PEA in reducing CD31 expression in colitic PPAR $\alpha$  null mice. In PPAR $\alpha$  null mice, DSS-treatment significantly increased the release of VEGF (C) and EGF (D) and these were unchanged by PEA administration, regardless of the concentrations used. (E) Western blot analysis and relative densitometric analysis (arbitrary units normalized on the expression of housekeeping protein  $\beta$ -actin) of VEGF-receptor (VEGF-R) and EGF-receptor (EGF-R) expression, showing similar results to VEGF and EGF release. Results are expressed as mean $\pm$ SD. \*\*\* $p$ <0.001 versus untreated mice.

doi:10.1371/journal.pone.0156198.g002

administration of MK866, but not of GW9662 significantly inhibited its effects even at the highest dose (Fig 2A–2D)

### The anti-angiogenic effect of PEA depend upon Akt/mTOR/p70S6K and HIF-1 $\alpha$ pathways downregulation

In order to verify whether PEA has a direct anti-angiogenic effect or this effect was related to its anti-inflammatory properties, we evaluated the Akt/mTOR/p70S6K pathway, that is directly involved in the angiogenesis. In the inflamed colon of DSS-treated mice phosphor-Akt, phosphor-mTOR and p70S6K- phosphorylation, were significantly up-regulated, and all were dose-dependently and significantly reduced by intraperitoneal administration of PEA (Fig 3A and 3B). The expression of the hypoxia-Inducible Factor (HIF)-1 $\alpha$  was also significantly reduced by -43,3 and -64% after treatment with PEA at 2 and 10 mg/kg, respectively (Fig 3A and 3B).

Similarly to what observed in the mouse colon, the expression of phosphor-Akt, -mTOR, -p70S6K and HIF-1 $\alpha$  were all significantly overexpressed in the mucosa of UC patients (14,7  $\pm$  1,5 vs 1,4 $\pm$ 0,7, 13 $\pm$ 1 vs 1,4 $\pm$ 0,3, 12 $\pm$ 0,8 vs 1 $\pm$ 0,4 and 8,5 $\pm$ 2,7 vs 0,4 $\pm$ 0,1 OD = mm<sup>2</sup>, respectively vs. control; all  $p$ <0,001; Fig 3C and 3D), and they were significantly reduced by PEA in a dose-dependent fashion (all  $p$ <0,001, Fig 3C and 3D).

In both mouse and human specimens the ability of PEA to reduce the overexpression of Akt/mTOR/p70S6K and HIF-1 $\alpha$  pathways was significantly inhibited by concomitant administration of MK866 but not of GW9662, further supporting the concept that its effect involves the PPAR $\alpha$  activation (Fig 4A–4D). This finding was also supported by the observation that

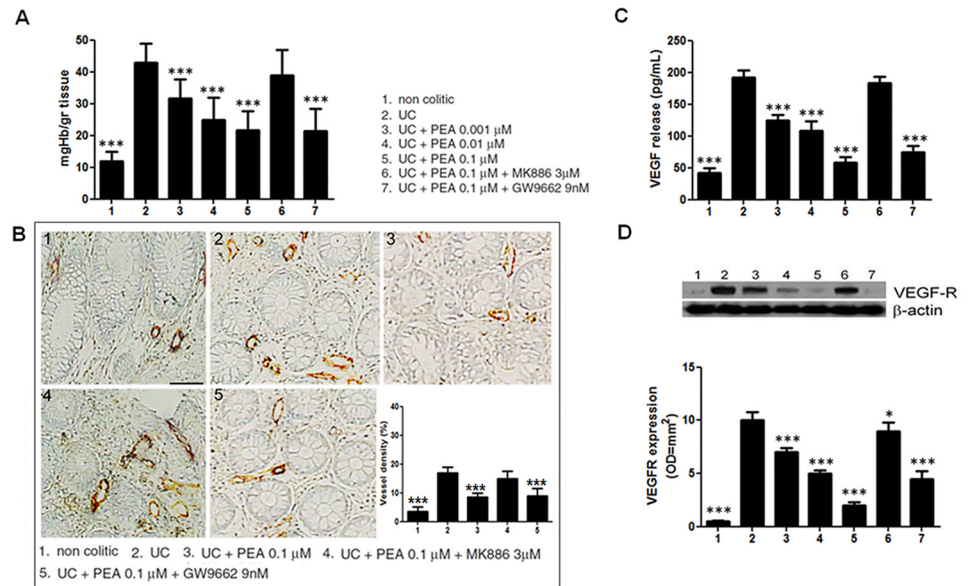


**Fig 3. Effects of palmitoylethanolamide (PEA) on molecular markers of angiogenesis in human.** (A) Ulcerative colitis caused a significant increase of Hb-content in colonic mucosa, PEA is able to reduce, in a dose-dependent fashion, the Hb-content in colitis patients; this effect persisted in presence of PPAR $\gamma$  antagonist (GW9662) while it was nullified by PPAR $\alpha$  antagonist (MK866). (B) Immunohistochemical images showing the expression of CD31 on: colonic mucosa of controls (panel 1), UC patients colonic mucosa in presence of PEA (0,1  $\mu$ M) alone (panel 3), PEA (0,1  $\mu$ M) plus MK866 3  $\mu$ M (panel 4), and PEA (0,1  $\mu$ M) plus GW9662 (9nM) (panel 5). Magnification 20X; scale bar: 100 $\mu$ m. The graph summarizes the relative quantification of CD31 expression (%) on human colonic mucosa in the same experimental groups, and, as described in mice, PEA administration caused a significant reduction of CD31 expression, except after co-administration of PPAR $\alpha$  antagonist. (C) VEGF release resulted increase in ulcerative colitis patients and it was significantly reduced by PEA treatment in a PPAR $\alpha$  dependent manner (D) Western blot analysis and relative densitometric analysis (arbitrary units normalized on the expression of housekeeping protein  $\beta$ -actin) of VEGF-receptor (VEGF-R) expression, showing a similar behavior to VEGF release. Results are expressed as mean $\pm$ SD. \* $p$ <0.05, \*\* $p$ <0.01 and \*\*\* $p$ <0.001 versus untreated biopsies from ulcerative colitis patients.

doi:10.1371/journal.pone.0156198.g003

PEA failed to significantly affect the Akt/mTOR/p70S6K and HIF-1 $\alpha$  pathways in PPAR $\alpha$  null mice (Fig 5).

## Discussion

Current therapies for inflammatory bowel disease are still challenging because of the relatively high rate of failure, the high costs and the risk of severe side effects due to immunosuppressive agents [30,31]. New molecules able to target different steps and pathways of the inflammatory response appear therefore a promising strategy for the treatment of these diseases.

Angiogenesis has been recently identified as a key event in the context of intestinal inflammation, whose extent significantly correlates with both the severity and the progression of the diseases [5–8], and favors the drift toward colonic carcinogenesis [32]; inhibition of angiogenesis appears thus as a synergistic and promising therapeutic strategy in IBDs [33,34].

VEGF is implicated in the regulation of the angiogenic process in sustained inflammation, and contributes to mucosal tissue remodeling, vascular permeability and leukocyte infiltration of the inflamed mucosa [35–37]. Here we demonstrated that, both in vivo and in ex vivo, PEA, in a concentration dependent manner, significantly reduced VEGF release and the expression of its receptor, in mice and human inflamed colon, respectively; this result was also associated with a significant decrease of mucosal hemoglobin content and CD31 positive vessels density.

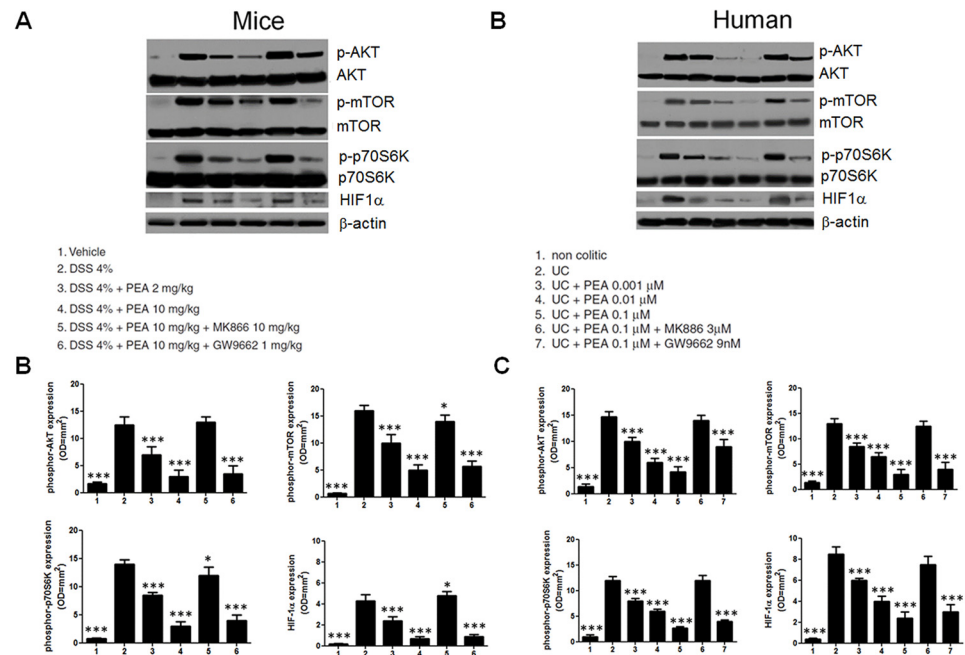


**Fig 4. Effects of palmitoylethanolamide (PEA) on Akt/mTOR/p70S6K axis activation and HIF-1 $\alpha$  expression in DSS-induced colitis and in ulcerative colitis.** (A) Western Blot analysis and (B) relative densitometric analysis showing the effects of PEA (2 mg/Kg and 10 mg/Kg), given alone or in the presence of MK866 (10 mg/Kg) or GW 9662 (1 mg/Kg), on the expression of phosphor-Akt, phosphor-mTOR, phosphor-p70S6K and HIF-1 $\alpha$  in mice with DSS-induced colitis. Western blot analysis (C) and relative densitometric analysis showing the effects of PEA at increasing concentration (0.001  $\mu$ M, 0.01  $\mu$ M and 0.1  $\mu$ M) given alone and in the presence of MK866 (3  $\mu$ M) or GW9662 (9 nM), on the expression of phosphor-Akt, phosphor-mTOR, phosphor-p70S6K and HIF-1 $\alpha$  in UC patients biopsies. In both human and mice, colitis induced the activation of pro-angiogenic Akt/mTOR/p70S6K pathway, and PEA resulted able to reduce it, in a dose-dependent and PPAR $\alpha$  dependent fashion. Results are expressed as mean  $\pm$  SD. \* $p$ <0.05, \*\* $p$ <0.01 and \*\*\* $p$ <0.001 versus DSS-treated mice (A and B) or vs untreated colonic biopsies from UC patients (C and D).

doi:10.1371/journal.pone.0156198.g004

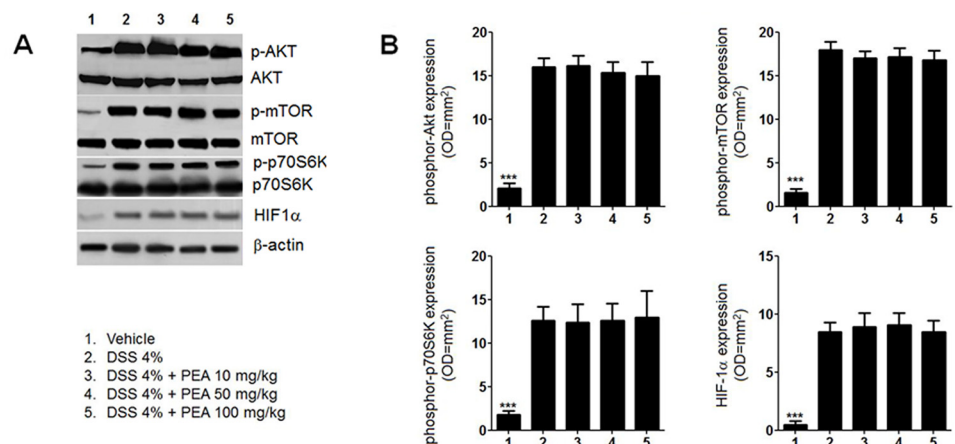


**Fig 5. Palmitoylethanolamide (PEA) failed to significantly affect DSS-induced Akt/mTOR/p70S6K axis activation and HIF-1 $\alpha$  expression in PPAR $\alpha$  null (KO) mice.** (A) Western Blot analysis and (B) relative densitometric analysis showing the effects of PEA (10–100 mg/kg) on the expression of phosphor-Akt, phosphor-mTOR, phosphor-p70S6K and HIF-1 $\alpha$  in DSS-treated PPAR $\alpha$  null (KO) mice. DSS exposure significantly induced the activation of the pro-angiogenic Akt/mTOR/p70S6K pathway as compared to untreated mice, but treatment with PEA had no significant effect in treated mice, regardless of the concentration used. Results are expressed as mean  $\pm$  SD. \*\*\* $p$ <0.001 versus untreated mice.

doi:10.1371/journal.pone.0156198.g005



It has been described that PEA is able to exert an antiangiogenic activity in other experimental models of chronic inflammation, likely supporting the concept that this ability is dependent by its anti-inflammatory effects [21,22,38]. However, we recently demonstrated that PEA directly reduces the release of pro-angiogenic factors in an in vitro model of colon cancer cells, through an Akt-mTOR pathway-dependent VEGF inhibition; these results suggest that the anti-angiogenic activity displayed by PEA in the inflamed colon is not solely related by its anti-inflammatory effects [23].

In our setting, we therefore investigated whether PEA-dependent VEGF signaling inhibition modulated by the Akt/mTOR axis. Different molecular pathways are involved in the angiogenesis, but the activation of Akt/mTOR axis has been specifically related to neo-vascularization in the development of inflammation-sustained colon cancer [39–41]. In particular, it induces the over-expression of HIF-1 $\alpha$ , a transcriptional factor related to hypoxia, that cooperates with reactive oxygen species (ROS), stimulating the release of VEGF and eventually neo-angiogenesis [42–44]. Our results demonstrated that PEA, in a PPAR- $\alpha$  selective and concentration dependent-manner, significantly reduced the phosphorylation of Akt, mTOR and p70S6 proteins in mice colon and ex-vivo human mucosa, leading to downstream inhibition of HIF-1 $\alpha$  with consequent inhibition of VEGF and EGF secretion and the respective receptors expression.

Remarkably, here we also showed that all the above-described pleiotropic effects of PEA are specifically related to the activation of the PPAR- $\alpha$  pathway. Although the role of PPAR- $\gamma$  as putative site of action of anti-inflammatory and anti-cancer drugs has been specifically addressed [45,46], the importance of PPAR- $\alpha$  pathway is recently emerging [16,23,27]. In keeping with this, we have demonstrated that the inhibition of the mTOR/Akt axis depends on PPAR- $\alpha$  activation, supporting its contribution in IBD-related angiogenesis and suggesting its protective role in inflammation-associated carcinogenesis. In addition, we provide data suggesting that PEA is able to act on the process of angiogenesis by directly modulating the endothelial cell's functioning, as demonstrated by its effect to significantly inhibit inflammatory-associated proliferation and migration of HUVEC cells (S1 Fig).

As stated, anti-angiogenic drugs represent an intriguing approach to treat IBDs, due to the effect on both inflammation and tumorigenesis. However, the efficacy of anti-angiogenic drugs is limited by the complexity and redundancy of the molecular pathways converging in neovascularization. In this context, PEA appears as a very interesting compound, since together with its activity on the Akt/mTOR pathway, it also significantly reduces the p38/MAPK/NF- $\kappa$ B axis [47–49]. It has been indeed previously demonstrated that PEA is able to inhibit the NF- $\kappa$ B (nuclear factor kappa-light-chain-enhancer of activated B cells) pro-inflammatory pathway, determining a strong downregulation of cyclooxygenase (COX)-2 and inducible nitric oxide synthase (iNOS) expression, with a consequent reduction of prostaglandins and nitric oxide release [48, 49]. While the role of these mediators in the inflammatory process is well established, there is evidence about their involvement in neo-vascularization and tumor growth, supporting the inflammation-associated carcinogenesis assumption [50, 51]. Interestingly, besides such anti-angiogenic and anti-inflammatory activity, PEA, as the others cannabinomimetic fatty acid derivatives, also exerts an antiproliferative effect on cancer cells, supporting its protective effects in both inflammation and cancer prevention [23, 52, 53].

To date, mesalamine is the unique drug, widely used in IBD, with both anti-inflammatory and potential anti-carcinogenic properties [54, 55]. However, even if rare, severe side effects to this compound, such as pancreatitis and interstitial nephritis, have been described [56]. PEA is a safe drug with a well known toxicological profile and it is already available as orally administered supplement in clinical practice [57, 58].

Although further studies are needed, palmitoylethanolamide, due to its anti-inflammatory and anti-angiogenic effects, might represent a promising “food therapy” for the prevention of

inflammation-associated colon cancer, and, most importantly, be part of a combined and multi-target therapy in the management of inflammation-associated angiogenesis and the potential anti-carcinogenic activity.

## Supporting Information

**S1 Fig. Palmitoylethanolamide reduced migration and proliferation in DSS-treated HUVEC cells.**  
(DOCX)

## Author Contributions

Conceived and designed the experiments: GS GE. Performed the experiments: TI EC SG L. Seguella NN. Analyzed the data: AD MP FM. Contributed reagents/materials/analysis tools: RC GA GdP L. Steardo. Wrote the paper: AD MP.

## References

1. Paleolog EM. Angiogenesis in rheumatoid arthritis. *Arthritis Res.* 2002; 4:81–90.
2. Sluimer JC, Daemen MJ. Novel concepts in atherogenesis: angiogenesis and hypoxia in atherosclerosis. *J Pathol.* 2009; 218:7–29. doi: [10.1002/path.2518](https://doi.org/10.1002/path.2518) PMID: [19309025](https://pubmed.ncbi.nlm.nih.gov/19309025/)
3. Crawford TN, Alfaro DV 3rd, Kerrison JB, Jablon EP. Diabetic retinopathy and angiogenesis. *Curr Diabetes Rev. United Arab Emirates;* 2009 Feb; 5(1):8–13.
4. Carmeliet P, Jain RK. Angiogenesis in cancer and other diseases. *Nature.* 2000; 407:249–57. PMID: [11001068](https://pubmed.ncbi.nlm.nih.gov/11001068/)
5. Tas SW, Maracle CX, Balogh E, Szekanecz Z. Targeting of proangiogenic signalling pathways in chronic inflammation. *Nat Rev Rheumatol.* 2016 Feb; 12(2):111–22. doi: [10.1038/nrrheum.2015.164](https://doi.org/10.1038/nrrheum.2015.164) PMID: [26633288](https://pubmed.ncbi.nlm.nih.gov/26633288/)
6. Jackson JR, Seed MP, Kircher CH, Willoughby DA, Winkler JD. The codependence inflammation of angiogenesis and chronic. *FASEB J.* 1997; 11:457–65. PMID: [9194526](https://pubmed.ncbi.nlm.nih.gov/9194526/)
7. Alkim C, Alkim H, Koksar AR, Boga S, Sen I. Angiogenesis in Inflammatory Bowel Disease. *Int J Inflamm.* 2015; 2015:970890 doi: [10.1155/2015/970890](https://doi.org/10.1155/2015/970890) PMID: [26839731](https://pubmed.ncbi.nlm.nih.gov/26839731/)
8. Danese S, Sans M, de la Motte C, Graziani C, West G, Phillips MH, et al. Angiogenesis as a novel component of inflammatory bowel disease pathogenesis. *Gastroenterology. AGA Institute American Gastroenterological Association;* 2006 Jun; 130(7):2060–73.
9. Olsson A-K, Dimberg A, Kreuger J, Claesson-Welsh L. VEGF receptor signalling—in control of vascular function. *Nat Rev Mol Cell Biol.* 2006 May; 7(5):359–71. PMID: [16633338](https://pubmed.ncbi.nlm.nih.gov/16633338/)
10. Ferrara N. Role of vascular endothelial growth factor in the regulation of angiogenesis. *Kidney Int.* 1999; 56:794–814. PMID: [10469350](https://pubmed.ncbi.nlm.nih.gov/10469350/)
11. Davaatseren M, Hwang J-T, Park JH, Kim M-S, Wang S, Sung MJ. Allyl isothiocyanate ameliorates angiogenesis and inflammation in dextran sulfate sodium-induced acute colitis. *PLoS One.* 2014 Jan; 9(7):e102975. doi: [10.1371/journal.pone.0102975](https://doi.org/10.1371/journal.pone.0102975) PMID: [25051185](https://pubmed.ncbi.nlm.nih.gov/25051185/)
12. Son MK, Jung KH, Hong S-W, Lee H-S, Zheng H-M, Choi M-J, et al. SB365, Pulsatilla saponin D suppresses the proliferation of human colon cancer cells and induces apoptosis by modulating the AKT/mTOR signalling pathway. *Food Chem. Elsevier Ltd;* 2013 Jan; 136(1):26–33.
13. Karar J, Maity A. PI3K/AKT/mTOR Pathway in Angiogenesis. *Front Mol Neurosci.* 2011 Jan; 4(51):1–8.
14. Clottes E. Hypoxia-inducible factor 1: regulation, involvement in carcinogenesis and target for anticancer therapy. *Bull Cancer.* 2005 Feb; 92(2):119–27. PMID: [15749641](https://pubmed.ncbi.nlm.nih.gov/15749641/)
15. Hadjipanayi E, Schilling AF. Hypoxia-based strategies for angiogenic induction: the dawn of a new era for ischemia therapy and tissue regeneration. *Organogenesis.* 2013 Oct 1; 9(4):261–72. doi: [10.4161/org.25970](https://doi.org/10.4161/org.25970) PMID: [23974216](https://pubmed.ncbi.nlm.nih.gov/23974216/)
16. Lo Verme J, Fu J, Astarita G, La Rana G, Russo R, Calignano A, et al. The Nuclear Receptor Peroxisome Proliferator-Activated Receptor-alpha Mediates the Anti-Inflammatory Actions of Palmitoylethanolamide. *Mol Pharmacol.* 2005; 67(1):15–9. PMID: [15465922](https://pubmed.ncbi.nlm.nih.gov/15465922/)

17. Conti S, Costa B, Colleoni M, Parolaro D, Giagnoni G. Antiinflammatory action of endocannabinoid palmitoylethanolamide and the synthetic cannabinoid nabilone in a model of acute inflammation in the rat. *Br J Pharmacol*. 2002; 135:181–7. PMID: [11786493](#)
18. Costa B, Conti S, Giagnoni G, Colleoni M. Therapeutic effect of the endogenous fatty acid amide, palmitoylethanolamide, in rat acute inflammation: inhibition of nitric oxide and cyclo-oxygenase systems. *Br J Pharmacol*. 2002 Oct; 137(4):413–20. PMID: [12359622](#)
19. Ross R a., Brockie HC, Pertwee RG. Inhibition of nitric oxide production in RAW264.7 macrophages by cannabinoids and palmitoylethanolamide. *Eur J Pharmacol* 2000 Aug; 401(2):121–30. PMID: [10924916](#)
20. Farquhar-smith WP, Jaggar SI, Rice ASC. Attenuation of nerve growth factor-induced visceral hyperalgesia via cannabinoid CB 1 and CB 2 -like receptors. *Pain*. 2002; 97:11–21. PMID: [12031775](#)
21. De Filippis D, D'Amico A, Cipriano M, Petrosino S, Orlando P, Di Marzo V, et al. Levels of endocannabinoids and palmitoylethanolamide and their pharmacological manipulation in chronic granulomatous inflammation in rats. *Pharmacol Res*. Elsevier Ltd; 2010 Apr; 61(4):321–8.
22. Cipriano M, Esposito G, Negro L, Capoccia E, Sarnelli G, Scuderi C, et al. Palmitoylethanolamide Regulates Production of Pro-Angiogenic Mediators in a Model of beta Amyloid-Induced Astrogliosis In Vitro. *CNS Neurol Disord Drug Targets*. United Arab Emirates; 2015; 14(7):828–37.
23. Sarnelli G, Gigli S, Capoccia E, Iuvone T, Cirillo C, Seguella L et al. Antiproliferative and antiangiogenic effects of palmitoylethanolamide in Caco-2 human colon cancer cell involve a selective PPAR-alpha dependent inhibition of Akt/mTOR pathway. *Phytotherapy Research*; 2016 2016 Mar 1. [Epub ahead of print]
24. Capasso R, Izzo AA, Fezza F, Pinto A, Capasso F, Mascolo N, et al. Inhibitory effect of palmitoylethanolamide on gastrointestinal motility in mice. *Br J Pharmacol*. 2001; 134:945–50. PMID: [11682441](#)
25. Costa B, Comelli F, Bettoni I, Colleoni M, Giagnoni G. The endogenous fatty acid amide, palmitoylethanolamide, has anti-allodynic and anti-hyperalgesic effects in a murine model of neuropathic pain: involvement of CB(1), TRPV1 and PPARgamma receptors and neurotrophic factors. *Pain*. International Association for the Study of Pain; 2008 Oct 3; 139(3):541–50.
26. Brown WH, Gillum MP, Lee H, Paulo J, Camporez G, Zhang X. Fatty acid amide hydrolase ablation promotes ectopic lipid storage and insulin resistance due to centrally mediated hypothroidism. *Proc Natl Acad Sci USA*. 2012; 109:14966–71. doi: [10.1073/pnas.1212887109](#) PMID: [22912404](#)
27. Esposito G, Capoccia E, Turco F, Palumbo I, Lu J, Steardo A, et al. Palmitoylethanolamide improves colon inflammation through an enteric glia/toll like receptor 4-dependent PPAR-α activation. *Gut*. 2014 Aug; 63(8):1300–12. doi: [10.1136/gutjnl-2013-305005](#) PMID: [24082036](#)
28. Tsujii M, Kawano S, Tsuji S, Kobayashi I, Takei Y, Nagano K, et al. Colonic mucosal hemodynamics and tissue oxygenation in patients with ulcerative colitis: investigation by organ reflectance spectrophotometry. *Gastroenterol*. 1995 Apr; 30(2):183–8.
29. Bhaskar L, Ramakrishna BS, Balasubramanian KA. Colonic mucosal antioxidant enzymes and lipid peroxide levels in normal subjects and patients with ulcerative colitis. *J Gastroenterol Hepatol*. 1995 Mar-Apr; 10(2):140–3. PMID: [7787158](#)
30. Grevenit P, Thomas A, Lodhia N. Medical Therapy for Inflammatory Bowel Disease. *Surg Clin North Am*. 2015 Dec; 95(6):1159–82. doi: [10.1016/j.suc.2015.08.004](#) PMID: [26596920](#)
31. Martínez-Montiel MP, Casis-Herce B, Gómez-Gómez GJ, Masedo-González A, Yela-San Bernardino C, Piedracoba C, et al. Pharmacologic therapy for inflammatory bowel disease refractory to steroids. *Clin Exp Gastroenterol*. 2015 Aug 17; 8:257–69. doi: [10.2147/CEG.S58152](#) PMID: [26316792](#)
32. Setia S, Nehru B, Sanyal SN. The PI3K/Akt pathway in colitis associated colon cancer and its chemoprevention with celecoxib, a Cox-2 selective inhibitor. *Biomed Pharmacother*. Elsevier Masson SAS; 2014 Jul; 68(6):721–7.
33. Hatoum O a, Heidemann J, Binion DG. The intestinal microvasculature as a therapeutic target in inflammatory bowel disease. *Ann N Y Acad Sci* 2006 Aug; 1072:78–97. PMID: [17057192](#)
34. Chidlow JH, Langston W, Greer JJM, Ostanin D, Abdelbaqi M, Houghton J, et al. Differential angiogenic regulation of experimental colitis. *Am J Pathol [Internet]*. American Society for Investigative Pathology; 2006 Dec; 169(6):2014–30.
35. Ferrante M, Pierik M, Henckaerts L, Joossens M, Claes K, Van Schuerbeek N, et al. The role of vascular endothelial growth factor (VEGF) in inflammatory bowel disease. *Inflamm Bowel Dis*. 2006 Sep; 12(9):870–8. PMID: [16954806](#)
36. Goebel S, Huang M, Davis WC, Jennings M, Siahaan TJ, Alexander JS, et al. VEGF-A stimulation of leukocyte adhesion to colonic microvascular endothelium: implications for inflammatory bowel disease. *Am J Physiol Gastrointest Liver Physiol*. 2006 Apr [cited 2015 Sep 25]; 290(4):G648–54. PMID: [16293653](#)

37. Scaldaferrri F, Vetrano S, Sans M, Arena V, Straface G, Stigliano E, et al. VEGF-A links angiogenesis and inflammation in inflammatory bowel disease pathogenesis. *Gastroenterology*. AGA Institute American Gastroenterological Association; 2009 Feb; 136(2):585–95.e5.
38. De Filippis D, Russo A, De Stefano D, Maiuri MC, Esposito G, Cinelli MP et al. (2007). Local administration of WIN 55,212–2 reduces chronic granuloma-associated angiogenesis in rat by inhibiting NF-kappa B activation. *J Mol Med* 85: 635–645 PMID: [17447045](#)
39. Hay N. The Akt-mTOR tango and its relevance to cancer. *Cancer Cell*. 2005 Sep; 8(3):179–83. PMID: [16169463](#)
40. Morgensztern D, McLeod HL. PI3K/Akt/mTOR pathway as a target for cancer therapy. *Anticancer Drugs*. 2005 Sep; 16(8):797–803. PMID: [16096426](#)
41. Shaw RJ, Cantley LC. Ras, PI(3)K and mTOR signalling controls tumour cell growth. *Nature*. 2006 May 25; 441(7092):424–30. PMID: [16724053](#)
42. Yuan G, Nanduri J, Khan S, Semenza GL, Prabhakar NR. Induction of HIF-1alpha expression by intermittent hypoxia: involvement of NADPH oxidase, Ca2+ signaling, prolyl hydroxylases, and mTOR. *J Cell Physiol* [Internet]. 2008 Dec; 217(3):674–85.
43. Laughner E, Taghavi P, Chiles K, Mahon PC, Semenza GL. HER2 (neu) signaling increases the rate of hypoxia-inducible factor 1alpha (HIF-1alpha) synthesis: novel mechanism for HIF-1-mediated vascular endothelial growth factor expression. *Mol Cell Biol*. 2001 Jun; 21(12):3995–4004. PMID: [11359907](#)
44. Glover LE, Colgan SP. Hypoxia and metabolic factors that influence IBD pathogenesis. *Gastroenterology*. 2011; 140(6):1748–55. doi: [10.1053/j.gastro.2011.01.056](#) PMID: [21530741](#)
45. Han S, Roman J. Peroxisome proliferator-activated receptor gamma: a novel target for cancer therapeutics? *Anticancer Drugs*. 2007 Mar; 18(3):237–44. PMID: [17264754](#)
46. Dubuquoy L, Rousseaux C, Thuru X, Peyrin-Biroulet L, Romano O, Chavatte P, et al. PPARgamma as a new therapeutic target in inflammatory bowel diseases. *Gut*. 2006 Sep; 55(9):1341–9. PMID: [16905700](#)
47. Dormond-Meuwly A, Roulin D, Dufour M, Benoit M, Demartines N, Dormond O. The inhibition of MAPK potentiates the anti-angiogenic efficacy of mTOR inhibitors. *Biochem Biophys Res Commun*. Elsevier Inc.; 2011 Apr 22; 407(4):714–9.
48. Scuderi C, Esposito G, Blasio A, Valenza M, Arietti P, Steardo L, et al. Palmitoylethanolamide counteracts reactive astrogliosis induced by beta-amyloid peptide. *J Cell Mol Med* [Internet]. 2011 Dec; 15(12):2664–74.
49. Gee E, Milkiewicz M, Haas TL. p38 MAPK activity is stimulated by vascular endothelial growth factor receptor 2 activation and is essential for shear stress-induced angiogenesis. *J Cell Physiol*. 2010 Jan; 222(1):120–6. doi: [10.1002/jcp.21924](#) PMID: [19774558](#)
50. Xu W, Liu LZ, Loizidou M, Ahmed M, Charles IG. The role of nitric oxide in cancer. *Cell Res*. 2002 Dec; 12(5–6):311–20. PMID: [12528889](#)
51. Montrose DC, Nakanishi M, Murphy RC, Zarini S, McAleer JP, Vella AT, et al. The role of PGE2 in intestinal inflammation and tumorigenesis. *Prostaglandins Other Lipid Mediat*. 2015 Jan-Mar; 116–117:26–36 doi: [10.1016/j.prostaglandins.2014.10.002](#) PMID: [25460828](#)
52. De Petrocellis L, Bisogno T, Ligresti A, Bifulco M, Melck D, Di Marzo V. Effect on cancer cell proliferation of palmitoylethanolamide, a fatty acid amide interacting with both the cannabinoid and vanilloid signalling systems. *Fundam Clin Pharmacol*. 2002 Aug; 16(4):297–302. PMID: [12570018](#)
53. Di Marzo V, Melck D, Orlando P, Bisogno T, Zagoory O, Bifulco M et al. Palmitoylethanolamide inhibits the expression of fatty acid amide hydrolase and enhances the anti-proliferative effect of anandamide in human breast cancer cells. *Biochem J*. 2001 Aug 15; 358(Pt 1):249–55. PMID: [11485574](#)
54. Tang J, Sharif O, Pai C. Mesalamine protects against colorectal cancer in inflammatory bowel disease. *Digestive and Liver disease* 2010; 55(6):1696
55. Rubin DT, LoSavio A, Yadron N, Huo D, Hanauer SB. Aminosalicylate therapy in the prevention of dysplasia and colorectal cancer in ulcerative colitis
56. Cunliffe RN, Scott BB. Monitoring for drug side-effects in inflammatory bowel disease *APT* 2002 66(4):647–662
57. Paladini A, Fusco M, Cenacchi T, Schievano C, Piroli A, Varrassi G. Palmitoylethanolamide, a Special Food for Medical Purposes, in the Treatment of Chronic Pain: A Pooled Data Meta-analysis. *Pain Physician* 2016; 19:11–24 PMID: [26815246](#)
58. Orefice NS, Alhouayek M, Carotenuto A, Montella S, Barbato F, Comelli A, et al. Oral Palmitoylethanolamide Treatment Is Associated with Reduced Cutaneous Adverse Effects of Interferon-beta1a and Circulating Proinflammatory Cytokines in Relapsing-Remitting Multiple Sclerosis. *Neurotherapeutics*. 2016 Apr; 13(2):428–38. doi: [10.1007/s13311-016-0420-z](#) PMID: [26857391](#)



# Rifaximin Improves *Clostridium difficile* Toxin A-Induced Toxicity in Caco-2 Cells by the PXR-Dependent TLR4/MyD88/NF- $\kappa$ B Pathway

Giuseppe Esposito<sup>1\*</sup>, Nicola Nobile<sup>1</sup>, Stefano Gigli<sup>1</sup>, Luisa Seguella<sup>1</sup>, Marcella Pesce<sup>2</sup>, Alessandra d'Alessandro<sup>2</sup>, Eugenia Bruzzese<sup>3</sup>, Elena Capoccia<sup>1</sup>, Luca Steardo<sup>1</sup>, Rosario Cuomo<sup>2</sup> and Giovanni Sarnelli<sup>2\*</sup>

<sup>1</sup> Department of Physiology and Pharmacology "Vittorio Erspamer", Sapienza University of Rome, Rome, Italy, <sup>2</sup> Department of Clinical Medicine and Surgery, University of Naples Federico II, Naples, Italy, <sup>3</sup> Department of Translational Medical Science, University of Naples Federico II, Naples, Italy

## OPEN ACCESS

### Edited by:

Raffaele Capasso,  
University of Naples Federico II, Italy

### Reviewed by:

Laurent Ferrier,  
Institut National de la Recherche  
Agronomique, France  
Ignazio Castagliuolo,  
University of Padova, Italy

### \*Correspondence:

Giovanni Sarnelli  
sarnelli@unina.it;  
Giuseppe Esposito  
giuseppe.esposito@uniroma1.it

### Specialty section:

This article was submitted to  
Gastrointestinal and Hepatic  
Pharmacology,  
a section of the journal  
Frontiers in Pharmacology

Received: 01 March 2016

Accepted: 25 April 2016

Published: 09 May 2016

### Citation:

Esposito G, Nobile N, Gigli S,  
Seguella L, Pesce M, d'Alessandro A,  
Bruzzese E, Capoccia E, Steardo L,  
Cuomo R and Sarnelli G (2016)  
Rifaximin Improves *Clostridium difficile*  
Toxin A-Induced Toxicity in Caco-2  
Cells by the PXR-Dependent  
TLR4/MyD88/NF- $\kappa$ B Pathway.  
Front. Pharmacol. 7:120.  
doi: 10.3389/fphar.2016.00120

**Background:** *Clostridium difficile* infections (CDIs) caused by *Clostridium difficile* toxin A (TcdA) lead to severe ulceration, inflammation and bleeding of the colon, and are difficult to treat.

**Aim:** The study aimed to evaluate the effect of rifaximin on TcdA-induced apoptosis in intestinal epithelial cells and investigate the role of PXR in its mechanism of action.

**Methods:** Caco-2 cells were incubated with TcdA and treated with rifaximin (0.1–10  $\mu$ M) with or without ketoconazole (10  $\mu$ M). The transepithelial electrical resistance (TEER) and viability of the treated cells was determined. Also, the expression of zona occludens-1 (ZO-1), toll-like receptor 4 (TLR4), Bcl-2-associated X protein (Bax), transforming growth factor- $\beta$ -activated kinase-1 (TAK1), myeloid differentiation factor 88 (MyD88), and nuclear factor-kappaB (NF- $\kappa$ B) was determined.

**Results:** Rifaximin treatment (0.1, 1.0, and 10  $\mu$ M) caused a significant and concentration-dependent increase in the TEER of Caco-2 cells (360, 480, and 680% vs. TcdA treatment) 24 h after the treatment and improved their viability (61, 79, and 105%). Treatment also concentration-dependently decreased the expression of Bax protein (–29, –65, and –77%) and increased the expression of ZO-1 (25, 54, and 87%) and occludin (71, 114, and 262%) versus TcdA treatment. The expression of TLR4 (–33, –50, and –75%), MyD88 (–29, –60, and –81%) and TAK1 (–37, –63, and –79%) were also reduced with rifaximin versus TcdA treatment. Ketoconazole treatment inhibited these effects.

**Conclusion:** Rifaximin improved TcdA-induced toxicity in Caco-2 cells by the PXR-dependent TLR4/MyD88/NF- $\kappa$ B pathway mechanism, and may be useful in the treatment of CDIs.

**Keywords:** Caco-2 cells, *Clostridium difficile* toxin A, pregnane X receptor, rifaximin, pseudomembranous colitis

## INTRODUCTION

Pseudomembranous colitis is a condition of the large intestine characterized by inflammation and bleeding (Surawicz and McFarland, 1999). It is mainly caused by the anaerobic Gram-positive bacteria, *Clostridium difficile*. These spore producing bacteria colonize the large intestine and produce toxins [*Clostridium difficile* toxin A (TcdA) and *Clostridium difficile* toxin B (TcdB)] which lead to severe diarrhea, colitis, shock and death in severe cases (Rupnik et al., 2009; Leffler and Lamont, 2015). The cost of treatment and duration of hospitalization is also significantly increased in affected individuals (Jodlowski et al., 2006). *Clostridium difficile* infections (CDIs) are common in hospital settings due to excessive use of antibiotics, which wash out the normal gastrointestinal flora, making individuals more vulnerable to bacterial attack (Rupnik et al., 2009). Currently available treatment strategies for CDIs include the use of specific antibiotics against *Clostridium difficile*, fecal transplant and surgery (Waltz and Zuckerbraun, 2016). However, treatment of severe and recurrent CDIs remains a challenge, with limited treatment options available (Ebigbo and Messmann, 2013).

Rifaximin, a synthetic analog of rifamycin, is a broad spectrum antibiotic effective against several Gram-positive as well as Gram-negative aerobic and anaerobic bacteria (Scarpignato and Pelosini, 2006). It is poorly absorbed on oral administration and has no systemic adverse events (Scarpignato and Pelosini, 2005). Rifaximin is mainly used for the treatment of travelers' diarrhea, hepatic encephalopathy, and irritable bowel syndrome (Layer and Andresen, 2010; Sanchez-Delgado and Miquel, 2015; Cash et al., 2016). Besides its antibiotic effect, rifaximin is a gut-specific activator of human pregnane X receptor (PXR), which is a nuclear receptor expressed in the small intestine that is involved in maintaining the integrity of the intestinal epithelial barrier (Ma et al., 2007; Cheng et al., 2010; Wan et al., 2015).

The aim of the present study was to evaluate the effect of rifaximin on TcdA-induced apoptosis, using the Caco-2 cell line as a model for the human intestinal barrier, and to investigate the role of PXR in its mechanism of action.

## MATERIALS AND METHODS

Caco-2 cells were purchased from European Collection of Cell Cultures (ECACC, Public Health England Porton Down, Salisbury, UK). Cell medium, chemicals and reagents used for cell culture, and TcdA were purchased from Sigma-Aldrich (St. Louis, MO, USA), unless otherwise stated. Instruments, reagents, and materials used for western blot analysis were obtained from Bio-Rad Laboratories (Milan, Italy). Rabbit anti-zona occludens-1 (ZO-1), anti-occludin and anti-glyceraldehyde-3-phosphate dehydrogenase (GAPDH) antibodies were procured from Cell Signaling Technology (Danvers, MA, USA). Rabbit anti-toll-like receptor 4 (TLR4), mouse anti-ZO-1, anti-Bcl-2-associated X protein (Bax), mouse anti-MyD88, rabbit anti-transforming growth factor- $\beta$ -activated kinase-1 (pTAK1), and mouse anti-TAK1 antibody were purchased from Santa Cruz Biotechnology (Santa Cruz, CA, USA) and horseradish peroxidase (HRP) was

obtained from Dako (Milan, Italy). Fluorescein isothiocyanate-conjugated anti-rabbit antibody and Texas red conjugated anti-mouse antibody were purchased from Abcam (Cambridge, UK), and custom oligonucleotides for electrophoretic mobility shift assay (EMSA) analysis were synthesized by TIB Molbiol (Berlin, Germany).

## Cell Culture

Caco-2 cells were cultured in 6-well plates in Dulbecco's Modified Eagle Medium (DMEM) containing 10% fetal bovine serum (FBS), 1% penicillin-streptomycin, 2 mM L-glutamate, and 1% non-essential amino acids. A total of  $1 \times 10^6$  cells/well were plated and incubated for 24 h. Upon reaching confluence, the cells were washed three times with phosphate-buffered saline (PBS), detached with trypsin/ethylene diamine tetraacetic acid (EDTA), plated in a 10 cm diameter petri dish and allowed to adhere for further 24 h.

The Caco-2 cells were randomly divided into six groups: vehicle group, 30 ng/ml TcdA group, 30 ng/ml TcdA plus 0.1  $\mu$ M rifaximin, 30 ng/ml TcdA plus 1  $\mu$ M rifaximin (Alfa Wasserman S.p.A, Bologna, Italy), 30 ng/ml TcdA plus 10  $\mu$ M rifaximin, and 30 ng/ml TcdA plus 10  $\mu$ M rifaximin plus 10  $\mu$ M PXR antagonist ketoconazole. Rifaximin concentrations were chosen on the basis of previous studies (Terc et al., 2014). Depending upon the experiments, Caco-2 cells were cultured in either 6-well plates or 96-well plates. The cells were treated with different concentrations of rifaximin (0.1–10  $\mu$ M) and incubated at 37°C for 24 h, followed by TcdA exposure (30 ng/ml) for 24 h.

## Transepithelial Electrical Resistance Measurement

The transepithelial electrical resistance (TEER) of the epithelial cell monolayer was determined using the EVOM volt-ohm meter (World Precision Instruments Germany, Berlin, Germany) according to the method described by Wells et al. (1998). Briefly, cells plated between 14 and 21 days were used for experimentation, and each epithelial cell layer with a TEER value greater than 1000  $\Omega/\text{cm}^2$ , was considered to have tight adhesion. TEER was calculated using the following formula:  $\text{TEER} (\Omega/\text{cm}^2) = (\text{Total resistance} - \text{blank resistance}) (\Omega) \times \text{Area} (\text{cm}^2)$ .

## Western Blot Analysis

Protein expression in the Caco-2 cells was evaluated using western blot analysis. Following the treatments, the cells ( $1 \times 10^6$  cells/well) were harvested, washed twice with ice-cold PBS and centrifuged at  $180 \times g$  for 10 min at 4°C. The pellet of cells obtained after centrifugation was resuspended in 100  $\mu$ l ice-cold hypotonic lysis buffer [10 mM 4-(2-hydroxyethyl)-1-piperazineethanesulfonic acid (HEPES), 1.5 mM  $\text{MgCl}_2$ , 10 mM KCl, 0.5 mM phenylmethylsulfonylfluoride, 1.5  $\mu$ g/ml soybean trypsin inhibitor, 7  $\mu$ g/ml pepstatin A, 5  $\mu$ g/ml leupeptin, 0.1 mM benzamide and 0.5 mM dithiothreitol (DTT)]. The suspension was rapidly passed through a syringe needle five to six times to lyse the cells and then centrifuged for 15 min at  $13,000 \times g$  to obtain the cytoplasmic fraction. The proteins

from the cytoplasmic fraction were mixed with a non-reducing gel loading buffer [50 mM Tris(hydroxymethyl)aminomethane (Tris), 10% sodium dodecyl sulfate (SDS), 10% glycerol, 2 mg bromophenol/ml] at a 1:1 ratio, and boiled for 3 min followed by centrifugation at  $10,000 \times g$  for 10 min. The protein concentration was determined using the Bradford assay and 50  $\mu$ g of each homogenate was used for electrophoresis using polyacrylamide mini gels.

Proteins were transferred to nitrocellulose membranes that were saturated by incubation with 10% non-fat dry milk in 1X PBS overnight at 4°C and then incubated with rabbit anti-ZO-1, rabbit anti-occludin, rabbit anti-TLR4, rabbit anti-Bax, rabbit anti-p-TAK1, mouse anti-TAK1, mouse anti-MyD88, or rabbit anti-GAPDH antibodies, according to standard experimental protocols. Membranes were then incubated with the specific secondary antibodies conjugated to HRP. Immune complexes were identified by enhanced chemiluminescence detection reagents (Amersham Biosciences, Milan, Italy) and the blots were analyzed by scanning densitometry (GS-700 Imaging Densitometer; Bio-Rad, Segrate, Italy). Results were expressed as optical density (OD; arbitrary units;  $\text{mm}^2$ ) and normalized against the expression of the housekeeping protein GAPDH.

### Immunofluorescence Staining Analysis

Caco-2 cells were harvested, washed with PBS, fixed in 4% formaldehyde in PBS for 15 min and permeabilized with 0.3% Triton-X100 in PBS for 1 h. Two percent bovine serum albumin (BSA) was used to block the non-specific binding sites. The cells were then incubated overnight with mouse anti-ZO-1 (1:100) and rabbit anti-occludin antibody (1:100), or rabbit monoclonal anti-active caspase-3 (1:100; Abcam, Cambridge, UK) and further incubated in the dark with the appropriate secondary antibody (fluorescein isothiocyanate conjugated anti-rabbit or Texas red conjugated anti-mouse). The cells were analyzed using a microscope (Nikon Eclipse 80i), and images were captured by a high-resolution digital camera (Nikon Digital Sight DS-U1). Appropriate negative controls were done by omitting primary or secondary antibodies.

### Cytotoxicity Assay

The 3-[4,5-dimethylthiazol-2-yl]-2,5 diphenyltetrazolium bromide (MTT) assay was used to determine cell proliferation and survival in the Caco-2 cells (Mosmann, 1983). The cells ( $5 \times 10^4$  cells/well) were plated in 96-well plates and allowed to adhere for 3 h. DMEM was then replaced with fresh medium and the cells were untreated or treated with 30 ng/ml TcdA alone or together with increasing concentrations of rifaximin (0.1, 1.0, and 10  $\mu$ M) dissolved in ultrapure and pyrogen-free sterile vehicle, in the presence or absence of 10  $\mu$ M ketoconazole. After 4 h, 25  $\mu$ l MTT (5 mg/ml MTT in DMEM) was added to the cells and the mixture was incubated for a further 3 h at 37°C. Subsequently, the cells were lysed and the dark blue crystals were solubilized using a 100  $\mu$ l solution containing 50% *N,N*-dimethylformamide and 20% (w/v) SDS (pH 4.5). The OD of each well was determined using a microplate spectrophotometer equipped with a 620 nm filter (PerkinElmer, Inc; Waltham, MA, USA).

### Electrophoretic Mobility Shift Assay

Electrophoretic mobility shift assay was performed to detect nuclear factor-kappaB (NF- $\kappa$ B) activation in Caco-2 cells after TcdA with or without rifaximin treatment. Briefly, 10 mg of cell extracts were incubated in a binding buffer (8 mM HEPES, pH 7.0, 10% glycerol, 20 mM KCl, 4 mM  $\text{MgCl}_2$ , 1 mM sodium pyrophosphate) containing 1.0 mg of poly(dI-dC) and  $\gamma$ - $^{32}\text{P}$  end-labeled probe. The probe had a sequence as follows: A) 5' AAC TCC GGG AAT TTC CCT GGC CC3' and B) 5' GGG CCA GGG AAA TTC CCG GAG TT3'. Nuclear extracts were incubated for 15 min with radiolabelled oligonucleotides ( $2.5$ – $5.0 \times 10^4$  cpm) in a 20 ml reaction buffer containing 2 mg poly(dI-dC), 10 mM Tris-HCl (pH 7.5), 100 mM NaCl, 1 mM EDTA, 1 mM DTT 1 mg/ml BSA, and 10% (v/v) glycerol. Nuclear protein-oligonucleotide complexes were resolved by electrophoresis on a 6% non-denaturing polyacrylamide gel in Tris-Borate-EDTA buffer at 150 V for 2 h at 4°C. The gel was dried and autoradiographed with an intensifying screen at  $-80^\circ\text{C}$  for 20 h. The relative bands were quantified by densitometric scanning with Versadoc (Bio-Rad Laboratories) and a computer program (Quantity One Software, Bio-Rad Laboratories).

### DNA Fragmentation Assay

Following treatments Caco-2 cells were harvested, lysed with 400  $\mu$ l sodium chloride EDTA buffer (75 mM NaCl and 25 mM EDTA) containing 1% (w/v) SDS and 2 U/ml proteinase K, and incubated for 2 h at 55°C. Proteins were precipitated by adding 140  $\mu$ l 5 M NaCl. After centrifugation, DNA in the supernatant was precipitated by addition ethanol and centrifugation was performed again (15 min;  $11,000 \times g$ ). After washing with 70% ethanol (v/v), the DNA was re-suspended in H<sub>2</sub>O, separated by agarose gel electrophoresis and stained with ethidium bromide.

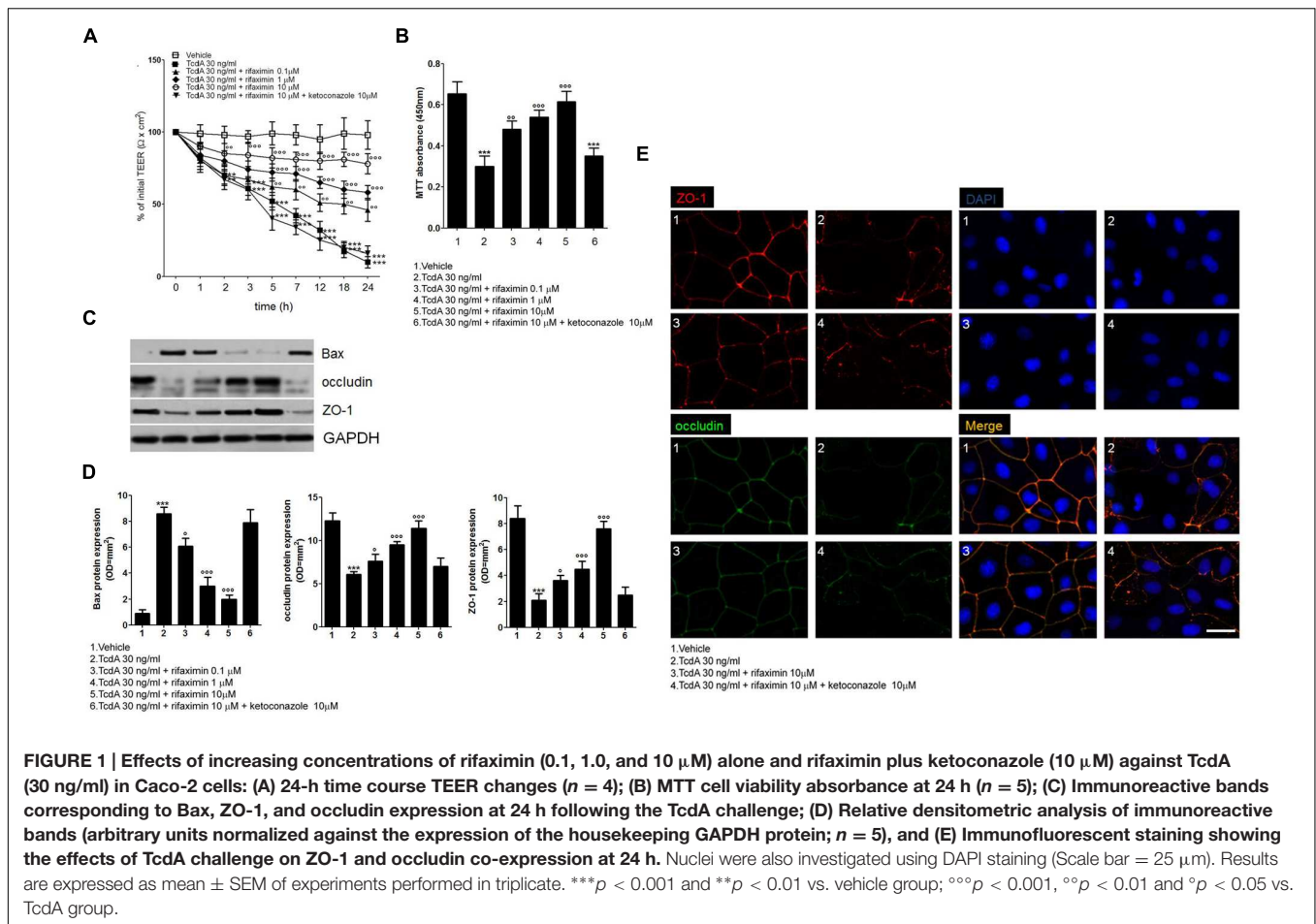
### Statistical Analysis

Results were expressed as mean  $\pm$  SEM of  $n = 5$  experiments in triplicate. Statistical analysis was performed using parametric one way analysis of variance (ANOVA) and Bonferroni's *post hoc* test was used for multiple comparisons. *P*-values  $< 0.05$  were considered significant.

## RESULTS

### Transepithelial Electrical Resistance

The TEER values in the presence of rifaximin (0.1–10  $\mu$ M) alone or in the presence of ketoconazole (10  $\mu$ M) were determined in order to evaluate the barrier integrity of Caco-2 cells exposed to 24 h of TcdA challenge. As seen in **Figure 1A**, a significant time-dependent reduction in TEER was observed starting from 2 h after 30 ng/ml TcdA exposure when compared with the vehicle group. The TEER values at 2, 3, 5, 7, 12, 18, and 24 h were  $-30$ ,  $-37$ ,  $-49$ ,  $-57$ ,  $-70$ ,  $-82$ , and  $-91\%$  versus the vehicle group, respectively. Starting at 5 h following the start of the toxin challenge, the effect of TcdA on TEER decrease was significantly counteracted by rifaximin treatment in a concentration-dependent manner. The TEER observed in the 0.1  $\mu$ M rifaximin group at 5, 7, 12, 18, and 24 h was 19, 43, 56,



177, and 360%, and in the 1.0  $\mu$ M rifaximin group was 36, 69, 103, 233, and 480%, when compared with the TcdA group. When rifaximin 10 mM was used, TEER reduction was seen starting at 2 h following TcdA stimulus and continued for all the time point intervals (24, 28, 57, 93, 150, 350, and 680% vs. the TcdA group at 2, 3, 5, 7, 12, 18, and 24 h; **Figure 1A**). The effect of rifaximin on the TEER was abolished by the treatment with ketoconazole (**Figure 1A**).

## Cell Viability and Cytotoxicity

As seen in **Figure 1B**, a significant decrease in Caco-2 cell viability ( $-54\%$ ) was observed at 24 h following the TcdA challenge, when compared with the vehicle group (assumed to be 100% viable cells). Under the same experimental conditions, rifaximin caused a significant and concentration-dependent inhibition of cytotoxicity induced by TcdA, resulting in an increased viability of the cultured cells (61, 79, and 105% with 0.1, 1.0, and 10  $\mu$ M rifaximin, respectively, vs. TcdA group). The effect of rifaximin was almost totally inhibited by ketoconazole (**Figure 1B**).

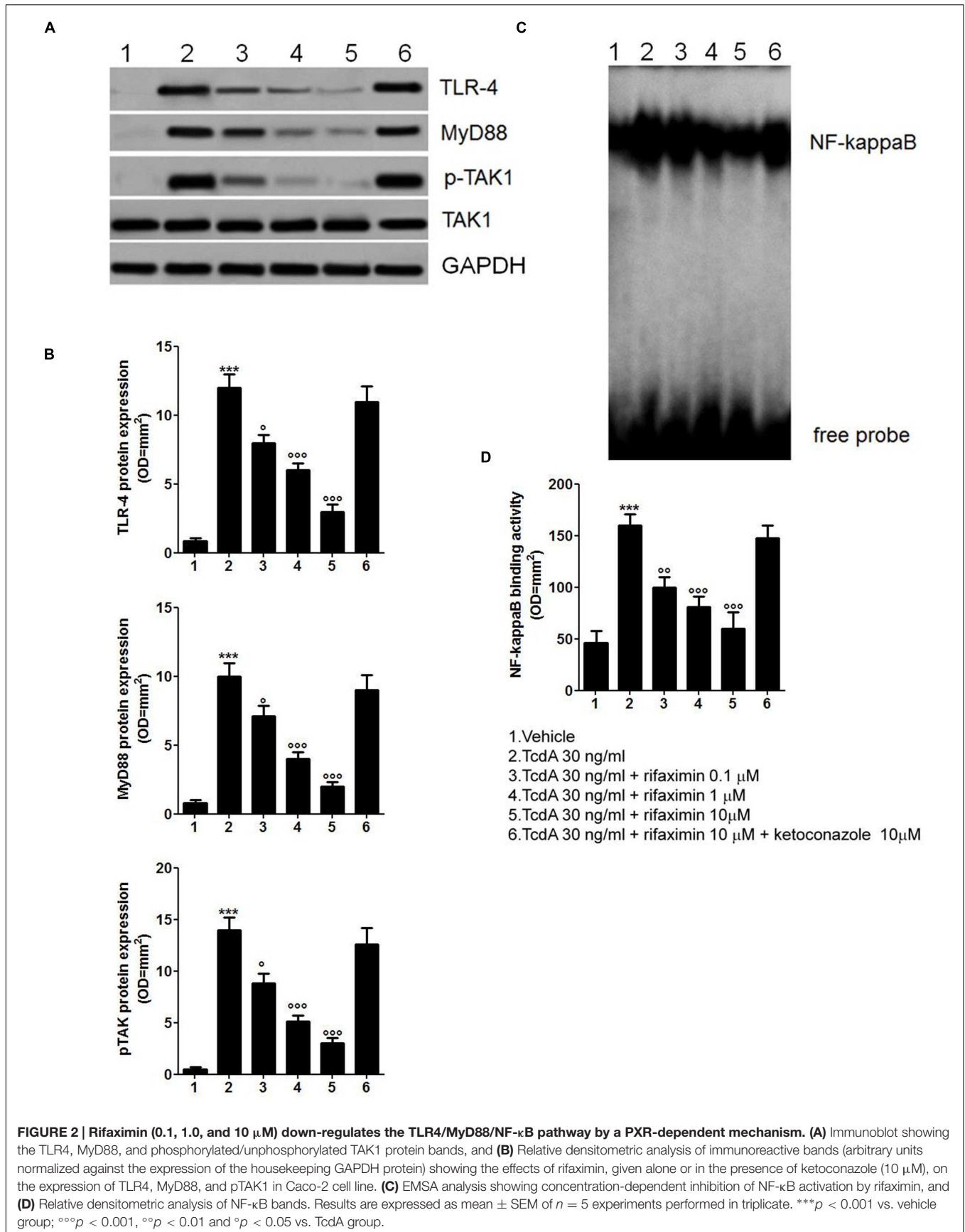
## Western Blot and Immunofluorescence Staining

The TcdA challenge caused a significant increase in pro-apoptotic Bax protein expression in Caco-2 cell homogenates

(955%;  $p < 0.001$  vs. vehicle), as seen in **Figures 1C,D**. Treatment with rifaximin resulted in a concentration-dependent decrease in Bax protein expression under the same experimental conditions ( $-29$ ,  $-65$ , and  $-77\%$  with 0.1, 1.0, and 10  $\mu$ M rifaximin, respectively, vs. TcdA group). Here again, this anti-apoptotic effect of rifaximin was reverted by ketoconazole (**Figures 1C,D**). To further confirm the ability of rifaximin to significantly affect the TcdA-induced apoptosis also the DNA fragmentation and the expression of caspase-3 were significantly and, in a similar PXR-manner, reduced (**Supplementary Figure S1**).

Also, there was a significant decrease in the expression of ZO-1 ( $-75\%$ ) and occludin ( $-50\%$ ) 24 h after the TcdA exposure (**Figures 1C,D**), versus their respective vehicle groups. Along with its protective effect on cell viability, rifaximin concentration-dependently increased ZO-1 (0.1, 1.0, and 10  $\mu$ M rifaximin: 25, 54, and 87%, respectively, vs. TcdA group) and occludin (71, 114, and 262%, respectively, vs. TcdA group) expression. Immunofluorescence analysis (**Figures 1C-E**) showed that rifaximin, at a dose of 10  $\mu$ M, resulted in an impressive preservation of epithelial barrier architecture, counteracting TcdA-induced decrease in ZO-1 and occludin co-expression in cultured cells (**Figure 1E**). Once again, ketoconazole caused complete loss of the





rifaximin-mediated rescue of ZO-1 and occludin proteins (Figures 1C,D).

### TLR4/MyD88/NF- $\kappa$ B Expression

There was a significant increase in the expression of TLR4 (1411%) and myeloid differentiation factor 88 (MyD88; 1250%), and phosphorylation of TAK1 (2800%) in the Caco-2 cells 24 h after the TcdA challenge, when compared with the vehicle group (Figures 2A,B). The EMSA analysis showed significant up-regulation of NF- $\kappa$ B activity by TcdA versus the vehicle group (348%; Figures 2A,B). Rifaximin at 0.1, 1.0, and 10  $\mu$ M inhibited TLR4 expression (-33, -50, and -75%) and reduced MyD88 (-29, -60, and -81%) and TAK1 expression (-37, -63, and -79%) in a concentration-dependent manner, when compared with the TcdA group (Figures 2A,B). Also, rifaximin caused a significant and concentration-dependent decrease in the expression of NF- $\kappa$ B (-38, -50, and -63% at 0.1, 1.0, and 10  $\mu$ M, respectively, vs. TcdA group; Figures 2C,D). These effects of rifaximin were inhibited by ketoconazole (Figure 2).

## DISCUSSION

In the present study, treatment with rifaximin significantly increased the TEER in Caco-2 cells in a time-dependent manner when compared with TcdA treatment. Treatment also reduced the cytotoxicity of the TcdA challenge and improved cell viability. Further, rifaximin caused a concentration-dependent decrease in the expression of Bax, caspase-3, and an increase in ZO-1 and occludin expression, and inhibited the expression of TLR4, MyD88, TAK1, and NF- $\kappa$ B in the Caco-2 cells. These effects of rifaximin were inhibited by the PXR antagonist, ketoconazole.

Transepithelial electrical resistance measurement is used as an index of monolayer confluence and integrity in cell culture experiments (Huynh-Deleme et al., 2005). TEER has also been used to measure the paracellular permeability of cell monolayers (Madara et al., 1988). In the present study, TcdA challenge caused a time-dependent marked loss of electrical resistance and barrier integrity of the Caco-2 cells, as seen by the reduction in the TEER after the challenge. Rifaximin treatment improved the TEER values and cell viability in a concentration-dependent manner, demonstrating its efficacy in the prevention of TcdA-induced apoptosis and maintaining barrier integrity. That the effects of rifaximin were inhibited by the PXR antagonist ketoconazole, indicates the mechanism of action of rifaximin involves PXR.

Treatment with rifaximin also caused a decrease in the expression of Bax, and an increase in the expression of ZO-1 and occludin in the Caco-2 cells, in a concentration-dependent manner, and preserved the epithelial barrier architecture in the cultured cells. ZO-1 is a tight junction protein that interacts with the transmembrane protein occludin to maintain the cell barrier integrity (Fanning et al., 1998). while Bax is a protein involved in the promotion of apoptosis (Pawlowski and Kraft, 2000; Westphal et al., 2011) Thus, a decrease in Bax expression should decrease the likelihood of apoptosis, and an increase in ZO-1 and occludin expression should ensure maintenance of barrier integrity, which is what was seen in the present

study, with rifaximin effectively maintaining the integrity of the Caco-2 epithelial cell barrier and down-regulating the apoptotic signaling pathway. Again, these effects of rifaximin were completely reversed by ketoconazole, suggesting a PXR-dependent mechanism of action.

Rifaximin treatment also down-regulated the TLR4/MyD88/NF- $\kappa$ B pathway induced by TcdA, through a PXR-dependent mechanism. TLR4 is a transmembrane receptor that is overexpressed in tumor cells (Rakoff-Nahoum and Medzhitov, 2009). TLR4 and its adaptor proteins MyD88 and TAK1 are involved in the activation of the NF- $\kappa$ B pathway causing the release of inflammatory mediators (Akira and Hoshino, 2003; O'Neill et al., 2003; Sato et al., 2005; Kawai and Akira, 2007) In the present study, treatment with rifaximin caused a significant reduction in the expression of TLR4, MyD88, TAK1, and NF- $\kappa$ B after the TcdA challenge, indicating its usefulness in the prevention of TcdA-induced apoptosis by acting on the inflammatory environment. Once again, ketoconazole co-incubation showed complete loss of rifaximin-mediated suppression of these proteins, indicating a role for PXR in these changes.

Pregnane X receptor is a receptor belonging to the nuclear receptor subfamily that are present in the liver and intestine, which are involved in the clearance of xenobiotics from cells (Mani et al., 2013; Smutny et al., 2013). Activation of PXR promotes the expression of several enzymes and transporters that assist in detoxification and removal of xenobiotics, and help in maintaining the integrity of the intestinal barrier (Zhang et al., 2008; Mencarelli et al., 2010). PXR activation also leads to inhibition of the NF- $\kappa$ B pathway and reduces the expression of inflammatory mediators (Cheng et al., 2010; Dou et al., 2012; Zhang et al., 2015) In the present study, reversal of the effects of rifaximin by the PXR antagonist ketoconazole confirm the role of PXR in its mechanism of action. Thus, it appears that rifaximin activates PXR in Caco-2 cells leading to a reduction in TcdA-induced inflammation by down-regulation of the TLR4/MyD88/NF- $\kappa$ B pathway, and improvement of the cell layer integrity.

Rifaximin is a poorly absorbed antibiotic with a favorable safety profile (Scarpignato and Pelosini, 2005). Due to its poor absorption, most of the drug is available in the intestine to locally exert its effects on TcdA-induced apoptosis in the colon. Thus, it may be a promising molecule in the treatment of CDIs.

## CONCLUSION

Rifaximin effectively inhibited TcdA-induced apoptosis in a cellular model of the intestinal barrier by a PXR-dependent TLR4/MyD88/NF- $\kappa$ B pathway mechanism. Further studies in clinical settings are required to confirm its efficacy in the treatment of CDIs.

## AUTHOR CONTRIBUTIONS

GS and GE authored the paper and designed the study; NN, SG, LSe, and EC performed the experiments; MP, AdA, and EB

performed data analysis and co-authored the paper; RC and LSt contributed to critical revision of the paper. All authors approved the submission of the manuscript.

## FUNDING

The preparation of this paper was funded in part by Alfa Wassermann.

## ACKNOWLEDGMENTS

The authors would like to thank Nishad Parkar, Ph.D., of Springer Healthcare Communications for providing medical writing assistance in the form of drafting the introduction and discussion, and English editing of the manuscript. This assistance was funded by Alfa Wassermann.

## REFERENCES

- Akira, S., and Hoshino, K. (2003). Myeloid differentiation factor 88-dependent and -independent pathways in toll-like receptor signaling. *J. Infect. Dis.* 187, S356–S363. doi: 10.1086/374749
- Cash, B. D., Lacy, B. E., Rao, T., and Earnest, D. L. (2016). Rifaximin and eluxadoline – newly approved treatments for diarrhea-predominant irritable bowel syndrome: what is their role in clinical practice alongside alosetron? *Expert Opin. Pharmacother.* 17, 311–322. doi: 10.1517/14656566.2016.1118052
- Cheng, J., Shah, Y. M., Ma, X., Pang, X., Tanaka, T., Kodama, T., et al. (2010). Therapeutic role of rifaximin in inflammatory bowel disease: clinical implication of human pregnane X receptor activation. *J. Pharmacol. Exp. Ther.* 335, 32–41. doi: 10.1124/jpet.110.170225
- Dou, W., Mukherjee, S., Li, H., Venkatesh, M., Wang, H., Kortagere, S., et al. (2012). Alleviation of gut inflammation by Cdx2/Pxr pathway in a mouse model of chemical colitis. *PLoS ONE* 7:e36075. doi: 10.1371/journal.pone.0036075
- Ebigbo, A., and Messmann, H. (2013). Challenges of *Clostridium difficile* infection. *Med. Klin. Intensivmed. Notfmed.* 108, 624–627. doi: 10.1007/s00063-013-0258-7
- Fanning, A. S., Jameson, B. J., Jesaitis, L. A., and Anderson, J. M. (1998). The tight junction protein ZO-1 establishes a link between the transmembrane protein occludin and the actin cytoskeleton. *J. Biol. Chem.* 273, 29745–29753. doi: 10.1074/jbc.273.45.29745
- Huynh-Delorme, C., Huet, H., Noel, L., Frigieri, A., and Kolf-Clauw, M. (2005). Increased functional expression of P-glycoprotein in Caco-2 TC7 cells exposed long-term to cadmium. *Toxicol. In Vitro* 19, 439–447. doi: 10.1016/j.tiv.2004.08.003
- Jodlowski, T. Z., Oehler, R., Kam, L. W., and Melnychuk, I. (2006). Emerging therapies in the treatment of *Clostridium difficile*-associated disease. *Ann. Pharmacother.* 40, 2164–2169. doi: 10.1345/aph.1H340
- Kawai, T., and Akira, S. (2007). Signaling to NF-kappaB by Toll-like receptors. *Trends Mol. Med.* 13, 460–469. doi: 10.1016/j.molmed.2007.09.002
- Layer, P., and Andresen, V. (2010). Review article: rifaximin, a minimally absorbed oral antibacterial, for the treatment of travellers' diarrhoea. *Aliment. Pharmacol. Ther.* 31, 1155–1164. doi: 10.1111/j.1365-2036.2010.04296.x
- Leffler, D. A., and Lamont, J. T. (2015). *Clostridium difficile* infection. *N. Engl. J. Med.* 372, 1539–1548. doi: 10.1056/NEJMra1403772
- Ma, X., Shah, Y. M., Guo, G. L., Wang, T., Krausz, K. W., Idle, J. R., et al. (2007). Rifaximin is a gut-specific human pregnane X receptor activator. *J. Pharmacol. Exp. Ther.* 322, 391–398. doi: 10.1124/jpet.107.121913
- Madara, J. L., Stafford, J., Barenberg, D., and Carlson, S. (1988). Functional coupling of tight junctions and microfilaments in T84 monolayers. *Am. J. Physiol.* 254, G416–G423.

## SUPPLEMENTARY MATERIAL

The Supplementary Material for this article can be found online at: <http://journal.frontiersin.org/article/10.3389/fphar.2016.00120>

**FIGURE S1 | (A)** Agarose gel electrophoresis of cultured Caco-2 cell DNA in the presence of TcdA (30 ng/ml) alone or in the presence of increasing concentration of rifaximin (0.1–10  $\mu$ M) for 24 h. Rifaximin (10  $\mu$ M) was tested either alone, or in the presence of the PXR antagonist ketoconazole (10  $\mu$ M). Ketoconazole alone was unable to exert any significant effect on DNA damage. The results are representative of  $n = 3$  independent experiments. **(B)** Western blot analysis showing immunoreactive bands referred to the pro-apoptotic active Caspase-3 protein. TcdA (30 ng/ml) induced a significant increase of Caspase-3 expression, that was significantly and concentration-dependently reduced by Rifaximin, whose effect was significantly inhibited by ketoconazole (10  $\mu$ M). Ketoconazole alone had no pro-apoptotic effect. **(C)** Relative quantification of immunoreactive bands of active caspase-3 protein (arbitrary units). Results are expressed as the mean  $\pm$  SEM of  $n = 4$  experiments performed in triplicate. \*\*\* $P < 0.001$  vs. vehicle group; °°° $P < 0.001$ , °° $P < 0.01$  vs. TcdA group.

- Mani, S., Dou, W., and Redinbo, M. R. (2013). PXR antagonists and implication in drug metabolism. *Drug Metab. Rev.* 45, 60–72. doi: 10.3109/03602532.2012.746363
- Mencarelli, A., Migliorati, M., Barbanti, M., Cipriani, S., Palladino, G., Distrutti, E., et al. (2010). Pregnane-X-receptor mediates the anti-inflammatory activities of rifaximin on detoxification pathways in intestinal epithelial cells. *Biochem. Pharmacol.* 80, 1700–1707. doi: 10.1016/j.bcp.2010.08.022
- Mosmann, T. (1983). Rapid colorimetric assay for cellular growth and survival: application to proliferation and cytotoxicity assays. *J. Immunol. Methods* 65, 55–63. doi: 10.1016/0022-1759(83)90303-4
- O'Neill, L. A., Dunne, A., Edjeback, M., Gray, P., Jefferies, C., and Wietek, C. (2003). Mal and MyD88: adapter proteins involved in signal transduction by Toll-like receptors. *J. Endotoxin Res.* 9, 55–59. doi: 10.1177/09680519030090010701
- Pawlowski, J., and Kraft, A. S. (2000). Bax-induced apoptotic cell death. *Proc. Natl. Acad. Sci. U.S.A.* 97, 529–531. doi: 10.1073/pnas.97.2.529
- Rakoff-Nahoum, S., and Medzhitov, R. (2009). Toll-like receptors and cancer. *Nat. Rev. Cancer* 9, 57–63. doi: 10.1038/nrc2541
- Rupnik, M., Wilcox, M. H., and Gerding, D. N. (2009). *Clostridium difficile* infection: new developments in epidemiology and pathogenesis. *Nat. Rev. Microbiol.* 7, 526–536. doi: 10.1038/nrmicro2164
- Sanchez-Delgado, J., and Miquel, M. (2015). Role of rifaximin in the treatment of hepatic encephalopathy. *Gastroenterol. Hepatol.* 2015, 3. [Epub ahead of print].
- Sato, S., Sanjo, H., Takeda, K., Ninomiya-Tsuji, J., Yamamoto, M., Kawai, T., et al. (2005). Essential function for the kinase TAK1 in innate and adaptive immune responses. *Nat. Immunol.* 6, 1087–1095. doi: 10.1038/ni1255
- Scarpignato, C., and Pelosini, I. (2005). Rifaximin, a poorly absorbed antibiotic: pharmacology and clinical potential. *Chemotherapy* 51, 36–66. doi: 10.1159/000081990
- Scarpignato, C., and Pelosini, I. (2006). Experimental and clinical pharmacology of rifaximin, a gastrointestinal selective antibiotic. *Digestion* 73, 13–27. doi: 10.1159/000089776
- Smutny, T., Mani, S., and Pavek, P. (2013). Post-translational and post-transcriptional modifications of pregnane X receptor (PXR) in regulation of the cytochrome P450 superfamily. *Curr. Drug Metab.* 14, 1059–1069. doi: 10.2174/1389200214666131211153307
- Surawicz, C. M., and McFarland, L. V. (1999). Pseudomembranous colitis: causes and cures. *Digestion* 60, 91–100. doi: 10.1159/000007633
- Terc, J., Hansen, A., Alston, L., and Hirota, S. A. (2014). Pregnane X receptor agonists enhance intestinal epithelial wound healing and repair of the intestinal barrier following the induction of experimental colitis. *Eur. J. Pharm. Sci.* 55, 12–19. doi: 10.1016/j.ejps.2014.01.007

- Waltz, P., and Zuckerbraun, B. (2016). Novel therapies for severe *Clostridium difficile* colitis. *Curr. Opin. Crit. Care* doi: 10.1097/MCC.0000000000000282 [Epub ahead of print].
- Wan, Y. C., Li, T., Han, Y. D., Zhang, H. Y., Lin, H., and Zhang, B. (2015). Effect of pregnane xenobiotic receptor activation on inflammatory bowel disease treated with rifaximin. *J. Biol. Regul. Homeost. Agents* 29, 401–410.
- Wells, C. L., van de Westerlo, E. M., Jechorek, R. P., Haines, H. M., and Erlandsen, S. L. (1998). Cytochalasin-induced actin disruption of polarized enterocytes can augment internalization of bacteria. *Infect. Immun.* 66, 2410–2419.
- Westphal, D., Dewson, G., Czabotar, P. E., and Kluck, R. M. (2011). Molecular biology of Bax and Bak activation and action. *Biochim. Biophys. Acta* 1813, 521–531. doi: 10.1016/j.bbamcr.2010.12.019
- Zhang, B., Xie, W., and Krasowski, M. D. (2008). PXR: a xenobiotic receptor of diverse function implicated in pharmacogenetics. *Pharmacogenomics* 9, 1695–1709. doi: 10.2217/14622416.9.11.1695
- Zhang, J., Ding, L., Wang, B., Ren, G., Sun, A., Deng, C., et al. (2015). Notoginsenoside R1 attenuates experimental inflammatory bowel disease via pregnane X receptor activation. *J. Pharmacol. Exp. Ther.* 352, 315–324. doi: 10.1124/jpet.114.218750
- Conflict of Interest Statement:** The authors declare that the research was conducted in the absence of any commercial or financial relationships that could be construed as a potential conflict of interest.
- The handling Editor declared a shared affiliation, though no other collaboration, with the authors MP, Ad'A, EB, RC, and GS, and states that the process nevertheless met the standards of a fair and objective review.
- Copyright © 2016 Esposito, Nobile, Gigli, Seguella, Pesce, d'Alessandro, Bruzzese, Capoccia, Steardo, Cuomo and Sarnelli. This is an open-access article distributed under the terms of the Creative Commons Attribution License (CC BY). The use, distribution or reproduction in other forums is permitted, provided the original author(s) or licensor are credited and that the original publication in this journal is cited, in accordance with accepted academic practice. No use, distribution or reproduction is permitted which does not comply with these terms.

# Enteric glia: A new player in inflammatory bowel diseases

E Capoccia,<sup>1</sup> C Cirillo,<sup>2</sup> S Gigli,<sup>1</sup> M Pesce,<sup>3</sup> A D'Alessandro,<sup>3</sup>  
R Cuomo,<sup>3</sup> G Sarnelli,<sup>3</sup> L Steardo<sup>1</sup> and G Esposito<sup>1</sup>

International Journal of  
Immunopathology and Pharmacology  
2015, Vol. 28(4) 443–451  
© The Author(s) 2015  
Reprints and permissions:  
sagepub.co.uk/journalsPermissions.nav  
DOI: 10.1177/0394632015599707  
iji.sagepub.com



## Abstract

In addition to the well-known involvement of macrophages and neutrophils, other cell types have been recently reported to substantially contribute to the onset and progression of inflammatory bowel diseases (IBD). Enteric glial cells (EGC) are the equivalent cell type of astrocyte in the central nervous system (CNS) and share with them many neurotrophic and neuro-immunomodulatory properties. This short review highlights the role of EGC in IBD, describing the role played by these cells in the maintenance of gut homeostasis, and their modulation of enteric neuronal activities. In pathological conditions, EGC have been reported to trigger and support bowel inflammation through the specific over-secretion of S100B protein, a pivotal neurotrophic factor able to induce chronic inflammatory changes in gut mucosa. New pharmacological tools that may improve the current therapeutic strategies for inflammatory bowel diseases (IBD), lowering side effects (i.e. corticosteroids) and costs (i.e. anti-TNF $\alpha$  monoclonal antibodies) represent a very important challenge for gastroenterologists and pharmacologists. Novel drugs capable to modulate enteric glia reactivity, limiting the pro-inflammatory release of S100B, may thus represent a significant innovation in the field of pharmacological interventions for inflammatory bowel diseases.

## Keywords

enteric glia, S100B, enteric nervous system, inflammatory bowel diseases, nitric oxide

Date received: 12 January 2015; accepted: 3 July 2015

## Introduction

Ulcerative colitis (UC) and Crohn's disease (CD) represent the two major clinically defined forms of inflammatory bowel disease (IBD) that may affect the whole gastrointestinal tract and the colonic mucosa, respectively, and are associated with an increased risk of developing colon cancer.<sup>1,2</sup> Even though widespread, IBD is more common in developed countries, with the highest incidence rates and prevalence registered in North America and Europe. However, a substantial variation in the epidemiology of IBD has been lately observed with an alarming rise in prevalence in previously reported low-incidence areas, such as Asia, further pointing out the urgent need of new pharmacological approaches in the management of these diseases.

Usually, therapies for IBD include chronic administration of glucocorticosteroids and sulfasalazine derivatives. However, these drugs are

not always effective and cannot be used for long-term maintenance.<sup>3</sup> In fact, steroids are useful in the short-term treatment of acute flares, but they may induce a number of systemic adverse reactions during prolonged therapy.<sup>4,5</sup> Sulfasalazine and its derivative 5-aminosalicylic acid (5-ASA) are effective only in mild-to-moderate phases of the disease and in preventing relapses.<sup>4-7</sup> The introduction of monoclonal anti-tumor necrosis

<sup>1</sup>Department of Physiology and Pharmacology 'Vittorio Erspamer', University Sapienza of Rome, P.le Aldo Moro 5, 00185, Rome, Italy

<sup>2</sup>Laboratory for Enteric NeuroScience (LENS), TARGID, KU Leuven, Herestraat 49, 3000, Leuven, Belgium

<sup>3</sup>Department of Clinical and Experimental Medicine, University of Naples Federico II, Via S. Pansini 5, 80131, Naples, Italy

### Corresponding author:

Giuseppe Esposito MsC. PhD, Department of Physiology and Pharmacology, "Vittorio Erspamer", University Sapienza of Rome, Rome, 00185, Italy.

Email: giuseppe.esposito@uniroma1.it

factor-alpha (TNF $\alpha$ ) antibodies (Infliximab and Adalimumab) in the therapy of IBD has radically changed their management, since these drugs are effective both in controlling moderate-to-severe forms of UC and CD and providing an efficient prevention of their relapses.<sup>8</sup> However, the long-term safety concerns of these drugs (i.e. the possibility to allow the developing of aggressive form of cancer, particularly leukemia and lymphoma<sup>9</sup>), together with the high costs, limit the ordinary use of these therapeutics. Moreover, a poor response to anti-TNF $\alpha$  therapy has been observed in some forms of UC and CD.<sup>10</sup> For these reasons, there is an urgent need for novel effective drugs, with manageable side toxicity and low costs for patients. In this perspective, the identification and characterization of new therapeutic targets for the development of innovative anti-IBD drugs appear to be crucial. The etiology of IBD has been extensively studied and several efforts have been made aiming at a better understanding of the pathophysiological mechanisms underlying the disease. Different studies have demonstrated the involvement of some risk factors including infectious agents, viruses and bacteria, autoimmune response, food allergies, hereditary factors, and co-morbid stressing conditions.<sup>11,12</sup> Generally, CD and UC have been univocally identified as autoimmune pathologies and the mucosal macrophages and lymphocytes infiltration has been considered as the main responsible for the chronic inflammation, occurring in the gut mucosa. Severe dysfunction of the mucosal immune system has been thus described to play an important role in the pathogenesis of IBD.<sup>13,14</sup> In general, a wide range of inflammatory cells in the gut, such as mucosal CD4+ T cells, are thought to play a central role in both the induction and the persistence of chronic inflammation by producing pro-inflammatory cytokines.<sup>15</sup> Several studies have demonstrated that the levels of T helper 1 (Th1)-related cytokines (e.g. TNF $\alpha$ , interferon gamma (IFN)- $\gamma$ , interleukin (IL)-12), as well as the concentration of other cytokines (e.g. IL-17A, IL-21, IL-23), are increased in the inflamed mucosa of these patients when compared to normal subjects.<sup>16–20</sup> Pro-inflammatory cytokines may profoundly affect intestinal mucosal homeostasis by inducing chronic inflammatory changes, including T cell and macrophage proliferation, expression of adhesion molecules and chemokines, and secretion of other pro-inflammatory cytokines

that perpetuate, in turn, the chronic inflammation in the gut.<sup>19,20</sup>

### *From mucosal inflammation concept to the enteric-driven neuroinflammation concept*

In recent years, it has become clear that the mucosal immune system alone may not account for all the aspects of IBD pathogenesis and pursuit of new players in CD and UC pathophysiology led to investigate the involvement of the enteric nervous system (ENS) in intestinal inflammation, enlarging the concept of inflammation to neuro-inflammation in IBD.

Although in patients with IBD morphological abnormalities of the ENS have been consistently described, only in the last decade have recent studies highlighted the changes occurring in both enteric neurons and enteric glial cells during intestinal inflammation.<sup>21–24</sup>

The ENS takes part to the peripheral nervous system and it is located within the wall of the gastrointestinal tract. It has been considered the “brain of the gut” since, independently from the central nervous system (CNS), it coordinates many aspects of digestive functions such as motility, blood flow, and immune/inflammatory processes.<sup>25</sup> Many features of digestive function are guided by the ENS, a complex network of neurons and glia that works independently from the central nervous system. The ENS originates from the neural crest, which invades, proliferates, and migrates within the intestinal wall until the whole bowel is colonized with enteric neural crest-derived cells (ENCCs). Due to different factors and morphogens, the ENCCs develop further, differentiating into glia and neuronal sub-types, interplaying to form a functional nervous system.<sup>26</sup> Histologically, the ENS is organized in two major ganglionated plexuses, the myenteric (Auerbach’s) and the submucosal (Meissner’s and Henle’s) plexus (Figure 1a). These ganglia contain neuron cell bodies and are interconnected by bundles of nerve processes. The myenteric plexus is located between the longitudinal and circular muscle throughout the gut, from the esophagus to the rectum. It mainly innervates the *muscularis externa* and controls intestinal motility. The sub-mucosal plexus, lying between the mucosa and the circular muscle, is involved in the regulation of bowel secretion, especially in the small intestine where it is most located. A number of

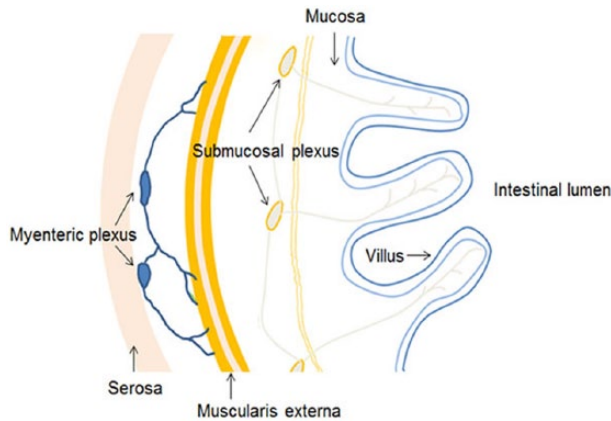


**Figure 1a.** Schematic representation of the gut wall. Myenteric plexus innervates the muscularis externa and controls the intestinal motility; the submucosal plexus innervates the submucosal blood vessels and is basically involved in the control of the intestinal secretory functions.

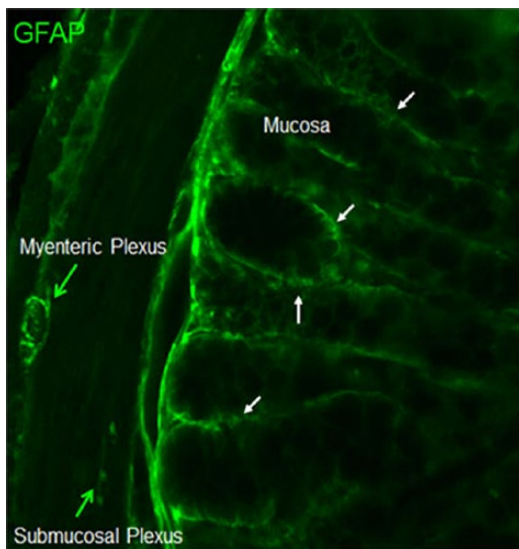


**Figure 1b.** GFAP immunofluorescence staining in the enteric nervous system. The figure shows the localization of myenteric plexus and submucosal plexus networks in mice intestine indicated by green arrows. White arrows indicate the close proximity of enteric glial cell processes with epithelial cells in the mucosa. Magnification 100 $\times$ .

morphological and functional distinct neurons are located in both plexuses, including primary afferent neurons, sensitive to chemical and mechanical stimuli, interneurons, and motor neurons. Most of the enteric neurons involved in motor functions are located in the myenteric plexus with some primary afferent neurons located in submucosal plexus.<sup>27</sup>

Though not fully understood, the neuroinflammatory process occurring during IBD refers to

several structural and functional abnormalities occurring in the ENS. In these conditions both macroscopic changes (hypertrophy and hyperplasia of nerve bundles and ganglia) and neurotransmitter release adaptations in the ENS are commonly observed.<sup>22</sup> In patients with IBD, morphological changes occurring in the ENS, ranging from the alteration of submucosal plexus structure to the retraction of neuronal fibers and the appearance of neuromatous lesions, are observed.<sup>23</sup>

Moreover, although the exact mechanism(s) at the basis of such alteration has/have not been fully understood, it is commonly accepted that the increased apoptosis of enteric neurons and EGC is closely correlated to several functional disturbances observed in IBD patients, such as gut dysmotility and increased sensory perception.<sup>21–23</sup>

#### *Enteric glia: The beautiful and the bad weather in the gut*

Enteric glial cells (EGC), the phenotypical equivalent of astrocytes into the CNS, are small cells with a star-like shape and are believed to represent the most abundant cells in the ENS;<sup>28</sup> EGCs are for these reasons considered as active partners in ENS function.<sup>29</sup> They display dynamic responses to neuronal inputs and may take part into the release of neuro-active factors. At present, EGCs of human gut are usually identified by the expression of the S100B and GFAP protein, as well as by the expression of more recently recognized markers such as Sox 10.<sup>30–33</sup> EGCs surround enteric neuron bodies and axons,<sup>34</sup> as well as intestinal blood vessels<sup>35</sup> while their processes extend into the mucosa.<sup>36</sup> Despite the previous assumption that EGCs may serve as mechanical support for enteric neurons, nowadays the knowledge on these cells is consistently expanded. Functionally, EGCs are believed to be responsible for many of peripheral neurons functions through the release of a variety of soluble factors.<sup>37</sup> Under physiological conditions, major histocompatibility complex class I (MHC I) molecules are constitutively expressed by EGCs, while MHC class II molecules are almost undetectable.<sup>38,39</sup> It has become increasingly clear that EGCs play a pivotal role in the regulation of intestinal homeostasis, leading to a more multifaceted and comprehensive knowledge of these cells.<sup>40</sup> Beside their trophic and cytoprotective functions toward enteric neurons, enteric glial cells play a key role in

the intestinal epithelial barrier homeostasis and integrity.<sup>41</sup> The intestinal barrier regulates the passage of the intestinal contents, preventing the diffusion of microbes and other pathogens (including viruses) through the mucosa. EGCs are in close proximity of gut epithelial cells and similarly to their counterparts in the CNS, they may affect intestinal permeability through the release of several mediators, directly controlling epithelial barrier functions.<sup>42</sup> Among the different EGC-related mediators, glial-derived neurotrophic factor (GDNF) plays a fundamental role in the preservation of mucosal integrity under the enteric glia surveillance. GDNF indeed exerts anti-inflammatory effects via a dual mechanism; on one hand, it inhibits EGCs apoptosis in an autocrine manner; on the other, via a paracrine mechanism, it lowers the level of pro-inflammatory cytokines, such as IL-1 $\beta$  and TNF $\alpha$ , that significantly increases during IBD and gut infections.<sup>43</sup> Recently it has been shown that EGCs can assure the integrity of the intestinal barrier through the release of S-nitrosoglutathione (GSNO).<sup>44</sup> The effect of this metabolite is associated with the overexpression of tight junction associated-proteins, for example zonula occludens-1 (ZO-1) and occludin, that in turn prevents the intestinal barrier breakdown during an inflammatory insult, linking with actin cytoskeleton ring and myosin light chain (MLC). Thus, EGCs play important functions in the maintenance of ENS homeostasis, but they may also proliferate and be activated in response to injury and inflammation, undergoing reactive gliosis (entero-gliosis).<sup>45,46,47</sup> In these conditions, EGCs activity is profoundly altered and, following injury and inflammation, these activated cells undergo a dynamic process associated with an increased proliferation and a pro-inflammatory phenotype.<sup>45,47,48</sup> Enteroglia activation is characterized by the over-release of neurotrophins, growth factors, and cytokines that, in turn, recruit infiltrating immune cells such as macrophages, neutrophils, and mast cells in the colonic mucosa.<sup>47-49</sup> During the onset and perpetuation of the inflammatory state of the mucosa, EGCs control of mucosal integrity is markedly altered.<sup>50</sup> These results are in line with several studies<sup>50-53</sup> showing that EGCs can regulate the expression of genes responsible for adhesion, differentiation, and proliferation of epithelial cells,<sup>54</sup> further confirming the importance of enteric glia in the epithelial barrier homeostasis. In the context of

signaling molecules released by EGCs, the production of transforming growth factor- $\beta$ 1 (TGF- $\beta$ 1) and vascular endothelial growth factor (VEGF) might be involved in the onset and metastasis of colon cancer during IBD, thanks to their effects on the epithelial cells proliferation and formation of new blood vessels.<sup>55</sup> Very interestingly, different evidences let hypothesize that EGCs act as *primum movens* in triggering and amplifying the inflammatory cascade during chronic inflammatory insult of the gut.<sup>45,46,56</sup> An intriguing correlation between the degree of enteric gliosis and severity of gut inflammation has been also reported and an intimate interaction between EGCs and the mucosal immune system has been observed.<sup>50,57</sup>

#### *EGC drive neuroinflammation in IBD: The role of S100B protein and its partnership with nitric oxide*

In recent years, it has been assumed that EGCs are involved in the chronic mucosal inflammation in UC; and many EGC-related signaling molecules thought to orchestrate such neuroinflammatory cross-talk are under extensive investigation.<sup>58,59</sup> The S100B protein, one of the typical markers of EGC, seems to play a crucial role in IBD.<sup>45</sup> S100B is the homodimer of subunit and belongs to a Ca<sup>2+</sup>-Zn<sup>2+</sup> binding proteins super-family that comprises more than 20 proteins.<sup>35</sup> In the gut, S100B protein is constitutively expressed by EGCs<sup>45</sup> while other members of S100 family, such as S100A8, S100A9, and S100A12 are expressed only under inflammatory conditions by phagocytes and intestinal epithelial cells.<sup>45,60</sup> The role exerted by S100B in gut inflammation has been only recently highlighted.<sup>45,61</sup> S100B is a pivotal signaling molecule that participates at the onset and progression of the inflammatory status, as it coordinates a wide range of signal activation pathways, directly correlated with the severity of tissue damage.<sup>61</sup> This is highlighted by the observation that rectal specimens from early diagnosed UC patients show an increased S100B protein expression (Figure 2a).<sup>45</sup>

The upregulation of S100B runs in parallel with an increased production of NO via the stimulation of iNOS protein expression. This is a very important point since a large group of studies pointed out that in UC patients an abnormal NO secretion by pro-inflammatory cytokines has been observed due to the progressive activation of iNOS protein.<sup>62,63</sup> In more detail, researches performed by comparing



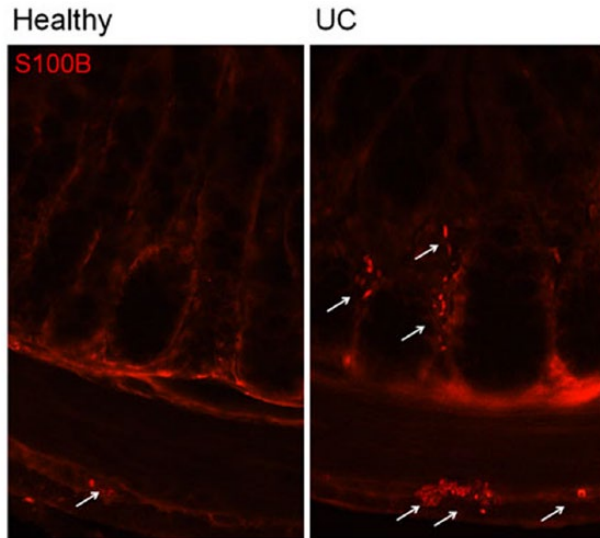


**Figure 2a.** S100B protein in ulcerative colitis (UC). Immunofluorescence analysis showing the upregulation of S100B protein in UC versus healthy specimen. Arrows indicate S100B protein expression spots in both in myenteric plexus and in mucosa. Magnification 100 $\times$ .

patients with UC and healthy subjects demonstrated that rectal specimens from UC patients show an increased immunoreactivity for S100B protein and a significantly enhanced protein secretion and expression.<sup>56</sup> This upregulation cannot be considered a mere epiphenomenon because it is related to the specific activation of inducible NO synthase (iNOS) protein leading to an increase of NO level. Thus, S100B upregulation has a prominent role during ulcerative colitis. The correlation between S100B upregulation and NO production is very interesting since, as previously described, UC is characterized by abnormal mucosal NO production.<sup>63</sup> EGCs ability of modulating NO levels via S100B release has been confirmed also in absence of a chronic inflammatory scenario. In fact, the administration of micromolar concentration of exogenous S100B is able to induce a concentration-dependent activation of iNOS expression and a subsequent enhanced NO production, in rectal mucosa of healthy subjects.<sup>56</sup> In line with this it has been suggested that EGCs modulate the NO-dependent inflammatory response through the release of S100B within the intestinal milieu and let hypothesize that S100B release might be a first step in the onset of inflammation.<sup>64</sup> Once released, S100B may accumulate at the RAGE (Receptor for

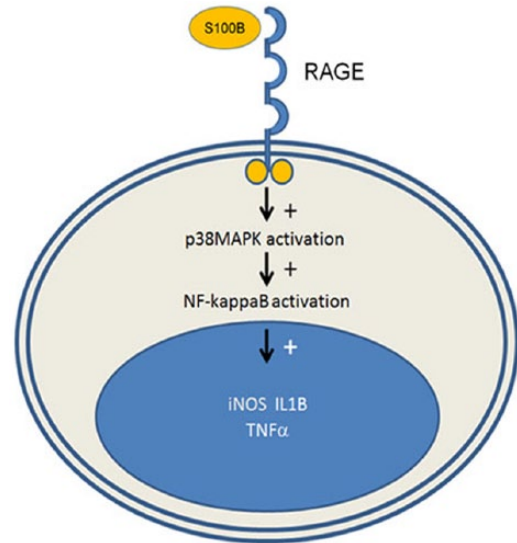


**Figure 2b.** Schematic representation of the S100B pro-inflammatory signaling. The linkage between S-100B and RAGE is able to increase the production of NO and other pro-inflammatory cytokines via the activation of NF $\kappa$ B.

Advanced Glycation End products) site in micromolar concentrations.<sup>65,66</sup> Such interaction leads then to mitogen-activated protein kinase (MAPK) phosphorylation and consequent nuclear factor-kappaB (NF- $\kappa$ B) activation which, in turn, induces the transcription of different cytokines, such as iNOS protein, IL-1B, TNF $\alpha$  (Figure 2b).<sup>67,68</sup> Although the mechanisms by which EGCs and their signaling molecule S100B may coordinate such a complex inflammatory scenario is just initially conceived; more recently, a close relationship with toll-like receptors (TLRs) activation has been proposed.<sup>61</sup> In fact, the direct interaction between S100B and RAGE receptors during colitis has to be considered an initial event triggering the activation of a specific downstream pathway involved in the maintenance of a persistent enteroglia-sustained inflammation in the human gut. RAGE is also involved in the enteroglia TLRs signaling network, and it has become clear that, since EGCs express different TLR subtypes depending upon their pathophysiological functions;<sup>69</sup> these cells may be involved in a wider network of neuro-immunological pathways. Supporting this hypothesis, a specific S100B/RAGE/TLR-4 axis during gut inflammation has thus been observed as a pivotal molecular mechanism sustaining EGC activation during UC.<sup>61</sup>

### Conclusions and perspectives: Could we consider EGC targeting as a novel approach to develop anti-IBD drugs?

The urgent need of new pharmacological approaches that may enlarge the tools against IBD, as well as a better knowledge on new molecular players involved in the triggering and perpetuation of inflammation in the gut is a very important challenge for pharmacologists and gastroenterologists. This review highlighted the importance of EGCs as fundamental cell type within the ENS that participate to the modulation of inflammatory responses in the human gut. ENS alterations, featured by apoptotic bodies of neurons and glia,<sup>70</sup> especially in submucosal plexi, is commonly observed in human IBD, and it has been postulated to play a fundamental role in the occurrence of disorders of intestinal motility and or secretion.<sup>21,23</sup>

EGCs trigger and promote chronic inflammation in the intestinal mucosa since these cells over-release S100B that in turn determinates NO production. Such detrimental loop is responsible for a substantial recruitment of other target cells, including immune cells. In fact, EGC-derived S100B is able to affect peripheral macrophages and intestinal mucosal immune cell. A better understanding of the molecular mechanisms underlying EGC dysfunction, might constitute a new approach to increase the efficacy of new enteric-glia oriented drugs that may overcome the lack of long-term effectiveness of immunosuppressant agents used for IBD.

In the next future, molecules capable to selectively target EGC-mediated neuroinflammation, might represent a novel approach to develop new therapeutic strategies for IBD. In this context, the possibility to interfere with the S100B/NO axis may pave the way to a significant improvement of the actual therapies against UC or CD. To this aim, in preclinical studies, we demonstrated that the specific inhibition of S100B protein activity with pentamidine, an antiprotozoal drug, resulted in a marked reduction of EGC-mediated neuroinflammation severity in mice.<sup>71</sup> Similar results were obtained *in vivo* in mice and in human UC-deriving cultured biopsies with palmitoylethanolamide (PEA), an endogenous autacoid local inflammation antagonist (ALIA)-mide, able to downregulate S100B protein expression and to inhibit S100B-dependent activation of TLR-4 on enteric

glia.<sup>61</sup> Both pharmacological approaches resulted in a significant downregulation of inflammatory parameters, and improved significantly the disease course through a selective enteroglia-specific targeting, although in a preclinical evidence.

In conclusion, most of the studies on the role of enteric glia have been carried out in preclinical animal models of IBD. Although this might appear as a limitative factor due to the unpreventable differences emerging by the IBD process *in vivo* and the human disease, EGCs powerfully emerge as a very intriguing target on which develop selective drugs to treat CD and UC.

### Acknowledgements

We are grateful to Luisa Seguella for her technical assistance to manuscript preparation.

### Declaration of conflicting interests

The author(s) declared no potential conflicts of interest with respect to the research, authorship, and/or publication of this article.

### Funding

This research received no specific grant from any funding agency in the public, commercial, or not-for-profit sectors.

### References

1. Rhodes JM and Campbell BJ (2002) Inflammation and colorectal cancer: IBD-associated and sporadic cancer compared. *Trends in Molecular Medicine* 8: 10–16.
2. M'Koma AE (2013) Inflammatory bowel disease: An expanding global health problem. *Clinical Medicine Insights Gastroenterology* 6: 33–47.
3. Fasci-Spurio F, Aratari A, Margagnoni G, et al. (2012) Oral beclomethasone dipropionate: A critical review of its use in the management of ulcerative colitis and Crohn's disease. *Current Clinical Pharmacology* 7: 131–136.
4. Hanauer SB and Stathopoulos G (1991) Risk-benefit assessment of drugs used in the treatment of inflammatory bowel disease. *Drug Safety* 6: 192–219.
5. Engel MA and Neurath MF (2010) New pathophysiological insights and modern treatment of IBD. *Journal of Gastroenterology* 45: 571–583.
6. Ham M and Moss AC (2012) Mesalamine in the treatment and maintenance of remission of ulcerative colitis. *Expert Review of Clinical Pharmacology* 5(2): 113–123.
7. Ford AC, Achkar JP, Khan KJ, et al. (2011) Efficacy of 5-aminosalicylates in ulcerative colitis: Systematic

- review and meta-analysis. *American Journal of Gastroenterology* 106: 601–616.
8. Spurio FF, Aratari A, Margagnoni G, et al. (2012) Early treatment in Crohn's disease: Do we have enough evidence to reverse the therapeutic pyramid? *Journal of Gastrointestinal and Liver Diseases* 21: 67–73.
  9. Rosh JR, Gross T, Mamula P, et al. (2007) Hepatosplenic T-cell lymphoma in adolescents and young adults with Crohn's disease: A cautionary tale? *Inflammatory Bowel Diseases* 13: 1024–1030.
  10. Guerra I and Bermejo F (2014) Management of inflammatory bowel disease in poor responders to infliximab. *Clinical and Experimental Gastroenterology* 7: 359–367.
  11. Frolkis A, Dieleman L, Barkema DVM, et al. (2013) Environment and the inflammatory bowel diseases. *Canadian Journal of Gastroenterology* 27(3): e18–e24.
  12. Molodecky NA and Kaplan GG (2010) Environmental risk factors for inflammatory bowel disease. *Gastroenterology & Hepatology* 6(5): 339–346.
  13. Pastorelli L, De Salvo C, Mercado JR, et al. (2013) Central role of the gut epithelial barrier in the pathogenesis of chronic intestinal inflammation: Lessons learned from animal models and human genetics. *Frontiers in Immunology* 4: 280.
  14. Rescigno M (2011) The intestinal epithelial barrier in the control of homeostasis and immunity. *Trends in Immunology* 32: 256–264.
  15. Shih DQ and Targan SR (2008) Immunopathogenesis of inflammatory bowel disease. *World Journal of Gastroenterology* 14(3): 390–400.
  16. Nikolaus S, Bauditz J and Gionchetti P. (1998) Increased secretion of pro-inflammatory cytokines by circulating polymorphonuclear neutrophils and regulation by interleukin 10 during intestinal inflammation. *Gut* 42(4): 470–476.
  17. Cobrin GM and Abreu MT (2005) Defects in mucosal immunity leading to Crohn's disease. *Immunological Reviews* 206: 277–295.
  18. Nunes T, Bernardazzi C and de Souza HS (2014) Interleukin-33 and inflammatory bowel diseases: Lessons from human studies. *Mediators of Inflammation* 2014: 423957.
  19. Andoh A, Yagi Y, Shioya M, et al. (2008) Mucosal cytokine network in inflammatory bowel disease. *World Journal of Gastroenterology* 14(33): 5154–5161.
  20. Scaldaferri F and Fiocchi C (2007) Inflammatory bowel disease: Progress and current concepts of etiopathogenesis. *Journal of Digestive Diseases* 8(4): 171–178.
  21. Geboes K and Collins S (1998) Structural abnormalities of the nervous system in Crohn's disease and ulcerative colitis. *Neurogastroenterology and Motility* 10: 189–202.
  22. Lakhan SE and Kirchgessner A (2010) Neuroinflammation in inflammatory bowel disease. *Journal of Neuroinflammation* 7: 37.
  23. Villanacci V, Bassotti G, Nascimbeni R, et al. (2008) Enteric nervous system abnormalities in inflammatory bowel diseases. *Neurogastroenterology and Motility* 20(9): 1009–1016.
  24. Bassotti G, Villanacci V, Fisogni S, et al. (2007) Enteric glial cells and their role in gastrointestinal motor abnormalities: Introducing the neuro-gliopathies. *World Journal of Gastroenterology* 13(30): 4035–4041.
  25. Goyal RK and Hirano I (1996) The enteric nervous system. *New England Journal of Medicine* 334(17): 1106–1115.
  26. Laranjeira C and Pachnis V (2009) Enteric nervous system development: Recent progress and future challenges. *Autonomic Neuroscience* 151(1): 61–69.
  27. Furness JB and Costa M (1980) Types of nerves in the enteric nervous system. *Neuroscience* 5(1): 1–20.
  28. Gabella G (1981) Ultrastructure of the nerve plexuses of the mammalian intestine: The enteric glial cells. *Neuroscience* 6(3): 425–436.
  29. Rühl A, Nasser Y and Sharkey KA (2004) Enteric glia. *Neurogastroenterology and Motility* 16 Suppl 1: 44–49.
  30. Bjorklund H, Dahl D and Seiger A (1984) Neurofilament and glial fibrillary acid protein-related immunoreactivity in rodent enteric nervous system. *Neuroscience* 12(1): 277–287.
  31. Ferri GL, Probert L, Cocchia D, et al. (1982) Evidence for the presence of S-100 protein in the glial component of the human enteric nervous system. *Nature* 297(5865): 409–410.
  32. Hoff S, Zeller F, von Weyhern CW, et al. (2008) Quantitative assessment of glial cells in the human and guinea pig enteric nervous system with an anti-Sox8/9/10 antibody. *Journal of Comparative Neurology* 509(4): 356–371.
  33. Jessen KR and Mirsky R (1980) Glial cells in the enteric nervous system contain glial fibrillary acidic protein. *Nature* 286(5774): 736–737.
  34. Gershon MD and Rothman TP (1991) Enteric glia. *Glia* 4(2): 195–204.
  35. Liu YA, Chung YC, Pan ST, et al. (2013) 3-D imaging, illustration, and quantitation of enteric glial network in transparent human colon mucosa. *Neurogastroenterology and Motility* 25(5): e324–338.
  36. Hanani M and Reichenbach A (1994) Morphology of horseradish peroxidase (HRP)-injected glial cells in the myenteric plexus of the guinea-pig. *Cell and Tissue Research* 278(1): 153–160.

37. Rühl A (2006) Glial regulation of neuronal plasticity in the gut: Implications for clinicians. *Gut* 55(5): 600–602.
38. Geboes K, Rutgeerts P, Ectors N, et al. (1992) Major histocompatibility class II expression on the small intestinal nervous system in Crohn's disease. *Gastroenterology* 103(2): 439–447.
39. Koretz K, Momburg F, Otto HF, et al. (1987) Sequential induction of MHC antigens on autochthonous cells of ileum affected by Crohn's disease. *American Journal of Pathology* 129(3): 493–502.
40. Bassotti G, Villanacci V, Antonelli E, et al. (2007) Enteric glial cells: New players in gastrointestinal motility? *Laboratory Investigation* 87(7): 628–632.
41. Yu YB and Li YQ (2014) Enteric glial cells and their role in the intestinal epithelial barrier. *World Journal of Gastroenterology* 20(32): 11273–11280.
42. Savidge TC, Sofroniew MV and Neunlist M (2007) Starring roles for astroglia in barrier pathologies of gut and brain. *Laboratory Investigations* 87(8): 731–736.
43. Zhang DK, He FQ, Li TK, et al. (2010) Glial-derived neurotrophic factor regulates intestinal epithelial barrier function and inflammation and is therapeutic for murine colitis. *Journal of Pathology* 222: 213–222.
44. Savidge TC, Newman P, Pothoulakis C, et al. (2007) Enteric glia regulate intestinal barrier function and inflammation via re-release of S-nitrosoglutathione. *Gastroenterology* 132(4): 1344–1358.
45. Cirillo C, Sarnelli G, Esposito G, et al. (2011) S100B protein in the gut: The evidence for enteroglial sustained intestinal inflammation. *World Journal of Gastroenterology* 17(10): 1261–1266.
46. Esposito G, Cirillo C, Sarnelli G, et al. (2007) Enteric glial-derived S100B protein stimulates nitric oxide production in celiac disease. *Gastroenterology* 133(3): 918–925.
47. Burns AJ and Pachnis V (2009) Development of the enteric nervous system: Bringing together cells, signals and genes. *Neurogastroenterology and Motility* 21: 100–102.
48. Von Boyen GB, Steinkamp M, Geerling I, et al. (2006) Proinflammatory cytokines induce neurotrophic factor expression in enteric glia: A key to the regulation of epithelial apoptosis in Crohn's disease. *Inflammatory Bowel Diseases* 12: 346–354.
49. Sharkey KA (2015) Emerging roles for enteric glia in gastrointestinal disorders. *Journal of Clinical Investigation* 125(3): 918–925.
50. Cabarrocas J, Savidge TC and Liblau RS (2003) Role of enteric glial cells in inflammatory bowel disease. *Glia* 41: 81–93.
51. Neunlist M, Van Landeghem L, Bourreille A, et al. (2008) Neuro-glial crosstalk in inflammatory bowel disease. *Journal of Internal Medicine* 263: 577–583.
52. Cheadle GA, Costantini TW, Lopez N, et al. (2013) Enteric glia cells attenuate cytomix-induced intestinal epithelial barrier breakdown. *PLoS One* 8(7): e69042.
53. Bach-Ngohou K, Mahé MM, Aubert P, et al. (2010) Enteric glia modulate epithelial cell proliferation and differentiation through 15-deoxy- $\Delta^{12,14}$ -prostaglandin J<sub>2</sub>. *Journal of Physiology* 588: 2533–2544.
54. Van Landeghem L, Mahé MM, Teusan R, et al. (2009) Regulation of intestinal epithelial cells transcriptome by enteric glial cells: Impact on intestinal epithelial barrier functions. *BMC Genomics* 10: 507.
55. Neunlist MP, Aubert P, Bonnaud S, et al. (2007) Enteric glia inhibit intestinal epithelial cell proliferation partly through a TGF- $\beta$ 1-dependent pathway. *American Journal of Physiology Gastrointestinal and Liver Physiology* 292(1): G231–241.
56. Cirillo C, Sarnelli G, Esposito G, et al. (2009) Increased mucosal nitric oxide production in ulcerative colitis is mediated in part by the enteroglial derived S100B protein. *Neurogastroenterology and Motility* 21(11): e1209–1112.
57. Cornet A, Savidge TC, Cabarrocas J, et al. (2001) Enterocolitis induced by autoimmune targeting of enteric glial cells: A possible mechanism in Crohn's disease? *Proceedings of the National Academy of Sciences of the United States of America* 98(23): 13306–13311.
58. Von Boyen GBT, Steinkamp M, Reinshagen M, et al. (2004) Proinflammatory cytokines increase glial fibrillary acidic protein expression in enteric glia. *Gut* 53(2): 222–228.
59. Von Boyen G and Steinkamp M (2010) The role of enteric glia in gut inflammation. *Neuron Glia Biology* 6(4): 231–236.
60. Leach ST, Yang Z, Messina I, et al. (2007) Serum and mucosal S100 proteins, calprotectin (S100A8/S100A9) and S100A12, are elevated at diagnosis in children with inflammatory bowel disease. *Scandinavian Journal of Gastroenterology* 42(11): 1321–1331.
61. Esposito G, Capoccia E, Turco F, et al. (2014) Palmitoylethanolamide improves colon inflammation through an enteric glia/toll like receptor 4-dependent PPAR- $\alpha$  activation. *Gut* 63(8): 1300–1312.
62. Linehan JD, Kolios G, Valatas V, et al. (2005) Effect of corticosteroids on nitric oxide production in inflammatory bowel disease: Are leukocytes the site of action? *American Journal of Physiology Gastrointestinal and Liver Physiology* 288(2): G261–267.
63. Menchen L, Colon AL, Madrigal JL, et al. (2004) Activity of inducible and neuronal nitric oxide synthases in colonic mucosa predicts progression of ulcerative colitis. *American Journal of Gastroenterology* 99(9): 1756–1764.
64. Cirillo C, Sarnelli G, Turco F, et al. (2011) Proinflammatory stimuli activates human-derived

- enteroglia cells and induces autocrine nitric oxide production. *Neurogastroenterology and Motility* 23(9): e372–e382.
65. Donato R (2007) RAGE: A single receptor for several ligands and different cellular responses: the case of certain S100 proteins. *Current Molecular Medicine* 7(9): 711–724.
66. Schmidt AM, Yan SD, Yan SF, et al. (2001) The multiligand receptor RAGE as a progression factor amplifying immune and inflammatory responses. *Journal of Clinical Investigation* 108(7): 949–955.
67. Esposito G, De Filippis D, Cirillo C, et al. (2006) The astroglial-derived S100beta protein stimulates the expression of nitric oxide synthase in rodent macrophages through p38 MAP kinase activation. *Life Sciences* 78(23): 2707–2715.
68. Lam AG, Koppal T, Akama KT, et al. (2001) Mechanism of glial activation by S100B: Involvement of the transcription factor NFkappaB. *Neurobiology of Aging* 22(5): 765–772.
69. Turco F, Sarnelli G, Cirillo C, et al. (2014) Enteroglia-derived S100B protein integrates bacteria-induced Toll-like receptor signaling in human enteric glial cells. *Gut* 63(1): 105–115.
70. Bassotti G, Villanacci V, Nascimbeni R, et al. (2009) Enteric neuroglial apoptosis in inflammatory bowel diseases. *Journal of Crohn's & Colitis* 3(4): 264–270.
71. Esposito G, Capoccia E, Sarnelli G, et al. (2012) The antiprotozoal drug pentamidine ameliorates experimentally induced acute colitis in mice. *Journal of Neuroinflammation* 9: 277.